TASTE-MASKING OF EFAVIRENZ THROUGH MICROENCAPSULATION

Marise Nel (BSc(Hons) MedSci)

A full thesis submitted in partial fulfilment of the requirements for the degree of

Magisterii Scientiae (Pharmaceutical Science)

Faculty of Natural Science, School of Pharmacy

Discipline of Pharmaceutics

University of the Western Cape, Belville, South Africa

UNIVERSITY *of the*
WESTERN CAPE

School of
PHARMACY

Supervisor: Prof. Marique Elizabeth Aucamp

Co-Supervisor: Prof. Halima Samsodien

November 2021

DECLARATION

I **Marise Nel** declare that

(i) The research reported in this thesis, except where otherwise indicated, is my original work.

(ii) This thesis has not been submitted for any degree or examination at any other University.

(iii) This thesis does not contain other persons' data, pictures, graphs or other information, unless specifically acknowledged as being sourced from other persons.

(iv) This thesis does not contain other persons' writing, unless specifically acknowledged as being sourced from other researchers. Where other written sources have been quoted, then:

a. their words have been re-written but the general information attributed to them has been referenced;

b. where their exact words have been used, their writing has been placed inside quotation marks, and referenced.

(v) Where I have reproduced a publication of which I am author, co-author or editor, I have indicated in detail which part of the publication was actually written by myself alone and have fully referenced such publications. This thesis does not contain text, graphics or tables copied and pasted from the Internet, unless specifically acknowledged, and the source being detailed in the thesis and in the References sections.

Signed:  Date: __10/11/2021__

DEDICATION

This thesis is a dedication to myself, my hopes, my dreams and my curiosity.

Nothing in life is to be feared. It is only to be understood. – *Marie Curie*

PUBLICATIONS AND PRESENTATIONS

- Using natural excipients to enhance the solubility of poorly water-soluble antiretroviral drug, efavirenz.

  Submitted to Journal of Drug Delivery Science and Technology in August 2021 (Appendix B)

- Virtual podium presentation at the annual Research Symposium hosted by the School of Pharmacy at the University of the Western Cape in 2021

- E-poster and oral presentation at AAPS PharmSci 360 virtual conference in 2020

  ***Title of poster**: Taste-masking efavirenz through microencapsulation using the technique of spray-drying*

ABSTRACT

Background: It is a well-known fact that a significant gap exists in the development of child-friendly dosage forms, detrimentally affecting paediatric patient compliance, especially in the treatment of debilitating diseases such as human-immunodeficiency virus (HIV) infection. Although not recommended as first-line treatment, efavirenz (EFV) still forms part of the South African Department of Health's treatment regimen for HIV-infected children. EFV is however an extremely bitter-tasting drug, known to cause "burning-mouth" syndrome and therefore paediatric patient compliance related to EFV dosage forms has generally proven low partly due to poor palatability. A multitude of taste-masking strategies may be applied in an effort to alleviate this factor. One of these strategies, which is well-known and more widely applied in food sciences than in pharmaceutical sciences, is that of compound microencapsulation through spray-drying and ionic gelation. In this study the potential of utilizing EFV-loaded microcapsules obtained *via* spray-drying and EFV-loaded calcium-alginate beads obtained *via* ionic gelation as possible taste-masking strategies were investigated.

Aim: Produce EFV micro-particles encapsulated by pea protein isolate, inulin and/or sodium alginate to facilitate taste masking of the active drug particles.

Methods: Spray-drying was used to prepare microencapsulated EFV using pea protein isolate (PPI) and inulin (IN) as wall forming agents. Different spray-drying process parameters were used in order to identify the most efficient and optimal conditions. Moisture content and yield of the spray-drying process were determined after each spray drying trial. The spray-dried powders were characterised through hot stage microscopy (HSM), differential scanning calorimetry (DSC), thermogravimetric analysis (TGA), Fourier-transform infrared spectroscopy (FTIR), powder X-ray diffraction (PXRD) and scanning electron microscopy (SEM). The achieved encapsulation efficiency (%EE) and drug loading (%DL) were also determined. Drug release at pH 6.8 was determined *via in vitro* dissolution and the results were used to inform the taste-masking efficiency achieved via spray-drying.

EFV-loaded calcium-alginate beads were prepared by first dissolving EFV (2 mg/mL) in a 2 % w/v sodium alginate solution and stirred until homogenously dispersed. The solution was then dropped into a 1 % w/v $CaCl_2$ solution. After rinsing, the formed beads were allowed to air dry for 120 h. The dried beads were evaluated with respect to moisture content, size, weight, drug loading, encapsulation efficiency, surface morphology swelling and *in vitro* drug release in both acidic and alkaline media. The *in vitro* drug release data was extrapolated to inform the achieved taste-masking efficiency.

Results: Microencapsulation of EFV *via* spray-drying using the natural excipients PPI and IN as encapsulating agents proved relatively successful. However, the resulting powders did not consist of microspheres in the true sense but rather presented with a more agglomerated/fused nature when EFV was added. FT-IR and DSC results showed that EFV was successfully loaded into the spray-dried powders and that the EFV was sufficiently dispersed in the powders to allow for detection. The use of an aqueous buffered solution for the preparation of the spray-drying feed solution produced an EFV containing powder with adequate taste-masked properties. EFV drug release from T10, T19 and T21 proved significantly lower compared to the marketed product Stocrin® film-coated tablets, suggesting that these formulations could potentially be associated with better palatability compared to the marketed product that is manipulated (crushed and ground) to enable children to take a daily EFV dose. On the other hand, the use of an ethanol-based solution for preparation of the feed solution did not produce powders with sufficient taste-masking properties. The downfall related to the spray-drying strategy was the overall stability of resulting powders. Visually the powders underwent significant colour and textural changes to such a degree that the powders would not maintain physical integrity for even 1 month upon exposure to either 40°C/75% RH or 30°C/65% RH conditions.

EFV-loaded calcium-alginate beads were successfully produced through ionic gelation with 55 – 69% drug loading efficiency. Thermal and spectroscopic analyses suggest that complete encapsulation of EFV was achieved. The swelling behaviour of the beads proved to be pH-dependent with the lowest and highest degree of swelling respectively observed in pH 1.2 and pH 7.2. Drug dissolution was linked to the swelling of the beads to some degree with the highest EFV dissolution also observed in pH 7.2. Overall, the drug release patterns together with the swelling behaviour of the beads suggest that maximum drug release will occur in the lower duodenum and small intestine. A small amount of drug release occurs in pH 6.8 media, suggesting that some drug release will occur in the oral cavity. These results suggest that sufficient taste-masking was not entirely achieved.

Conclusions:

The use of natural excipients PPI and IN as encapsulating agents proved relatively successful. The use of an aqueous buffered solution for the preparation of the spray-drying feed solution produced an EFV containing powder with adequate taste-masked properties. The downfall related to the spray-drying strategy was the overall stability of resulting powders. Future work may include investigating the use of hydrophobic amino acids like leucine as an additional excipient. This will ideally help improve the physical stability of the spray-dried powders by reducing the particle surface energy.

EFV-loaded calcium-alginate beads have some advantageous properties as an oral dosage form. The ease of manufacturing and patient drug delivery provide some good argument for further optimisation of this technology. The physical and morphological nature of drug loaded microbeads holds great advantage to the paediatric population due to the ease of dose scale up and potential mixing of a single dose with food or milk. Future work may involve investigating the coating of the EFV loaded calcium-alginate beads as a method to further delay the diffusion and release of EFV, especially into a pH 6.8 environment. This may ultimately lead to improved taste-masking, which might render a potentially marketable formulation. Additionally, EFV loaded alginate beads require further characterisation with regards to encapsulation of EFV and the solubility effect of sodium alginate on EFV. Only after further characterisation will more robust conclusions and predictions be able to be made.

Keywords: paediatric drug development; taste-masking; spray-drying; ionic gelation

Acknowledgements

I would like to thank the following people who assisted, supported and trained me in various aspects of this project:

Firstly, I would like to express my deepest appreciation and gratitude to Prof. Aucamp. Thank you for believing in my and giving me the opportunity to be part of your research team. Even though I did not know anything about pharmaceutics you gave me this opportunity. Thank you for allowing me to think and grow as a researcher. I am sincerely grateful for your patience, support and guidance. The completion of my dissertation would not have been possible without you.

I am also extremely grateful to the pharmaceutics research group: Candi, Yves, Geoffrey, Nnamdi, Bola, Jean and Rami. Thank you for your advice, insight and support.

To Mr Kippie, thank you for patiently training me on the analytical equipment and always being a friendly face.

To Prof Samsodien, thank you for your guidance, support and for always having a spare of everything on hand.

To my friends and family, thank you for your love and support throughout this journey.

A special thank you to my fiancé, Armand, for graciously giving me the time, space and support to complete my Master's project.

I would also like to thank Prof Baker and Dr. Waryo from the SensorLab-UWC as part of the Department of Chemistry for performing the contact angle measurements.

The financial assistance of the National Research Foundation (NRF) towards this research is also hereby acknowledged. Opinions expressed and conclusions arrived at, are those of the author and are not necessarily to be attributed to the NRF. (Grant number: MND190614447631)

I also acknowledge and deeply appreciate the Royal Society of the United Kingdom for their financial assistance that made this project possible (Grant number: FL\R1\191360).

Lastly, thank you to the University of the Western Cape and the UWC School of Pharmacy for their facilities, resources and support staff.

LIST OF ABBREVIATIONS

HIV	Human Immunodeficiency Virus
AIDS	Aquired Immunodeficiency Syndrome
ART	Antiretroviral treatment
ARVs	Antiretrovirals
UNAIDS	Joint United Nations Programme on HIV and AIDS
UNICEF	United Nations Children's Fund
WHO	World Health Organisation
COVID-19	Coronavirus disease of 2019
TB	Tuberculosis
NRTI	Nucleoside reverse transcriptase inhibitor
NNRTI	Non-nucleoside reverse transcriptase inhibitor
PI	Protease inhibitor
FI	Fusion inhibitor
AZT	Azidothymidine/Zidovudine
FDA	Federal Drug Administration
DNA	Deoxyribonucleic acid
RNA	Ribonucleic acid
FDC	Fixed dose combination
HAART	Highly active antiretroviral treatment
API	Active pharmaceutical ingredient
ABC+3TC+EFV	Abacavir, lamivudine and efavirenz
ABC+3TC+LPV/r	Abacavir, lamivudine and lopinavir/ritonavir
ABC	Abacavir
LPV/r	Lopinavir/ritonavir
NVP	Nevaripine
3TC	Lamivudine
RAL	Raltegravir
EFV	Efavirenz
BCS	Biopharmaceutical classification system
TDF	Tenovir disoproxil fumarate
FTC	Emtricitabine
CCR5	Chemokine receptor 5
CYP	Cytochrome P-450 enzyme
DTG	Dolutegravir
PPI	Pea protein isolate
IN	Inulin
SLS	Sodium lauryl sulphate
SA	Sodium alginate
HSM	Hot stage microscopy
TGA	Thermogravimetric analysis
DSC	Differential scanning calorimetry
EI	Efavirenz and inulin physical mixture
EP	Efavirenz and pea protein isolate physical mixture
EPI	Efavirenz, inulin and pea protein isolate physical mixture
SEM	Scanning electron microscopy
PXRD	Powder X-ray diffraction
FT-IR	Fourier transform infrared spectroscopy

GRAS	Generally recognised as safe
pKa	Negative log base ten of the acid dissociation constant (Ka value)
DVS	Dynamic vapour sorption
RH	Relative humidity
HPLC	High performance liquid chromatography
RSD	Relative standard deviation

LIST OF FIGURES

LIST OF TABLES

LIST OF EQUATIONS

Table of Contents

CHAPTER 1

The human immunodeficiency virus in paediatric populations

1.1 Introduction

Infection with the human immunodeficiency virus (HIV) is a chronic viral infection that causes significant and progressive immune depletion. Ultimately, when untreated, this infection results in the development of acquired immunodeficiency syndrome (AIDS) (Fauci, 1988). To date, the global health sector has achieved many and significant successes in the prevention and treatment of HIV/AIDS, yet it remains a major global health issue.

Paediatric HIV is considered a neglected disease by many due to the slow development and research of antiretrovirals (ARVs) suitable to be administered to the paediatric population (Lee et al., 2016; Van Riet-Nales et al., 2017). Currently, the two main problems associated with the effective treatment of paediatric HIV are the limited number of ARVs developed and approved for paediatric use and low patient compliance due to the lack of 'child-friendly' dosage forms (Cram et al., 2009; Dubrocq, Rakhmanina & Phelps, 2017). It is essential that paediatric medicines are formulated to best suit the age, physiologic condition, and treatment requirements of children. This chapter will provide an overview of HIV/AIDS in Africa and how this pandemic in Africa compares with the global statistics. Additionally, the current available ARVs will be explored in relation to the treatment of paediatric HIV-positive patients, highlighting critical shortcomings and challenges.

1.2 HIV/AIDS in Africa and beyond

It has been over 40 years since the discovery of HIV/AIDS and yet, to this day, it remains one of the most devastating pandemics in sub-Saharan Africa. Today, no region in the world is without cases of HIV/AIDS, illustrating the magnitude of the burden this disease is causing worldwide (**Figure 1.1**). Despite sub-Saharan Africa continuing to bear the majority burden of HIV-1 infections, during the last decade more and more countries have started to report stabilisation and decline in prevalence (Simon, Ho & Karim, 2006). This can be attributed to major advances in drug development and successful prevention efforts by government and education systems to promote protective sex while combating vertical transmission, multi-partner sex, and needle sharing among drug users (Gregson et al., 2006; Simon, Ho & Karim, 2006).

Despite these efforts and medical advances, there are still a significantly high number of new HIV infections and AIDS-related deaths occurring annually, thus necessitating the need for further research (Becerra, Bildstein & Gach, 2016). At the end of 2020, a total of 37.7 million people were living with HIV/AIDS globally, while 1.5 million people became newly infected and roughly 900 000 were living in the African region (UNAIDS, 2021a). This, in comparison with 2014 statistics where 2 million people were newly infected with HIV globally, of which 1.4

million people were living in the African region, shows that steady progress is being made with this pandemic (UNAIDS, 2015). However, despite the lower incidence rates Africa still consistently shows at least a five-fold higher incidence rate for new HIV infections, when compared to other regions.

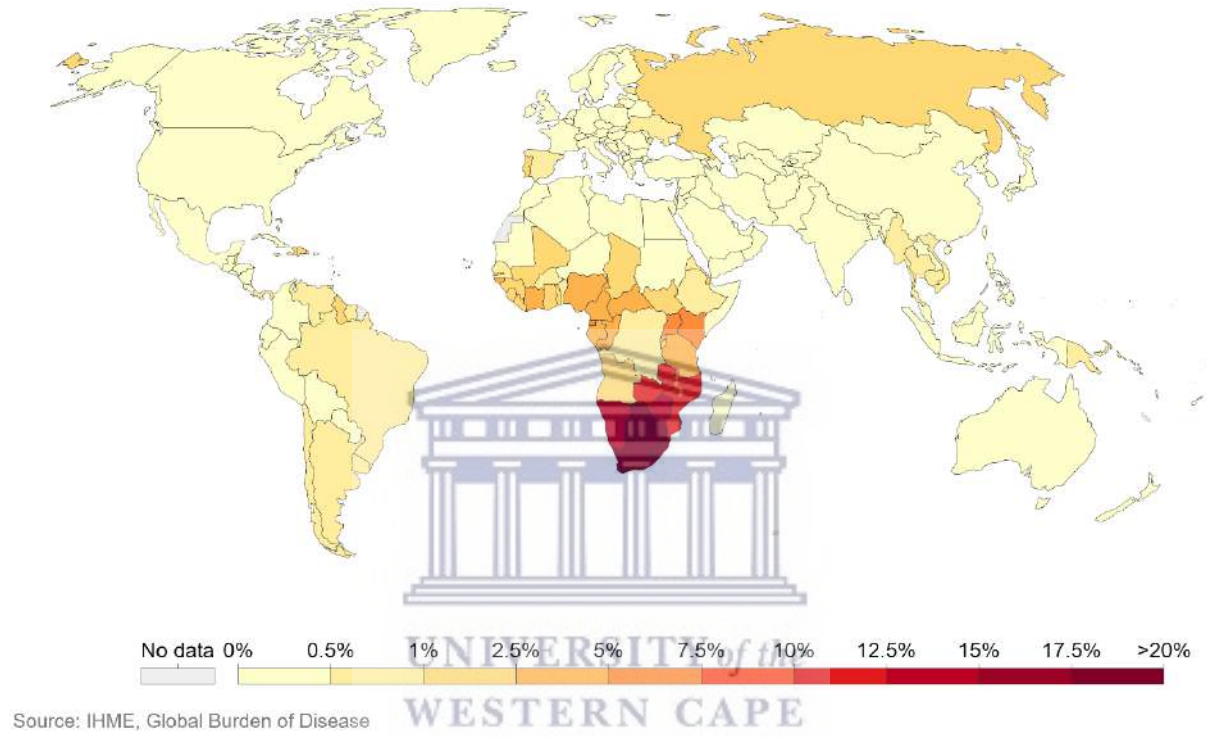

Figure 1.1: Heat map showing the world distribution and share of the population infected with HIV in 2017. No region in the world is untouched by the HIV/AIDS epidemic. Dark red regions show that the biggest HIV burden is carried by sub-Saharan Africa (Adapted from Roser & Ritchie, (2019)).

From UNAIDS, UNICEF, and WHO health reports it is undeniably clear that Africa is central to the global HIV/AIDS crisis (**Figure 1.1**) (UNAIDS, 2017; World Health Organisation, 2018; UNICEF, 2020a). Therefore, research that is focused on optimising prevention programs, drug development as well as strengthening support systems specifically for the African region may prove to be particularly valuable in the fight against HIV/AIDS. This strategy may sound relatively obvious but remains complicated since African regions present with various unique challenges associated with geographic, social, cultural, and economic factors. The majority of people living with HIV/AIDS reside in low-income and rural areas where access to transport, medical and general services are very limited (World Health Organisation, 2018).

Inaccessibility to care and treatment, weak economies, poor infrastructure, extreme climate conditions, and insufficient political leadership are a few examples of typical challenges faced by African countries which also impact the fight against HIV/AIDS.

The development of innovative, scalable, sustainable, cost-effective, and “Africa-friendly” ARV dosage forms is crucial to improve the course of the disease. The development of pharmaceutical solutions to aid in protecting ARVs against the harsh African climatic conditions should also be considered as an important aspect. Since climatic conditions are different in the various regions of the world, special consideration should be made during the development of medicines aimed at the African market. This becomes important when we consider the fact that developing African countries do not necessarily have sufficient resources to manufacture essential pharmaceutical products. As a result, essential drugs are mostly imported into developing countries. The development and manufacturing of these pharmaceutical drugs in regions other than the target region should be done in such a manner that product stability is optimised for the climatic conditions of the target regions.

One of the most notable impacts of HIV/AIDS, besides the obvious human cost, is on the economy of Africa and subsequently its ability to handle the pandemic (Piot et al., 2001; Dixon, McDonald & Roberts, 2002). HIV/AIDS-stricken countries have subsequently reduced labor forces, productivity, and exports (Dixon, McDonald & Roberts, 2002; Resch et al., 2011). Due to subsequent increases in imports as a result of reduced local productivity, products become more expensive and populations poorer (Dixon, McDonald & Roberts, 2002; Tavares & Tang, 2011). This seemingly never-ending loop of events leads to a constant need for resources in Africa. External, international sources of funds, medicines, and services are needed to continue and strengthen the fight against HIV/AIDS. (Banda, 2013; Banda, Wangwe & Macintosh, 2016).

1.2.1 Potential impact of COVID-19 pandemic on the HIV/AIDS fight

The COVID-19 pandemic has unarguably challenged the global health sector significantly. At the time of writing, this infectious viral disease affected an estimated 210 million people worldwide and resulted in the death of 4.4 million people. **Figure 1.2** depicts the estimated annual number of deaths recorded for 2016, 2018, and 2020, respectively, due to HIV/AIDS, Tuberculosis (TB), and malaria. However devastating the COVID-19 disease currently is, it should not undermine the seriousness of long-standing diseases such as HIV, TB, and malaria of which the cumulative mortality average to more than 2.5 million people every year (**Figure 1.2**).

Irrespective of the relative devastation of the COVID-19 pandemic, the outbreak of this virus was, and still is, associated with a lot of uncertainty and panic within the health systems, governments as well as in the general public. In South Africa and many other countries, this panic led to a total shutdown and subsequently the redirection of medical resources to fight the COVID-19 pandemic. The redirection of medical supplies and staff to COVID-19 hotspots left existing health issues such as HIV, TB, and malaria exposed and neglected (Amimo, Lambert & Magit, 2020; UNICEF, 2020a). Developing countries generally have vulnerable economies which means that they can barely fight the problems they had before the COVID-19 pandemic. With the outbreak of this pandemic, additional pressure has been placed on the economies and health systems within these countries. Due to a lack of sufficient resources, these countries would have had to decide whether to prioritise COVID-19, which most countries did. This means that fewer resources were available for other health issues and this impacted the distribution and supply of medicines such as ARVs (UNICEF, 2020a). According to the UNAIDS 2021 global AIDS update report, many countries experienced service interruptions during 2020 with regards to HIV/AIDS testing and treatment initiations. Theoretically, this could also have included understaffed and understocked clinics during COVID-19 related lockdowns. Many countries reported declines in HIV testing, diagnosis referrals, and treatment initiations (UNAIDS, 2021b). The delay and interruption of treatment regimens could very possibly have short and long-term detrimental effects such as increased HIV/AIDS-related deaths and more resistant HIV strains.

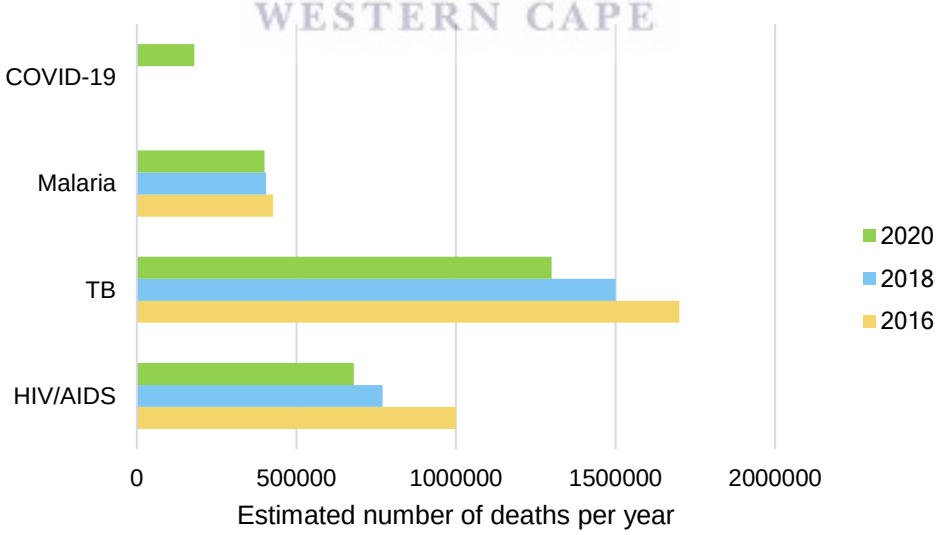

Figure 1.2: Estimated number of deaths per year as a result of HIV/AIDS, TB, malaria, and COVID-19. Data is given for 2016, 2018, and 2020, except for COVID-19 where data is given only for 2020. (UNAIDS, 2017, 2018, 2019; World Health Organization, 2017, 2019; World Health Organisation, 2021).

However, since the COVID-19 pandemic is not over yet data has not been collected from all countries and regions. When the focus is back on HIV/AIDS and other diseases patients will potentially need their treatment regimens to be re-evaluated and intensified in cases where resistance might have emerged. The COVID-19 pandemic has however also resulted in the development and growth of the world health systems. For example, the adoption of health care innovations such as multi-month dispensing of medications, self-testing, medicine delivery services, and the development and use of virtual platforms for support and information has been accelerated by the COVID-19 pandemic (UNAIDS, 2021b).

1.3 Antiretroviral drugs (ARVs)

1.3.1 Discovery and development of ARVs

ARVs are drugs used to treat a retroviral infection; in particular HIV. The global distribution/accessibility of antiretroviral treatment (ART) to people living with HIV has increased significantly in the last decade (World Health Organization, 2016; UNAIDS, 2017). According to World Health Organization (WHO) statistics, only 40% of those living with HIV in 2016 were receiving antiretroviral therapy while in 2020 this number had increased to 73%. The benefits of ART used to be almost exclusively restricted to industrialised countries, but global efforts have resulted in great strides being achieved in extending these benefits to resource-limited settings where >90% of infected individuals live (Lodha & Manglani, 2012) (**Figure 1.3**). But alas, despite these major efforts, according to the UNAIDS statistics, only 62% of those living with HIV in 2018 were actually receiving ART (UNAIDS, 2019).

The overarching purpose of research and drug development in the fight against HIV remains to cure the disease, however, up until this point in time, no cure has been found. However, drugs exist that suppress the viral load by targeting viral entry, reverse transcriptase activity, genomic integration, and viral maturation ultimately meaning that people can live long and healthy lives even with HIV/AIDS (Zhan et al., 2016). ARVs are commonly divided into 6 classes based on their mechanisms of action (Anabwani, Woldetsadik & Kline, 2005; Zhan et al., 2016). As shown in **Figure 1.4** each class has a unique mode of function targeting different stages of the viral life cycle.

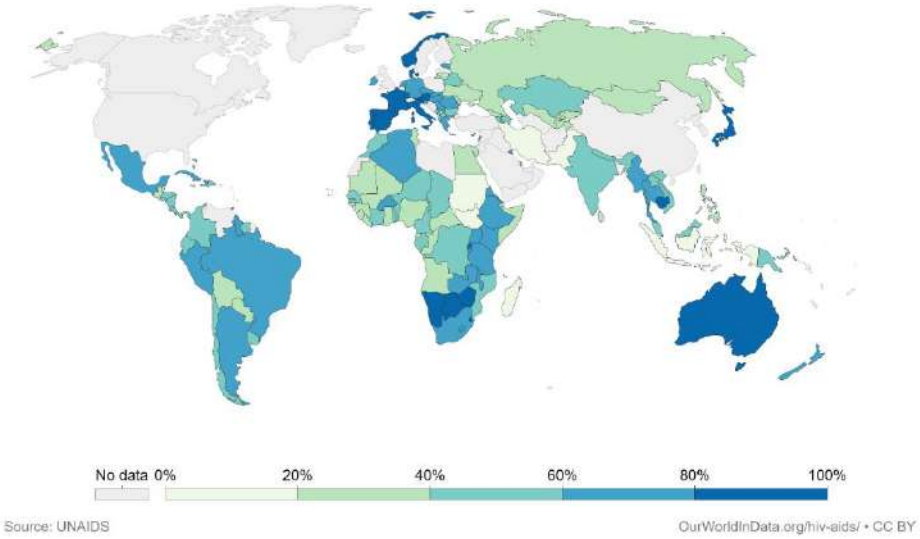

Figure 1.3: World distribution heat map showing the share of people living with HIV who were receiving ART in 2017, shown as the percentage of people living with HIV. Data shown includes several ARV medicines used to suppress viral replication in the body. (Adapted from: (Roser & Ritchie, 2019))

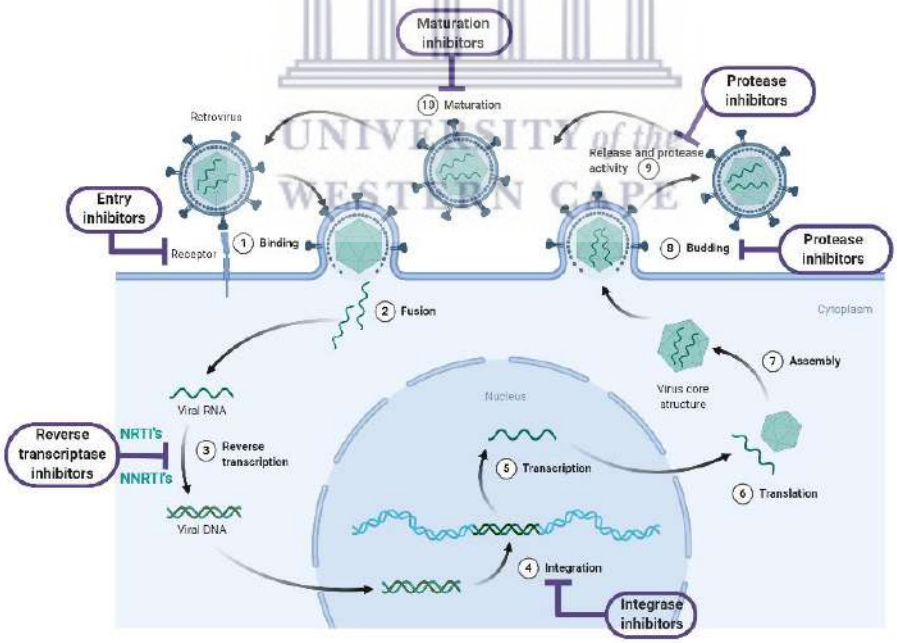

Figure 1.4: Schematic showing the simplified life cycle of the human immunodeficiency virus (HIV) and the points of target for the different classes of the current antiretroviral drugs (ARV). [Prepared using BioRender.com]

The first ARV, azidothymidine (AZT), was discovered in 1985 and became FDA approved in 1987 (Esté & Cihlar, 2010). Still used today, AZT, also called zidovudine, acts to terminate the

synthesis of proviral DNA from the viral RNA template thereby inhibiting viral replication (Hirsch, 1988). The development of AZT and other early nucleoside reverse transcriptase inhibitors showed that the treatment of HIV is possible, and these drugs paved the way for the discovery and development of new generations of ARV drugs. Fast-tracked, 35 years further, massive advances have been made in ARV research and development with about 30 FDA-approved ARVs available on the market as well as multiple fixed-dose combination (FDC) therapies, either approved or in the pipeline towards approval. While single-drug therapy led to initial improvement in the clinical and immunological status of patients, the effects could not be sustained due to the rapid development of viral resistance. This is a result of the short life-cycle of the virus and the high error rate during reverse transcription causing the virus to mutate rapidly, resulting in high genetic variability of the virus and the development of drug resistance (Lodha & Manglani, 2012). The major turning point in ART was the introduction of highly active antiretroviral therapy (HAART) in the late 1990s; a potent combination therapy strategy where three or more active agents are used together. HAART clinical trials have shown promising outcomes in reducing morbidity and mortality while also reducing drug resistance compared to monotherapy (Esté & Cihlar, 2010).

The advent of ARV treatment has led to huge successes in the prevention and treatment of HIV/AIDS, especially during the last decade. In eastern and southern Africa the number of AIDS-related deaths has dropped by 49% between 2010 and 2019, reflecting the effect of scaled-up ARV therapy in these regions (UNAIDS, 2020). In addition, there has been a 38% reduction in the number of new HIV infections in eastern and southern Africa between 2010 and 2019. Other regions of the world also showed significant reductions in AIDS-related deaths and new HIV infections for this period, but to a lesser extent (UNAIDS, 2020). Among children, the number of AIDS-related deaths has also significantly declined between 2010 (240 000 deaths) and 2019 (110 000 deaths) reflecting the increased access to paediatric ART (UNICEF, 2020a).

1.3.2 Commonly prescribed ARVs and their limitations

Despite major advances, as highlighted in preceding paragraphs some of the earliest challenges associated with ARV development and therapy remain today. Treatment adherence, long-term drug toxicity, drug resistance, and tolerability of ARVs remain some of the major treatment obstacles across the range of ARVs (Gulick, 2003).

The effectiveness of ARV therapy mainly depends on patient compliance and adherence (Dahourou & Leroy, 2017). According to the WHO adherence project, adherence is defined

as “the extent to which a person’s behaviour – taking medication, following a diet, and/or executing lifestyle changes, corresponds with agreed recommendations from a health care provider” (World Health Organisation, 2003). In the treatment of HIV/AIDS, adherence to therapy typically varies between 37 - 83% and depends greatly on the specific drug as well as demographic characteristics of patient populations (World Health Organisation, 2003). Individual-level factors that influence adherence include the complexity of treatment regimens, palatability, and side effects (Murphy et al., 2004; Mills et al., 2006; Kagee et al., 2011). For example, adherence decreases as the number of tablets or capsules and doses per day increase (Esté & Cihlar, 2010). Poor adherence represents a significant challenge to population health initiatives where treatment success is determined primarily by adherence to long-term therapies – such as HIV/AIDS. Poor adherence to ARV regimens results in suboptimal therapeutic drug levels, which in turn can lead to the emergence of viral drug resistance (Anabwani, Woldetsadik & Kline, 2005). One potential strategy that has been previously identified to improve adherence is by simplifying drug treatment regimens.

The drug variety available today enables the use of combination drug therapy for reduced risk of resistance development and increased potency. Despite the availability of various drug options, there is no ARV on the market that comes without some adverse effect(s), as outlined in **Table 1.1**. These range from nausea, rashes, and anaemia to more severe adverse effects such as myopathy, pancreatitis, and renal impairment (Warnke, Barreto & Temesgen, 2007). Any associated adverse effects have a negative impact on patient compliance as they affect the patient’s quality of life and willingness to adhere to treatment (Psichogiou et al., 2017).

1.3.3 Paediatric dosage forms and ART

i. Paediatric pharmaceutical dosage forms

The development of drug formulations that are appropriate for children can present significant challenges. The paediatric population is a heterogeneous group consisting of different developmental stages and age groups as follows: neonates (0 – 1 month), infants (1 month – 2 years), children (2 – 12 years), and adolescents (12 – 16 years). Each of these groups has unique needs, including those related to pharmaceutical dosage forms (Nunn & Williams, 2005). Apart from ensuring the correct dosage, these formulations should be “child-friendly” to enable children to willingly take them. The oral drug administration route is the most frequently used in adults as well as children. However, oral drug administration poses additional development challenges as these dosage forms have to allow ease of swallowing and acceptable palatability (Sam et al., 2012). In addition, factors such as weight and stages of growth and development dictate treatment options. (King et al., 2002). Children are

characterised by height and weight increases until beyond adolescence, as well as by changes in the size and functionality of their organs. Consequently, a dose might have to be adapted as children grow and develop. Considering these mentioned factors it is clear why drug formulations, allowing the possibility of flexible dosing, are preferred among the paediatric population (Bastiaans, 2016). It should furthermore be highlighted that when considering paediatric dosage forms the combination of these factors, rather than each factor alone should be taken into account.

Table 1.1: Potential adverse effects associated with ten of the most common ARVs prescribed and used by HIV/AIDS patients. Table was compiled using information from https://aidsinfo.nih.gov/drugs**.**

ARV	ARV Class	Possible adverse drug effect
Lamivudine	NRTI	Associated with Hepatitis B viral resistance emergence
Emtricitabine	NRTI	Side effects (ex. dizziness, liver problems)
Efavirenz	NNRTI	High risk for birth defects Neuropsychiatric side effects
Nevirapine	NNRTI	Hepatotoxicity Low genetic barrier
Ritonavir	PI	Drug-drug interactions (ex. Etravirine, atorvastatin and oxycodone)
Raltegravir	Integrase Inhibitor	Side effects (ex. nausea, muscle pain) Low genetic barrier
Lopinavir	Protease inhibitor	Liver problems Pancreatitis Skin rash
Tipranavir	PI	Drug-drug interactions (ex. Aspirin, sofosbuvir and ritonavir)
Tenovir disoproxil fumarate	NRTI	Drug-drug interactions (ex. Adefovir, didanosine and ritonavir)
Dolutegravir	Integrase inhibitor	Allergic reactions Liver diseases and abnormalities

Oral drug dosage forms include solid and liquid dosage forms, each of which has advantages and disadvantages (Krause & Breitkreutz, 2008; Ranmal, Cram & Tuleu, 2016). Various aspects determine acceptability among children, such as tablet size, daily dose, and drug palatability. As a result paediatric formulations primarily involve liquids or low-dose dispersible formulations, which are easy to swallow and allow for easy dose alterations (Walsh et al., 2018). Liquid formulations, however, contain excipients, that can be toxic to newborns. These formulations might also require the administration of larger volumes thus affecting the packaging size since liquid formulations are often packaged in glass bottles in relatively large volumes (Bastiaans, 2016). Additionally, these formulations often require cool and dry storage conditions which means special transportation needs and final at-user storage conditions are required, typically to maintain the required cold chain. Solvents such as ethanol and propylene glycol are often used in drug formulation to achieve adequate drug solubility despite their possible adverse effects in children. Other excipients, potentially harmful to this vulnerable population include, certain preservatives and artificial sweeteners (sucrose, aspartame), and colourants (xanthines, tartrazine) (Rouaz et al., 2021).

On the other hand, solid preparations are generally significantly easier to handle, procure and store and therefore, on a global level, preference is given to paediatric dispersible and solid preparations. Additionally, solid preparations exhibit greater chemical and physical stability compared to liquid formulations (Ranmal, Cram & Tuleu, 2016; Walsh et al., 2018). Solid dosage forms do however have their own limitations since many children, depending on age, are unable to swallow whole tablets or capsules. Luckily a variety of more suitable solid dosage forms are available, which include powders, chewable tablets, granules, mini-tablets, sprinkles, and fast dispersing dosage forms (Amirav, 2008; Vanprapar et al., 2010; Preis, 2015; Salem et al., 2015; Giralt et al., 2017). These dosage forms have shown preference and superiority above their liquid dosage form counterparts as illustrated by the granular dosage form of the asthma drug montelukast (Singulair®, Merck) and the sprinkle dosage form of the antiepileptic drug divalproex sodium (Depakote®, AbbVie). Singulair® oral granules have been associated with improved paediatric patient compliance when compared to the alternative inhalable drug dosage form (Amirav, 2008). Similarly, Depakote® sprinkles exhibit prolonged absorption and subsequently require less frequent dosing compared to the syrup formulation of the same active pharmaceutical ingredient (API). The sprinkles also have improved palatability and this dosage form has shown improved paediatric patient compliance (Cloyd et al., 1992). The paediatric success of these solid dosage forms is linked to their small size, ease of administration, and treatment efficiency. Despite these successes in paediatric drug formulation, not all diseases benefit equally from these effective dosage forms. Some diseases

such as HIV, TB, and malaria are unevenly concentrated in underdeveloped countries where the geographic, social, and economic factors form additional hurdles to the success of these drug formulations. Subsequently, pharmaceutical development of child-friendly solid dosage forms for these diseases has lagged behind. Barriers that have delaying effects on the development of new paediatric formulations include poor incentives for investment in the paediatric drug market and the magnitude of physical, social, and pharmacokinetic factors that need consideration during development (Schlatter, Deathe & Vreeman, 2016). Another major consideration relating to paediatric drug development is the process of clinical trials. Clinical trials are required for the approval to introduce a drug into the market and are often lengthy and expensive. Clinical trials involving children are a lot stricter and the regulations more intense than those involving adults and sometimes this results in companies opting for an adult-based clinical trial even for paediatric medications (Conroy et al., 2000). The data collected is then extrapolated to the paediatric population. Ideally, all paediatric medications should go through paediatric clinical trials but the cost and time associated with these processes make it difficult. It is imperative that the design and choice of drug dosage forms also consider these factors to ensure the success of paediatric drugs even in developing countries.

ii. Adherence among paediatric HIV patients

As already mentioned, adherence is a crucial success factor for anyone on ART as almost perfect compliance to treatment is required. In children, however, achieving adherence poses special challenges. The management of paediatric ART involves interaction between children, their caregivers and healthcare providers (Nahirya-Ntege et al., 2012). These challenges include that infants and younger children are dependent on others for drug administration and as highlighted, child-friendly formulations are often not available. Additionally, developmental and psychological factors that are associated with growth and development pose additional problems as treatment regimens need to be re-evaluated and adjusted as children age and grow (Anabwani, Woldetsadik & Kline, 2005).

Studies have found that a common factor limiting adherence in the paediatric population is drug palatability (Dubrocq, Rakhmanina & Phelps, 2017) since often the taste of a drug is still not considered when nominating new compounds for drug development (Cram et al., 2009). However, compared to adults, children have a heightened preference for sweet-tasting and greater rejection of bitter-tasting foods and oral substances (Dubrocq, Rakhmanina & Phelps, 2017). Children infected with HIV often fail to adhere to their treatment because of poor drug taste. Studies have shown that up to 14% of children report problems with palatability while at

least 6% discontinue ART on a particular drug because of poor palatability (Lin et al., 2011). Among all the factors reported influencing adherence, up to 81% of caregivers cited better palatability as the most helpful intervention to increase ARV therapy adherence in children (Lin et al., 2011; Nahirya-Ntege et al., 2012). Improved taste of ARV drugs in children has proven to lead to better adherence, resulting in better clinical outcomes and reduced family stress (Chiappetta, Hocht & Sosnik, 2010; Lin et al., 2011). Improving the palatability of ARVs is crucial for increasing paediatric patient compliance and subsequently also ART effectiveness. Further limitations to paediatric ARV treatment are the emerging toxicities associated with ART, along with the lack of pharmacokinetic and safety data in children and overcoming drug resistance (Krause & Breitkreutz, 2008).

iii. Paediatric ARV status and challenges

Paediatric HIV is considered a neglected disease by many since research and development of paediatric ARVs has been slow due to ethical, economic, and practical reasons (Lee et al., 2016; Intini, Bonifazi & Migliaccio, 2019). The ethical and economic challenges associated with drug trials in children hinder the development of new paediatric drugs. Furthermore, the development of special dosage forms for the paediatric population is not considered as financially rewarding to the pharmaceutical industry compared to the development of adult medicines (Penazzato et al., 2018). This is because the paediatric drug market is only a fraction of the adult drug market size (Lee et al., 2016; Penazzato et al., 2018). Additionally, only 25% of ARVs approved for adults are also approved for treating children younger than 2 years, resulting in limited paediatric therapy options (Waalewijn et al., 2019). This is an unacceptable way forward as an estimated 1.7 million HIV patients are children, most of whom live in low- and middle-income countries (UNAIDS, 2019). Globally, an estimated 919 000 children (aged 0 – 14 years) received ART in 2016, only about 43% of all children living with HIV (UNAIDS, 2017). It is crucial that ART is available, in its full capacity, to the paediatric population as early initiation increases the chances of maximal viral suppression while reducing the viral reservoir to allow for normal development and growth in children (Waalewijn et al., 2019). With our current knowledge and treatment options, HIV-infected children can expect to live a full adult life, but with the necessity to continue lifelong treatment (Bastiaans, 2016). The South African National Department of Health is currently recommending that all HIV-infected children are initiated on ART independent of their immune status or the presence of overt disease symptoms (South African National Department of Health, 2019).

It is no secret that, in many ways, children are very different from adults and so children should also be treated differently with regards to drug and pharmaceutical dosage form development.

Compared to adults, disease progression in children is significantly faster and in the absence of intervention the mortality rate reaches up to 50% for HIV-infected children before the age of 2 years (Lodha & Manglani, 2012; Dahourou & Leroy, 2017). The pharmacokinetic and pharmacodynamic properties of drugs influence the choices of drug therapy in children (King et al., 2002). Drug metabolism in children is significantly different from adult drug metabolism as it is subject to physiological factors. Several pharmacokinetic and pharmacodynamic drug properties, such as absorption, distribution, metabolism, and excretion, are influenced by age-related factors such as body composition and enzyme bioavailability (Ivanovska et al., 2014). ARVs are no exception, but still, children are often prescribed ARVs designed for the adult population. It is imperative that pharmaceutical companies understand the significance of developmental changes for the pharmacokinetics of ARVs, in order to optimise treatment strategies, minimise toxicities and provide the least invasive regimens to paediatric patients (Ivanovska et al., 2014). In this regard, there has been a universal drive to develop better paediatric ARV dosage forms. In South Africa, no fixed guidelines exist on paediatric ARV dosage regimens for infants weighing < 3 kg as it requires the input of a medical professional to make individual-level recommendations. For children weighing between 3 - 40 kg, weight-dependent dosing regimens are described in the 2019 ART Clinical Guidelines compiled by the National Department of Health (South African National Department of Health, 2019) (**Table 1.2**). For all individuals weighing more than 40 kg, standard adult dosage regimens are recommended (**Table 1.2**). ARVs are often formulated so that the same drug exists in the same dosage form type but differs in the incorporated drug dose. This allows for the relatively simple tailoring of the drug dose, enabling age-related dosage changes. This might seem advantageous but from the recent guidelines, it became apparent that most of the currently available dosage forms do not meet the requirements for easy dose adjustment to obtain suitable paediatric doses (South African National Department of Health, 2019).

Currently, for ARVs, only a few dosage forms are marketed that have been developed with the paediatric population in mind but mostly children must rely on adult dosage forms in the instances where syrup formulations are not available. For example, in the case of a 3-year-old child that cannot swallow a whole tablet, caregivers often take it upon themselves to manipulate the dosage form to render it more suitable for consumption. During this process, the dosage often becomes reduced due to small losses during handling, or in some cases, this can lead to overdose if measurements are not done carefully. Liquid dosage forms have long been the gold standard for paediatric medications and many paediatric ARVs are available in liquid dosage forms due to their relative ease of administration and flexible dosing. These liquids often require cold-chain transport, packaging in big glass bottles, and

refrigerated storage – all of which pose difficulties in most African countries (Musiime et al., 2014). In rural Africa most homes either do not have electricity supply or the supply is erratic and unreliable. Another challenge is the transport of large volumes from the clinic to the homes. In large parts of Africa, the parents or caregivers usually live in rural settings, meaning that they must walk long distances to and from the clinic while carrying large volumes of liquid formulations. For example, take the liquid formulation containing abacavir, lamivudine, lopinavir, and ritonavir, of which a 10 kg child must take 28 mL daily. This equals about 2.5 L every three months, meaning that caregivers have to carry about 17 bottles containing 160 mL each. (Schlatter, Deathe & Vreeman, 2016).

As illustrated in **Table 1.2** the dosage regimens for paediatric ART are numerous and in some cases complex. When considering the first-line paediatric regimens, abacavir, lamivudine and efavirenz (ABC+3TC+EFV) and abacavir, lamivudine and lopinavir/ritonavir (ABC+3TC+LPV/r) one quickly realises that a child sometimes needs to take multiple tablets and/or capsules daily. In cases where FDCs are available these tablets often exist as large dosage forms which are not necessarily suited for swallowing by a young child. Take ABC tablets as an example, these tablets exist either as 60 mg ABC scored tablets or 300 mg unscored tablets. For children weighing between 10 - 15 kg, the option is given to take 12 mL of the oral solution or 240 mg in tablet form. If the only available dosage form is the ABC tablets a child would have to swallow 4 x 60 mg tablets since the 300 mg tablet cannot be scored accurately. The need for a young child to swallow multiple tablets might pose difficulties in getting the child to complete the daily dose as well as adhere to the dosage regimen in the long term.

The large number of paediatric patients who require medication for other conditions, such as TB or malaria further stresses the need for simple ART dosage regimens. Complex dosage regimens as well as those that require multiple tablets/capsules to be taken can negatively affect adherence (Malek et al., 2017). Ideally, the goal should be to minimise the number of different dosage forms patients need to take daily to promote easy and efficient drug administration for adequate patient adherence (Esté & Cihlar, 2010).

Table 1.2: Paediatric and adult dosage regimens compared in relation to the available formulations of a few ARVs commonly prescribed for paediatric use.

ARV drug	Available formulations	Paediatric dosage regimen	Adult dosage regimen
Efavirenz (EFV)	Capsules: 50 mg, 200 mg Tablets: 50 mg, 200 mg, 600 mg FDC tablet: TEE 300/200/600 mg	Avoid if < 10 kg If > 10 kg; 200 mg ONCE daily If > 25 kg; 400 mg ONCE daily	600 mg ONCE daily
Dolutegravir (DTG)	Tablets: 50 mg FDC tablet: TLD 300/300/50 mg	Avoid if < 20 kg If > 20 kg; 50 mg ONCE daily	50 mg ONCE daily
Lopinavir/ritonavir (LPV/r)	Oral solution: 80/20 mg/mL Tablets: 200/50 mg, 100/25 mg	300/75 mg/ m^2 LPV/r TWICE daily If < 10 kg: 100 mg TWICE daily If > 10 kg: 200 mg TWICE daily If > 25 kg: 300 mg TWICE daily If > 30 kg: 400 mg TWICE daily	400 mg TWICE daily
Abacavir (ABC)	Oral solution: 20 mg/mL Tablets: 60 mg (scored, dispersible), 300 mg (not scored) FDC: ABC/3TC 600/300 mg	3,5 mL per 5 kg TWICE daily If ≤ 25 kg: 300 mg ONCE daily OR If ≥ 25 kg: 300 mg TWICE daily 1 x FDC ONCE daily	300 mg TWICE daily OR 600 mg ONCE daily
Nevirapine	Tablets: 200 mg; 400 mg Oral suspension: 10 mg/mL	Age < 1 month: 2 - 10 mg/kg per dose TWICE daily Age > 1 month: 20 – 40 mg per day	200 mg ONCE daily for 14 days, then 200 mg TWICE daily

ARV drug	Available formulations	Paediatric dosage regimen	Adult dosage regimen
Zidovudine (AZT)	Oral solution: 10 mg/mL	180-240 mg/m²/dose TWICE daily	300 mg TWICE daily
	Tablets: 100 mg, 300 mg (not scored)	If ≤ 14 kg: 100 mg ONCE daily If ≥ 14 kg: 2 x 100 mg AM 1 x 100 mg PM If ≥ 20 kg: 2 x 100 mg TWICE daily If ≥ 25 kg: 300 mg TWICE daily	
	FDC: AZT/3TC 300/150 mg	If ≥ 25 kg: 1 x FDC TWICE daily	
Atazanavir/ritonavir (ATV/r)	Capsules: 150 mg, 200 mg	Avoid if ≤ 15 kg If ≥ 15 kg: 200 mg ONCE daily If ≥ 30 kg: 2 x 150 mg ONCE daily	300 mg ONCE daily
Lamivudine (3TC)	Oral solution: 10 mg/mL	4 mg/kg TWICE daily	300 mg ONCE daily
	Tablets: 150 mg	If ≥ 10 kg: 8 mg/kg ONCE daily	
	FDC tablets: ABC/3TC 600/300 mg TLD 300/300/50 mg	If > 25 kg: 300 mg ONCE daily	

*Note: TLD: tenofovir/lamivudine/dolutegravir; TEE: tenofovir/emtricitabine/efavirenz

iv. Advances in paediatric ART

Even though new HIV infections among children have declined significantly in recent years, there is still a very high number of new HIV infections and AIDS-related deaths occurring each year, necessitating the need for further ARV research (Becerra, Bildstein & Gach, 2016). FDA-approved ARVs for children have been lagging behind those for adults but nevertheless, recent advances are showing promise. These include sprinkles, tablets with multiple break lines, chewable tablets, dispersible tablets, liquids, and powders. For example, fixed-dose combination (FDC) tablets containing zidovudine and lamivudine developed by Kayitare *et al.* (2009) contain three essential features required for a paediatric HIV formulation, namely: flexibility in dosing, fast disintegration, and high bioavailability (Kayitare et al., 2009). Rectangular tablets were developed with multiple break lines on both sides to allow for flexible and adequate dosing. These FDC tablets are available on the market and are reported to be well tolerated but still with some drug-associated toxicities. It is worthy to note that initial tolerability studies were done among children in Europe and Thailand, countries with a very different economy than most African countries. These FDC tablets require clean water or another liquid in order to be administered which may affect the success of this dosage form in Africa. The WHO has presented a list of optimal drug formulations for paediatric drug formulations that fulfill certain defined criteria to guide paediatric ARV programs. These criteria relate to dosing flexibility, approval by a quality assurance body, user-friendliness, optimised supply chain, and comparative cost (UNICEF, 2020b). **Table 1.3** summarises the current first-line paediatric ART and related dosage forms considered as optimal by the WHO.

Over the last decade, the pharmaceutical manufacturer, Cipla developed a co-formulated sprinkle formulation of lopinavir/ritonavir (LVP/r). This novel formulation was developed in response to the longstanding need and demand for an easy to administer, heat-stable paediatric ARV formulation. From the available information, it appears that melt extrusion technology was employed resulting in a formulation containing 40/10 mg LPV/r pellets per capsule (Clayden, 2012; World Health Organization & UNICEF, 2015). Musiime et al. (2014) performed a comparative bioavailability study on this formulation. This dosage form holds promise in the African context as it does not require cold-chain transport or special storage conditions and it can be administered with any food or liquid.

Powders as oral dosage forms have also been explored for the paediatric ARV market. Powder dosage forms can be sprinkled on food or suspended in liquids for easy administration making this a viable dosage form for children of almost any age (Salem et al., 2015).

Additionally, no refrigerated transport or storage is required. More simple transport and storage requirements render this dosage form full of potential in the African context.

Table 1.3: Paediatric ARV dosage forms forming the first-line ART regimens as accepted by the WHO.

ARV drug	Dosage form	Positive attributes	Negative attributes
LPV/r	Tablet	Stable	Dose adjustment
NVP	Oral solution Dispersible scored tablet	Dose adjustment	Supply chain Palatability
AZT/3TC	Dispersible scored tablet	Dose adjustment	Palatability
ABC/3TC	Dispersible scored tablet	Dose adjustment	Palatability
RAL	Chewable scored tablet	Food/drink independent	Twice daily dosing
EFV	Scored tablets	Dose adjustment	Palatability

*Adapted from UNICEF (2020)

*Note: LPV/r: Lopinavir/ritonavir; NVP: Nevirapine; AZT: Azidothymidine; 3TC: Lamivudine ABC: Abacavir; RAL: Raltegravir; EFV: Efavirenz

1.4 HIV co-infections

As devastating as HIV infection is, it is unfortunately sometimes accompanied by other deadly conditions such as TB, malaria, and hepatitis B. About 13% of people living with TB are also living with HIV and consequently, these patients are required to take both TB and HIV medication (Rabie et al., 2015). The need to take multiple medications can lead to or contribute to poor adherence among patients especially if treatment regimens become complex. To promote better adherence to ARVs, and other medications, simple dosage regimens are essential (Malek et al., 2017). More than 70% of patients with HIV/TB coinfections live in sub-Saharan Africa, contributing to the unique set of factors that require consideration in drug development and distribution initiatives to fight these pandemics on the African continent (UNAIDS, 2018). Data suggest that the increase in ART access has been associated with a decline in TB risk among HIV-infected individuals. As ART access worldwide has increased from 46% in 2015 to 73% in 2020, the TB incidence in HIV-infected persons decreased by 9% between 2015 and 2020 (UNAIDS, 2016; World Health Organization, 2020). The need to address TB co-morbidities in HIV-infected children is further exemplified by the observation

that early infancy poses a heightened TB infection risk among HIV-infected children (Rabie et al., 2015). This highlights the importance of further drug research and development aimed at ARVs and TB medications that are compatible and safe with each other.

1.5. The era of personalised medicine for paediatrics

Personalised medicine is an emerging and evolving field of health care where the unique clinical, genetic, genomic and environmental information of each patient is used to optimise medical care at an individual level. This allows for maximising the probability of positive patient response while reducing the risk of adverse effects. The reasoning that underlines personalised medicine is based on the fact that genetic, genomic, and environmental variation found among humans result in variation in the response to medications (Chan & Ginsburg, 2011). One particular example is the liver metabolism cytochrome P450 enzymes which represent the most common route of drug elimination. Within this family of enzymes, there are both fast- and slow-metabolising variants and these variants are associated with under- and over-dosing of drugs when not considered prior to determining dosage regimens (Rodriguez-Novoa et al., 2005; Wyen et al., 2008; Cabrera et al., 2009).

Building computer-based medicine/disease models hold a very interesting and promising prospective for personalised health care. In recent years there have been attempts to construct mathematical and mechanistic models for complex diseases such as HIV/AIDS (Prague, Commenges & Thiébaut, 2013; Attarian & Tran, 2017). These models are computer-based and the idea is that a model predicts certain outcomes given the data regarding a particular disease, drug, or patient. When considering the already mentioned multitude of factors that can affect the adherence, efficiency and overall patient experience of ART, the modeling of HIV disease and ART patient response can be a very insightful and valuable tool to have. Furthermore, a model like this potentially has the power to predict patient response to ART at an individual level. To develop a model like this historic information about the type of ARV, viral mutations, patient genetics, patient compliance, drug pharmacokinetics/pharmacodynamics, patient socio-economy, and geography would need to be collected and incorporated into the model's "brain" as possible variables (Prague, Commenges & Thiébaut, 2013). This model can then use the combination of factors that is assumed to determine the patient response in order to predict future patient events given certain facts about a drug or a patient. Africa is in a prime position to pioneer advances in the field of personalised medicine. The genetic diversity in Africa is higher than in any other continent making it the ideal system to study in order to develop mathematical models (Campbell & Tishkoff, 2008; Pereira et al., 2021). Additionally, Africa faces very unique and

extreme challenges. By studying and incorporating these factors into models we can create more robust and accurate models. This is definitely no easy task, as each variable factor and condition that needs to be accounted for makes developing a model more complex.

It is obvious that the benefit of an ART model can be extended to everyone affected by HIV. However, it is possible that the paediatric population may benefit even more than the adult population. The paediatric population is generally more unpredictable as a result of more variables as highlighted in paragraph 1.3.3 (ii). Considering this, the inclusion of data from the paediatric population into the development of disease/medicine models can potentially lead to even more robust models with greater prediction power. On the other hand, because of the unique properties of the paediatric population, it may also be beneficial to develop a separate paediatric model which may deliver more accurate and relevant predictions specifically aimed at children.

1.6 Relevance and proposed impact of the current study

As illustrated in the above sections, a significant gap exists in the development of child-friendly dosage forms. This detrimentally affects paediatric patient compliance, especially in the treatment of debilitating diseases such as HIV infection. EFV is an extremely bitter-tasting drug, known to cause “burning-mouth” syndrome and therefore paediatric patient compliance related to EFV dosage forms has generally proven low partly due to poor palatability. In the current study, we propose to make EFV, more child-friendly by means of taste masking the drug through microencapsulation. This study explored two different microencapsulation techniques and the potential to obtain taste-masked EFV-loaded microcapsules which could potentially be furthered to paediatric dosage form development.

1.7 Conclusion

This chapter provided the context and challenges that several health systems, especially those in Africa are dealing with in regards to the treatment of paediatric HIV-infected patients. The challenge of providing acceptable dosage forms, specifically aimed at treating children has been highlighted. Although this study will focus on the development of a prototype child-friendly dosage form containing an ARV and that being said, only a single first-line ARV, efavirenz, it is envisioned that this study will provide a foundation for future innovation in the area of paediatric dosage form development. In this thesis, the focus will be on the taste-masking strategies for poorly palatable drugs. In order to design and formulate a suitable paediatric dosage form to address some of the adherence issues highlighted in previous

paragraphs, it is imperative to perform complete pre-formulation and formulation studies. The first step in these types of studies is to understand the solid-state chemistry of compounds as well as the processes involved. The subsequent chapters will emphasise these aspects.

1.8 References

Amimo, F., Lambert, B. & Magit, A. 2020. What does the COVID-19 pandemic mean for HIV, tuberculosis, and malaria control? *Tropical Medicine and Health*. 48(1). DOI: 10.1186/s41182-020-00219-6.

Amirav, I. 2008. Real-life effectiveness of Singulair® (Montelukast) in 506 children with mild to moderate asthma. *Israel Medical Association Journal*. 10(4):287–291.

Anabwani, G.M., Woldetsadik, E.A. & Kline, M.W. 2005. Treatment of human immunodeficiency virus (HIV) in children using antiretroviral drugs. *Seminars in Pediatric Infectious Diseases*. 16(2):116–124. DOI: 10.1053/j.spid.2005.12.007.

Attarian, A. & Tran, H. 2017. An Optimal Control Approach to Structured Treatment Interruptions for HIV Patients: A Personalized Medicine Perspective. *Applied Mathematics*. 08(07):934–955. DOI: 10.4236/am.2017.87074.

Banda, G. 2013. Finance as a "forgotten technological capability" for promoting African local pharmaceutical manufacture. *International Journal of Technology Management and Sustainable Development*. 12(2):117–135. DOI: 10.1386/tmsd.12.2.117_1.

Banda, G., Wangwe, S. & Macintosh, M. 2016. The Pharmaceutical Industry in Africa. In *Making Medicines in Africa*. M. Mackintosh, G. Banda, P. Tibandebage, & W. Wamae, Eds. London: Palgrave Macmillan. 5–24. DOI: 10.1057/9781137546470.

Bastiaans, D. 2016. Making things easier: How to improve antiviral drug treatment for children. Radboud University.

Becerra, J.C., Bildstein, L.S. & Gach, J.S. 2016. Recent Insights into the HIV / AIDS Pandemic. *Microbial Cell*. 3(9):451–475. DOI: 10.15698/mic2016.09.529.

Cabrera, S.E., Santos, D., Valverde, M.P., Domínguez-Gil, A., González, F., Luna, G. & García, M.J. 2009. Influence of the cytochrome P450 2B6 genotype on population pharmacokinetics of efavirenz in human immunodeficiency virus patients. *Antimicrobial Agents and Chemotherapy*. 53(7):2791–2798. DOI: 10.1128/AAC.01537-08.

Campbell, M.C. & Tishkoff, S.A. 2008. African genetic diversity: Implications for human demographic history, modern human origins, and complex disease mapping. *Annual Review of Genomics and Human Genetics*. 9:403–433. DOI: 10.1146/annurev.genom.9.081307.164258.

Chan, I.S. & Ginsburg, G.S. 2011. Personalized Medicine: Progress and Promise. *Annual Review of Genomics and Human Genetics*. 12(1):217–244. DOI: 10.1146/annurev-genom-082410-101446.

Chiappetta, D.A., Hocht, C. & Sosnik, A. 2010. A Highly Concentrated and Taste-Improved Aqueous Formulation of Efavirenz for a More Appropriate Pediatric Management of the Anti-HIV Therapy A Highly Concentrated and Taste-Improved Aqueous Formulation of Efavirenz

for a More Appropriate Pediatric Manage. *Current HIV Research*. 8(3):223–231. DOI: 10.2174/157016210791111142.

Clayden, P. 2012. *Novel lopinavir/ritonavir sprinkle formulation for children in resource-limited settings*. Available: https://i-base.info/htb/19902 [Accessed:2021, August 25].

Cloyd, J.C., Kriel, R.L., Jones-Saete, C.M., Ong, B.Y., Jancik, J.T. & Remmel, R.P. 1992. Comparison of sprinkle versus syrup formulations of valproate for bioavailability, tolerance, and preference. *The Journal of Pediatrics*. 120(4, Part 1):634–638. DOI: 10.1016/S0022-3476(05)82496-5.

Conroy, S., McIntyre, J., Choonara, I. & Stephenson, T. 2000. Drug trials in children: Problems and the way forward. *British Journal of Clinical Pharmacology*. 49(2):93–97. DOI: 10.1046/j.1365-2125.2000.00125.x.

Cram, A., Breitkreutz, J., Desset-brèthes, S., Nunn, T. & Tuleu, C. 2009. Challenges of developing palatable oral paediatric formulations. *International Journal of Pharmaceutics*. 365:1–3. DOI: 10.1016/j.ijpharm.2008.09.015.

Dahourou, D.L. & Leroy, V. 2017. Challenges and perspectives of compliance with pediatric antiretroviral therapy in Sub-Saharan Africa. *Medecine et Maladies Infectieuses*. 47(8):511–518. DOI: 10.1016/j.medmal.2017.07.006.

Dixon, S., McDonald, S. & Roberts, J. 2002. The impact of HIV and AIDS on Africa's economic development. *British Medical Journal*. 324(7331):232–234. DOI: 10.1136/bmj.324.7331.232.

Dubrocq, G., Rakhmanina, N. & Phelps, B.R. 2017. Challenges and Opportunities in the Development of HIV Medications in Pediatric Patients. *Pediatric Drugs*. 19(2):91–98. DOI: 10.1007/s40272-016-0210-4.

Esté, J.A. & Cihlar, T. 2010. Current status and challenges of antiretroviral research and therapy. *Antiviral Research*. 85(1):25–33. DOI: 10.1016/j.antiviral.2009.10.007.

Fauci, A.S. 1988. The Human Immunodeficiency Virus: Infectivity and Mechanisms of Pathogenesis. *Science*. 239(4840):617–622. Available: https://www.jstor.org/stable/1700182.

Giralt, A.N., Nöstlinger, C., Lee, J., Salami, O., Lallemant, M., Ouma, O., Nyamongo, I. & Marchal, B. 2017. Understanding the acceptability and adherence to paediatric antiretroviral treatment in the new formulation of pellets (LPV/r): The protocol of a realist evaluation. *British Medical Journal Open*. 7(3):1–9. DOI: 10.1136/bmjopen-2016-014528.

Gregson, S., Garnett, G.P., Nyamukapa, C.A., Hallett, T.B., Lewis, J.J.C., Mason, P.R., Chandiwana, S.K. & Anderson, R.M. 2006. HIV decline associated with behavior change in eastern Zimbabwe. *Science*. 311(5761):664–666. DOI: 10.1126/science.1121054.

Gulick, R.M. 2003. New antiretroviral drugs. *Clinical Microbiology and Infection*. 9(3):186–193. DOI: 10.1046/j.1469-0691.2003.00570.x.

Hirsch, M.S. 1988. Azidothymidine. *The Journal of Infectious Diseases*. 157(3):427–431. Available: https://www.jstor.org/stable/30136643.

Intini, A., Bonifazi, D. & Migliaccio, G. 2019. Challenges and New Frontiers on the Paediatric Drug Discovery and Development. In *Drug Discovery and Development - New Advances*. 2020th ed. V. Gaitonde, P. Karmakar, & A. Trivedi, Eds. London, UK: IntechOpen Ltd. 1–13.

DOI: 10.5772/intechopen.85635.

Ivanovska, V., Rademaker, C.M.A., van Dijk, L. & Mantel-Teeuwisse, A.K. 2014. Pediatric Drug Formulations: A Review of Challenges and Progress. *Pediatrics*. 134(2):361–372. DOI: 10.1542/peds.2013-3225.

Kagee, A., Remien, R.H., Berkman, A., Hoffman, S., Campos, L. & Swartz, L. 2011. Structural barriers to ART adherence in Southern Africa: Challenges and potential ways forward. *Global Public Health*. 6(1):83–97. DOI: 10.1080/17441691003796387.

Kayitare, E., Vervaet, C., Ntawukulilyayo, J.D., Seminega, B., Bortel, V. & Remon, J.P. 2009. Development of fixed dose combination tablets containing zidovudine and lamivudine for paediatric applications. *International Journal of Pharmaceutics*. 370(1–2):41–46. DOI: 10.1016/j.ijpharm.2008.11.005.

King, J.R., Kimberlin, D.W., Aldrovandi, G.M. & Acosta, E.P. 2002. Antiretroviral Pharmacokinetics in the Paediatric Population. *Clinical Pharmacokinetics*. 41(14):1115–1133. DOI: 10.2165/00003088-200241140-00001.

Krause, J. & Breitkreutz, J. 2008. Improving Drug Delivery in Paediatric Medicine. *Pharmaceutical Medicine*. 22(1):41–50. DOI: 10.1007/BF03256681.

Lee, J.S.F., Sagaon Teyssier, L., Dongmo Nguimfack, B., Collins, I.J., Lallemant, M., Perriens, J. & Moatti, J.P. 2016. An analysis of volumes, prices and pricing trends of the pediatric antiretroviral market in developing countries from 2004 to 2012. *BMC Pediatrics*. 16(1):1–8. DOI: 10.1186/s12887-016-0578-x.

Lin, D., Seabrook, Jamie A. Matsui, D.M., King, S.M., Rieder, M.J. & Finkelstein, Y. 2011. Palatability, adherence and prescribing patterns of antiretroviral drugs for children with human immunodeficiency virus infection in Canada. *Pharmacoepidemiology and drug safety*. 20(12):1246–1252. DOI: 10.1002/pds.2236.

Lodha, R. & Manglani, M. 2012. Antiretroviral therapy in children: Recent advances. *Indian Journal of Pediatrics*. 79(12):1625–1633. DOI: 10.1007/s12098-012-0903-9.

Malek, W., Yager, J., Britt, N., Morse, C., Hecox, Z., Hoye-simek, A., Sullivan, S. & Patel, N. 2017. Clinical outcomes associated with single tablet regimens: relationship between antiretroviral therapy pill burden and control of concomitant comorbidities among HIV-Infected patients. *Journal of HIV & Retro virus*. 3(1:5):1–7. DOI: 10.21767/2471-9676.100032.

Mills, E.J., Nachega, J.B., Buchan, I., Orbinski, J., Attaran, A., Singh, S., Rachlis, B., Wu, P., Cooper, C., Thabane, L., Wilson, K., Guyatt, G.H. & Bangsberg, D.R. 2006. Adherence to antiretroviral therapy in sub-Saharan Africa and North America: A meta-analysis. *Journal of the American Medical Association*. 296(6):679–690. DOI: 10.1001/jama.296.6.679.

Murphy, D.A., Marelich, W.D., Huffman, D. & Steers, W.N. 2004. Predictors of antiretroviral adherence. *AIDS Care*. 16(4):471–484. DOI: 10.1080/09540120410001683402.

Musiime, V., Fillekes, Q., Kekitiinwa, A., Kendall, L., Keishanyu, R., Namuddu, R., Young, N., Opilo, W., Lallemant, M., Walker, A.S., Burger, D. & Gibb, D.M. 2014. The pharmacokinetics and acceptability of lopinavir/ritonavir minitab sprinkles, tablets, and syrups in African HIV-infected children. *Journal of Acquired Immune Deficiency Syndromes*. 66(2):148–154. DOI: 10.1097/QAI.0000000000000135.

Nahirya-Ntege, P., Cook, A., Vhembo, T., Opilo, W., Namuddu, R., Katuramu, R.,

Tezikyabbiri, J., Naidoo-James, B. & Gibb, D. 2012. Young HIV-infected children and their adult caregivers prefer tablets to syrup antiretroviral medications in Africa. *PLoS ONE*. 7(5):1–8. DOI: 10.1371/journal.pone.0036186.

Nunn, T. & Williams, J. 2005. Formulation of medicines for children. *British Journal of Clinical Pharmacology*. 59(6):674–676. DOI: 10.1111/j.1365-2125.2005.02410.x.

Penazzato, M., Watkins, M., Morin, S., Lewis, L., Pascual, F., Vicari, M., Lee, J., Hargreaves, S., eDoherty, M., Siberry, G.K. 2018. Catalysing the development and introduction of paediatric drug formulations for children living with HIV: a new global collaborative framework for action. *The Lancet HIV*. 5(5):e259–e264. DOI: 10.1016/S2352-3018(18)30005-5.

Pereira, L., Mutesa, L., Tindana, P. & Ramsay, M. 2021. African genetic diversity and adaptation inform a precision medicine agenda. *Nature Reviews Genetics*. 22(5):284–306. DOI: 10.1038/s41576-020-00306-8.

Piot, P., Bartos, M., Ghys, P.D., Walker, N. & Schwartländer, B. 2001. The global impact of HIV/AIDS. *Nature*. 410(6831):968–973. DOI: 10.1038/35073639.

Prague, M., Commenges, D. & Thiébaut, R. 2013. Dynamical models of biomarkers and clinical progression for personalized medicine: The HIV context. *Advanced Drug Delivery Reviews*. 65(7):954–965. DOI: 10.1016/j.addr.2013.04.004.

Preis, M. 2015. Orally Disintegrating Films and Mini-Tablets—Innovative Dosage Forms of Choice for Pediatric Use. *AAPS PharmSciTech*. 16(2):234–241. DOI: 10.1208/s12249-015-0313-1.

Psichogiou, M., Poulakou, G., Basoulis, D., Paraskevis, D., Markogiannakis, A. & Daikos, G.L. 2017. Recent Advances in Antiretroviral Agents: Potent Integrase Inhibitors. *Current Pharmaceutical Design*. 23(18). DOI: 10.2174/1381612823666170329142059.

Rabie, H., Frigati, L., Hesseling, A.C. & Garcia-prats, A.J. 2015. Review article Tuberculosis : opportunities and challenges for the 90-90-90 targets in HIV-infected children. *Journal of the International AIDS society*. 18(Suppl 6):1–11. DOI: 10.7448/IAS.18.7.20236.

Ranmal, S.R., Cram, A. & Tuleu, C. 2016. Age-appropriate and acceptable paediatric dosage forms: Insights into end-user perceptions, preferences and practices from the Children's Acceptability of Oral Formulations (CALF) Study. *International Journal of Pharmaceutics*. 514(1):296–307. DOI: 10.1016/j.ijpharm.2016.07.054.

Resch, S., Korenromp, E., Stover, J., Blakley, M., Krubiner, C., Thorien, K., Hecht, R. & Atun, R. 2011. Economic returns to investment in AIDS treatment in low and middle income countries. *PLoS ONE*. 6(10). DOI: 10.1371/journal.pone.0025310.

Rodriguez-Novoa, S., Barreiro, P., Rendon, A., Jimenez-Nacher, I., Gonzalez-Lahoz, J. & Soriano, V. 2005. Influence of 516G>T Polymorphisms at the Gene Encoding the CYP450-2B6 Isoenzyme on Efavirenz Plasma Concentrations in HIV-Infected Subjects. *Clinical Infectious Diseases*. 40(9):1358–1361. DOI: 10.1086/429327.

Roser, M. & Ritchie, H. 2019. *HIV / AIDS*. Available: https://ourworldindata.org/hiv-aids [Accessed:2020, May 13].

Rouaz, K., Chiclana-Rodriguez, B., Nardi-ricart, A., Suñe-Pou, M., Mercade-Frutos, D., Sune-Negre, J., Peres-Lozano, P. & Garcia-Montoya, E. 2021. Excipients in the paediatric

population: A Review. *Pharmaceutics*. 13(387):1–44. DOI: 10.3390/pharmaceutics13030387.

Salem, A.H., Chiu, Y.L., Valdes, J.M., Nilius, A.M. & Klein, C.E. 2015. A novel ritonavir paediatric powder formulation is bioequivalent to ritonavir oral solution with a similar food effect. *Antiviral Therapy*. 20(4):425–432. DOI: 10.3851/IMP2932.

Sam, T., Ernest, T.B., Walsh, J. & Williams, J.L. 2012. A benefit/risk approach towards selecting appropriate pharmaceutical dosage forms - An application for paediatric dosage form selection. *International Journal of Pharmaceutics*. 435(2):115–123. DOI: 10.1016/j.ijpharm.2012.05.024.

Schlatter, A.F., Deathe, A.R. & Vreeman, R.C. 2016. The need for pediatric formulations to treat children with HIV. *AIDS Research and Treatment*. 2016. DOI: 10.1155/2016/1654938.

Simon, V., Ho, D.D. & Karim, Q.A. 2006. Seminar HIV / AIDS epidemiology , pathogenesis , prevention , and treatment. *Science*. 368(9534):489–504. Available: http://ac.els-cdn.com/S0140673606691575/1-s2.0-S0140673606691575-main.pdf?_tid=73556fba-fefe-11e5-91e3-00000aab0f6b&acdnat=1460280631_b48fc461d14c43bfa3381b19edf104a2.

South African National Department of Health. 2019. *2019 ART Clinical Guidelines*. Available: https://www.knowledgehub.org.za/elibrary/2019-art-clinical-guidelines-management-hiv-adults-pregnancy-adolescents-children-infants.

Tavares, R. & Tang, V. 2011. Regional economic integration in Africa: Impediments to progress? *South African Journal of International Affairs*. 18(2):217–233. DOI: 10.1080/10220461.2011.588826.

UNAIDS. 2015. *AIDS by the numbers*. Available: http://search.unaids.org [Accessed:2020, May 13].

UNAIDS. 2016. *Global Aids Update*. Available: https://www.unaids.org/sites/default/files/media_asset/global-AIDS-update-2016_en.pdf [Accessed:2020, May 13].

UNAIDS. 2017. *Ending Aids Progress Towards the 90-90-90 Targets*. DOI: UNAIDS/JC2900E.

UNAIDS. 2018. *Ending tuberculosis and AIDS a joint response in the era of the sustainable development goals*. Available: https://www.who.int/conferences/tb-global-ministerial-conference/WHO_EndTB_Conference_Highlights.pdf [Accessed:2020, May 13].

UNAIDS. 2019. *2019 Fact sheet*. V. 1. Available: https://www.unaids.org/en/resources/fact-sheet [Accessed:2020, May 15].

UNAIDS. 2020. UNAIDS Data 2020. *Programme on HIV/AIDS*. 1–248. Available: https://www.unaids.org/en/resources/documents/2020/unaids-data%0Ahttp://www.unaids.org/sites/default/files/media_asset/20170720_Data_book_2017_en.pdf.

UNAIDS. 2021a. *Fact sheet 2021*. Available: https://www.unaids.org/en/resources/fact-sheet [Accessed:2021, July 10].

UNAIDS. 2021b. *Global AIDS update: Confronting inequalities*. Available: https://www.unaids.org/en/resources/documents/2021/2021-global-aids-update [Accessed:2021, July 10].

UNICEF. 2020a. *Reimagining a resilient HIV response for children, adolescents and pregnant women living with HIV*. Available: http://www.childrenandaids.org/sites/default/files/2020-12/2020 World AIDS Day Report.pdf [Accessed:2020, August 20].

UNICEF. 2020b. *Paediatric Antiretroviral Medicines : Market & Supply Update*. Available: https://www.unicef.org/supply/media/2581/file/ARV-market-and-supply-update.pdf [Accessed:2020, May 10].

Vanprapar, N., Cressey, T.R., Chokephaibulkit, K., Muresan, P., Plipat, N., Sirisanthana, V., Prasitsuebsai, W., Hongsiriwan, S., Eksaengsri, A., Toye, M., Smith, M.E., McIntosh, K., Capparelli, E., Yogev, R. 2010. A chewable pediatric fixed-dose combination tablet of stavudine, lamivudine, and nevirapine: Pharmacokinetics and safety compared with the individual liquid formulations in human immunodeficiency virus-infected children in Thailand. *Pediatric Infectious Disease Journal*. 29(10):940–944. DOI: 10.1097/INF.0b013e3181e2189d.

Van Riet-Nales, D.A., Kozarewicz, P., Aylward, B., de Vries, R., Egberts, T.C.G., Rademaker, C.M.A. & Schobben, A.F.A.M. 2017. Paediatric Drug Development and Formulation Design—a European Perspective. *AAPS PharmSciTech*. 18(2):241–249. DOI: 10.1208/s12249-016-0558-3.

Waalewijn, H., Turkova, A., Rakhmanina, N., Cressey, T.R., Penazzato, M., Colbers, A. & Burger, D.M. 2019. Optimizing Pediatric Dosing Recommendations and Treatment Management of Antiretroviral Drugs Using Therapeutic Drug Monitoring Data in Children Living With HIV. *Therapeutic drug monitoring*. 41(4):431–443. DOI: 10.1097/FTD.0000000000000637.

Walsh, J., Ranmal, S.R., Ernest, T.B. & Liu, F. 2018. Patient acceptability, safety and access: A balancing act for selecting age-appropriate oral dosage forms for paediatric and geriatric populations. *International Journal of Pharmaceutics*. 536(2):547–562. DOI: 10.1016/j.ijpharm.2017.07.017.

Warnke, D., Barreto, J. & Temesgen, Z. 2007. Therapeutic review: Antiretroviral drugs. *Journal of Clinical Pharmacology*. 47(12):1570–1579. DOI: 10.1177/0091270007308034.

World Health Organisation. 2003. *Adherence to long term therapies - evidence for action*. Available: https://www.who.int/chp/knowledge/publications/adherence_full_report.pdf [Accessed:2020, May 18].

World Health Organisation. 2021. *Global Tuberculosis Report 2021*. Available: https://www.who.int/teams/global-tuberculosis-programme/tb-reports [Accessed:2021, October 16].

World Health Organization. 2016. *Combined Global Demand Forecasts for Antiretroviral Medicines and Hiv Diagnostics in Low-and Middle-Income Countries From 2015 To 2020*. Available: http://apps.who.int/iris/bitstream/10665/250088/1/9789241511322-eng.pdf?ua=1 [Accessed:2020, May 10].

World Health Organization. 2017. *Global Tuberculosis Report*. DOI: 10.1177/2165079915607875.

World Health Organization. 2019. *World Malaria Report 2019*. Available: https://www.who.int/publications-detail/world-malaria-report-2019 [Accessed:2020, May 10].

World Health Organization. 2020. *Global Tuberculosis Report*. Available: https://www.who.int/publications/i/item/9789240013131 [Accessed:2021, February 05].

World Health Organization & UNICEF. 2015. *Fact Sheet on Lopinavir and Ritonavir (Lpv/R) Oral Pellets*. Available: http://www.who.int/hiv/pub/guidelines/arv2013/en/index.html [Accessed:2020, May 13].

World Health Organisation. 2018. Updated recommendations on first-line and second-line antiretroviral regimens and post-exposure prophylaxis and recommendations on early infant diagnosis of HIV: interim guidelines. Supplement to the 2016 consolidated guidelines on the use of antiretrovir. *World Health Organization*. (December):1–79. Available: https://apps.who.int/iris/bitstream/handle/10665/277395/WHO-CDS-HIV-18.51-eng.pdf?ua=1.

Wyen, C., Hendra, H., Vogel, M., Hoffmann, C., Knechten, H., Brockmeyer, N.H., Bogner, J.R., Rockstroh, J., Esser, S., Mauss, S., Jaeger, H., Harrer, T., van Lunzen, J., Skoetz, N., Jetter, A., Groneuer, C., Fatkenheur, G., Khoo, S.H., Egan, D., Back, D.J. & Owen, A. 2008. Impact of CYP2B6 983T>C polymorphism on non-nucleoside reverse transcriptase inhibitor plasma concentrations in HIV-infected patients. *Journal of Antimicrobial Chemotherapy*. 61(4):914–918. DOI: 10.1093/jac/dkn029.

Zhan, P., Pannecouque, C., De Clercq, E. & Liu, X. 2016. Anti-HIV Drug Discovery and Development: Current Innovations and Future Trends. *Journal of Medicinal Chemistry*. 59(7):2849–2878. DOI: 10.1021/acs.jmedchem.5b00497.

CHAPTER 2

A developmental perspective on paediatric dosage forms

2.1 Introduction

Pharmaceutical pre-formulation is a vital stage in the drug development process where the physico-chemical, toxicological, pharmacological, and biopharmaceutical properties of an active pharmaceutical ingredient (API) and all potential excipients to be used are studied. This multidisciplinary stage usually forms the interface between the discovery of a drug candidate and the formulation of that drug into a dosage form that is suitable for patient administration. These studies strengthen the scientific foundation for the introduction of a new drug, conserve resources during development stages and generally result in enhanced product quality and safety. The information gained during pre-formulation studies is used to inform the potential formulation parameters that could be used to develop a pharmaceutical dosage form into an optimal drug delivery system, with the ultimate goal being to ensure exceptional quality medicines leading to improved global health (Gopinath & Naidu, 2011; Vilegave, Vidyasagar & Chandankar, 2013).

This chapter will therefore provide an overview of different pre-formulation parameters and focus will be given to those parameters that can guide taste-masking of APIs during dosage form development.

2.2 Pre-formulation in dosage form development

The pre-formulation profile of an API typically includes the physical and chemical properties thereof. In general, the collective term, physico-chemical properties are used as an over-arching definitive term to combine the parameters and characteristics that are investigated as part of pre-formulation studies. An in-depth discussion on these properties will be provided followed by linkage and ultimately translation of these properties to API taste-masking strategies.

2.2.1 Physico-chemical properties of pharmaceutical ingredients

The physico-chemical properties of pharmaceutical ingredients carry significant value during drug formulation. From molecular level to shelf life, physico-chemical properties are determinants for properties at various levels. These properties also influence drug bioavailability and therefore it is crucial to characterise and understand the physico-chemical properties of the relative compounds to ensure therapeutic success. These properties and their importance will be discussed in the following sections.

2.2.1.1 Inherent chemical properties

Inherent properties are the “built-in” characteristics of the molecule which can only be altered by chemical modification (Aulton, 2017). It is a well-known fact that drug compounds have to successfully interact with their target receptors to achieve a therapeutic outcome. Inherent properties that govern such interactions include dissociation constant (pKa), partition coefficient (LogP/LogD), chirality, and intrinsic solubility (Chaurasia, 2016; Patel, 2016). Since these properties are inherent to the chemical characteristics of the molecule it inevitably have a direct impact on one another thus highlighting the importance to be defined during pre-formulation studies as they guide potential drug molecule modifications, choices of solvents, excipients, and even dosage form formulation strategies.

i. pKa

The pKa, LogP and solubility profiles of an API are used to predict the efficiency and strength of drug-target interactions. Drug particles have to be in a solubilised state in order to be systemically absorbed and ultimately have a therapeutic effect. The ionisation constant (pKa) of a compound indicates the ionisation state thereof as a function of pH and influences properties such as drug permeability, partition coefficient, and the aqueous solubility (as a function of pH) (Lee et al., 2007; Aulton, 2017). The pKa value of a compound indicates the potential absorption site of the drug. The particular pKa of an API can be exploited during pre-formulation in order to achieve more desirable biopharmaceutical properties. For example, drug pKa values can be used to choose suitable salt-forming agents and the solubility of the salts can also be predicted (Maurin, Grant & Stahl, 2008). Complexation with macrocyclic molecules such as cyclodextrins has been investigated for their ability to result in pKa shifts in the API which imposes different absorption properties to the formulation compared to the API alone (Ghosh & Nau, 2012).

ii. logP

Partition coefficients (logP) are ratio values that are used to describe how the unionised form of a solute will be distributed at equilibrium between two immiscible solvents (aqueous and organic phases). In pharmaceutical sciences, the oil/water partition coefficient is used as a measure of a molecule’s lipophilicity (Aulton, 2017). This can provide insight into the preference of a drug to a hydrophilic versus lipophilic environment and therefore provides insights into its ability to cross lipid membranes in the body, ultimately determining the absorption behavior of a compound (Patel, 2016; Aulton, 2017).

iii. Solubility

One particularly important objective of pre-formulation studies is to optimise drug solubility. This is important because a drug must first be in solution in order to be absorbed into the systemic circulation, meaning that the drug has to be dissolved in order to have a therapeutic

effect (Sugano et al., 2007; Savjani, Gajjar & Savjani, 2012). The intrinsic or equilibrium solubility of a drug is the maximum amount of drug that can dissolve into a specific volume of solvent at a specific temperature. It is important to know the intrinsic solubility of a drug compound prior to formulation because if the solubility needs to be adjusted in order to deliver a therapeutic dose, the strategy to do so should be designed and evaluated during pre-formulation. The intrinsic solubility of a compound is determined by its inherent properties, such as logP and pKa but also by many other parameters such as the types of molecular bonds, molecular volume, and the energy involved with the specific crystal lattice (Patel, 2016). In summary, factors that can affect the solubility profile of a drug may include the type of solvent, solvent temperature and pH, choice of excipients, ionisability of the compound in the solvent, and the solid-state form of the API compound (Sugano et al., 2007; Savjani, Gajjar & Savjani, 2012). Establishing how the solubility of the drug is affected by potential excipients can also guide the choice of excipients for optimal drug performance. The evaluation, description and occasional manipulation of solubility are essential to ensure sufficient bioavailability and ultimately an acceptable therapeutic outcome.

iv. Organoleptic properties

Organoleptic properties of compounds include their odour, taste, and colour (**Table 2.1**) (Chaurasia, 2016). These properties are particularly important if an oral dosage form is required since the API has to be relatively desirable to lead to successful oral administration. Any unappealing features of the API or excipient(s) need to be recorded during the pre-formulation stage. Undesirable visual features can be addressed by coating the drug with a more pleasing textured or coloured coating. Unpleasant odours or tastes can be overcome by taste-masking the API by one of many approaches (Chaurasia, 2016; Zheng et al., 2018). If any substances need to be added to improve the organoleptic properties, these substances need to be included in the pre-formulation studies in order to evaluate their effect on the solubility, stability and bioavailability of the API.

Table 2.1: Organoleptic parameters that are typically evaluated during pre-formulation studies and the relevant analytic tools used.

Evaluation parameter	Method of analysis
Colour	Visual
Odour	Manual
Taste	E-tongue testing

2.2.1.2 Solid-state chemistry of pharmaceutical ingredients

It is a well-known fact that APIs can exist in several different solid forms, each with unique pharmaceutically relevant properties which will affect its solubility, stability, and ultimately the bioavailability. In some instances, these different forms can interconvert spontaneously or through the addition of energy during pharmaceutical processing steps such as milling, mixing, granulation, to name but just a few. It is therefore required that formulators know the different forms and their respective properties since it affects the pharmaceutical manufacturing industry as a whole, from the drug discovery phase up to successful marketing of a dosage form (Byrn et al., 1994). The main objective of studying the solid-state chemistry of APIs is to deliver each drug in the optimal performing solid form. Just briefly, the most common solid-state forms that drugs may exist in include:

i. Crystalline polymorphs

Polymorphism is the ability of compounds to crystallise as more than one distinct crystalline species, each with a different internal lattice design. The different polymorphic forms of the same compound have different physico-chemical properties such as melting point, density, vapor pressure, solubility, and dissolution rate (Byrn et al., 1994; Brittain, Grant & Myrdal, 2009). Some crystalline forms of a compound tend to be more stable than other crystalline or amorphous forms of the same API. Further to this, it should be noted that the most stable crystalline form of a drug possesses the lowest free energy and therefore is the least likely to interconvert to another solid-state form during processing steps or storage and will also exhibit the lowest aqueous solubility than the other solid-state forms of the same drug (Singhal & Curatolo, 2004).

ii. Solvates and hydrates

Solvates are solid-state forms that contain solvent molecules within their crystal lattice structures. These solvent molecules are entrapped within the crystal and impart unique properties to the solid form (Patel, 2016; Healy et al., 2017). The solvent molecules are able to form strong interactions with the API that may improve physical stability. Alternatively, the solvent molecules can act as space fillers in the crystal structure without the formation of strong intramolecular interactions. This molecular packing role may also lead to improved stability of the solid form (Healy et al., 2017). Hydrates are a subcategory of solvates where the solvent entrapped in the crystal lattice structure is water. This presence of water molecules affects the intermolecular interactions and the degree of crystallinity. Subsequently, it has an effect on the solubility, dissolution rate, stability, and ultimately the bioavailability of the API (Healy et al., 2017).

iii. Salts

For basic and acidic drug compounds the process of salt formation is the simplest, most cost-effective strategy to address poor aqueous solubility and enhance bioavailability. The salt form

of a chemical entity may impact the wettability, diffusion layer thickness, and melting point. Salt formation is also generally associated with a significant increase in the solubility of a drug and therefore also the dissolution rate which translates into improved absorption profiles (Elder, Holm & De Diego, 2013). Conversion into a salt form is one of the most common performance-improving techniques used to date (Patel, 2016).

iv. Co-crystals

Co-crystals are defined as a single crystal lattice containing two or more molecular species (Vishweshwar et al., 2006; Elder, Holm & De Diego, 2013; Steed, 2013). When a molecular recognition event between different solid molecular species occurs, co-crystals can form. This will only be thermodynamically favourable if the interaction between complementary functional groups results in hydrogen bonds that are energetically more favourable compared to those between the molecules of either component (Vishweshwar et al., 2006). The ability to create API-API co-crystals has led to the expansion of the range of solid-state forms available for formulation. Generally, crystalline species are preferred above amorphous forms because their characterisation is easier and more reproducible and these forms exhibit lower hygroscopicity, and greater chemical stability. In addition to these general advantages, co-crystals also offer improved ability to solubilise poorly soluble APIs compared to other crystalline species (Elder, Holm & De Diego, 2013).

v. Amorphous solid forms

These forms possess no long-range order of atoms/molecules in their molecular lattices, leading to higher levels of molecular free energy which results in higher solubility and also higher dissolution rates but this comes at the cost of reduced physical stability as amorphous forms can revert to more stable forms upon storage (Byrn et al., 1994). Some research has been done, with success, on stabilising amorphous solid forms using an array of different techniques (Mallick et al., 2008; Liu et al., 2010; Maclean et al., 2011; Shah et al., 2012).

2.2.1.3 Intrinsic dissolution

The intrinsic dissolution rate of a drug is defined as the rate at which mass is transferred per unit area of a solid dissolving surface (Aulton, 2017). The primary goal of dissolution and solubility studies is to understand the absorption behavior of a drug compound in order to predict its *in vivo* performance (Macheras & Dokoumetzidis, 2000). Ideally, a solid dosage form should be soluble only at a particular site depending on the intended site of action. The dissolution rate of a compound is not only dependent the drug itself but also on the formulation. Factors affecting *in vivo* dissolution rates of solids in liquids include a) the surface area of undissolved solids, b) the solubility of the solids in the liquid medium, c) the concentration of the solute in the solution at a given time and d) the dissolution rate constant (Aulton, 2017).

During pre-formulation studies dissolution of the drug alone and in combination with the excipients should be evaluated at all relevant biological pH values. This is to ensure that an adequate therapeutic dose can be achieved upon administration (Wang, Fotaki & Mao, 2009).

As mentioned already, many drug compounds possess undesirable palatability which results in therapeutic failure as a result of reduced patient compliance (**Chapter 1, Section 1.3.3**). Taste-masking of APIs may form part of the pre-formulation or formulation phases of dosage form development and it is important to note that it can potentially impact the physico-chemical properties of the drug. It is therefore imperative that all the potential changes in the physico-chemical properties are evaluated post-taste-masking. One of the most important aspects to evaluate is the drug release profile of the taste-masked formulation. This is due to the widely accepted fact that only the dissolved drug particles have the ability to elicit taste by interacting with the taste bud receptors (Keeley et al., 2019). This evaluation is typically done by *in vitro* dissolution testing and the importance is two-fold in the development of taste-masked drugs. First, dissolution allows for the prediction of the taste-masking efficiency by providing an estimate for the likely drug release in the oral cavity. Secondly, it also assesses the effect that taste-masking has on the pharmacokinetic profile (Gittings et al., 2014). Furthermore, in cases where an oral drug is to be taken with food or drink, it is also important to characterise the dissolution profile of the compound in typical foods or utilising a dissolution medium that allows mimicking of a fed gastric or fed intestinal state to ensure that there are no interactions that may interfere with the therapeutic effect. If the dissolution profile is sub-optimal, strategies to improve drug dissolution at the desired pH can be investigated (Kostewicz et al., 2002). Strategies that are typically used to improve drug bioavailability include preparing salts and solid forms, chemical modifications, and increasing surface area through micronisation (Sugano et al., 2007).

2.2.1.4 Permeability

The ability of a compound to cross biological membranes and ultimately reach the systemic circulation is referred to as permeability. For successful therapy following oral drug delivery sufficient intestinal absorption is required to ensure that the drug compound reaches its target site (Dahan, Miller & Amidon, 2009). Maximum solubility and permeability at the site of absorption are crucial for optimal oral bioavailability. The permeability of a drug is assessed in order to predict if drug bioavailability is adequate for successful therapeutic responses. The development of permeability assays, such as *in situ* perfusion models and non-cellular parallel artificial membrane assays, have been designed to assist in evaluating the permeability of drug compounds (Volpe, 2010). These *in situ*, *ex vivo,* and *in vitro* approaches greatly

contribute to driving drugs into *in vivo* clinical studies during drug development to facilitate their introduction into the market.

2.2.1.5 Stability

In pharmaceutical formulation, the ultimate goal is to produce a product that will remain both physically and chemically stable throughout any manufacturing and storage processes (Aucamp & Milne, 2019). The stability of a particular pharmaceutical formulation can be defined as its capability to remain within its physical, chemical, microbiological, therapeutic, and toxicological specifications throughout its shelf-life (Bajaj, Singla & Sakhuja, 2012). The stability of a compound can be subdivided into chemical stability (chemical integrity and potency), physical stability (appearance, palatability, uniformity and dissolution), and microbial stability (**Table 2.2**) (Chaurasia, 2016). The primary objective of determining stability is to elucidate under which conditions the compound is prone to degradation. Typical mechanisms by which chemical degradation occurs most frequently include oxidation, hydrolysis, and photolysis. Stability testing forms an important part of dosage form development as it ensures drug safety, efficiency, and quality. The stability of the drug is determined when in solution as well as in solid-state (Patel, 2016). Stability testing in solution includes investigating the effect of pH, ionic strength, addition of co-solvents, light, temperature, and oxygen on the drug. It is also important to determine if and how any excipients might affect the stability of the API. The information gained through stability testing can inform suitable molecular modifications and will guide the transport, storage, and lifetime recommendations of the final dosage form (Bajaj, Singla & Sakhuja, 2012; Aashigari et al., 2019).

Table 2.2: Parameters typically evaluated during pre-formulation in order to assess the stability of a compound (Chaurasia, 2016; Patel, 2016).

Evaluation parameter	Method of analysis
Solid-state stability	Raman, XRD, DSC
Solution stability	Raman, HPLC
Chemical stability	HPLC, TGA, DSC, Raman
Microbiological stability	HPLC, PCR

i. Physical stability

The physical stability of a compound relates to the three-dimensional conformational form. The physico-chemical properties of a particular solid-state form of an API relates to its physical stability and every solid-state form has different properties. In order for a drug to be considered physically stable, the solid-state form used during design and formulation must remain stable

throughout. This means that the original physical properties such as appearance, colour, and solid-state are retained. The physical stability may affect the performance, visual uniformity, and drug release rate (Aashigari et al., 2019). Comprehensive knowledge of all the potential solid-state forms of a compound together with knowledge on solid-state transformations is required to accurately assess and track the physical stability of a compound. Yet again, it is also important to consider and evaluate the physical stability of any excipient that may form part of the formulation (Aucamp & Milne, 2019).

ii. Chemical stability

The chemical stability of a compound relates to the chemical nature and potency and the ability of a compound to withstand loss with regards to its chemical activity and properties (Waterman & Adami, 2005). Chemical instability is assessed by monitoring the loss of drug potency or the formation of degradation products. Through assessing the chemical stability of compounds, degradation mechanisms can be identified and understood. This can in turn aid in the design of stabilisation methods or some cases the redesign or modification of the API (Magnin et al., 2004).

iii. Microbiological stability

Microorganisms are all around us and can sometimes get into a final pharmaceutical product. This microbial contamination can originate from process equipment, the environment as well as the water used during processing and manufacturing. Microbial contamination results in microbial instability such that the quality and performance of the product are affected. In extreme cases where microbes produce toxic byproducts, contamination can result in life-threatening consequences. Preservatives can be added during formulation to counter microbial contamination in cases where the drug compound or excipients are prone to microbial instability. Alternative non-preservative approaches have also received mentionable attention lately to further reduce any potentially harmful and toxic effects (Dao et al., 2018). Early on in dosage form development, it is necessary that formulators establish specified guidelines to control and resist antimicrobial activity in pharmaceutical products.

2.2.2 Physico-mechanical properties

2.2.2.1 Bulk characterisation

Bulk characterisation involves the investigation of interparticle interactions as well as the interaction of different particulate surfaces with water vapor. These properties include bulk density, surface morphology, flowability, deformation, moisture content, crystallinity, and particle packing (**Table 2.3**) (Chaurasia, 2016; Patel, 2016).

The size and shape of drug particles can influence the powder flow characteristics which in turn would influence the final dosage form properties such as drug dissolution rate, dose

uniformity, stability, and sedimentation rates. The size of particles can be reduced to an extent in order to get more optimal drug properties. For example, a multitude of particle size reduction strategies exists and can be used to improve the bioavailability of a drug (Khadka et al., 2014).

Table 2.3: Parameters typically evaluated in order to characterise the bulk properties of a drug compound.

Evaluation parameter	Method of analysis
Particle size and shape	Scanning electron microscopy (SEM), Particle size analysis
Density	Angle of repose, bulk density, tapped density, true density
Hygroscopicity	TGA/Vapour sorption analysis
Flowability	Carr's compressibility index and Hausner ratios

Hygroscopicity of compounds is evaluated to characterise their tendency to absorb moisture from their environment. The moisture sorption data is used to describe the physical stability of the drug. This information is important because significant changes in moisture content could affect the stability of a solid dosage form. For example, if it is known that a particular drug substance is moisture sensitive, the vapor sorption data will reflect this and guide excipient selection to ensure both optimal physical and chemical stability of the drug compound (Allada et al., 2016). The density of a drug compound plays a crucial part in determining the size of the final dosage form, determining the flow properties of solids and is an important parameter in the process of tableting. Powder flowability is loosely defined as the ability of a powder to flow and it can range from free-flowing to cohesive. Powder flow properties can influence the final product weight and uniformity while from a manufacturing point of view, flowability can govern the efficiency and rate of production. The determination of flow properties during pre-formulation can also influence excipient selection during formulation stages and may be a deciding factor in the choice between compression and granulation processes (Prescott & Barnum, 2000).

2.2.3 Compatibility

Compatibility between excipients and the API needs to be evaluated during the pre-formulation stages. Compatibility between an API and excipient/s is considered satisfactory when there are no adverse effects on the safety, therapeutic efficacy, or stability of the API. Compatibility is crucial to ensure maximum stability of the active compound (Patel et al., 2015). The

evaluation of the compatibility between compounds can be assessed using thermal methods such as differential scanning calorimetry (DSC), microcalorimetry, and hot stage microscopy (HSM). Alternatively, spectroscopy, microscopic techniques such as scanning electron microscopy (SEM), or chromatographic techniques (HPLC) can be used to evaluate the chemical and physical compatibility between compounds (Pani et al., 2012; Chaurasia, 2016). Drug-excipient incompatibility can potentially result in changes in the physical, chemical, microbiological, or therapeutic properties and stability of a formulation. Physical incompatibilities are those that do not involve changes in the chemical nature of the API but rather involve changes in the colour, odour, flow properties, and sedimentation rate. In cases where such change significantly affects the performance of the API, the formulation strategy would need to be revised. Interactions between an API and excipient that involve chemical degradation are known as chemical incompatibilities and these lead to the formation of unstable chemical entities. Therapeutic incompatibilities could also arise if interactions between the API and excipient take place once the formulation is administered into the body. Incompatibilities can complicate and compromise the development process or the viability of a commercial drug product (Patel, 2016). Therefore these tests are important to inform the optimal API-excipient combinations necessary for a successful and marketable drug formulation.

Pharmaceutical pre-formulation studies form a significant part of pharmaceutical dosage form development. As discussed in the preceding paragraphs multiple factors should be considered during the pharmaceutical pre-formulation stage and this stage can be a relatively involved and intricate process. In conclusion pharmaceutical pre-formulation is the cornerstone of successful formulation of pharmaceutical dosage forms that is safe and effective.

2.3 Taste-masking as a pre-formulation strategy to improve organoleptic properties

Oral drug delivery is one of the most common and convenient drug administration routes and based on this the taste of a drug is an important factor that influences the likelihood that patients will take an oral drug. The stimulation of taste buds on the surface of the tongue results in the perception referred to as taste. Humans can experience and distinguish among five components of taste namely sour, salt, sweet, bitter, and umami/savory (Ayenew et al., 2009). Bitterness is the taste most commonly associated with APIs and many oral drugs fail clinically as a result of bad taste, especially among paediatric and elderly populations. This is because, compared to adults, children have a heightened preference for sweet-tasting and greater rejection for bitter-tasting substances (Dubrocq, Rakhmanina & Phelps, 2017).

Masking the bitter taste of some drugs is an important parameter for improved patient compliance and treatment quality (Wagh & Ghadlinge, 2009). As a result, there has been a mentionable drive towards taste-masking bitter drugs to reduce the bitterness in an attempt to make the drugs more palatable to improve patient compliance (Gao et al., 2006; Khan et al., 2007; Xu, Li & Zhao, 2008; Orlu-Gul et al., 2013; Almurisi et al., 2020).

Various taste-masking strategies can be used to mask the taste of unpalatable drugs. One approach is to construct physical barriers “around” the drug particles, subsequently altering the ability of the drug to interact with taste receptors. This is typically achieved through coating, granulation, or encapsulation. The addition of a coating layer can protect the API and shield the unpleasant taste. Granulation effectively lowers the surface area of the drug that comes into contact with the tongue upon oral intake and so reduces the extent of the bitterness experienced. Another approach is to modify the drug solubility by chemical derivatisation, complexation, and the use of ion-exchange resins or solid dispersions. For example, the solubility of a drug can be manipulated by creating specific interactions between the drug and hydrophobic polymers, thereby decreasing the solubility of a drug in an aqueous environment such as the mouth (Ayenew et al., 2009). The taste of a drug is only sensitised when the drug is dissolved in saliva and it comes in contact with the taste buds. Therefore, taste-masking methods focus on making drugs insoluble at a salivary pH of 6.8 (Al-kasmi et al., 2017). Cyclodextrins are commonly used as complexing agents to mask the unpleasant taste of drugs. The cyclodextrins form a complex around the drug by wrapping around it and inhibiting its interaction with the taste buds. Ion-exchange resins are high molecular weight polymers with either cationic or anionic functional groups forming insoluble resonates with oppositely charged drug molecules. Other approaches are centered on simply altering the human taste perception by adding excipients such as sweeteners, flavours, and bitter blockers (Pein et al., 2014). The addition of sweeteners often serve as an auxiliary method when combining it with another techniques to ensure good overall taste-masking performance. There is no single approach that is perfect for all taste-masking needs and depending on certain parameters such as dosage form, drug dose, desired bioavailability and target patient group, different taste-masking techniques might be employed as each holds specific advantages and applications (Vummaneni & Nagpal, 2015). These techniques can be used to not only improve taste, but in some cases also the stability and performance of the product.

With the availability of a plethora of taste-masking technologies and the constant development of new techniques, it is important to make an objective analysis of taste. There are three main methods to evaluate taste-masking efficiency: human taste panels, animal models, and analytical techniques. Human taste panels are challenging with respect to cost, time, toxicity

of drugs, and ethical considerations. Moreover, taste preferences are personal and because it is dependent on the physical and physiological conditions of each individual, human taste panels can lead to variable and inconsistent results. Animal models, although not being a true representation of human taste sensation and preference (Choi et al., 2014), it still shows some level of application and value at least in the elimination of severely unpalatable preparations. *In vitro* analytical techniques that have been adopted over the past several decades show the most promise for future taste assessment. Electronic sensing systems show particular promise as it is fast, relatively inexpensive in terms of experimental setup and execution, and low in risk (Jain et al., 2010; Choi et al., 2014). On the downside, these electronic sensing systems are highly specialised and expensive equipment, thus making acquiring of these systems challenging.

Another popular technique for evaluating taste-masking of pharmaceuticals is *in vitro* dissolution testing in a simulated oral cavity environment. It has been recognised that to accurately predict the most likely release profile of an API in the oral cavity the dissolution testing should ideally mimic the oral environment as closely as possible (Gittings et al., 2014). Important factors to consider when attempting to mimic the oral cavity include the volume, saliva, and agitation in the oral cavity. Currently, there is no standard pharmacopoeial approved dissolution test for taste-masked particles and as a result, a magnitude of different dissolution methods exist, all of which employ vastly different experimental parameters (Gittings et al., 2014; Keeley et al., 2019). The advantages and limitations of the existing dissolution methods for taste-masked particles have been highlighted in literature (Gittings et al., 2014). One example of a commonly used strategy for taste-masked particles is the single medium pH 6.8 dissolutions. Although the chemical environment in the oral cavity is accurately represented by pH 6.8 these dissolutions often employ biologically irrelevant volumes by performing tests at volumes as high as 900 mL. Despite there not currently being an optimal or accepted standard method for conducting drug dissolution in simulated oral cavity environments, a lot of studies make use of normal *in vitro* dissolution testing. Despite some limitations associated with this strategy, the results obtained do provide trustworthiness to the data and subsequent conclusions/predictions made.

2.4 Taste-masking to enhance paediatric dosage forms

As mentioned, the palatability of oral drug formulations is a key determinant for the acceptability and compliance to drug therapy, especially in children. Additionally, adequate taste testing is important to ensure that the designed dosage form meets the unique needs of children and should ideally form part of early paediatric drug development protocols.

Hoang Thi *et al.* (2012) used spray-drying to encapsulate acetaminophen within a microcapsule composed of sodium caseinate and lecithin, for paediatric drug application. This resulted in a significant decrease in early drug release and therefore it was possible to mask the drug bitterness upon administration into the mouth. The combined use of cyclodextrins and sweeteners by Orlu-Gul *et al.* (2013) resulted in the development of a taste-masked hydrocortisone paediatric solution. The cyclodextrin complexation was used to optimise the drug solubility while the addition of the neotame sweetener suppressed the drug bitterness. In another study, Salman *et al.* (2018) evaluated the tolerability of two midazolam drug formulations, an inherently bitter drug, in a clinical setting. Compared to the unflavored liquid formulation, the novel chewable chocolate-based tablets were found to have higher tolerability in children while remaining equally efficient, safe and, display adequate bioavailability. However, it may be valuable to question the safety of this formulation considering the risk of overdosing given the pleasant taste of the tablets.

Specific considerations are needed when masking the taste of drugs for the paediatric population. The use of excipients is one very important example of this. In addition to APIs, excipients are also metabolised differently by children compared to adults. Therefore the use of certain excipients may not be appropriate or the levels will be restricted for paediatric drug formulation. When designing an age-appropriate paediatric formulation, the excipients should be selected based on a benefit-risk approach, encompassing all aspects of the proposed excipients, including but not limited to, toxicity, tolerability, physico-chemical properties and patients' age (Walsh et al., 2014). For example, the use of ethanol in paediatric medicines is discouraged, and when the use of ethanol in drug formulation is unavoidable ethanol levels are restricted to a maximum of 0.5% in oral medicines intended for children under the age of 6 years (Marek & Kraft, 2014). This is because ethanol metabolism is not as efficient in children as in adults because of physiologic immaturity of the metabolic enzyme, alcohol dehydrogenase. Ethanol exposure can result in possible acute toxicity or chronic toxicity, with prolonged medicinal exposure for the treatment of pediatric chronic diseases. Some of the most frequently observed alcohol-related toxicities in children include hypoglycemia, acidosis, and electrolyte abnormalities (Zuccotti & Fabiano, 2011). However, it is recognised that in certain cases small amounts of ethanol are required in the formulation process. Therefore, it is important to note that just like with the selection of an appropriate taste-masking approach, the selection of excipients needs to be done on a case-by-case basis.

2.5 Microencapsulation as a taste-masking strategy

In the context of pharmaceutical dosage form development, encapsulation can be defined as a process whereby APIs are surrounded by a coating, or embedded in a homogeneous or heterogeneous matrix, to give small capsules with many functional properties (Rodríguez et al., 2016). The compound that covers or encapsulates the API is referred to as the coating material, wall former, or encapsulant and is responsible for controlling the drug release and improving the stability of the active compound (Quintero, Rojas & Ciro, 2018). Another beneficial property imposed by encapsulation is the protection from potentially harmful environmental conditions such as oxygen, light, and pH. Microencapsulation can be considered a special type of encapsulation whereby a thin layer of coating is applied to small particles of a solid, droplets of liquid, and dispersions. The products of the microencapsulation process are capsules in the micrometer to millimeter range, known as microcapsules or microparticles (Sri et al., 2012). Every microparticle produced consists of an inner and outer layer. The inner layer, or core, is defined as the specific material to be coated, it can be in liquid or solid form and is generally the API. The outer layer, or coating/shell, serves to protect core materials from volatilisation, oxidation and in some cases mask the unpleasant taste of the core material (Ayenew et al., 2009). Some general properties of the ideal coating layer include that it should i) stabilise the core material, ii) be inert relative to active ingredients, iii) allow for controlled release under specific conditions and iv) be economical.

Microcapsules can have different morphologies, depending mainly on the core material and the deposition process of the shell/coating material (**Figure 2.1**). Mononuclear microcapsules simply contain the shell around the core while polynuclear capsules have many cores enclosed within a single shell. Matrix encapsulated microparticles are a third morphology type, where the core material is distributed homogeneously into the shell material.

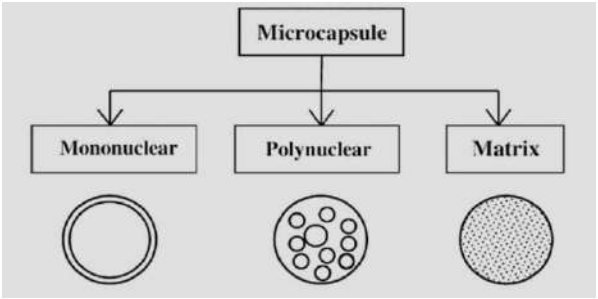

Figure 2.1: Microcapsule morphologies in a schematic. The three major types of microcapsule morphology are mononuclear-, polynuclear- and matrix encapsulated microcapsules (Adapted from Sri *et al.*, 2012).

Reasons for using microencapsulation in dosage form development include (Bansode et al., 2010):

- Sustained or controlled drug release;
- Taste-masking of bitter drugs;
- Converting liquid drugs into powder forms;
- Stabilise drugs that are sensitive to light, moisture or oxygen;
- Prevent unwanted drug-drug interactions;
- Reduce drug toxicity and GIT irritation; and
- Targeted drug delivery.

Many different methods exist for the production of microcapsules and in general, these methods can be divided into three groups (Al-kasmi et al., 2017):

i. *Chemical polymerisation* is the most common among chemical encapsulation methods. A chosen monomer is dissolved in a liquid core material and then dispersed in an aqueous phase. The polymerisation reaction can be set by co-reactant or free radical resulting in rapid polymerisation at the interface where capsule shell generation occurs. For example, Yang *et al.* (2008) produced microcapsules using a chain extender molecule to produce self-healing polymers of toluene diisocyanate. A toluene diisocynate prepolymer was dissolved into chlorobenzene and then slowly poured into a gum arabic solution, heated and a chain extender was added resulting in the formation of a polyurethane shell at the interface between the aqueous phase and oil phase.

ii. *Physico-chemical encapsulation* can be achieved by either coacervation (phase separation) or the ionotropic gelation method.

   a) In a coacervation method, the drug is dispersed in a polymer solution and then the solubility of polymer is partially decreased resulting in precipitation and the formation of a continuous coating of the wall polymer around core particles.

      For example, Nori *et al.* (2011) successfully encapsulated propolis extract by complex coacervation using isolated soy protein and pectin as encapsulant agents. Aqueous soy protein isolate was added to the propolis extract and homogenised. A pectin solution was added and then the mixture was cooled to promote sedimentation of the microcapsules. The produced microcapsules maintained desired propolis properties and were alcohol-free, stable, and exhibited antioxidant and antimicrobial activity.

b) Ionotropic gelation involves the dropwise addition of a drug-loaded anionic polymer to an aqueous solution of polyvalent cations. The diffusion of cations into the polymeric drops leads to the formation of a three-dimensional lattice.

For example, Khazaeli, Pardakhty, and Hassanzadeh (2008) prepared ibuprofen beads through ionotropic gelation. Ibuprofen drug was added to a sodium alginate polymer solution and then dropped into a cationic metal solution to prepare ibuprofen beads.

iii. Examples of *mechanical microencapsulation* are fluid bed coating, solvent evaporation/extraction, and spray-drying.

a) In fluid bed coating, the drug is suspended in air at a predetermined temperature. The polymer solution is then sprayed, the solvent evaporates and subsequently, the polymer encapsulates the drug particles.

For example, Shin *et al.* (2018) developed an extended-release pellet system of imidafenacin using a fluid-bed coater. Spherical sugar pellets were first layered with the drug and hypromellose by inputting the solution into a fluid-bed coater and then subsequently coated with Eudragit RS copolymers.

b) Solvent evaporation/extraction involves the dissolution of the drug and polymer in an organic solvent. The solution is then added to the aqueous phase and the organic solvent evaporates allowing the polymer to encapsulate the drug.

For example, ethyl cellulose micro/nanocapsules have been prepared using an emulsification-solvent evaporation method (Abbaspoor, Ashrafi & Salehi, 2018). Ethyl cellulose powder was dissolved in benzene and ethanol, and following stirring linseed oil was added to the polymeric solution. The polymeric solution then was added to the aqueous solution (polyethylene glycol and sodium lauryl sulphate in nitric acid solution) and the dispersion was concentrated by continuous open-top stirring resulting in the removal of the solvent by evaporation and formation of micro/nanocapsules.

c) The process of spray-drying is also based on solvent evaporation but does not necessarily involve an organic solvent. Both drug and polymer are dissolved in an appropriate solvent and then sprayed into a chamber at controlled temperature. The solvent evaporates and the drug is encapsulated by the polymer.

In this thesis, special emphasis will be given to spray-drying and ionic gelation as methods of microencapsulation. For this reason, the next sections will be dedicated to discussing spray-drying and ionic gelation within the pharmaceutical context.

2.5.1 Microencapsulation through spray-drying

Spray-drying is defined as the transformation of a feed from a fluid state into a dried product by spraying the feed into a hot gaseous drying medium. The feed can either be a solution, suspension, emulsion, or paste and depending on the physical and chemical properties of the feed solution as well as the operation design, the resulting dried product can either be powder, granules, or agglomerates (Nath & Satpathy, 1998). This technique is widely applicable and versatile since it can be used for both heat resistant and heat-sensitive drugs, for both water-soluble and water-insoluble drugs and both hydrophilic and hydrophobic drugs, polymers, and other substances. Additionally, it is a one-step continuous operation process and easy to scale up making it suitable for pharmaceutical applications (Desai & Park, 2005).

The apparatus used for spray-drying is referred to as a spray-dryer and the basic design is shown in **Figure 2.2**. The spray-drying process may be described by three major phases namely atomisation, droplet-to-particle conversion and particle collection. The first important transformation is the formation of droplets by atomisation, which increases the droplet surface area. The feed solution is pumped to an atomiser, which breaks up the liquid feed into a spray of fine droplets. Once the droplet has formed and ejected by the atomiser the droplets are ejected into a drying gas chamber under the influence of turbulent gas flow where moisture vaporisation occurs, resulting in the formation of dry powder particles. Finally, the dried particles are separated from the drying medium and are then collected in a collection vessel (Santos et al., 2017). Successful spray-drying relies on achieving high retention of the core material during processing and storage.

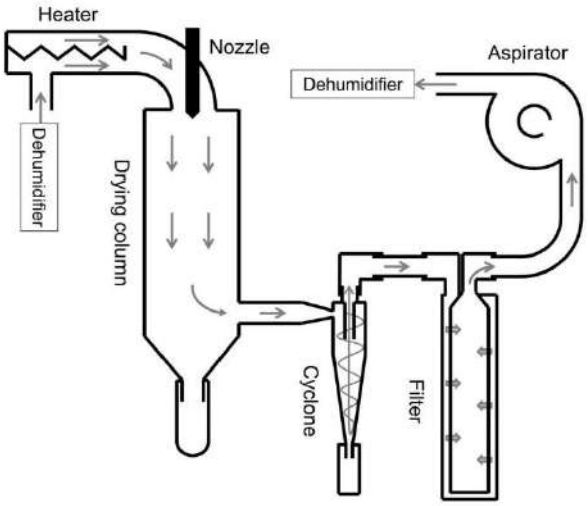

Figure 2.2: Annotated schematic showing the typical design of a spray-dryer. Functional principles and components of a Büchi B-290 Mini spray-dryer (Adapted from Grasmeijer *et al.*, 2013).

2.5.1.1 Spray-drying process parameters

Some of the most relevant chemical and biochemical properties related to the spray-dried powder include mean particle size, particle size distribution, bulk density, porosity, moisture content, texture and particle shape. In this regard, the particular properties of spray-dried products can be somewhat controlled by modifying the spray-drying process parameters. Controllable process parameters that should be optimised for each experiment include (Rane et al., 2007; Santos et al., 2017):

- Atomisation pressure
    - Since atomisation is carried out under pressure, the process has an impact on droplet size. For a given device and fixed feed solution, microcapsule droplet size decreases with increasing pressure.
- Feed flow rate
    - The rate at which the feed stock solution is pumped into the atomiser can be controlled. Given that atomisation pressure is kept constant particle size can be increased with increasing feed flow rates.
- Feed viscosity
    - When the feed viscosity is higher, a great percentage of atomisation energy needs to be supplied to the nozzle to overcome the viscous forces. Consequently, less energy remains for droplet fission, resulting in larger particle sizes.
- Inlet temperature
    - Inlet temperature refers to the temperature of the heated drying gas, measured right before it enters the drying chamber and it reflects the capacity of the gas to dry the droplets. Hence, higher inlet temperatures enable higher solvent evaporation rates and decreased particle size since the moisture content is decreased more rapidly. However, inlet temperature should be selected wisely while considering the feed stock properties and other process parameters.
- Drying gas flow rate
    - The gas flow rate should be balanced as it needs to be low enough to ensure complete moisture removal, but it should also be high enough to ensure adequate separation efficiency during cyclone separations procedure.
- Outlet temperature
    - The outlet temperature is not directly regulated by the operator but rather results from heat and mass exchanges inside the drying chamber. The outlet temperature is a function of inter-related parameters such as the inlet temperature, the drying gas flow rate and the feed properties.

2.5.1.2 Examples of using spray-drying in the pharmaceutical industry

Spray-drying is a powerful and popular drying technique used in the pharmaceutical industry today. The very first pharmaceutical application of spray-drying obtained dry plant extracts from active raw materials. Since then spray-drying has become a popular drying technique with various applications, often favoured above other drying methods because of its versatility and ability to produce high-quality homogenous powders.

Listed below are a few examples of the application of spray-drying in a pharmaceutical context:

- Spray-drying can be used to improve the dissolution rate of drugs. Vogt, Kunath and Dressman (2008) used spray-drying in the preparation of rapidly dissolving formulations of fenofibrate, a cholesterol drug. First, the drug was micronised using a bead mill and then the nano-particulate dispersion was spray-dried to produce a powder that exhibited a higher dissolution rate than commercial formulations.
- Spray-drying can be used to preserve or enhance nanoparticle stability during storage, by transforming nano-suspensions into powders. Cerdeira, Mazzotti and Gander (2013) prepared itraconazole and miconazole nano-suspensions and subsequently used spray-drying to convert the nano-suspensions into dry powder forms to improve long term stability.
- Rane *et al.* (2007) illustrated that controlled crystallisation of poorly water-soluble drugs can be achieved with spray-drying in presence of a protective carrier, such as a hydrophilic polymer. This resulted in reduced particle size, increase surface area and enhanced drug dissolution.
- Bora, Borude and Bhise (2008) used spray-drying technology to produce taste-masked microspheres of the bitter anti-nausea drug, ondansetron hydrochloride. Eudragit and chitosan were used to form a polymeric coating around the drug, thereby minimising drug interaction with the taste buds.
- Controlled drug release can be achieved by spray-drying. Desai and Park (2005) prepared chitosan–tripolyphosphate microspheres containing the drug acetaminophen. It was found that the surface morphology of the microspheres and release rate of the drug could be controlled by varying process parameters used during spray-drying.

Spray-drying is a widely used method for the production of fine particles, coarse powders, agglomerates or granulates. The characteristics of the spray-dried particles can be controlled and maintained throughout the operation. Spray-drying has been successfully applied in the

pharmaceutical industry to both APIs and also final pharmaceutical formulations. Spray-drying presents a wide field for research and development in pharmaceutical science.

2.5.2 Microencapsulation through ionic gelation

Ionic gelation is an ionic polymerisation technique where the starting solution, an aqueous polymeric solution with ions of low molecular mass, interacts with electrolytes containing ions of the opposite charge. The oppositely charged ions react and form a relatively insoluble gel (Kurozawa & Hubinger, 2017). For pharmaceutical applications, the API is typically loaded into the starting aqueous polymeric solution. Typical polymers that are used in drug delivery systems include alginates, chitosan, gellan gum, chitin and gum arabic (Anandhakumar et al., 2017; Vidart et al., 2018; Nalini et al., 2019). The release of the encapsulated material is subject to the gel phase changes which are determined by the external environment. Different external stimuli that can serve as triggers for gel phase change and subsequent release of the encapsulated API include pH, temperature, osmotic pressure, and mechanical forces (Kurozawa & Hubinger, 2017).

Advantages of using ionic gelation in drug delivery systems include low cost and the fact that there is no need for specialised equipment, high processing temperatures or the use of organic solvents (Kurozawa & Hubinger, 2017). The technique of ionic gelation is more applicable for hydrophobic compounds and has indeed proved very successful for drugs with poor aqueous solubility (Mirghani et al., 2000; Almeida & Almeida, 2004; Arica et al., 2005; Rastogi et al., 2007). The natural nature of typical polymer systems further renders it attractive for use in drug delivery and this strategy has gained much popularity in the pharmaceutical industry.

Listed below are a few examples of the application of ionic gelation strategies in the pharmaceutical context:

i. Nalini et al. (2019) showed that the synthesis of alginate/chitosan nanoparticles loaded with the hydrophobic drug quercetin resulted in increased chemical stability and reduced toxicity of the drug. The preparation of the nanoparticles was done in two steps. The basic quercetin nanoparticle was prepared through chitosan ionic gelation followed by complexation with alginate. The resulting particle size was in the nanometer range (118 – 255 nm) and high encapsulation efficiency (82.4%) and moderate loading capacity (46.5%) were achieved. Further, sustained pH-dependent drug release was achieved with enhanced stability in acidic media to protect quercetin against enzymatic and pH-related degradation.

ii. Anandhakumar et al. (2017) prepared doxorubicin nanoparticles *via* ionic gelation using chitosan with an additional collagen peptide film on the outside. The prepared collagen peptide–chitosan nanoparticles were pH-responsive with regards to drug release indicating their potential in delivering anti-tumor drugs in response to the extracellular pH of the tumor environment for cancer therapy. Additionally, bi-phasic drug release was achieved with an initial release burst followed by a sustained release for a period of up to 7 days further indicating their potential use in cancer therapy.

iii. Vidart et al. (2018) used a blend of alginate and sericin to prepare encapsulated diclofenac sodium particles in the millimeter size range. The inclusion of sericin into the matrix resulted in a significant delay in drug release compared to alginate-only matrix systems. The delayed drug release over a period of 6 hours achieved here also indicated the potential need for less frequent dosing and subsequently better patient adherence.

iv. Miladi et al. (2015) prepared chitosan nanoparticles for the encapsulation of osteoporosis drug alendronate. Here, the choice of a chitosan-based matrix was motivated by the preference of the oral drug delivery route. Chitosan is known to have mucoadhesive properties rendering chitosan nanoparticles a potential alternative alendronate oral dosage form. High encapsulation efficiencies (up to 70%) were achieved with significantly higher drug release observed in an acidic environment compared to a neutral environment.

The ionic gelation method is widely used due to the high stability of synthesised particles, the ease of using water-based solutions, the simple cost-effective process as well as the ability to work easily with poorly water-soluble drugs. A lot of the recent research done on ionic gelation is targeted at developing new drug delivery systems.

2.6 Conclusion

In this thesis, the non-nucleoside reverse transcriptase inhibitor, efavirenz, will be explored as a model ARV for taste-masking purposes. Two microencapsulation techniques namely, spray-drying and ionic gelation were utilised in this study as taste-masking strategies and the design of these processes was done in correlation with the physico-chemical properties of efavirenz. Additionally, the potential use of vegetable proteins and natural sugars as wall-formers was incorporated into this study.

2.7 References

Aashigari, S., Goud, R., Sneha, S., Vykuntam, U. & Potnuri, N. 2019. Stability studies of pharmaceutical products. *World Journal of Pharmaceutical Research*. 8(1):479–492. DOI: 10.20959/wjpr20191-13872.

Abbaspoor, S., Ashrafi, A. & Salehi, M. 2018. Synthesis and characterization of ethyl cellulose micro/nanocapsules using solvent evaporation method. *Colloid and Polymer Science*. 296(9):1509–1514. DOI: 10.1007/s00396-018-4371-2.

Al-kasmi, B., Bashir, M.H.D., Bashimam, M. & El-zein, H. 2017. Mechanical microencapsulation: The best technique in taste masking for the manufacturing scale - Effect of polymer encapsulation on drug targeting. *Journal of Controlled Release*. 260(June):134–141. DOI: 10.1016/j.jconrel.2017.06.002.

Allada, R., Maruthapillai, A., Palanisamy, K. & Chappa, P. 2016. Hygroscopicity categorization of pharmaceutical solids by gravimetric sorption analysis: A systematic approach. *Asian Journal of Pharmaceutics*. 10(4):279–286.

Almeida, P. & Almeida, A. 2004. Cross-linked alginate-gelatine beads: a new matrix for controlled release of pindolol. *Journal of Controlled Release*. 97(3):431–439. DOI: 10.1016/j.conrel.2004.03.015.

Almurisi, S.H., Doolaanea, A.A., Akkawi, M.E., Chatterjee, B. & Sarker, M.Z.I. 2020. Taste masking of paracetamol encapsulated in chitosan-coated alginate beads. *Journal of Drug Delivery Science and Technology*. 56:101520. DOI: 10.1016/j.jddst.2020.101520.

Anandhakumar, S., Krishnamoorthy, G., Ramkumar, K.M. & Raichur, A.M. 2017. Preparation of collagen peptide functionalized chitosan nanoparticles by ionic gelation method: An effective carrier system for encapsulation and release of doxorubicin for cancer drug delivery. *Materials Science and Engineering C*. 70:378–385. DOI: 10.1016/j.msec.2016.09.003.

Arica, B., Çaliş, S., Atilla, P., Durlu, N.T., Çakar, N., Kaş, H.S. & Hincal, A.A. 2005. In vitro and in vivo studies of ibuprofen-loaded biodegradable alginate beads. *Journal of Microencapsulation*. 22(2):153–165. DOI: 10.1080/02652040400026319.

Aucamp, M. & Milne, M. 2019. The physical stability of drugs linked to quality-by-design (QbD) and in-process technology (PAT) perspectives. *European Journal of Pharmaceutical Sciences*. 139. DOI: 10.1016/j.ejps.2019.105057.

Aulton, M. 2017. Dissolution and Solubility. In: *Pharmaceutics: The Science of Dosage Form Design*. Fifth ed. M. Aulton & K. Taylor, Eds. London: Elsevier. 18–35.

Ayenew, Z., Puri, V., Kumar, L. & Bansal, A. 2009. Trends in Pharmaceutical Taste Masking Technologies: A Patent Review. *Recent Patents on Drug Delivery & Formulation*. 3(1):26–39. DOI: 10.2174/187221109787158364.

Bajaj, S., Singla, D. & Sakhuja, N. 2012. Stability testing of pharmaceutical products. *Journal of Applied Pharmaceutical Science*. 2(3):129–138. DOI: 10.7324/JAPS.2012.2322.

Bansode, S.S., Banarjee, S.K., Gaikwad, D.D., Jadhav, S.L. & Thorat, R.M. 2010. Microencapsulation: A review. *International Journal of Pharmaceutical Sciences Review and Research*. 2(1):38–43.

Bora, D., Borude, P. & Bhise, K. 2008. Taste masking by spray-drying technique. *AAPS PharmSciTech*. 9(4):1159–1164. DOI: 10.1208/s12249-008-9154-5.

Brittain, H.G., Grant, D.J. & Myrdal, P.B. 2009. Effects of polymorphism and solid-state solvation on solubility and dissolution rate. In: *Polymorphism in Pharmaceutical Solids*. H.G. Brittain, Ed. New York: Informa Healthcare. 436–481.

Byrn, S.R., Pfeiffer, R.R., Stephenson, G., Grant, D.J.W. & Gleason, W.B. 1994. Solid-State Pharmaceutical Chemistry. *Chemical Materials*. 6:1148–1158. DOI: 10.1021/cm00044a013.

Cerdeira, A.M., Mazzotti, M. & Gander, B. 2013. Formulation and drying of miconazole and itraconazole nanosuspensions. *International Journal of Pharmaceutics*. 443(1–2):209–220. DOI: 10.1016/j.ijpharm.2012.11.044.

Chaurasia, G. 2016. Pharmaceutical preformulation studies in formulation and development of new drug: A review. *International Journal of Pharmaceutical Sciences and Research*. 7(6):2313–2320. DOI: 10.13040/IJPSR.0975-8232.7(6).2313-20.

Choi, D.H., Kim, N.A., Nam, T.S., Lee, S. & Jeong, S.H. 2014. Evaluation of taste-masking effects of pharmaceutical sweeteners with an electronic tongue system. *Drug Development and Industrial Pharmacy*. 40(3):308–317. DOI: 10.3109/03639045.2012.758636.

Dahan, A., Miller, J.M. & Amidon, G.L. 2009. Prediction of Solubility and Permeability Class Membership: Provisional BCS Classification of the World's Top Oral Drugs. *The AAPS Journal*. 11(4):740–746. DOI: 10.1208/s12248-009-9144-x.

Dao, H., Lakhani, P., Police, A., Kallakunta, V., Ajjarapu, S.S., Wu, K.W., Ponkshe, P., Repka, M.A., Murthy, S.N. 2018. Microbial Stability of Pharmaceutical and Cosmetic Products. *AAPS PharmSciTech*. 19(1):60–78. DOI: 10.1208/s12249-017-0875-1.

Desai, K.G.H. & Park, H.J. 2005. Preparation and characterization of drug-loaded chitosan-tripolyphosphate microspheres by spray drying. *Drug Development Research*. 64(2):114–128. DOI: 10.1002/ddr.10416.

Dubrocq, G., Rakhmanina, N. & Phelps, B.R. 2017. Challenges and Opportunities in the Development of HIV Medications in Pediatric Patients. *Pediatric Drugs*. 19(2):91–98. DOI: 10.1007/s40272-016-0210-4.

Elder, D.P., Holm, R. & De Diego, H.L. 2013. Use of pharmaceutical salts and cocrystals to address the issue of poor solubility. *International Journal of Pharmaceutics*. 453(1):88–100. DOI: 10.1016/j.ijpharm.2012.11.028.

Gao, Y., Cui, F., Guan, Y., Yang, L., Wang, Y. & Zhang, L. 2006. Preparation of roxithromycin-polymeric microspheres by the emulsion solvent diffusion method for taste masking. *International Journal of Pharmaceutics*. 318(103):62–69. DOI: 10.1016/j.ijpharm.2006.03.018.

Ghosh, I. & Nau, W.M. 2012. The strategic use of supramolecular pKa shifts to enhance the bioavailability of drugs. *Advanced Drug Delivery Reviews*. 64(9):764–783. DOI: 10.1016/j.addr.2012.01.015.

Gittings, S., Turnbull, N., Roberts, C.J. & Gershkovich, P. 2014. Dissolution methodology for taste masked oral dosage forms. *Journal of Controlled Release*. 173(1):32–42. DOI: 10.1016/j.jconrel.2013.10.030.

Gopinath, R. & Naidu, R. a S. 2011. Pharmaceutical Preformulation Studies – Current Review. *International Journal of Pharmaceutical & Biological Archives*. 2(5):1391–1400.

Grasmeijer, N., de Waard, H., Hinrichs, W.L.J. & Frijlink, H.W. 2013. A User-Friendly Model for Spray Drying to Aid Pharmaceutical Product Development. *PLoS ONE*. 8(9). DOI: 10.1371/journal.pone.0074403.

Healy, A.M., Worku, Z.A., Kumar, D. & Madi, A.M. 2017. Pharmaceutical solvates, hydrates and amorphous forms: A special emphasis on cocrystals. *Advanced Drug Delivery Reviews*. 117:25–46. DOI: 10.1016/j.addr.2017.03.002.

Hoang Thi, T.H., Morel, S., Ayouni, F. & Flament, M.P. 2012. Development and evaluation of taste-masked drug for paediatric medicines - Application to acetaminophen. *International Journal of Pharmaceutics*. 434(1–2):235–242. DOI: 10.1016/j.ijpharm.2012.05.047.

Jain, H., Panchal, R., Pradhan, P., Patel, H. & Pasha, T.Y. 2010. Electronic tongue: A new taste sensor. *International Journal of Pharmaceutical Sciences Review and Research*. 5(2):91–96.

Keeley, A., Teo, M., Ali, Z., Frost, J., Ghimire, M., Rajabi-Siahboomi, A., Orlu, M. & Tuleu, C. 2019. In Vitro Dissolution Model Can Predict the in Vivo Taste Masking Performance of Coated Multiparticulates. *Molecular Pharmaceutics*. 16(5):2095–2105. DOI: 10.1021/acs.molpharmaceut.9b00060.

Khadka, P., Ro, J., Kim, H., Kim, I., Kim, J.T., Kim, H., Cho, J.M., Yun, G., Lee, J. 2014. Pharmaceutical particle technologies: An approach to improve drug solubility, dissolution and bioavailability. *Asian Journal of Pharmaceutical Sciences*. 9(6):304–316. DOI: 10.1016/j.ajps.2014.05.005.

Khan, S., Kataria, P., Nakhat, P. & Yeole, P. 2007. Taste masking of ondansetron hydrochloride by polymer carrier system and formulation of rapid-disintegrating tablets. *AAPS PharmSciTech*. 8(2):1–7.

Khazaeli, P., Pardakhty, A. & Hassanzadeh, F. 2008. Formulation of ibuprofen beads by ionotropic gelation. *Iranian Journal of Pharmaceutical Research*. 7(3):163–170.

Kostewicz, E.S., Brauns, U., Becker, R. & Dressman, J.B. 2002. Forecasting the oral absorption behavior of poorly soluble weak bases using solubility and dissolution studies in biorelevant media. *Pharmaceutical Research*. 19(3):345–349. DOI: 10.1023/A:1014407421366.

Kurozawa, L.E. & Hubinger, M.D. 2017. Hydrophilic food compounds encapsulation by ionic gelation. *Current Opinion in Food Science*. 15:50–55. DOI: 10.1016/j.cofs.2017.06.004.

Lee, P.H., Ayyampalayam, S.N., Carreira, L.A., Shalaeva, M., Coselmon, S.B.R., Poole, S., Gifford, E. & Lombardo, F. 2007. In silico prediction of ionization constants of drugs. *Molecular Pharmaceutics*. 4(4):498–512. DOI: 10.1016/b0-08-045044-x/00143-7.

Liu, Y., Sun, C., Hao, Y., Jiang, T., Zheng, L. & Wang, S. 2010. Mechanism of dissolution enhancement and bioavailability of poorly water soluble celecoxib by preparing stable amorphous nanoparticles. *Journal of Pharmacy and Pharmaceutical Science*. 13(4):589–606.

Macheras, P. & Dokoumetzidis, A. 2000. On the heterogeneity of drug dissolution and release. *Pharmaceutical Research*. 17(2):108–112. DOI: 10.1023/A:1007596709657.

Maclean, J., Medina, C., Daurio, D., Alvarez-nunez, F., Jona, J., Munson, E. & Nagapudi, K. 2011. Manufacture and performance evaluation of a stable amorphous complex of an acidic drug molecule and neusilin. *Journal of Pharmaceutical Science*. 100(8):3332–3344. DOI: 10.1002/jps.

Magnin, D.R., Robl, J.A., Sulsky, R.B., Augeri, D.J., Huang, Y., Simpkins, L.M., Taunk, P.C., Betebenner, D.A., Robertson, J.G., Abboa-Offei, B.E., Wang, A., Cap, M., Xin,L., Tao, L., Sitkoff, D.F., Malley, M.F., Gougoutas, J.Z., Khanna, A., Huang, Q., Han, S., Parker, R.A., Hamann, L.G. 2004. Synthesis of novel potent dipeptidyl peptidase IV inhibitors with enhanced chemical stability: Interplay between the N-terminal amino acid alkyl side chain and the cyclopropyl group of r -Aminoacyl- L - cis -4 , 5-methanoprolinenitrile-based inhibitors. *Journal of Medicinal Chemistry*. 47(10):2587–2598. DOI: 10.1021/jm049924d.

Mallick, S., Pattnaik, S., Swain, K., De, P.K., Saha, A., Ghoshal, G. & Mondal, A. 2008. Formation of physically stable amorphous phase of ibuprofen by solid state milling with kaolin. *European Journal of Pharmaceutics and Biopharmaceutics*. 68:346–351. DOI: 10.1016/j.ejpb.2007.06.003.

Marek, E. & Kraft, W.K. 2014. Ethanol pharmacokinetics in neonates and infants. *Current Therapeutic Research*. 76:90–97. DOI: 10.1016/j.curtheres.2014.09.002.

Maurin, M., Grant, D.J. & Stahl, P. 2008. The physicochemical background: Fundamentals

of ionic equilibria. In: *Handbook of Pharmaceutical Salts Properties, Selection, and Use*. P. Stahl & C. Wermuth, Eds. Zurich: Wiley-VCH. 9–14.

Miladi, K., Sfar, S., Fessi, H. & Elaissari, A. 2015. Enhancement of alendronate encapsulation in chitosan nanoparticles. *Journal of Drug Delivery Science and Technology*. 30:391–396. DOI: 10.1016/j.jddst.2015.04.007.

Mirghani, A., Idkaidek, N.M., Salem, M.S. & Najib, N.M. 2000. Formulation and release behavior of diclofenac sodium in Compritol 888 matrix beads encapsulated in alginate . *Drug Development and Industrial Pharmacy*. 26(7):791–795. DOI: 10.1081/DDC-100101301.

Nalini, T., Basha, S.K., Mohamed Sadiq, A.M., Kumari, V.S. & Kaviyarasu, K. 2019. Development and characterization of alginate/chitosan nanoparticulate system for hydrophobic drug encapsulation. *Journal of Drug Delivery Science and Technology*. 52:65–72. DOI: 10.1016/j.jddst.2019.04.002.

Nath, S. & Satpathy, G.R. 1998. A systematic approach for investigation of spray drying processes. *Drying Technology*. 16(6):1173–1193. DOI: 10.1080/07373939808917459.

Nori, M.P., Favaro-Trindade, C.S., de Alencar, S.M., Thomazini, M., de Camargo Balieiro, J.C. & Contreras Castillo, C.J. 2011. Microencapsulation of propolis extract by complex coacervation. *LWT - Food Science and Technology*. 44(2):429–435. DOI: 10.1016/j.lwt.2010.09.010.

Orlu-Gul, M., Fisco, G., Parmar, D., Gill, H. & Tuleu, C. 2013. A new reconstitutable oral paediatric hydrocortisone solution containing hydroxypropyl-β-cyclodextrin. *Drug Development and Industrial Pharmacy*. 39(7):1028–1036. DOI: 10.3109/03639045.2012.696654.

Pani, N.R., Nath, L.K., Acharya, S. & Bhuniya, B. 2012. Application of DSC, IST, and FTIR study in the compatibility testing of nateglinide with different pharmaceutical excipients. *Journal of Thermal Analysis & Calorimetry*. 108:219–226. DOI: 10.1007/s10973-011-1299-x.

Patel, P. 2016. Preformulation studies: An integral part of formulation design. In: *Pharmaceutical Formulation Design - Recent Practices*. U. Ahmad & J. Akhtar, Eds. London: IntechOpen. 3–18. DOI: DOI: http://dx.doi.org/10.5772/intechopen.82868.

Patel, P., Ahir, K., Patel, V., Manani, L. & Patel, C. 2015. Drug-Excipient compatibility studies : First step for dosage form development. *The Pharma Innovation Journal*. 4(5):14–20. Available: http://www.thepharmajournal.com/archives/2015/vol4issue5/PartA/4-4-9.pdf.

Pein, M., Preis, M., Eckert, C. & Kiene, F.E. 2014. Taste-masking assessment of solid oral dosage forms – A critical review. *International Journal of Pharmaceutics*. 465(1–2):239–254. DOI: 10.1016/j.ijpharm.2014.01.036.

Prescott, J.K. & Barnum, R.A. 2000. On powder flowability. *Pharmaceutical Technology*. 24(10):60-84.

Quintero, J., Rojas, J. & Ciro, G. 2018. Vegetable proteins as potential encapsulation agents: a review. *Food Research*. 2(3):208–220. DOI: 10.26656/fr.2017.2(3).261.

Rane, Y.M., Mashru, R.C., Sankalia, M.G., Sutariya, V.B. & Shah, P.P. 2007. Investigations on factors affecting chitosan for dissolution enhancement of oxcarbazepine by spray dried microcrystal formulation with an experimental design approach. *Drug Development and Industrial Pharmacy*. 33(9):1008–1023. DOI: 10.1080/03639040601179749.

Rastogi, R., Sultana, Y., Aqil, M., Ali, A., Kumar, S., Chuttani, K. & Mishra, A.K. 2007. Alginate microspheres of isoniazid for oral sustained drug delivery. *International Journal of Pharmaceutics*. 334:71–77. DOI: 10.1016/j.ijpharm.2006.10.024.

Rodríguez, J., Martín, M.J., Ruiz, M.A. & Clares, B. 2016. Current encapsulation strategies for bioactive oils: From alimentary to pharmaceutical perspectives. *Food Research International*. 83:41–59. DOI: 10.1016/j.foodres.2016.01.032.

Salman, S., Tang, E.K.Y., Cheung, L.C., Nguyen, M.N., Sommerfield, D., Slevin, L., Lim, L.Y. & von Ungern Sternberg, B.S. 2018. A novel, palatable paediatric oral formulation of midazolam: pharmacokinetics, tolerability, efficacy and safety. *Anaesthesia*. 73(12):1469–1477. DOI: 10.1111/anae.14318.

Santos, D., Maurico, A.C., Sencades, V., Santos, J.D., Fernandes, M.H. & Gomes, P.. 2017. Spray Drying: An Overview. *IntechOpen*. DOI: 10.5772/intechopen.72247.

Savjani, K.T., Gajjar, A.K. & Savjani, J.K. 2012. Drug solubility: Importance and enhancement techniques. *ISRN Pharmaceutics*. 2012:1–10. DOI: 10.5402/2012/195727.

Shah, N., Sandhu, H., Phuapradit, W., Pinal, R., Iyer, R., Albano, A., Chatterji, A., Anand, S., Choi, D.S., Tang, K., Tian, H., Chokshi, H., Singhal, D., Malick, W. 2012. Development of novel microprecipitated bulk powder (MBP) technology for manufacturing stable amorphous formulations of poorly soluble drugs. *International Journal of Pharmaceutics*. 438(1–2):53–60. DOI: 10.1016/j.ijpharm.2012.08.031.

Shin, T.H., Im, S.H., Goh, M.S., Lee, E.S., Ho, M.J., Kim, C.H., Kang, M.J. & Choi, Y.W. 2018. Novel extended-release multiple-unit system of imidafenacin prepared by fluid-bed coating technique. *AAPS PharmSciTech*. 19(6):2639–2645. DOI: 10.1208/s12249-018-1100-6.

Singhal, D. & Curatolo, W. 2004. Drug polymorphism and dosage form design: a practical perspective. *Advanced Drug Delivery Reviews*. 56:335–347. DOI: 10.1016/j.addr.2003.10.008.

Sri, J., Seethadevi, A., Prabha, K.S. & Muthuprasanna, P. 2012. Microencapsulation : A review. *International Journal of Pharma and Bio Sciences*. 3(1):509–531.

Steed, J.W. 2013. The role of co-crystals in pharmaceutical design. *Trends in Pharmacological Sciences*. 34(3):185–193. DOI: 10.1016/j.tips.2012.12.003.

Sugano, K., Okazaki, A., Sugimoto, S., Tavornvipas, S., Omura, A. & Mano, T. 2007. Solubility and dissolution profile assessment in drug discovery. *Drug Metabolism and Pharmacokinetics*. 22(4):225–254. DOI: 10.2133/dmpk.22.225.

Vidart, J.M.M., da Silva, T.L., Rosa, P.C.P., Vieira, M.G.A. & da Silva, M.G.C. 2018. Development of sericin/alginate particles by ionic gelation technique for the controlled release of diclofenac sodium. *Journal of Applied Polymer Science*. 135(12):1–12. DOI: 10.1002/app.45919.

Vilegave, K., Vidyasagar, G. & Chandankar, P. 2013. Preformulation studies of pharmaceutical new drug molecule & products: An overview. *American Journal of Pharmacy and Health Research*. 1(3):1–20.

Vishweshwar, P., Mcmahon, J.A., Bis, J.A. & Zaworotko, M.J. 2006. Pharmaceutical Co-Crystals. *Journal of Pharmaceutical Sciences*. 95(3):499–516. DOI: 10.1002/jps.

Vogt, M., Kunath, K. & Dressman, J.B. 2008. Dissolution enhancement of fenofibrate by micronization, cogrinding and spray-drying: Comparison with commercial preparations. *European Journal of Pharmaceutics and Biopharmaceutics*. 68(2):283–288. DOI: 10.1016/j.ejpb.2007.05.010.

Volpe, D.A. 2010. Application of method suitability for drug permeability classification. *The AAPS Journal*. 12(4):670–678. DOI: 10.1208/s12248-010-9227-8.

Vummaneni, V. & Nagpal, D. 2015. Taste Masking Technologies: An Overview and Recent Updates Taste Masking Technologies : An Overview and Recent. *International Journal of Research in Pharmaceutical and Biomedical Sciences. 3(2):510-524*.

Wagh, V.D. & Ghadlinge, S. V. 2009. Taste Masking Methods and Techniques in Oral Pharmaceuticals: Current Perspectives. *Journal of Pharmacy Research*. 2(6):1049–1054.

Walsh, J., Cram, A., Woertz, K., Breitkreutz, J., Winzenburg, G., Turner, R. & Tuleu, C. 2014. Playing hide and seek with poorly tasting paediatric medicines: Do not forget the excipients. *Advanced Drug Delivery Reviews*. 73:14–33. DOI: 10.1016/j.addr.2014.02.012.

Wang, Q., Fotaki, N. & Mao, Y. 2009. Biorelevant Dissolution : Methodology and Application in Drug Development. *Dissolution Technologies*. 16(3). DOI: 10.14227/DT160309P6.

Waterman, K.C. & Adami, R.C. 2005. Accelerated aging: Prediction of chemical stability of pharmaceuticals. *International Journal of Pharmaceutics*. 293:101–125. DOI: 10.1016/j.ijpharm.2004.12.013.

Xu, J., Bovet, L.L. & Zhao, K. 2008. Taste masking microspheres for orally disintegrating tablets. *International Journal of Pharmaceutics*. 359:63–69. DOI: 10.1016/j.ijpharm.2008.03.019.

Yang, J., Keller, M.W., Moor, J.S., White, S.R. & Sottos, N.R. 2008. Microencapsulation of isocyanates for self-healing polymers. *Macromolecules*. 41(24):9650–9655. DOI: 10.1021/ma801718v.

Zheng, X., Wu, F., Hong, Y., Shen, L., Lin, X. & Feng, Y. 2018. Developments in taste-masking techniques for traditional chinese medicines. *Pharmaceutics*. 10(157):1–22. DOI: 10.3390/pharmaceutics10030157.

Zuccotti, G.V. & Fabiano, V. 2011. Safety issues with ethanol as an excipient in drugs intended for pediatric use. *Expert Opinion on Drug Safety*. 10(4):499–502. DOI: 10.1517/14740338.2011.565328.

CHAPTER 3

A pharmaceutical perspective on efavirenz and potential microencapsulating materials

3.1 Introduction

As discussed in the two preceding chapters the lack of child-friendly dosage forms has been highlighted in combination with the serious situation of treating HIV-infected children with dosage forms which are not ideal for children. The life-long burden of HIV treatment has been disseminated and it became apparent that the development of dosage forms that will enhance treatment adherence of children will be of great benefit to the paediatric population. It was also mentioned that this study involves the investigation of microencapsulation as a potential pre-formulation strategy to facilitate taste-masking of ARVs typically used in the treatment regimens of children. Therefore, for the purpose of this study, efavirenz (EFV) was chosen as an ARV to explore microencapsulation strategies.

EFV is an FDA-approved non-nucleoside reverse transcriptase inhibitor (NNRTI) that shows to have good inhibitory activity against HIV-1 (Adkins & Noble, 1998). EFV forms part of the HAART treatment regimens and is approved for both adult and paediatric patients. Currently, as highlighted in Chapter 2, there is a worldwide need for paediatric-specific drug formulations. While the use of EFV is associated with proven ARV efficacy and is approved for use in the paediatric population, the available EFV formulations do not have ideal properties for optimal drug delivery in this population group. In this chapter, the physical, chemical, and pharmacokinetic properties of EFV will be reviewed while emphasising some challenges that have been encountered with the formulation of this drug by other researchers. Additionally, some strategies will be discussed that can be used to better formulate this ARV for the paediatric population.

3.2 Physico-chemical properties of efavirenz

EFV (**Figure 3.1**) is described as a benzoxazinone derivative with an empirical formula of $C_{14}H_9ClF_3NO_2$ (Rakhmanina & van den Anker, 2010). EFV is a non-hygroscopic, white crystalline powder with a molecular weight of 315.68 g/mol and it is classified as a BCS class II drug because of its low aqueous solubility (~4 µg/mL) and high permeability which may be attributed to its high lipophilicity (logP = 5.4) and ionisation constant (pKa) of 10.2 (Rakhmanina & van den Anker, 2010). The drug is soluble in organic solvents such as methanol and dichloromethane. Various solid-state forms of EFV have been identified over the years, which include both amorphous and crystalline forms of the compound (Mahapatra et al., 2010; Sathigari et al., 2012). A total of eight crystalline forms and one amorphous form have been patented for EFV since 1999. These solid-state forms are described in WO patent application publication No. 99/64405 and US patent application publications No. 8466279 B2, 5965729 and 2007/0026073 A1 (Clarke & Kukura, 1999; Radesca et al., 1999; Reddy et al.,

2013). The two crystalline forms most studied include those with orthorhombic and monoclinic crystal structures (Fandaruff *et al.*, 2014a). The melting point of EFV Form I, the most stable and common solid-state form, has been reported in literature as 136 - 141°C. (Kolhe, Chaudhari & More, 2013; Pinto, Cabral & de Sousa, 2014).

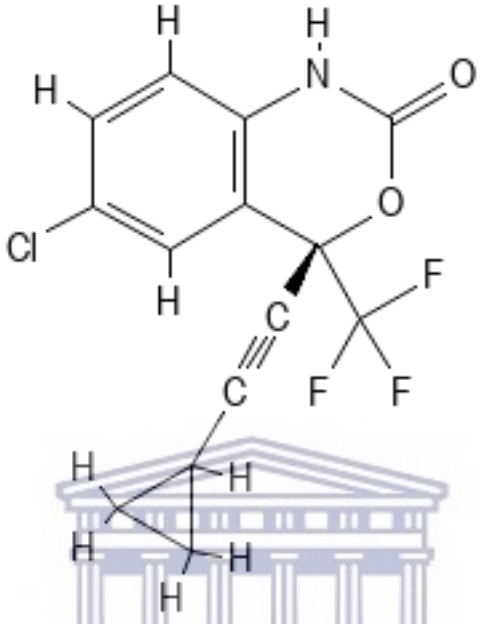

Figure 3.1: Chemical structure of efavirenz (National Center for Biotechnology Information, 2021).

EFV, like many other ARVs, exhibits photoreactivity in response to light exposure. EFV can undergo different photolysis processes that can result in structural changes and ultimately in altered physico-chemical properties (Abou-zied et al., 2002; Kakde & Kale, 2011; Jordaan & Shapi, 2017). EFV stability has also been reported to be affected by pH, oxidation, and humidity (Maurin et al., 2002; Kakde & Kale, 2011). These factors ideally need to form part of stability testing of any EFV formulations to ensure adequate safety and activity of the compound. This is further important when determining optimal storage conditions of proposed formulations. For example, EFV exhibits thermal stability up to a temperature of 255.8°C while being prone to light-mediated degradation. This means that special considerations are not needed for high temperatures when planning for packaging, distribution, and storage but the risk of light exposure does need to be accounted for when choosing storage containers and making recommendations for distribution and storage (Fandaruff *et al.*, 2014b).

3.3 Pharmacokinetic and pharmacodynamics properties of efavirenz

Peak EFV drug plasma concentrations are reached after 3 - 5 hours following oral administration (Maggiolo, 2009). The oral bioavailability of a single 600 mg dose is 40 - 50% and is increased when EFV is taken with food. The drug is highly protein-bound to human plasma proteins, especially to albumin (Adkins & Noble, 1998). EFV drug metabolism occurs in the liver where active EFV is converted to inactive hydroxylated metabolites by CYP2B6, a major isozyme part of the cytochrome P450 system. CYP2B6 is the cytochrome responsible for the 8-hydroxylation of EFV and a large proportion of its clearance (Rodriguez-Novoa et al., 2005). Several pharmacogenomics studies have shown that EFV metabolism and subsequent plasma levels are affected by the polymorphism of CYP2B6 (Tsuchiya et al., 2004; Nyakutira et al., 2008). In this regard, *in vitro* studies have shown that the CYP2B6 G516T polymorphism has been strongly associated with elevated EFV plasma concentrations and increased risk for adverse central nervous system effects. This polymorphism exhibits a high prevalence in the patients of African descent, the population that represents the majority of HIV-infected individuals (Nyakutira et al., 2008; Cabrera et al., 2009; Gengiah et al., 2015). The CYP2B6 T983C polymorphism has also been associated with increased levels of EFV (Wyen et al., 2008; Gengiah et al., 2015). Together, these clinical and *in vitro* studies suggest that CYP2B6 genotyping may allow clinicians to optimise ART in patients who initiate an EFV-based regimen. The drug exhibits a half-life of 40 – 55 hours, depending on the number of doses (Maggiolo, 2009). This long half-life allows for once-daily dosing but due to the low genetic barrier associated it is also prone to trigger viral resistance in cases of sub-optimal therapy.

3.4 Efavirenz in ART

As already described in Chapter 1, **section 1.3**, EFV forms a component of HAART and treatment guidelines recommend that EFV is combined with two NRTIs as a preferred first-line regimen for the treatment of HIV-1 infection. EFV is also considered one of the most cost-effective ARVs associated with sufficient viral suppression, making it ideal for low- to middle-income countries such as those in sub-Saharan Africa. According to the 2016 WHO forecasts for ARVs, EFV was one of the most in-demand APIs in 2016 (World Health Organization, 2016).

Currently, EFV is available in single once-a-day oral tablets and capsules, containing 50 – 600 mg of EFV (the recommended dose for adults is 600 mg/day). EFV is generally prescribed as part of HAART, where it is combined with tenofovir disoproxil fumarate (TDF)

and emtricitabine (FTC) in the commercially marketed fixed-dose regimen, Atripla (Esté & Cihlar, 2010). The recommended dosage for children according to the 2016 FDA guidelines is 25 mg/kg/day, with the additional consideration of the CYP2B6 genotype of the patient since CYP2B6 polymorphisms are known to affect EFV metabolism significantly. In the South African context, the Department of Health guides clinicians to prescribe 200 mg for children weighing 10 – 13.9 kg, 300 mg to children in the bodyweight range of 14 – 24.9 kg, 400 mg in children weighing 25 – 39.9 kg followed by these patients receiving the full adult dose of 600 mg once reaching a bodyweight of 40 kg and higher.

The ARV efficacy of EFV-based combination regimens is reportedly good, as has been demonstrated in many clinical trials around the world (Mugavero et al., 2008; Viljoen et al., 2010). EFV clinical outcomes have been compared to other ARVs, both as monotherapies and in combination therapies (Maggiolo, 2009). While multivariate analysis and large observational studies have reported that virological failure is less likely to occur when EFV instead of another third agent is used, clinical studies have shown more variable and complex results (Mugavero et al., 2008). Overall, no significant virological difference has been noted when comparing EFV with other NNRTIs. When compared to EFV, integrase inhibitors and CCR5 antagonists lead to greater increases in CD4 cell numbers and fewer adverse effects in the clinic (Markowitz et al., 2007; Maggiolo, 2009). It is however important to note that most EFV clinical studies included patients infected with HIV-1 subtype B; which is most prevalent in developed countries. It may therefore be suggested that clinical EFV studies involving patients infected with HIV-1 subtype C, the predominant subtype in developing countries, have to be prioritised to have more accurate and relevant understandings of EFV in the African clinical setting.

As mentioned in **Chapter 1, section 1.4**, TB and HIV co-infections occur relatively often as people who are infected with HIV or those who are malnourished are more likely to develop active TB because of suppressed immune systems. EFV is also considered as the NNRTI of choice in patients with tuberculosis (TB) co-infection (Cristofoletti et al., 2013; Phillips et al., 2020). EFV can be co-administered with TB medication without any required dosage adjustments or significant drug-drug interactions (Orrell et al., 2011).

As with any ARV, EFV use is associated with some adverse effects which include rashes, headache, dizziness, and fatigue (Adkins & Noble, 1998; Rakhmanina & van den Anker, 2010). One particular adverse effect associated with EFV-based regimens is the so-called burning mouth syndrome (BMS) (Page-Sharp et al., 2006). BMS has characteristically been described as the painful burning and itching of the oral cavity and lips (Gurvits & Tan, 2013). With palatability being a major determinant for paediatric patient adherence, the need to

develop a taste-masked EFV formulation is non-avoidable. Other associated disadvantages of EFV treatment include trouble sleeping, nightmares, and more frequent nausea compared to other ARVs (Orrell et al., 2011). The most frequently encountered side effects are neuropsychiatric symptoms such as agitation, hallucinations, depression, and amnesia. Neuropsychiatric symptoms can potentially impair the quality of life in some patients and can contribute to low adherence and virological failure (Maggiolo, 2009). However, these side effects are usually transient and resolve 2 - 4 weeks after treatment initiation, but have been shown to persist for up to 2 years in some patients (Rakhmanina & van den Anker, 2010). Adverse effects tend to be more extreme in slow EFV metabolisers and therefore genotype-driven dose adjustments need to be considered in all patients. Another shortcoming of EFV as part of HAART is the large inter-and intra-patient variability in the pharmacokinetics in children and adults mostly due to CYP2B6 polymorphisms (Brundage et al., 2004; Andriguetti et al., 2021).

It is worthy to note that EFV has been replaced in all recent treatment guidelines as a preferred first-line ARV (World Health Organisation, 2018; South African National Department of Health, 2019). A DTG based regimen is now recommended as the preferred first-line regimen for people living with HIV initiating ART. DTG has multiple advantages compared with EFV 600 mg, including lower potential for drug interactions, a shorter median time to viral suppression and a lower risk of resistance emergence. DTG is associated with a long half-life, low cost, low dosage and has already been formulated into a once-daily FDC. Co-administration of DTG with TB medication has also proved to be well-tolerated among TB/HIV patients. Additionally, DTG has also documented *in vitro* and clinical activity against HIV-2 infection, which is naturally resistant to EFV, making DTG more widely applicable (World Health Organisation, 2018). DTG is a brand new ARV on the market and subject to comprehensive clinical trials in children DTG will need to be formulated for the paediatric population. This process will take some time before an optimal DTG paediatric formulation is available with adequate clinical data to support its use in children. Even when this day comes, it will take some time to phase out EFV. Until then EFV remains one of the first choice ARVs for the paediatric population.

3.5 Efavirenz dosage forms and associated pharmaceutical formulation challenges

As with many ARVs, one of the most noticeable challenges with EFV dosage form formulation is the low aqueous solubility and poor bioavailability of the drug. This poses problems, particularly for paediatric formulations as poorly soluble ARVs are indeed soluble in some

organic compounds such as alcohol, yet alcohol is not ideal for paediatric formulations. Significant research has been done on improving the solubility of ARVs such as EFV. Solutions for improving EFV solubility have been focused on nano-crystals, complexation with cyclodextrins, encapsulation in polymeric micelles, micronisation, and co-micronisation. Several EFV formulations have been registered, developed and marketed since the approval of EFV by the FDA in 1998. These formulations range from oral tablets, capsules, liquids and even EFV loaded polymeric micelles. A formulation of fast dissolving EFV capsules/tablets using super-disintegrants was patented in 1998 by Mahooi-Morehead *et al.* but there is no proof that this formulation was marketed. Nanotechnologies have been employed to produce solid-lipid nanoparticles by a high-pressure homogenisation technique thereby improving the bioavailability of EFV (Gupta et al., 2017). Polymeric micelles made by incorporating EFV into the core of co-polymer micelles also exhibited improved EFV bioavailability (Chiappetta et al., 2010a). Chiappetta, Hocht & Sosnik (2010b) formulated a concentrated EFV solution by utilising water-immiscible triglyceride vehicles to achieve a highly concentrated aqueous EFV solution with apparent paediatric treatment potential. Taneja, Shilpi and Khatri (2016) used an antisolvent precipitation-ultrasonication technique to formulate EFV nanosuspensions with improved solubility and bioavailability compared to conventional drug suspensions (Taneja, Shilpi & Khatri, 2016). The use of polymers and cyclodextrins have also proven to increase the solubility and dissolution rate of EFV (Chadha et al., 2012). The use of polymer and cyclodextrin-based strategies have shown promising taste-masking capabilities (Szejtli & Szente, 2005). Similarly, the use of self-emulsifying drug delivery systems has resulted in increased drug solubility and bioavailability (Reddy, Reddy & Reddy, 2014). Solid self-emulsifying lipid formulations containing EFV have been produced using a series of oils, surfactants and solvents. These self-emulsifying lipid formulations exhibited increased solubility as well as increased dissolution rate compared to pure EFV (Reddy, Reddy & Reddy, 2014).

However, despite many of these techniques and approaches very little of this is applicable in the African setting as they are laborious and relatively expensive. A significant amount of the research on EFV has led to the production of suspensions, emulsions and solutions (Chiappetta et al., 2010a; Chiappetta, Hocht & Sosnik, 2010b). Some of these liquid formulations may well have improved palatability, but remain suboptimal in an African setting due to transport and storage challenges as discussed in Chapter 1. As mentioned, to children the taste of a drug is an important determinant of patient adherence and since many ARVs, including EFV, are inherently bitter it makes sense to adopt taste-masking strategies in an effort to address the adherence problem. Various taste-masking techniques have been developed as discussed in Chapter 2 where the focus has been given to spray-drying and

ionic gelation as taste-masking strategies. The next section of this chapter will focus on the two excipients used in this study as microencapsulation agents.

3.6 Excipients used as microencapsulation agents

In the process of microencapsulation through spray-drying the choice of coating material is an important factor. This is because the coating materials can interfere with the final product properties such as particle size, flowability and even shelf-life. The ideal properties of materials used for spray-drying include low viscosity at high concentrations, high solubility, good emulsifying capability, film-forming ability and also acceptable thermal properties (Quintero, Rojas & Ciro, 2018).

Recently, potential encapsulating agents with a natural origin have been given mentionable attention because of their safety in humans. One such example, that has been extensively studied, is vegetable proteins. These include proteins isolated from soybeans, peas, wheat, corn and barley. Vegetable proteins have many properties that render them attractive for use in drug development. Vegetable proteins are a renewable, sustainable and cost-effective option to obtain effective microencapsulation of compounds (Nesterenko et al., 2013). Their biodegradability, nutritional value and non-allergenic properties further add to the advantages of using vegetable proteins in the pharmaceutical field. Additionally, these compounds exhibit excellent gelling, film-forming, emulsifying and foaming capacity which further supports their use as encapsulating agents (Quintero, Rojas & Ciro, 2018). However, some vegetable proteins tend to have relatively low water solubility and exhibit high viscosity at high protein concentrations. These properties are not ideal for microencapsulation, but proteins can however be modified in order to overcome these limitations or enhance and diversify their functionality. Typical approaches used to modify vegetable proteins include enzymatic hydrolysis, deamination and acetylation. Protein modification can result in altered size, shape and functional properties (Nesterenko et al., 2014). Different types of plant proteins can be used for encapsulation. Soy proteins are widely available making them easy and inexpensive to source and these proteins are good barriers to oxygen, oil and carbon dioxide transfer but soy protein is associated with allergies. Proteins isolated from chickpeas exhibit non-allergenic properties as well as better solubility and emulsifying properties compared to soy protein isolate (Nesterenko et al., 2013). Proteins isolated from sunflower seeds have also become a popular choice linked to their availability in areas where soy is not common as well as their excellent functional properties. However, the quality of sunflower seed proteins are affected by phenolic compounds which may be detrimental to product quality (Nesterenko et al., 2013). The choice of protein most suitable for a particular microencapsulation process will depend

on the physico-chemical properties of the compound to be encapsulated as well as the desired final properties of the encapsulated product. In this study, it was decided to explore pea protein isolate as a potential microencapsulant for EFV through the process of spray-drying and the next few paragraphs will highlight previous studies which informed towards the successful use of this vegetable protein isolate in microencapsulation, either through spray-drying or coacervation.

3.7 Pea protein isolate as a microencapsulating agent

Pea protein isolates (PPI) are extracted from pea seeds and consist mainly of globulins. The globulin fraction in pea proteins contains three subfractions: legumin, vicilin and convicilin. These protein subfractions are found in all pea protein samples but because their ratios can vary, the emulsifying properties of different samples can vary. PPI possesses good gel-forming and emulsifying properties making it an ideal candidate for microencapsulation. The method used for the preparation of PPI from raw pea material can influence the functional properties of the final PPI product. Also, it should be noted that PPI prepared from different raw material batches will not always have precisely the same functional properties (Barać et al., 2015). Considering this, it may be beneficial to characterise each PPI batch before pharmaceutical processing.

The use of proteins in microencapsulation *via* spray-drying has been particularly useful in reducing the surface stickiness of compounds with a high content of low molecular weight carbohydrates (Jayasundera et al., 2011). This means that the powder product is less likely to adhere to the spray-dryer surfaces, which results in more powder collection, higher product yield and economic appeal. This is because of the surface-active property of proteins and their film-forming ability which can overcome the stickiness of solutions upon drying (Adhikari et al., 2009). PPI has been successfully used as an emulsifier for the microencapsulation of flaxseed oil (Bajaj, Tang & Sablani, 2015), lipophilic ingredients (Gharsallaoui et al., 2012), ascorbic acid and conjugated linoleic acid (Pereira et al., 2009; Costa et al., 2015). The use of PPI as an encapsulating agent has shown high microencapsulation efficiencies and good core retention with improved solubility and dissolution profiles. Pea proteins also exhibit anti-oxidant properties such that these proteins might improve the oxidative stability of microencapsulated particles. This holds additional benefits for the use of proteins as encapsulants in drug formulation as it may improve product stability and shelf-life (Tamm et al., 2016).

Polysaccharides are often added to proteins for microencapsulation and has been shown to increase the stability of emulsions with regards to pH, temperature and ionic strength.

Polysaccharide/protein interactions give new functions to pea proteins without chemical or enzymatic modification, particularly improved solubility, foaming and surfactant properties. The combination of proteins and polysaccharides has also been shown to enhance emulsion stability and protection of the core material rendering them valuable wall materials (Nesterenko et al., 2014). Polysaccharides like modified starches, gum arabic, lactose, and maltodextrin exhibit good oxidative stability but poor emulsifying capacity and emulsifying stability. Some of the advantageous properties of carbohydrates for microencapsulation are their low viscosities at high concentrations and excellent film-forming properties (da Silva et al., 2012; Fernandes et al., 2016; Pauck et al., 2017). One particularly useful carbohydrate, inulin, will be discussed in more detail below.

3.8 Inulin as a microencapsulating agent

Inulin (IN) (**Figure 3.2**) is a natural fructose poly- or oligosaccharide with unique physico-chemical properties providing a wide range of uses in the food and pharmaceutical industry. IN is a dietary fiber with long chain lengths found in various fruits and vegetables and is generally biochemically inert, non-toxic and can form hydrogels (Silva et al., 2016). The recent increased understanding of the chemistry and behaviour of IN has led to the increased use thereof in drug delivery systems. Properties that motivate its use in pharmaceutical applications include its low-calorie nature, ability to increase drug dissolution rates, and low viscosity of solutions (Roberfroid, 2007). Furthermore, IN exhibits various properties that render it a good candidate for spray-drying such as its gelling ability and prebiotic properties, relating to some form of health benefit. The degree of polymerisation of IN largely determines the physico-chemical characteristics such as morphology, solubility, rheology, thermal properties and physical and chemical stability associated with this polysaccharide. The variability of these properties renders IN useful for a wide range of pharmaceutical applications but also illustrates the need to characterise in a batch-wise manner (Mensink et al., 2015).

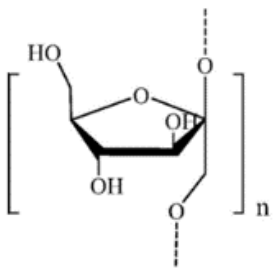

Figure 3.2: Molecular structure of inulin (Image adapted from Dong *et al.* (2014)).

Often carbohydrates are incorporated together with proteins to improve their emulsifying properties and to increase the viscosity of the final emulsion to a viscosity that is adequate for spray-drying. Recently, blends of PPI and maltodextrins have been utilised to encapsulate ascorbic acid through spray-drying and the resulting spherical microcapsules exhibited high core content retention (Gharsallaoui et al., 2012). In this project, the objective is to combine PPI and the polysaccharide, IN for the purpose of spray-drying and thereby encapsulating EFV.

3.9 Sodium alginate as microencapsulating agent *via* ionic gelation

Alginates are a family of natural, anionic copolymers with members consisting of varying proportions of guluronic and manuronic acid subunits, arranged in irregular patterns. The chemical nature of alginates renders these polymers suitable for chemical reactions and linkages due to the presence of hydroxyl and carbonyl groups within the backbone (**Figure 3.3**) (Borba et al., 2016). Alginates are extracted from brown algae through treatment with alkaline solutions. After filtration, the extract is precipitated with sodium chloride to produce an alginate salt. Further purification and conversion steps are performed to produce water-soluble sodium alginate powder. This water-soluble powder can then be used to produce a sodium alginate (SA) solution, the precursor for gel production (Lee & Mooney, 2012). More than 200 different alginates are manufactured and the particular ratio of guluronic and manuronic subunits within a batch of alginate is determined by the natural source from which it was extracted (Lee & Mooney, 2012). These different alginates exhibit different physical properties and drug release tendencies. The relative ratio of guluronic and manuronic subunits determines some physical properties of the gel such as mechanical strength, swelling behaviour, physical stability, viscoelasticity and transmittancy. For example, a higher ratio of guluronic units tends to impose stronger mechanical strength to the gel since these subunits exhibit a greater affinity for divalent cations and therefore lead to stronger ionic binding and physically stronger gels (Hecht & Srebnik, in press; Tønnesen & Karlsen, 2002). It is advisable that only ultrapure grades of alginates should be used in pharmaceutical applications. Alginate gelation occurs when divalent, cationic metal ions, most often calcium ions (Ca^{2+}), interact ionically with the negatively charged guluronic acid residues. The divalent metal ions have the ability to bind to two alginate chains simultaneously thereby resulting in cross-linking of the two chains (**Figure 3.4**). This calcium-dependent gelation results in the formation of a three-dimensional gel matrix. Varying affinities for alginates are exhibited by various cations and this selective ionic binding is the basis on which typical ionotropic hydrogels are formed. The strength of cross-linking relates to the particular cation that is used with the order of strength being: trivalent cations > divalent cations > monovalent cations. Calcium ions remain the most

popular for use in drug delivery systems despite not showing the strongest interaction strength. The preference of using Ca^{2+}- ions relates to the natural occurrence thereof, and subsequent safety, in the human body. The use of other divalent cations such as Pb^{2+}, Cu^{2+}, and Cd^{2+} is limited within drug delivery systems due to their associated toxicity. The use of Zn^{+2} has also been explored with success in drug delivery systems, but Zn-alginate gels are generally loose and mechanically weak (Hu et al., 2021).

Through drop-wise addition of a SA aqueous solution into a calcium chloride solution, calcium alginate beads can be produced. The gelation of the alginate is mediated by the ionic interaction of Ca^{2+}-ions with the carboxyl ($-COO^-$) groups of the guluronic acid residues (Bajpai & Sharma, 2004). This ionic interaction links guluronic monomers in different alginate molecules together resulting in the formation of the typical 'egg-box' structure as first described by Grant et al. (1973) (**Figures 3.3 and 3.4**). The solubility of alginates in water at room temperature without the need for heating and cooling cycles makes alginates particularly attractive for use in drug delivery systems. The multiparticulate nature of alginates imposes the advantages of reduced risk of dose dumping and reduced risk of local irritation (Patel et al., 2016). Also, the presence of carboxylic groups in the alginate structure confers pH sensitivity to this polymer which renders it particularly valuable in targeted drug delivery (Agüero et al., 2017). Using alginates for microencapsulation and drug delivery holds many other advantages such as high stability, minimized loss of encapsulated material, cost-effectiveness, suitability for acid and heat-sensitive drugs, non-toxic and biocompatibility (Almeida & Almeida, 2004; Patel et al., 2016).

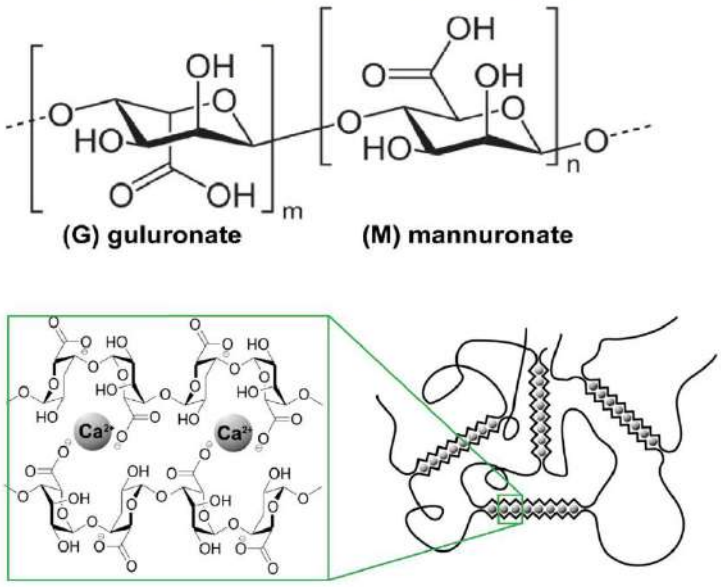

Figure 3.3: The structure of guluronate and mannuronate subunits of alginates and the cross-linking of the alginate chains as a result of calcium cation addition in the typical egg-box model as first described by Grant et al. (1973). Figure adapted from Bruchet and Melman (2015).

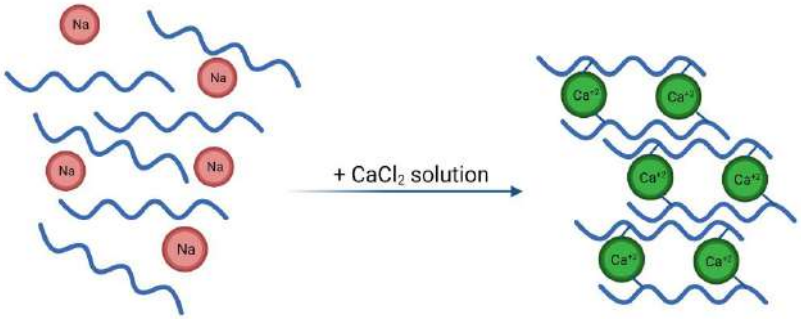

Figure 3.4: Schematic showing the replacement of sodium ions by calcium ions resulting in the cross-linking of alginate chains to form mechanically strong gel structures. [Prepared using BioRender.com]

Over the last 25 years, drug-loaded calcium-crosslinked alginate particles have been developed as a unique drug delivery system for an array of pharmaceutical drugs. Their use in formulations includes both single and multiple components containing beads, both water-soluble and poorly water-soluble drug entrapment, immediate and delayed-release dosage forms as well as formulation with or without the addition of polymer or hydrogel components. Ibuprofen-loaded alginate particles for oral drug delivery have been developed for controlled release by Arica *et al.*, (2005). The encapsulation efficiency achieved was extremely low, ranging between 1.15% and 14.8 but tended to increase as the concentration of the alginate polymer increased. It was noted that the smaller the diameter of the beads and the lower the alginate concentration used the faster the observed rate of drug release was. The encapsulation of diclofenac sodium with alginates following the dispersion in the lipid polymer, Compritol® 888 delivered similar results with greater polymer concentrations being associated with slower drug release (Mirghani et al., 2000). Patel, Sher and Pawar, (2006) achieved an encapsulation efficiency of between 81 and 96% with the water-soluble drug, metronidazole. They also illustrated that, for water-soluble drugs, an increase in curing time is associated with reduced encapsulation efficiency and subsequently also lower drug content. This was attributed to the rapid release of the drug from the alginate matrix and solubilisation into the aqueous curing medium. El-Kamel, Al-Gohary and Hosny (2003) reported a positive correlation between encapsulation efficiency and the SA concentration. They also reported higher encapsulation efficiencies when using higher calcium chloride concentrations. The same observation was also made by Mirghani *et al.*, (2000) and Rastogi *et al.*, (2007).

It has been suggested that the calcium alginate matrix formed is usually very permeable and therefore controlling the release of water-soluble drugs has proven difficult. Subsequently, the use of alginate beads is currently preferentially suggested for delivering either poorly water-

soluble drugs or macromolecules, especially if delayed/sustained drug release is desired (Almeida & Almeida, 2004). With this being said, the incorporation of water-soluble drugs into alginate beads has been very successful, with high encapsulation efficiencies and drug loading being achieved when short curing times are used. However, due to the surrounding aqueous environment, the inherent solubility of the drug in a matrix system resulted in rapid release of the drug from the matrix system, meaning that delayed release of water-soluble drugs was not achieved (Patel et al., 2016).

3.10 Conclusion

As discussed in Chapter 1, the development of paediatric drug formulations has been lagging behind adult ARV formulations. To allow HIV-positive children a fair chance to live full lives pharmaceutical formulations developed specifically for the paediatric population are necessary. In this chapter, EFV as an ARV being prescribed to children suffering from HIV has been discussed in terms of its known physico-chemical properties, pharmacodynamics, and pharmacokinetics as well as the incorporation thereof in pharmaceutical formulations. From a thorough literature review, it became apparent that EFV dosage formulation strategies are greatly affected by the poor solubility of this ARV. The chapter further discussed the rationale for incorporating PPI and IN as microencapsulating excipients to be used in a spray-drying process to potentially facilitate the microencapsulation of EFV. Since two microencapsulation strategies were investigated in this study, sodium alginate and the ionic gelation thereof with calcium cations were also discussed. The following section of the thesis will be dedicated to the experimental part which was embarked on in an effort to achieve possible taste-masking of the bitter-tasting EFV.

3.11 References

Abou-zied, O.K., Jimenez, R., Thompson, E.H.Z., Millar, D.P. & Romesberg, F.E. 2002. Solvent-Dependent Photoinduced Tautomerization of 2-(2′-Hydroxyphenyl) benzoxazole. *Journal of Physical Chemistry A*. 106:3665–3672. DOI: 10.1021/jp013915o

Adhikari, B., Howes, T., Bhandari, B.R. & Langrish, T.A.G. 2009. Effect of addition of proteins on the production of amorphous sucrose powder through spray drying. *Journal of Food Engineering*. 94(2):144–153. DOI: 10.1016/j.jfoodeng.2009.01.029.

Adkins, J.C. & Noble, S. 1998. Efavirenz. *Drugs*. 56(6):1055–1064. DOI: 10.2165/00003495-199856060-00014.

Agüero, L., Zaldivar-Silva, D., Peña, L. & Dias, M. 2017. Alginate microparticles as oral colon drug delivery device: A review. *Carbohydrate Polymers*. 168:32–43. DOI: 10.1016/j.carbpol.2017.03.033.

Almeida, P. & Almeida, A. 2004. Cross-linked alginate-gelatine beads: a new matrix for controlled release of pindolol. *Journal of Controlled Release*. 97(3):431–439. DOI: 10.1016/j.conrel.2004.03.015.

Andriguetti, B.N., Van Schalkwyk, H.K., Barrat, D.T., Tucci, J., Pumuye, P. & Somogyi, A.A. 2021. Large variability in plasma efavirenz concentration in Papua New Guinea HIV / AIDS patients associated with high frequency of CYP2B6 516T allele. *Clinical and Translational Science*. (May):1–11. DOI: 10.1111/cts.13120.

Arica, B., Çaliş, S., Atilla, P., Durlu, N.T., Çakar, N., Kaş, H.S. & Hincal, A.A. 2005. In vitro and in vivo studies of ibuprofen-loaded biodegradable alginate beads. *Journal of Microencapsulation*. 22(2):153–165. DOI: 10.1080/02652040400026319.

Bajaj, P.R., Tang, J. & Sablani, S.S. 2015. Pea Protein Isolates: Novel Wall Materials for Microencapsulating Flaxseed Oil. *Food and Bioprocess Technology*. 8(12):2418–2428. DOI: 10.1007/s11947-015-1589-6.

Bajpai, S.K. & Sharma, S. 2004. Investigation of swelling/degradation behaviour of alginate beads crosslinked with Ca2+ and Ba2+ ions. *Reactive and Functional Polymers*. 59(2):129–140. DOI: 10.1016/j.reactfunctpolym.2004.01.002.

Barać, M.B., Pešić, M.B., Stanojević, S.P., Kostić, A.Z. & Čabrilo, S.B. 2015. Techno-functional properties of pea (Pisum sativum) protein isolates-a review. *Acta Periodica Technologica*. 46:1–18. DOI: 10.2298/APT1546001B.

Borba, P.A.A., Pinotti, M., De Campos, C.E.M., Pezzini, B.R. & Stulzer, H.K. 2016. Sodium alginate as a potential carrier in solid dispersion formulations to enhance dissolution rate and apparent water solubility of BCS II drugs. *Carbohydrate Polymers*. 137:350–359. DOI: 10.1016/j.carbpol.2015.10.070.

Brundage, R.C., Yong, F.H., Fenton, T., Spector, S.A., Starr, S.E. & Fletcher, C. V. 2004. Intrapatient Variability of Efavirenz Concentrations as a Predictor of Virologic Response to Antiretroviral Therapy. *Antimicrobial Agents and Chemotherapy*. 48(3):979–984. DOI: 10.1128/AAC.48.3.979-984.2004.

Cabrera, S.E., Santos, D., Valverde, M.P., Domínguez-Gil, A., González, F., Luna, G. & García, M.J. 2009. Influence of the cytochrome P450 2B6 genotype on population pharmacokinetics of efavirenz in human immunodeficiency virus patients. *Antimicrobial Agents and Chemotherapy*. 53(7):2791–2798. DOI: 10.1128/AAC.01537-08.

Chadha, R., Arora, P., Bhandari, S. & Jain, D.V.S. 2012. Effect of hydrophilic polymer on complexing efficiency of cyclodextrins towards efavirenz-characterization and thermodynamic parameters. *Journal of Inclusion Phenomena and Macrocyclic Chemistry*. 72(3–4):275–287. DOI: 10.1007/s10847-011-9972-z.

Chiappetta, D.A., Hocht, C., Taira, C. & Sosnik, A. 2010a. Efavirenz-loaded polymeric micelles for pediatric anti-HIV pharmacotherapy with significantly higher oral bioavailaibility. *Nanomedicine*. 5(1):11–23. DOI: 10.2217/nnm.09.90.

Chiappetta, D.A., Hocht, C. & Sosnik, A. 2010b. A Highly Concentrated and Taste-Improved Aqueous Formulation of Efavirenz for a More Appropriate Pediatric Management of the Anti-HIV Therapy A Highly Concentrated and Taste-Improved Aqueous Formulation of Efavirenz for a More Appropriate Pediatric Manage. *Current HIV Research*. 8(3):223–231. DOI: 10.2174/157016210791111142.

Clarke, W. & Kukura, J. 1999. *Process for crystallization of a reverse transcriptase inhibitor using an anti-solvent.* Patent No. 5965729. USA.

Costa, A.M.M., Nunes, J.C., Lima, B.N.B., Pedrosa, C., Calado, V., Torres, A.G. & Pierucci, A.P.T.R. 2015. Effective stabilization of CLA by microencapsulation in pea protein. *Food Chemistry*. 168:157–166. DOI: 10.1016/j.foodchem.2014.07.016.

Cristofoletti, R., Nair, A., Abrahamsson, B., Groot, D., Kopp, S., Langguth, P., Polli, J., Shah, V. & Dressman, J. 2013. Biowaiver Monographs for Immediate Release Solid Oral Dosage Forms: Efavirenz. Journal of Pharmaceutical Sciences, 102(2):318-329. DOI: 10.1002/jps.23380

da Silva, F.C., Rodrigues, C., De Alencar, S.M., Thomazini, M., Carvalho, J.C. De, Pittia, P. & Favaro-trindade, C.S. 2012. Assessment of production efficiency , physicochemical properties and storage stability of spray-dried propolis , a natural food additive , using gum Arabic and OSA starch-based carrier systems. *Food and Bioproducts Processing*. 91(February):28–36.

Dong, F., Zhang, J., Yu, C., Li, Q., Ren, J., Wang, G., Gu, G. & Guo, Z. 2014. Synthesis of amphiphilic aminated inulin via ' click chemistry ' and evaluation for its antibacterial activity. *Bioorganic & Medicinal Chemistry Letters*. 24(18):4590–4593. DOI: 10.1016/j.bmcl.2014.07.029.

El-Kamel, A., Al-Gohary, O. & Hosny, E. 2003. Alginate-diltiazem hydrochloride beads : optimization of formulation factors , in vitro and in vivo availability. *Journal of Microencapsulation*. 20(2):211–225. DOI: 10.1080/02652040210162568.

Esté, J.A. & Cihlar, T. 2010. Current status and challenges of antiretroviral research and therapy. *Antiviral Research*. 85(1):25–33. DOI: 10.1016/j.antiviral.2009.10.007.

Fandaruff, C., Rauber, G.S., Araya-Sibaja, A.M., Pereira, R.N., De Campos, C.E.M., Rocha, H.V.A., Monti, G.A., Malaspina, T., Silva, M.A.S., Cuffini, S.L. 2014a. Polymorphism of anti-HIV drug efavirenz: Investigations on thermodynamic and dissolution properties. *Crystal Growth and Design*. 14(10):4968–4975. DOI: 10.1021/cg500509c.

Fandaruff, C., Araya-Sibaja, A.M., Pereira, R.N., Hoffmeister, C.R.D., Rocha, H.V.A. & Silva, M.A.S. 2014b. Thermal behavior and decomposition kinetics of efavirenz under isothermal and non-isothermal conditions. *Journal of Thermal Analysis and Calorimetry*. 115(3):2351–2356. DOI: 10.1007/s10973-013-3306-x.

Fernandes, R.V., Botrel, D.A., Silva, E.K., Borges, S.V., de Oliveira, C.R., Yoshida, M.I., de Andrade Feitosa, J.P. & de Paula, R.C.M. 2016. Cashew gum and inulin: New alternative for ginger essential oil microencapsulation. *Carbohydrate Polymers*. 153:133–142. DOI: 10.1016/j.carbpol.2016.07.096.

Gengiah, T.N., Botha, J.H., Yende-Zuma, N., Naidoo, K. & Abdool Karim, S.S. 2015. Efavirenz dosing: Influence of drug metabolizing enzyme polymorphisms and concurrent tuberculosis treatment. *Antiviral Therapy*. 20(3):297–306. DOI: 10.3851/IMP2877.

Gharsallaoui, A., Saurel, R., Chambin, O. & Voilley, A. 2012. Pea (Pisum sativum, L.) Protein Isolate Stabilized Emulsions: A Novel System for Microencapsulation of Lipophilic Ingredients by Spray Drying. *Food and Bioprocess Technology*. 5(6):2211–2221. DOI: 10.1007/s11947-010-0497-z.

Gupta, S., Kesarla, R., Chotai, N., Misra, A. & Omri, A. 2017. Systematic approach for the formulation and optimization of solid lipid nanoparticles of efavirenz by high pressure homogenization using design of experiments for brain targeting and enhanced bioavailability. *BioMed Research International*. DOI: 10.1155/2017/5984014.

Gurvits, G.E. & Tan, A. 2013. Burning mouth syndrome. *World Journal of Gastroenterology*. 19(5):665–672. DOI: 10.3748/wjg.v19.i5.665.

Hecht, H. & Srebnik, S. (in press). Structural Characterization of Sodium Alginate and Calcium Alginate. *Biomacromolecules*. 17:2160−2167. DOI: 10.1021/acs.biomac.6b00378.

Hu, C., Lu, W., Mata, A., Nishinari, K. & Fang, Y. 2021. Ions-induced gelation of alginate: Mechanisms and applications. *International Journal of Biological Macromolecules*. 177:578–588. DOI: 10.1016/j.ijbiomac.2021.02.086.

Jayasundera, M., Adhikari, B., Howes, T. & Aldred, P. 2011. Surface protein coverage and its implications on spray-drying of model sugar-rich foods: Solubility, powder production and characterisation. *Food Chemistry*. 128(4):1003–1016. DOI: 10.1016/j.foodchem.2011.04.006.

Jordaan, M.A. & Shapi, M. 2017. Investigation of the solvent-dependent photolysis of a

nonnucleoside reverse-transcriptase inhibitor, antiviral agent efavirenz. *Antiviral Chemistry and Chemotherapy*. 25(3):94–104. DOI: 10.1177/2040206617730170.

Kakde, R.B. & Kale, D.L. 2011. Stability Study and Densitometric Determination of Efavirenz in Tablet by Normal Phase Thin Layer Chromatography. *International Journal of PharmTech Research*. 3(3):1889–1896.

Kolhe, S., Chaudhari, P. & More, D. 2013. Dissolution Enhancement of Poorly Water Soluble Efavirenz by Hot Melt Extrusion Technique. *International Journal of Drug Development & Research*. 5(2):354–361.

Lee, K.Y. & Mooney, D.J. 2012. Alginate: Properties and biomedical applications. *Progress in Polymer Science*. 37(1):106–126. DOI: 10.1016/j.progpolymsci.2011.06.003.

Maggiolo, F. 2009. Efavirenz: A decade of clinical experience in the treatment of HIV. *Journal of Antimicrobial Chemotherapy*. 64(5):910–928. DOI: 10.1093/jac/dkp334.

Mahapatra, S., Thakur, T.S., Joseph, S., Varughese, S. & Desiraju, G.R. 2010. New solid state forms of the anti-HIV drug efavirenz. Conformational flexibility and high *Z′* issues. *Crystal Growth and Design*. 10(7):3191–3202. DOI: 10.1021/cg100342k.

Markowitz, M., Nguyen, B.Y., Gotuzzo, E., Mendo, F., Ratanasuwan, W., Kovacs, C., Prada, G., Morales-Ramirez, J.O., Crumpacker, C.S., Isaacs, R.D., Gilde, L.R., Wan, H., Miller, M.D., Wenning, L.A., Teppler, H. 2007. Rapid and durable antiretroviral effect of the HIV-1 integrase inhibitor raltegravir as part of combination therapy in treatment-naive patients with HIV-1 infection: Results of a 48-week controlled study. *Journal of Acquired Immune Deficiency Syndromes*. 46(2):125–133. DOI: 10.1097/QAI.0b013e318157131c.

Maurin, M.B., Rowe, S.M., Blom, K. & Pierce, M. 2002. Kinetics and mechanism of hydrolysis of Efavirenz. *Pharmaceutical Research*. 19(4):347–359. DOI: 10.1023/a:1015160132290.

Mensink, M.A., Frijlink, H.W., Van Der Voort Maarschalk, K. & Hinrichs, W.L.J. 2015. Inulin, a flexible oligosaccharide. II: Review of its pharmaceutical applications. *Carbohydrate Polymers*. 134:418–428. DOI: 10.1016/j.carbpol.2015.08.022.

Mirghani, A., Idkaidek, N.M., Salem, M.S. & Najib, N.M. 2000. Formulation and Release Behavior of Diclofenac Sodium in Compritol 888 Matrix Beads Encapsulated in Alginate Formulation and Release Behavior of Diclofenac Sodium in Compritol 888 Matrix Beads Encapsulated in Alginate. *Drug Development and Industrial Pharmacy*. 26(7):791–795. DOI: 10.1081/DDC-100101301.

Mugavero, M.J., May, M., Harris, R., Saag, M.S., Costagliola, D., Egger, M., Günthard, H.F., Dabis, F., Hogg, R., De Wolf, F., Fatkenheuer, G., Gill, M.J., Justice, A., Monforte, A., Lampe, F., Miro, J.M., Staszewski, S. & Sterne, J.A.C. 2008. Does short-term virologic failure translate to clinical events in antiretroviral-naïve patients initiating antiretroviral therapy in clinical practice? *AIDS*. 22(18):2481–2492. DOI: 10.1097/QAD.0b013e328318f130.

Nesterenko, A., Alric, I., Silvestre, F. & Durrieu, V. 2013. Vegetable proteins in microencapsulation: A review of recent interventions and their effectiveness. *Industrial Crops and Products*. 42(1):469–479. DOI: 10.1016/j.indcrop.2012.06.035.

Nesterenko, A., Alric, I., Violleau, F., Silvestre, F. & Durrieu, V. 2014. The effect of vegetable protein modifications on the microencapsulation process. *Food Hydrocolloids*. 41:95–102. DOI: 10.1016/j.foodhyd.2014.03.017.

National Center for Biotechnology Information. "PubChem Compound Summary for CID 64139,Efavirenz" *PubChem*, https://pubchem.ncbi.nlm.nih.gov/compound/Efavirenz. [Accessed: 18 October, 2021].

Nyakutira, C., Röshammar, D., Chigutsa, E., Chonzi, P., Ashton, M., Nhachi, C. & Masimirembwa, C. 2008. High prevalence of the CYP2B6 516G→T(*6) variant and effect on

the population pharmacokinetics of efavirenz in HIV/AIDS outpatients in Zimbabwe. *European Journal of Clinical Pharmacology*. 64(4):357–365. DOI: 10.1007/s00228-007-0412-3.

Orrell, C., Cohen, K., Conradie, F., Zeinecker, J., Ive, P., Sanne, I. & Wood, R. 2011. Efavirenz and rifampicin in the South African context: Is there a need to dose-increase efavirenz with concurrent rifampicin therapy? *Antiviral Therapy*. 16(4):527–534. DOI: 10.3851/IMP1780.

Page-Sharp, M., Kristensen, J.H., Beran, R.G., Rampono, J., Hale, T.W., Kohan, R. & Ilett, K.F. 2006. Burning Mouth Syndrome Due to Efavirenz Therapy. *The Annals of Pharmacotherapy*. 40:1471–1472. DOI: 10.1345/aph.1G667.

Patel, N., Lalwani, D., Gollmer, S., Injeti, E., Sari, Y. & Nesamony, J. 2016. Development and evaluation of a calcium alginate based oral ceftriaxone sodium formulation. *Progress in Biomaterials*. 5(2):117–133. DOI: 10.1007/s40204-016-0051-9.

Patel, Y.L., Sher, P. & Pawar, A.P. 2006. The Effect of Drug Concentration and Curing Time on Processing and Properties of Calcium Alginate Beads Containing Metronidazole by Response Surface Methodology. *AAPS PharmSciTech*. 7(4). DOI: 10.1208/pt070486.

Pauck, C., Beer, D. De, Aucamp, M., Liebenberg, W., Stieger, N., Human, C. & Joubert, E. 2017. LWT - Food Science and Technology Inulin suitable as reduced-kilojoule carrier for production of microencapsulated spray-dried green Cyclopia subternata (honeybush) extract. *LWT - Food Science and Technology*. 75:631–639. DOI: 10.1016/j.lwt.2016.10.018.

Pereira, H.V.R., Saraiva, K.P., Carvalho, L.M.J., Andrade, L.R., Pedrosa, C. & Pierucci, A.P.T.R. 2009. Legumes seeds protein isolates in the production of ascorbic acid microparticles. *Food Research International*. 42(1):115–121. DOI: 10.1016/j.foodres.2008.10.008.

Phillips, A.N., Bansi-Matharu, L., Venter, F., Havlir, D., Pozniak, A., Kuritzkes, D.R., Wensing, A., Lundgren, J.D., Pillay, D., Mellors, J., Cambiano, V., Jahn, A., Apollo, T., Mugurungi, O., Da Silva, J., Raizes, E., Ford, N., Siberry, G.K., Gupta, R.K., Barnabas, R., Revill, P., Cohn, J., Calmy, A., Bertagnolio, S. 2020. Updated assessment of risks and benefits of dolutegravir versus efavirenz in new antiretroviral treatment initiators in sub-Saharan Africa: modelling to inform treatment guidelines. *The Lancet HIV*. 3018(19):1–8. DOI: 10.1016/S2352-3018(19)30400-X.

Pinto, E.C., Cabral, L.M. & de Sousa, V.P. 2014. Development of a discriminative intrinsic dissolution method for efavirenz. *Dissolution Technologies*. 21(2):31–40. DOI: 10.14227/DT210214P31.

Quintero, J., Rojas, J. & Ciro, G. 2018. Vegetable proteins as potential encapsulation agents: a review. *Food Research*. 2(3):208–220. DOI: 10.26656/fr.2017.2(3).261.

Radesca, L., Maurin, M., Rabel, S. & Moore, J. 1999. *Crystalline efavirenz*. Patent No. WO 99/64405. USA.

Rakhmanina, N.Y. & van den Anker, J.N. 2010. Efavirenz in the therapy of HIV infection. *Expert Opinion on Drug Metabolism & Toxicology*. 6(1):95–103. DOI: 10.1517/17425250903483207.

Rastogi, R., Sultana, Y., Aqil, M., Ali, A., Kumar, S., Chuttani, K. & Mishra, A.K. 2007. Alginate microspheres of isoniazid for oral sustained drug delivery. *International Journal of Pharmaceutics*. 334:71–77. DOI: 10.1016/j.ijpharm.2006.10.024.

Reddy, M.S., Reddy, N.S. & Reddy, S.M. 2014. Solubility enhancement of poorly water soluble drug efavirenz by solid self emulsifying drug delivery systems. *International Journal of Pharma Research & Review*. 3(4):20–28. Available: http://www.ijpr.in/Data/Archives/2014/april/0602201402.pdf.

Reddy, P., Reddy, K., Reddy, R., Reddy, D. & Reddy, K. 2013. *Polymorphisms of efavirenz*.

Patent No. US 8466279 B2. USA.

Roberfroid, M.B. 2007. Inulin-Type Fructans: Functional Food Ingredients. *The Journal of Nutrition*. (5):2493–2502.

Rodriguez-Novoa, S., Barreiro, P., Rendon, A., Jimenez-Nacher, I., Gonzalez-Lahoz, J. & Soriano, V. 2005. Influence of 516G>T Polymorphisms at the Gene Encoding the CYP450-2B6 Isoenzyme on Efavirenz Plasma Concentrations in HIV-Infected Subjects. *Clinical Infectious Diseases*. 40(9):1358–1361. DOI: 10.1086/429327.

Sathigari, S.K., Radhakrishnan, V.K., Davis, V.A., Parsons, D.L. & Babu, R.J. 2012. Amorphous-state characterization of efavirenz-polymer hot-melt extrusion systems for dissolution enhancement. *Journal of Pharmaceutical Sciences*. 101(9):3456–3464. DOI: 10.1002/jps.23125.

Silva, E.K., Zabot, G.L., Bargas, M.A. & Meireles, M.A.A. 2016. Microencapsulation of lipophilic bioactive compounds using prebiotic carbohydrates: Effect of the degree of inulin polymerization. *Carbohydrate Polymers*. 152:775–783. DOI: 10.1016/j.carbpol.2016.07.066.

South African National Department of Health. 2019. *2019 ART Clinical Guidelines*. Available: https://www.knowledgehub.org.za/elibrary/2019-art-clinical-guidelines-management-hiv-adults-pregnancy-adolescents-children-infants.

Szejtli, J. & Szente, L. 2005. Elimination of bitter, disgusting tastes of drugs and foods by cyclodextrins. *European Journal of Pharmaceutics and Biopharmaceutics*. 61:115–125. DOI: 10.1016/j.ejpb.2005.05.006.

Tamm, F., Herbst, S., Brodkorb, A. & Drusch, S. 2016. Functional properties of pea protein hydrolysates in emulsions and spray-dried microcapsules. *Food Hydrocolloids*. 58:204–214. DOI: 10.1016/j.foodhyd.2016.02.032.

Taneja, S., Shilpi, S. & Khatri, K. 2016. Formulation and optimization of efavirenz nanosuspensions using the precipitation-ultrasonication technique for solubility enhancement. *Artificial Cells, Nanomedicine and Biotechnology*. 44(3):978–984. DOI: 10.3109/21691401.2015.1008505.

Tønnesen, H.H. & Karlsen, J. 2002. Alginate in Drug Delivery Systems Alginate in Drug Delivery Systems. *Drug Development and Industrial Pharmacy*. 28(6):621–630. DOI: 10.1081/DDC-120003853.

Tsuchiya, K., Gatanaga, H., Tachikawa, N., Teruya, K., Kikuchi, Y., Yoshino, M., Kuwahara, T., Shirasaka, T., Kimura, S., Oka, S. 2004. Homozygous CYP2B 6*6 (Q172H and K262R) correlates with high plasma efavirenz concentrations in HIV-1 patients treated with standard efavirenz-containing regimens. *Biochemical and Biophysical Research Communications*. 319(4):1322–1326. DOI: 10.1016/j.bbrc.2004.05.116.

Viljoen, M., Gous, H., Kruger, H.S., Riddick, A., Meyers, T.M. & Rheeders, M. 2010. Efavirenz Plasma Concentrations at 1, 3, and 6 Months Post-Antiretroviral Therapy Initiation in HIV Type 1-Infected South African Children. *AIDS Research and Human Retroviruses*. 26(6):613–619. DOI: 10.1089=aid.2009.0200

World Health Organization. 2016. *Combined Global Demand Forecasts for Antiretroviral Medicines and Hiv Diagnostics in Low-and Middle-Income Countries From 2015 To 2020*. Available: http://apps.who.int/iris/bitstream/10665/250088/1/9789241511322-eng.pdf?ua=1 [Accessed: 10 May 2020].

World Health Organisation. 2018. Updated recommendations on first-line and second-line antiretroviral regimens and post-exposure prophylaxis and recommendations on early infant diagnosis of HIV: interim guidelines. Supplement to the 2016 consolidated guidelines on the use of antiretrovir. *World Health Organization*. (December):1–79. Available: https://apps.who.int/iris/bitstream/handle/10665/277395/WHO-CDS-HIV-18.51-eng.pdf?ua=1.

Wyen, C., Hendra, H., Vogel, M., Hoffmann, C., Knechten, H., Brockmeyer, N.H., Bogner, J.R., Rockstroh, J., Esser, S., Jaeger, H., Harrer, T., Mauss, S., van Lunzen, J., Skoetz, N., Jetter, A., Groneuer, C., Fatkenheuer, G., Khoo, S.H., Egan, D., Back, D.J., Owen, A. 2008. Impact of CYP2B6 983T>C polymorphism on non-nucleoside reverse transcriptase inhibitor plasma concentrations in HIV-infected patients. *Journal of Antimicrobial Chemotherapy*. 61(4):914–918. DOI: 10.1093/jac/dkn029.

CHAPTER 4

Materials and Methods

4.1 Introduction

In this chapter, a complete description of the methodology and experimental procedures that were used in this study is provided. This includes optimisation of the spray-drying procedure and preliminary stability testing of selected spray-dried formulations. Furthermore, the chapter also presents the materials and analytical techniques used to analyse and characterise the compounds selected for this pre-formulation study.

4.2 Materials

The active pharmaceutical ingredient, efavirenz (EFV), batch number (B/N): IF-EF-190902 and pea protein isolate (PPI), B/N: 3700D04034180040 was sourced from DB Fine Chemicals (Pty) Ltd. (Rivonia, South Africa). Inulin (IN) with a degree of polymerisation > 10 was purchased from Savannah Fine Chemicals (Pty) Ltd. (Milnerton, Cape Town, South Africa). The purity of EFV raw material was confirmed using a World Health Organisation (WHO) reference standard, B/N: 2.0 with a certified purity of 99.9% purchased from Stargate Scientific (Johannesburg, South Africa). Chromatography-grade acetonitrile was purchased from Labchem, Johannesburg, South Africa. Analytical grade formic acid, sodium lauryl sulphate (SLS), and Tween® 20 (Polysorbate 20) was purchased from Sigma Aldrich (Germany). Bradford Reagent (B/N: SLCC0151) were purchased from Sigma Aldrich (Johannesburg, South Africa). Sodium alginate (SA), (B/N: SHBM2247), hydrochloric acid, B/N: SZBF2210V and calcium chloride B/N: MKBX8777V was also purchased from Sigma Aldrich (Johannesburg, South Africa). Sodium hydroxide (B/N: 1041959), sodium chloride (B/N: 1037400), potassium dihydrogen phosphate (B/N:1040257), sodium hydrogen carbonate (B/N:K50606329850) and disodium hydrogen phosphate (B/N: F1535286833) was purchased from Merck (Johannesburg, South Africa). Finally, distilled water was obtained from a Mili-Q Elix® Essential 3 Water Purification System from Merck® water purification system and ultrapure HPLC water with resistivity of 18.2 MΩ.cm^{-1} was obtained from a Lasec® Purite laboratory water system.

4.3 Methods

All procedures and analysis were done at the University of the Western Cape, School of Pharmacy, Discipline of Pharmaceutics, unless otherwise stated in the respective method descriptions below.

4.3.1 Physico-chemical characterisation of EFV, PPI and IN

The appropriate use of analytical methods has been proven valuable in characterising the physico-chemical, physico-mechanical and thermal properties of all the relevant compounds

utilised in the study as well as the final formulation. In this section, detailed descriptions are provided of the analytical techniques and evaluation parameters used to characterise the properties of all compounds.

4.3.1.1 Thermal Analysis

The thermal properties of the drug and wall forming agents were investigated using hot-stage microscopy (HSM), differential scanning calorimetry (DSC), and thermo-gravimetric analysis (TGA) (**Figure 4.1**). In this study thermal analytical techniques were used to evaluate the solid-state form of EFV, thermal stability of all relevant compounds and to aid in drug-excipient compatibility testing.

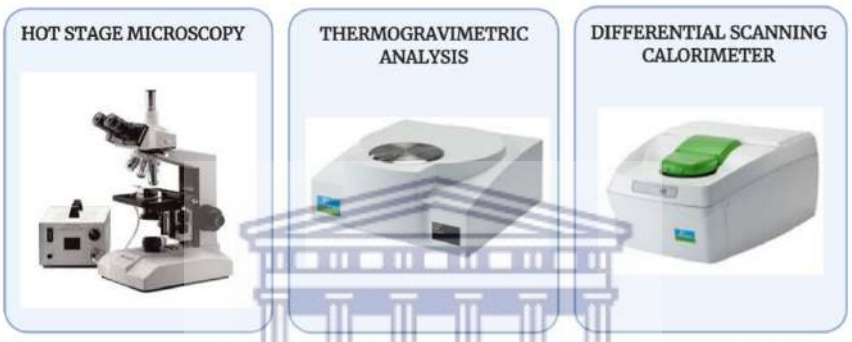

Figure 4.1: Schematic showing the series of thermal analysis techniques used to characterise the thermal properties of the components used in the present study. [Prepared with Biorender at https://biorender.com/]

i. Hot-stage microscopy (HSM)

HSM is a visual analytical technique often used as a complementary technique to characterise the physical properties of a compound as a function of temperature (Vitez et al., 1998). In the pharmaceutical industry, HSM is used to visually confirm sample phase transitions, such as melts, observed with other thermal techniques such as DSC and TGA. During this study thermal events of samples were recorded using a real-time Olympus UC30 (Tokyo, Japan) camera fitted to an Olympus SZX-ILLB200 (Tokyo, Japan) polarised light microscope to which a Linkam THMS600/720 heating stage (Surrey, UK) was attached. An external Volpi Intralux® 5100 halogen light source was used to aid visibility. The recorded images were analysed using Stream Essentials software® (Olympus, Tokyo, Japan). For all HSM analyses, small quantities of samples were placed on a microscope slide using a dissecting needle and subsequently a small drop of silicon oil was carefully dropped on the sample before a cover slide was placed on top. Photomicrographs were taken at regular time intervals or when a significant event was visually observed.

HSM was performed as a visual aid to TGA and DSC analysis and the relevant micrographs are presented in Appendix A.

ii. Thermogravimetric analysis (TGA)

TGA is a technique that monitors the amount of weight change of a substance as a function of temperature (Monajjemzadeh & Ghaderi, 2015). By measuring the mass loss of a sample, TGA determines the thermal profile of the substance which provides insight into the physical and chemical changes of the material in response to temperature (Barnes, Hardy & Lever, 1993; Monajjemzadeh & Ghaderi, 2015). The data obtained from TGA analyses can also be used to inform thermal stability. TGA analyses were done using a Perkin Elmer 4000 thermogravimetric system (Waltham, USA). To prepare the samples for analysis, an empty and clean crucible was tarred to zero using the built-in balance. Once stable, a small amount of sample, weighing between 1 - 3 mg, was transferred to the crucible and the weight was recorded. Analyses were carried out under a nitrogen purge of 20 mL/min and over a heating temperature range of 30 – 600°C using a heating rate of 10°C/min. The same heating program was used for all samples. The collected data was analysed using Pyris™ software.

iii. Differential scanning calorimeter (DSC)

This technique measures the difference in the amount of heat required to increase the temperature of a sample, as a function of temperature, relative to a reference sample. DSC was used to determine the melting point, heat of fusion, and thermal stability of chemical compounds. Additionally, DSC was used to detect any physical interactions or incompatibilities between the different microencapsulants that were used in this study (Barnes, Hardy & Lever, 1993; Monajjemzadeh & Ghaderi, 2015).

Samples, weighing 2 – 4 mg, were weighed into aluminium pans and subsequently sealed with aluminium lids. A DSC 8000 Perkin Elmer instrument (Waltham, USA), utilizing the Pyris™ software program and with an incorporated intra-cooling system was used to carry out all DSC analyses. The samples were heated at a heating rate of 10°C/min from 30 – 200°C. All analyses were performed under continuous dry nitrogen (99.8 %) purging with a flow rate of 20 mL/min. An empty aluminium sealed pan was used as a reference.

4.3.1.2 Fourier-transform infrared spectroscopy (FT-IR)

Fourier-transform infrared spectroscopy (FT-IR) measures the absorption of light as a function of wavelength to produce a spectroscopic fingerprint of the compounds (Markovich & Pidgeon, 1991; Dole et al., 2011).

FT-IR studies were done to detect any potential molecular interactions between EFV and the excipients, IN, PPI and SA, as well as any phase transformation or degradation of EFV during processing steps. FT-IR spectra were obtained using a Perkin-Elmer Spectrum 400 FT-IR spectrometer (Waltham, USA) fitted with a diamond attenuated total reflectance (ATR) crystal. For each sample, a spectrum was collected within the 650 – 4000 cm^{-1} range by placing a small amount of sample on the crystal surface and applying between 50 and 60 % force. The average of 4 scans was plotted as a spectrum by the program with frequency plotted against recorded percentage transmittance. Spectra were subsequently analysed using Spectrum® software version 6.3.5.0176 (Waltham, USA) for the absence or shift in the characteristic peak wavenumbers.

4.3.1.3 Particle Morphology and Crystalline Habit

i. Scanning electron microscopy (SEM)

In order to gain morphological information, such as shape and size, of the pure compounds and spray-dried particles, scanning electron microscopy (SEM) was used. SEM analysis of EFV, IN and PPI were done using an AURIGA Field Emission High-Resolution Scanning Electron Microscope (HRSEM), Zeiss (Germany). Analysis was also done for selected spray-dried powders. Powder samples were mounted onto aluminium stubs using carbon tape. The mounted samples were subsequently coated with a thin layer of gold-palladium. An accelerating voltage of 5 kV was used for images. The lament current was set at 2,359 amps.

SEM analysis was done at the University of the Western Cape, Department of Physics and Astronomy.

ii. X-ray powder diffraction (PXRD)

X-ray powder diffraction (PXRD) was used to determine the solid-state of EFV, PPI, IN as well as microencapsulated trials and samples at various points in this study. PXRD was also used to determine whether the drug remained in a crystalline state after being subjected to the spray-drying process. PXRD data were collected using a Bruker D8 Advance powder X-ray diffractometer (Karlsruhe, Germany). High voltage and the current were set to 40 kV and 40 mA, respectively. All diffraction runs were performed at ambient temperature using a diffraction range of 4 – 40° 2θ.

4.3.1.4 Dynamic vapour sorption analysis

Dynamic vapour sorption (DVS) analyses were performed using the Q5000SA vapour sorption analyser (TA Instruments, New Castle, USA). A humidity-temperature program was preset to the following: the temperature was controlled isothermally at 25°C with the first humidity ramp

set from 0 - 90% relative humidity (RH), subsequent desorption and adsorption phases were set to either range from 90 - 10% RH or 10 - 90% RH, respectively. For each vapour sorption run not more than 10 mg of sample was added to a metallised quartz sample holder. Each run started with a drying phase at 60°C for 60 min or until the weight fluctuation was less than 0.0001%.

4.3.2 High-performance liquid chromatography

High-performance liquid chromatography (HPLC) was used to quantify the amount of EFV throughout the various stages of this research study. Specific uses of HPLC analysis included determining EFV solubility, the achieved encapsulation efficiency and drug loading for microspheres prepared through spray-drying and ionic gelation methods, and finally drug release from these microspheres following dissolution studies. For accurate EFV quantification, it was crucial to select a suitable robust and reliable HPLC method. Since EFV is a well-known compound various HPLC methods have been developed and published in literature. Here, the method developed by Singh et al. (2013) was used for analysis throughout as a base onto which adjustments were made to optimise analysis on the particular system at UWC. The EFV concentration was quantified using an Azura Knauer (Berlin, Germany) HPLC system equipped with an autosampler, quaternary pump, DAD detector, and column temperature controller. The HPLC system was coupled with ClarityChrom® software for assisted result processing. A Phenomenex Kinetex (Torrance, CA, USA) C_{18}, 150 x 4.6 mm column, stacked with 5 µm particles, was used as the stationary phase. The mobile phase consisted of chromatography-grade acetonitrile and formic acid (0.1% v/v; pH 4.0) in a ratio of 60:40 %v/v, using isocratic elution at a flow rate of 1 mL/min. The detection wavelength was set to 246 nm. The injection volume was varied for different experimental objectives and the column temperature was maintained at ambient temperature. Linearity of this method was established across the concentration range of 0.01 – 2.00 mg/mL and regression was quantified to be $R^2 = 0.999$.

4.3.3 Solubility testing of pea protein isolate

PPI solubility was evaluated using the well-known Bradford assay which is a standard colorimetric protein assay (Sigma-Aldrich, 2011). This assay was done by first preparing a series of standard bovine serum albumin (BSA) protein solutions with protein concentrations ranging between 0.25 – 1.40 mg/mL in test tubes. Subsequently, 3 mL of the Bradford reagent was added to 0.1 mL of the BSA solution per test tube (Sigma-Aldrich, 2011). Using 1.5 mL of the final solution, transferred to a cuvette, the absorbance of the samples was recorded at 600 nm, using a Jenway® 6051 Colorimeter spectrophotometer (Staffordshire, UK). A correlation coefficient of 0.986 was obtained and was used for quantification of the protein

content in the PPI solution prepared in buffer solutions. The spectrophotometer was blanked with buffer solutions, containing no BSA, to which Bradford Reagent has been added.

4.3.4 Equilibrium *in vitro* solubility testing of EFV in combination with excipients and surface-active agents

Equilibrium solubility is defined as the amount of a substance that passes into solution to achieve saturation at a constant temperature (Aulton, 2017). The determination of solubility is critical as it governs which formulation strategies will be best for a particular drug to ensure optimal *in vivo* drug absorption (Khadka et al., 2014).

Equilibrium *in vitro* solubility testing of EFV was done in all bio-relevant media as well as in 1% v/v Tween® 20, 1% w/v SLS buffer solutions and distilled water. Aqueous buffered solutions at pH 1.2 (0.1 M hydrochloric acid), pH 4.5, pH 6.8, and pH 7.2 were prepared according to the International Pharmacopoeia buffer solution guidelines for dissolutions (World Health Organization, 2019). For the 1% v/v Tween® 20 and 1% w/v SLS buffer solutions, Tween® 20 and SLS was added to the different aqueous buffered solutions. Solubility was done by adding an excess amount of EFV while controlling the amounts of PPI to 8 mg/mL, to prevent clogging of the syringe filters, and IN to 5 mg/mL to prevent gel formation (**Figure 4.2**). The combinations that were used in the solubility testing were (a) EFV, (b) EFV and IN, (c) EFV and PPI and (d) EFV, IN and PPI. All combinations were tested in all relevant media as described above. Sampling, filtration, and drug concentration analysis was done after 24 h agitation in an orbital shaker incubator ES-80 maintained at 37.5 ± 0.5°C and using a shaking speed of 180 rpm. To filter samples, solutions were extracted from the glass beakers using a syringe and subsequently filtered into glass HPLC vials using 0.22 µm nylon syringe filters. The EFV concentration was quantified through HPLC analysis as described in **Section 4.3.2**.

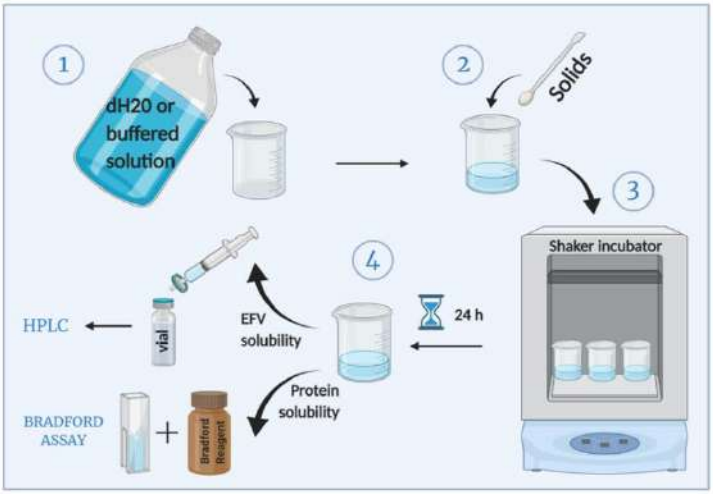

Figure 4.2: Schematic representing the methodology followed for *in vitro* solubility testing. [Prepared with Biorender at https://biorender.com/]

To further establish whether the excipients had a concentration-related effect on the solubility of EFV two additional experiments were conducted. For the combination EP, the amount of PPI added was reduced from 6 mg/mL to 2 mg/mL (EP (B)) and then to 1 mg/mL (EP (C)) to evaluate the solubility effect. For the combination EPI, the amount of IN added was increased to 10 mg/mL to 12 mg/mL (EPI (B)) and 24 mg/mL (EPI (C)). Processing and analysis were completed in the same manner as discussed above.

4.3.5 Spray-drying to produce EFV loaded microcapsules

The technique of spray-drying was used to produce EFV-loaded microcapsules by utilising PPI and IN as wall forming agents. First, a series of spray-drying trials was done to determine the processing parameters for optimal microencapsulation of EFV. Subsequently, these parameters were applied in order to produce EFV microcapsules. All of the spray-drying experiments for aqueous solutions were carried out by the Agricultural Research Council (ARC) Infruitec Nietvoorbij, Stellenbosch, South Africa. SLS, Tween® 20, and olive oil were investigated as potential solubility enhancers of EFV during the initial trial phases. Based on literature reports and safety guidelines surfactant concentrations ranging between 0.1 – 1% were tested for the three candidates with only those trials where powder was successfully collected from shown in **Table 4.1** (Li et al., 2008). Although success with higher concentrations surfactants have been reported, the potential irritant effect of the surfactants were considered and therefore lower concentrations were favoured (Ahlfors, Dahl & Lyberg, 2012; Craye et al., 2015).

A Büchi B-290 Mini spray-dryer (Büchi Labortechnik AG, Flawil, Switzerland) was used to carry out the spray-drying of various feed preparations (**Table 4.1**) as part of the process optimisation. Throughout the spray-drying process, the feed preparation was stirred using a magnetic stirrer bar and maintained at the target temperature (35 or 60 °C) using a heated magnetic stirrer. Spray-drying involves the atomisation of a liquid feed into very small droplets within a hot drying gas leading to the transformation of liquid droplets into solid particles (Cal & Sollohub, 2010). Here, pressurised and dehumidified air, generated by a Haug SO45-E2-ASY oil-free air compressor (Haug Kompressoren AG, St. Gallen, Switzerland) and a Büchi B-296 dehumidifier, was used as the drying medium. The dehumidifier standardises the drying air by removing moisture with a cold trap (<5°C). An inlet air temperature of 220°C was maintained and the outlet air temperature was continuously measured by the in-line temperature gauge.

All the ethanol-based solutions were spray-dried at the University of the Western Cape, School of Pharmacy, Discipline of Pharmaceutics by the candidate, Marise Nel. Here, a Büchi B-290

Mini spray-dryer (Buchi Labortechnik AG, Flawil, Switzerland) equipped with Inert Loop B-295 and an integrated two-fluid 0.7mm nozzle was used for spray-drying. The feeding solution was prepared by dissolving EFV in a 50% (v/v) solution of ethanol and water. The excipients, IN and PPI, were subsequently added at a 2:1 (w/w) ratio with EFV and the mixture was allowed to mix for 30 minutes at ambient temperature (**Table 4.2**). Compressed nitrogen was used as the drying medium to produce fine droplets. Liquid droplets were dried in the drying chamber, separated from the air in the cyclone and finally collected in the collection vessel. Drying conditions for all prepared samples were: aspirator 100%; pump flow rate 900 mL/h and compressed nitrogen flow rate 420 L/h. The inlet temperature was set to 170°C while the outlet temperature ranged between 94 – 105°C throughout.

The spray-dried powder was recovered in a glass vessel after separation from the drying air by a cyclone separator system. At the end of each experimental run and once the total volume of the feed preparation had been converted to powder, heating of the inlet air was terminated and the system was allowed to run until the inlet temperature had fallen below 80 °C.

After each experimental run, the mass of recovered powder was recorded (to three decimals) using a Sartorius Analytic A 120 S balance (Zeiss, Germany). The process yield (%) was then calculated using the following equation:

$$\%\,Yield = \frac{mP}{mSFP}\ x\ 100 \qquad \textit{Equation. 4.1}$$

Where *mP* represents the mass of powder recovered and *mSFP* represents the mass of solids in the feed preparation.

The mass of the product (not determined to the dry basis) was used to express percentage yield (%). The moisture content of IN, PPI and the spray-dried powders (collected immediately after spray-drying) was determined gravimetrically using an HR73 Halogen Moisture Analyser (Mettler-Toledo, Greifensee, Switzerland). Approximately 2 g of the sample was placed on an aluminium dish and desiccated for 60 minutes at 100°C.

Selected spray-dried powder products were subjected to physico-chemical characterization and *in vitro* dissolution testing in pH 6.8 for the evaluation of taste-masking.

Table 4.1: Spray-drying trials for EFV dispersed in various carrier matrices containing PPI, IN, SLS, Tween® 20 and olive oil as prepared by ARC Infruitec, Plant Bioactives Group for UWC.

	Spray-drying feed preparation								
Trial	**Mass of PPI (g)**	**Mass of IN (g)**	**Mass of EFV (g)**	**Mass of SLS (g)**	**Mass of Tween 20 (g)**	**Mass of olive oil (g)**	**Dissolution buffer at pH 6.8 (mL)**	**Solids concentration (%)**	**Temperature of feed (°C)**
1	25	25	-	-			500	10	35
2	50	50	-	-			500	20	35
3	37.5	37.5	-	-			500	15	35
4	56.25	18.75	-	-			500	15	35
5	30	30	-	-			300	20	60
6	45	15	-	-			400	15	60
7	15.8	15.8	8	0.4			400	10	60
8	13.8	13.8	12	0.4			400	10	60
9	15.95	15.95	8	0.1			400	10	60
10	16	16	8	-			400	10	60
14	14	14	8	-		4.0	400	10	60
15	15.8	15.8	8	-		0.4	400	10	60
19	14	14	8	-	4.0	-	400	10	60
20	15.8	15.8	8	-	0.4	-	400	10	60
21	15.9	15.9	8	-	0.2	-	400	10	60

Table 4.2: Spray-drying trials for EFV dispersed in an ethanol carrier matrix containing PPI and IN, done at UWC.

Trial	Formulation of feed suspension						
	Mass of EFV (g)	Mass of PPI (g)	Mass of IN (g)	Solvent system EtOH:dH_2O (%)	Solvent volume (mL)	Solids concentration (%)	Temperature of feed (°C)
22	8	16	16	100:0	400	10	25
23	8	16	16	50:50	400	10	40

4.3.6 Determination of percentage encapsulation efficiency (%EE) and drug content uniformity for spray-dried powders

Here, the encapsulation efficiency (EE) was determined as a percentage of drug that is successfully entrapped into the spray-dried powders relative to the drug amount loaded into the feed solution. The %EE is indicative of how efficient the used method is at encapsulating the drug.

Encapsulation efficiency was calculated as the percentage that was due to encapsulated EFV using **Equation 4.2**:

$$\%\ EE = \frac{actual\ drug\ concentration\ in\ powder}{loaded\ concentration\ in\ feed\ solution} \times 100 \qquad \textit{Equation 4.2}$$

Drug content uniformity was calculated based on the differences in quantified drug content of samples taken from different locations (top, middle and bottom) in the sample container. **Equation 4.3** below was used to calculate the drug content uniformity of the spray-dried powders.

$$Drug\ content\ uniformity = \frac{Drug\ concentration\ in\ sampled\ sample}{Average\ drug\ concentration\ in\ whole\ sample} \times 100 \qquad \textit{Equation 4.3}$$

4.3.7 Microencapsulation of efavirenz through ionic gelation

SA (2% w/v) was allowed to dissolve completely in distilled water under gentle stirring (100 rpm) at 50 ± 1°C. Upon complete solubilisation of SA, EFV raw material was added to the aqueous SA solution to a final 2 mg/mL EFV concentration and was then allowed to stir for 96 h or until EFV has dispersed complete homogenously and no dry EFV is visible. This solution was then added dropwise using a glass Pasteur pipette (1.2 ± 0.15 mm tip diameter) and a rubber pipette bulb, into 100 mL of a $CaCl_2$ (1% w/v) solution, under gentle stirring (100 rpm). The capsule formed was allowed to harden and stabilise for 15 min in the $CaCl_2$ solution and was subsequently removed and rinsed twice with distilled water (**Figure 4.3**). The $CaCl_2$ concentration of 1% w/v was selected based on literature reports that $CaCl_2$ concentrations ranging between 1 – 3% are typically used for ionic gelation. The lower end of this range was selected to maximise drug loading since literature has reported a decline in drug loading with higher $CaCl_2$ concentrations (Ishak et al., 2007). Curing times in the $CaCl_2$ solution vary greatly among literature reports where longer curing times have been associated with drug leeching. However, a curing time of 15 min has been a very popular choice according to literature and the risk of drug leeching here was considered minimum due to the hydrophobic nature of EFV (Bajpai & Sharma, 2004; Pasparakis & Bouropoulos, 2006; Patel et al., 2016; Nalini et al., 2019).

In another method, IN was added to the SA solution together with the EFV. This solution was then used to prepare the alginate beads as described above. Empty beads were also prepared by preparing the SA solution without the addition of EFV. In each case, the rinsed bead was allowed to dry at room temperature until a constant weight was achieved. Weight changes of the beads were monitored by weighing the beads at times 0 h, 24 h, 48 h and 120 h.

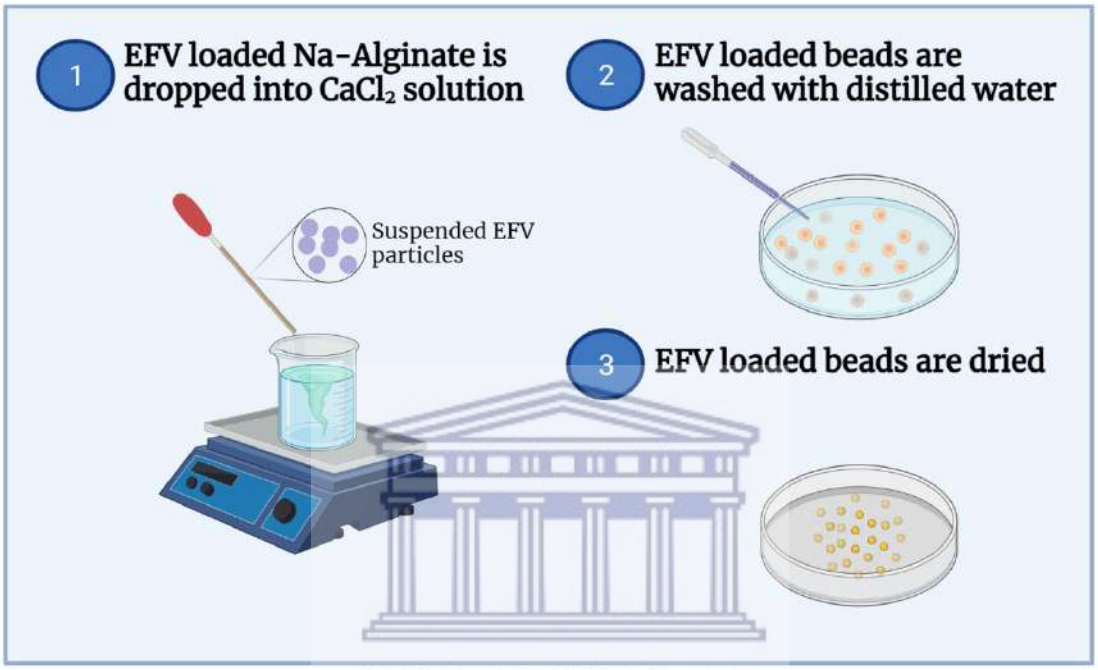

Figure 4.3: Schematic showing the simplified methodology followed for the production of EFV-loaded alginate beads. [Prepared using BioRender.com]

4.3.8 Determination of the size and symmetry of the beads

In the instances where EFV-loaded alginate beads were prepared the size of the beads was determined using an Olympus UC30 (Tokyo, Japan) camera fitted to an Olympus SZX-ILLB200 (Tokyo, Japan) polarised light microscope The measuring tool on the Stream Essentials software was used to measure the diameter of at least 4 beads at, at least 3 different positions for each bead. The degree of similarity between the 3 diameters was used to describe the degree of symmetry. The averages of the 3 diameters were used to calculate the actual size of the beads using **Equation 4.4** as given below:

$$Actual\ size\ (\mu m) = \frac{measured\ average\ diameter\ (\mu m)}{magnification\ factor} \qquad \textit{Equation 4.4}$$

4.3.9 Evaluation of the swelling behaviour of EFV-loaded alginate beads

The water uptake behaviour of the dried alginate beads was monitored over time by weight determinations. In order to best mimic the transition of a typical oral dosage form through the

GIT the experiment was set up to incorporate a transition between different pH environments. The beads were exposed to a pH 6.8 aqueous buffered medium for 30 min, followed by 2 h in pH 1.2 and 4.5 buffered media each and finally for 6 h in a pH 7.2 buffered medium. Samples of beads of known weight (~100 mg) were placed in a glass Petri dish containing 10 mL (enough to cover all beads) of the starting swelling solution and allowed to swell at 37.5°C ± 1°C. The beads were periodically removed and weighed. The weight of the swollen beads was determined by first blotting them onto filter paper to remove moisture adhering to the surface, immediately followed by weighing on an electronic balance. The same beads that the experiment was started with were transferred to each consecutive pH medium. For each sample, the experiment was done in triplicate.

The percentage swelling of the beads was calculated using **Equation 4.5** as given below:

$$\textit{Percentage swelling} = \left[\frac{final\ weight - initial\ dry\ weight}{initial\ dry\ weight}\right] \times 100 \qquad \textit{Equation 4.5}$$

4.3.10 Determination of percentage drug loading (%DL) and percentage encapsulation efficiency (%EE)

Percentage drug loading (%DL) can be defined as the mass percentage of a particle that is made up of the encapsulated drug. It, therefore, is indicative of the amount of drug that was successfully loaded into the microparticles as a function of weight. The determination of drug loading is important for the accurate calculation of the alginate beads weight required for a sufficient dose.

To determine the % DL achieved, exactly 10 beads were accurately weighed to which 10 mL pH 7.2 phosphate buffer solution was added and subsequently placed in an ultrasonic water bath for 30 min. The sample was allowed to rest overnight to allow for complete disintegration of the beads. Due to the insolubility of EFV in aqueous systems, 10 mL acetonitrile was added to the sample to solubilise the EFV that was released from the bead during swelling and breaking. The drug concentration in the resulting solution was quantified by HPLC. Theoretically, the concentration of EFV in the solution would represent the concentration of the EFV successfully loaded into the alginate bead. Results were based on triplicate determinations.

Drug loading capacity was calculated as the percentage (w/w) of the dry weight that was due to encapsulated EFV using the following equation:

$$\%\ Drug\ loading = \frac{total\ drug\ in\ solution\ (mg)}{weight\ of\ bead\ (mg)} \times 100 \qquad \textit{Equation 4.6}$$

The encapsulation efficiency (EE) is defined as the percentage of drug that is successfully entrapped into the bead. The %EE is indicative of how efficient the used method is at encapsulating the drug into the alginate matrix. To determine the %EE, the amount of drug that remained in the $CaCl_2$ solution was first determined. This was done by adding 3 mL of ACN to 3 mL of $CaCl_2$ solution directly after exactly 100 beads were formed. The drug concentration was then quantified using HPLC. Encapsulation efficiency was calculated as the percentage (w/w) of the total drug content using the following equation:

$$\%EE = \frac{total\ drug\ content - drug\ content\ in\ CaCl_2}{total\ drug\ content} \times 100 \qquad \textit{Equation 4.7}$$

4.3.11 *In vitro* dissolution testing

In vitro dissolution, or drug release tests, is an important dosage form developmental tool used to test the biopharmaceutical characteristics of a drug product while ensuring quality control of oral dosage forms (Siewert et al., 2003; Anand et al., 2011).

The USP basket dissolution method was used to evaluate the drug release from the spray-dried microcapsules and produced EFV-loaded alginate beads. The dissolution apparatus was set up according to pharmacopoeial guidelines (World Health Organization, 2019). *In vitro* dissolution testing was performed utilising a Hanson Research SRII 6-flask dissolution test station (California, USA) set to a rotational speed of 75 rpm at 37.0 ± 0.5°C. Each dissolution vessel (n = 6) contained 900 mL of the dissolution media. For dissolutions of the spray-dried trials each basket was loaded with spray-dried powder equivalent to 500 mg EFV only in pH 6.8 dissolution media. For dissolutions of EFV-loaded alginate beads, beads containing an equivalent amount of 100 mg drug were loaded into each basket. Dissolution was done over a period of 60 min for distilled water and pH 6.8 dissolution medium and over a period of 120 min for pH 1.2 and pH 7.2 dissolution medium. Withdrawals (2mL) were done at 1, 2, 5, 10, 20, 30, 45 and 60 min (and 120 min for pH 1.2 and pH 7.2). Drug concentration was quantified using HPLC as described in **section 4.3.2**. The current on-market product Stocrin® 600 mg film-coated tablets were crushed to a powder and also subjected to dissolution testing in pH 6.8 medium to allow for adequate comparisons to be made with regards to taste-masking. Crushing of the Stocrin® tablet was done in an attempt to best mimic the conditions under which the paediatric population would receive their dosage. Due to the difficulty of swallowing among younger children, caretakers often manipulate the dosage form by crushing tablets for easier administration. This action destroys the coating film around the tablet which may have a taste-masking function to some degree and therefore serves as a fair comparison of taste-masking efficiency. Dissolution of EFV-loaded calcium alginate beads in pH 6.8 media was also performed at 40°C to establish whether EFV release is accelerated at higher

temperatures. This was done to inform how EFV release will be affected when mixed with prepared food.

4.3.12 Preliminary stability testing

Stability testing forms a very important part of dosage form development as it ensures finished pharmaceutical product (FPP) safety, efficiency, and quality when FPPs are being stored in pharmacies, clinics and even in patients' homes. Here, preliminary stability testing was done on pure EFV, PPI, IN as well as all the physical mixtures of the different combinations of these compounds (**Figure 4.4**). Additionally, stability testing was also done for the selected spray-dried formulations. A Labcon FSIE-H20 humidity chamber (Krugersdorp, South Africa) was used to expose the compounds to the International Council for Harmonisation (ICH) storage conditions (International Conference of Harmonisation, 2009). Storage conditions used were 40°C / 75% RH for 2 months and 30°C / 65% RH for 2 months and samples were removed monthly from the humidity chamber for subsequent analysis. Physical and chemical stability was evaluated by HSM, TGA, DSC and FT-IR. Chemical potency was evaluated using HPLC, as described in **section 4.3.2**, by comparing the potency of EFV exposed to the storage conditions to the potency of pure EFV prior to exposure**.**

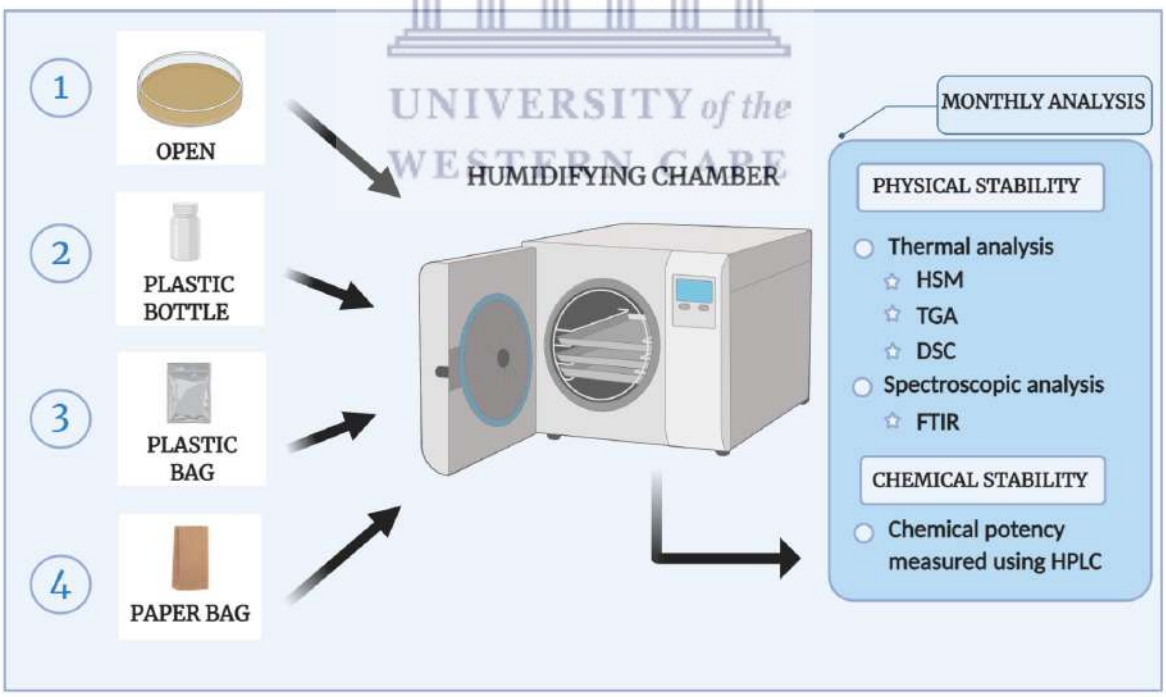

Figure 4.4: Schematic showing the methodology followed during stability testing of EFV and the chosen spray-dried formulations. On the left-hand side, the four different storage types are represented while on the right-hand side the series of analyses that were carried out in a monthly interval is shown. [Prepared with Biorender at https://biorender.com/]

Based on the preliminary 2-month stability study it was decided to investigate the stability for another two months but at a less harsh ICH stability condition. Furthermore, based on the stability that T10 exhibited as well as the fact that these investigations are only preliminary it was decided to not include T10 in this study but to add the T23 sample since no preliminary data were available for this trial, yet. Likewise, it was deemed necessary to evaluate the stability of T19 at 30°C/65% RH due to its chemical instability at 40°C/75% RH storage conditions. Trial 23 stability was also evaluated at 30°C/65% RH and for the sake of making accurate comparisons all three raw materials were again included for stability evaluation at 30°C/65% RH. The samples stored in sealed paper bags at 40°C/75% RH exhibited the best overall stability and therefore the storage of samples in paper bags at 30°C/65% RH was again evaluated. Open containers were again included to prove the most extreme exposure to the environment. A third, additional storage condition, namely a sealed glass polytop, was included for 30°C/65% RH stability evaluation.

4.3.13 Contact angle measurements

For assessment of wettability, contact angle measurements were performed in triplicate using the static sessile drop method. A Krüss Drop Shape Analyzer DSA 25 (Hamburg, Germany) was used and all analyses were performed at ambient temperature. Approximately, a spatula tip amount of each powder sample was placed onto a clean microscope slide. A second slide was then placed on top and powder samples were subsequently pressed lightly between the two glass slides to obtain a level and uniform powder bed. A single drop of deionised water (5 μL) was deposited on the powder bed. The right (R) and left (L) contact angle was then measured within 5 seconds of the drop landing on the powder bed surface. Furthermore, the time taken for the water drop to absorb into the powder was also recorded. All measurements were performed in triplicate, three independent water drops and measurements were done on different areas of the same sample. The size of the contact angle and the time taken for the absorption of the water drop is inversely proportional to the degree of powder wettability (Bracco & Holst, 2013).

Contact angle measurements were performed by Prof. Baker at SensorLab-UWC, Chemistry Department, Faculty of Natural Sciences, UWC.

4.3.14 Statistical Analysis

One-way ANOVA statistical testing was used to calculate statistical significance observed in the solubility values. All calculations were done using the One-way ANOVA Analysis Tool pack for Microsoft® Excel®. P values of ≤ 0.05 were considered significant.

4.4 Conclusion

This chapter provided detailed descriptions of the methodology and experimental procedures that were used in this study. The microencapsulation methods, spray-drying and ionic gelation, that were used in this explorative study as well as the stability testing conditions were described. Furthermore, the chapter also presented the materials and analytical techniques used to analyse and characterise the compounds selected for this formulation study. The experimental results will be presented and discussed in the following chapters.

4.5 References

Ahlfors, E.E., Dahl, J.E. & Lyberg, T. 2012. The development of T cell-dominated inflammatory responses induced by sodium lauryl sulphate in mouse oral mucosa. *Archives of Oral Biology*. 57(6):796–804. DOI: 10.1016/j.archoralbio.2011.11.005.

Anand, O., Yu, L.X., Conner, D.P. & Davit, B.M. 2011. Dissolution testing for generic drugs: An FDA perspective. *AAPS Journal*. 13(3):328–335. DOI: 10.1208/s12248-011-9272-y.

Aulton, M. 2017. Dissolution and Solubility. In *Pharmaceutics: The Science of Dosage Form Design*. Fifth ed. M. Aulton & K. Taylor, Eds. London: Elsevier. 18–35.

Bajpai, S.K. & Sharma, S. 2004. Investigation of swelling/degradation behaviour of alginate beads crosslinked with Ca2+ and Ba2+ ions. *Reactive and Functional Polymers*. 59(2):129–140. DOI: 10.1016/j.reactfunctpolym.2004.01.002.

Barnes, A.F., Hardy, M.J. & Lever, T.J. 1993. A review of the applications of thermal methods within the pharmaceutical industry. *Journal of Thermal Analysis*. 40(2):499–509. DOI: 10.1007/BF02546619.

Bracco, G. & Holst, B. 2013. Contact angle and wetting properties. In: *Surface science techniques*. V. 51. 3–34. DOI: 10.1007/978-3-642-34243-1.

Cal, K. & Sollohub, K. 2010. Spray Drying Technique . I : Hardware and Process Parameters. *Journal of Pharmaceutical Science*. 99(2):575–586. DOI: DOI 10.1002/jps.21886.

Craye, G., Löbmann, K., Grohganz, H., Rades, T. and Laitinen, R. 2015. Characterization of Amorphous and Co-Amorphous Simvastatin Formulations Prepared by Spray Drying. *Molecules*. 20(12):21532-21548. DOI: 10.3390/molecules201219784

Dole, M.N., Patel, P.A., Sawant, S.D. & Shedpure, P.S. 2011. Advance applications of fourier transform infrared spectroscopy. *International Journal of Pharmaceutical Sciences Review and Research*. 7(2):159–166.

International Conference of Harmonisation. 2009. *International conference on harmonisation of technical requirements for registration of pharmaceuticals for human use*. V. 8. Available: https://www.ich.org/ [Accessed:2021, April 15].

Ishak, R.A.H., Awad, G.A.S., Mortada, N.D. & Nour, S.A.K. 2007. Preparation , in vitro and in vivo evaluation of stomach-specific metronidazole-loaded alginate beads as local anti-Helicobacter pylori therapy. *Journal of Controlled Release*. 119:207–214. DOI: 10.1016/j.jconrel.2007.02.012.

Khadka, P., Ro, J., Kim, H., Kim, I., Kim, J.T., Kim, H., Cho, J.M., Yun, G., et al. 2014. Pharmaceutical particle technologies: An approach to improve drug solubility, dissolution and bioavailability. *Asian Journal of Pharmaceutical Sciences*. 9(6):304–316. DOI:

10.1016/j.ajps.2014.05.005.

Li, L., Leung, S., Gengenbach, T., Yu, J., Gao, G., Tang, P., Zhou, Q. and Chan, H. 2017. Investigation of L-leucine in reducing the moisture-induced deterioration of spray-dried salbutamol sulfate power for inhalation. *International Journal of Pharmaceutics*. 530(1-2):30-39. DOI: 10.1016/j.ijpharm.2007.12.020

Markovich, R.J. & Pidgeon, C. 1991. Introduction to Fourier Transform Infrared Spectroscopy and Applications in the Pharmaceutical Sciences. *Pharmaceutical Research*. 8(6):663–675.

Monajjemzadeh, F. & Ghaderi, F. 2015. Thermal Analysis Methods in Pharmaceutical Quality Control. *Journal of Molecular Pharmaceutics & Organic Process Research*. 3(1). DOI: 10.4172/2329-9053.1000e121.

Nalini, T., Basha, S.K., Mohamed Sadiq, A.M., Kumari, V.S. & Kaviyarasu, K. 2019. Development and characterization of alginate / chitosan nanoparticulate system for hydrophobic drug encapsulation. *Journal of Drug Delivery Science and Technology*. 52(March):65–72. DOI: 10.1016/j.jddst.2019.04.002.

Pasparakis, G. & Bouropoulos, N. 2006. Swelling studies and in vitro release of verapamil from calcium alginate and calcium alginate – chitosan beads. *International Journal of Pharmaceutics*. 323:34–42. DOI: 10.1016/j.ijpharm.2006.05.054.

Patel, N., Lalwani, D., Gollmer, S., Injeti, E., Sari, Y. & Nesamony, J. 2016. Development and evaluation of a calcium alginate based oral ceftriaxone sodium formulation. *Progress in Biomaterials*. 5(2):117–133. DOI: 10.1007/s40204-016-0051-9.

Siewert, M., Dressman, J., Brown, C.K. & Shah, V.P. 2003. FIP / AAPS Guidelines to Dissolution / in Vitro Release Testing of Novel / Special Dosage Forms *. *AAPS PharmSciTech*. 4(1):1–10. DOI: https://doi.org/10.1208/pt040107.

Sigma-Aldrich. 2011. *Bradford Protocol*. Available: https://www.sigmaaldrich.com/content/dam/sigma-aldrich/docs/Sigma/Bulletin/b6916bul.pdf.

Singh, A., Majumdar, S., Deng, W., Mohammed, N.., Chittiboyina, A.., Raman, V., Shah, S. & Repka, M. 2013. Development and characterization of taste masked Efavirenz pellets utilizing hot melt extrusion. *Journal of Drug Delivery Science and Technology*. 23(2):157–163. DOI: 10.1016/S1773-2247(13)50024-4.

Vitez, I.M., Newman, A.W., Davidovich, M. & Kiesnowski, C. 1998. The evolution of hot-stage microscopy to aid solid-state characterizations of pharmaceutical solids. *Thermochimica Acta*. 324(1–2):187–196. DOI: 10.1016/s0040-6031(98)00535-8.

World Health Organization. 2019. *Dissolution test for solid oral dosage forms*. Available: https://apps.who.int/phint/en/p/docf/ [Accessed:2020, February 02].

CHAPTER 5

Physico-chemical characterisation and compatibility evaluation of EFV and proposed excipients

Note: Part of this chapter has been submitted for peer-reviewing to the Journal of Drug Delivery Science and Technology. See ***Appendix B*** *for the submitted version.*

5.1 Introduction

As described in Chapter 3, every pharmaceutical formulation study hinges on the physico-chemical properties of the active pharmaceutical ingredient(s) (APIs) and excipients to be used in the final dosage form. For this study, it was therefore pertinent to investigate the physico-chemical properties of EFV and the excipients described in Chapter 4 and this chapter provides the results obtained during the physico-chemical characterisation. Furthermore, an extensive solubility profile of EFV is presented here as well as the results obtained from the compatibility evaluation of EFV with the proposed excipients.

5.2 Physico-chemical characterisation and compatibility of EFV in combination with PPI and IN

5.2.1 Thermal analysis

To encapsulate EFV through the process of spray-drying or ionic gelation, a significant part of this study was directed to pharmaceutical pre-formulation. Therefore, the thermal analysis served a two-fold purpose, namely to determine suitable process parameters as well as to establish the compatibility of EFV with the excipients used throughout this study.

At ambient temperature, EFV presents as an off-white powder with a highly electrostatic nature. DSC analysis confirmed the melting temperature (**Figure 5.1(a)**), observed as a single sharp endothermic peak at a temperature of 140.19°C with ΔH = 44.32 J/g. This temperature corresponds to the reported melting temperature of EFV Form I in literature (Fandaruff et al., 2014 (a); Wardhana et al., 2020). TGA showed that EFV remains thermally stable until 225°C when the onset of degradation was observed, associated with a weight loss of 91.95% (**Figure 5.2(a)**).

At ambient temperature IN presents as a fine white powder. As depicted in **Figure 5.1 (b)** IN exhibited a glass transition temperature at 136.63°C and no other endothermic or exothermic peaks were observed. The TGA thermogram collected for IN confirmed that the onset of degradation was at 222°C. The TGA thermogram further revealed weight loss due to heating in three steps at 246.45°C, 315.17°C and 360.10°C, accounting for a total of 81.14% weight loss, (**Figure 5.2 (b)**). A residue of 18.86% remained at the end of the run at 600°C.

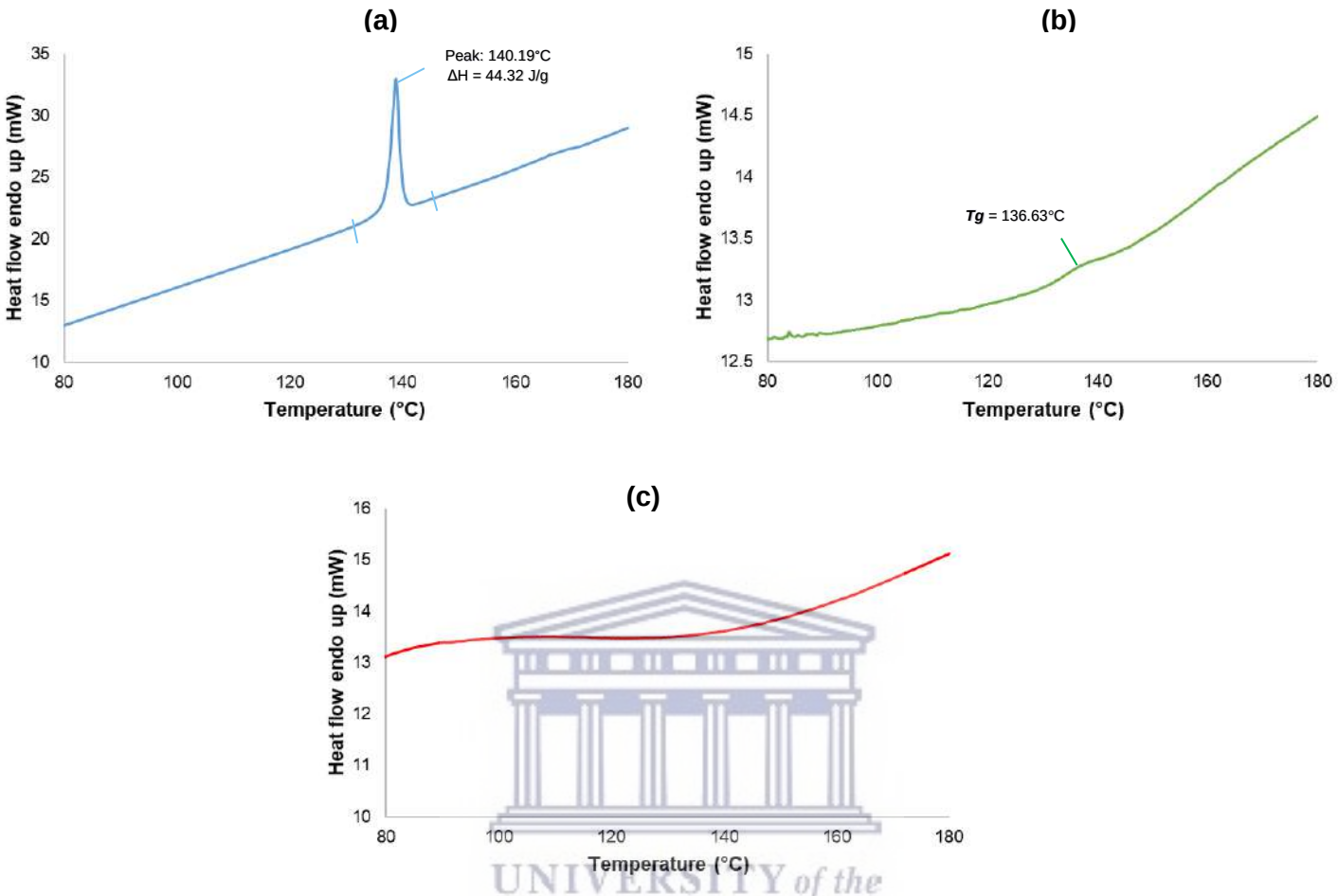

Figure 5.1: DSC thermograms of (a) EFV, (b) IN and (c) PPI, collected at a heating range of 30 – 190°C with only the range of 80 – 180°C depicted for better visualisation. The SLS thermogram is depicted for the range 80 – 205°C.

PPI presents as a cream-brown powder at ambient temperature and thermal analysis showed that it exhibits no dehydration, glass transition or melting (**Figure 5.1(c)**). A study by Lan, Chen and Rao (2018) reported the onset of protein denaturation at 80.03°C, which was noted as a processing parameter for the future spray-drying process used in this study. The TGA trace for PPI further revealed weight loss due to heating in two steps at 75.25°C and 313.40°C accounting for a total of 81.30% weight loss (**Figure 5.2(c)**). A residue of 18.21% remained at the end of the experimental run at 600°C.

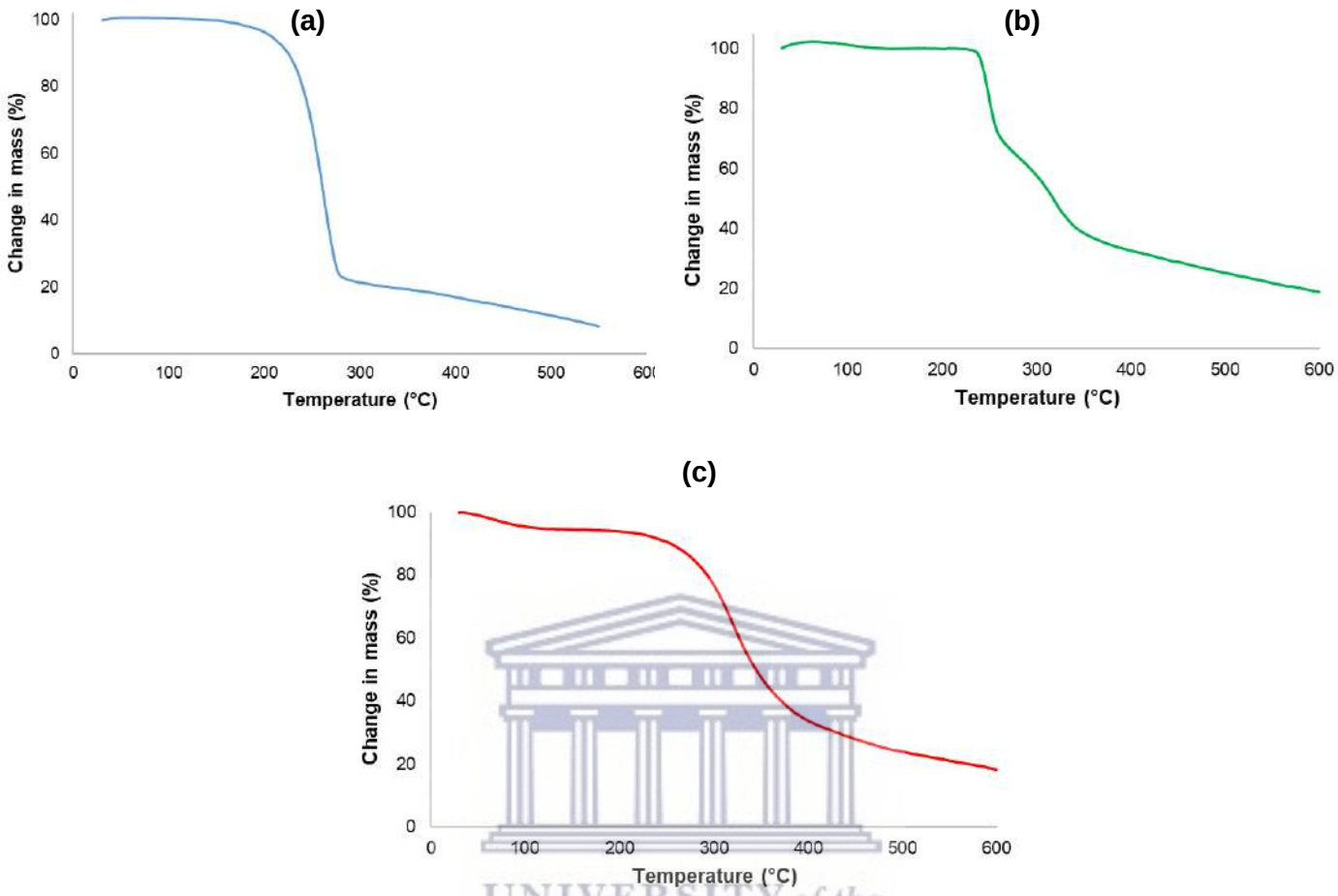

Figure 5.2: TGA thermograms for raw materials (a) EFV, (b) PPI, (c) IN, collected over a 30 – 600°C range.

The physical combinations of EFV with IN and PPI were also investigated using thermal analysis to establish thermal compatibility between EFV and these excipients. DSC analysis of physical mixtures of EFV and IN (EI) (1:4 w/w), EFV and PPI (EP) (1:4 w/w) and finally EFV, PPI and IN (EPI) (1:4:4 w/w/w) each showed a single endothermic peak at 139.60°C (ΔH = 6.14 J/g), 139.78°C (ΔH = 6.47 J/g) and 139.22°C (ΔH = 4.42 J/g), respectively thus suggesting that no observed incompatibility exists between EFV and the two excipients (**Figure 5.3**). Differences in the EFV endothermic peak size were solely attributed to the weight-dependent decrease in the EFV concentration in the prepared mixtures.

The TGA trace obtained for the physical mixture EI confirmed the onset of degradation to be 183.85°C and a total weight loss of 74.73% was quantified (**Figure 5.4**). A residue of 25.27% remained at the end of the EI sample run at 600°C. The physical mixture of EP exhibited an onset of degradation at 188.37°C and a total weight loss of 66.09% was quantified. A residue of 33.91%

remained at the end of the EP sample run at 600°C. The TGA trace obtained with EPI presented similarities to the EP and EI mixtures. For the EPI sample, onset of degradation was confirmed to be 187.90°C and a total weight loss of 54.11% was calculated. At the end of the run, a residue of 45.89% remained at 600°C for the EPI sample. TGA for the physical mixtures EI, EP and EPI revealed significant decreases in the onset of degradation temperature for all physical mixtures, exhibiting onset of degradation temperatures >40°C lower than pure EFV, IN and PPI alone (**Figure 5.4**). Despite the earlier onset of degradation, it was also observed that all physical mixtures were associated with less overall sample degradation compared to pure EFV. This can however be attributed to the fact that the samples were combinations. The decrease in degradation temperature observed in the physical mixtures can indicate potential incompatibilities between EFV and PPI/IN. Despite this, EFV was still detected on DSC thermograms of all physical mixtures, suggesting only partial degradation of EFV. Furthermore, when the temperature range is considered within which formulation related processes is planned to be performed, no significant interactions between EFV and IN/PPI is expected. For this reason, the decision was made to continue with the study despite the potential incompatibility.

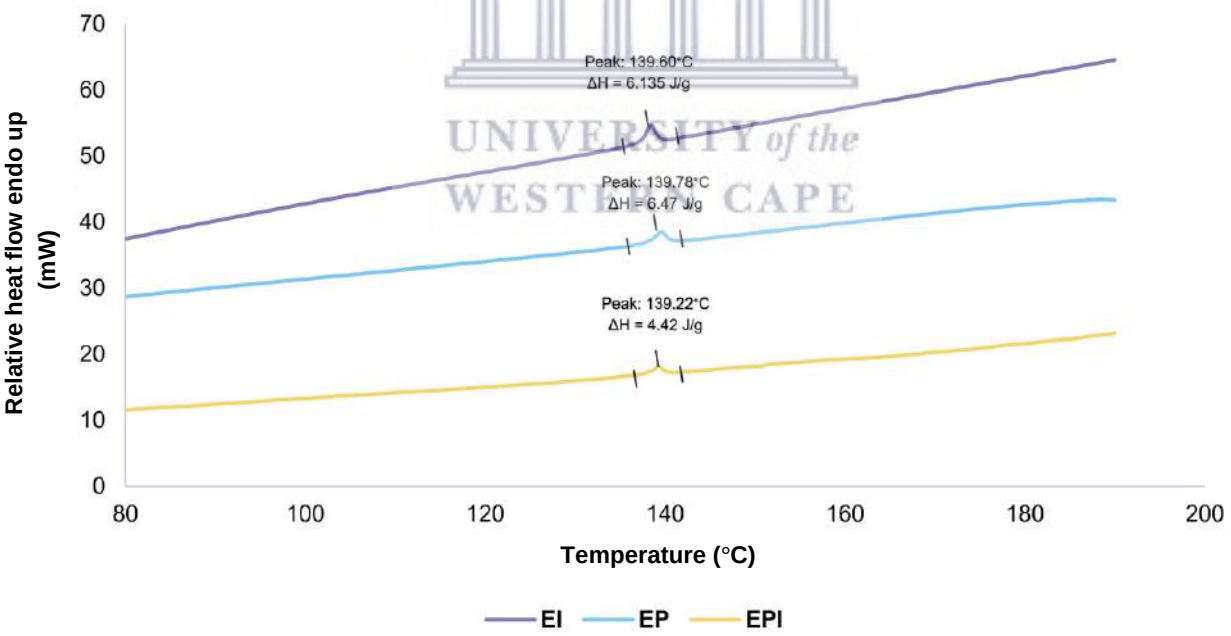

Figure 5.3: Overlay of DSC thermograms for the physical mixtures of EI, EP and finally EPI. DSC data were collected at a heating range of 30 – 190°C with only the range of 80 – 190°C depicted.

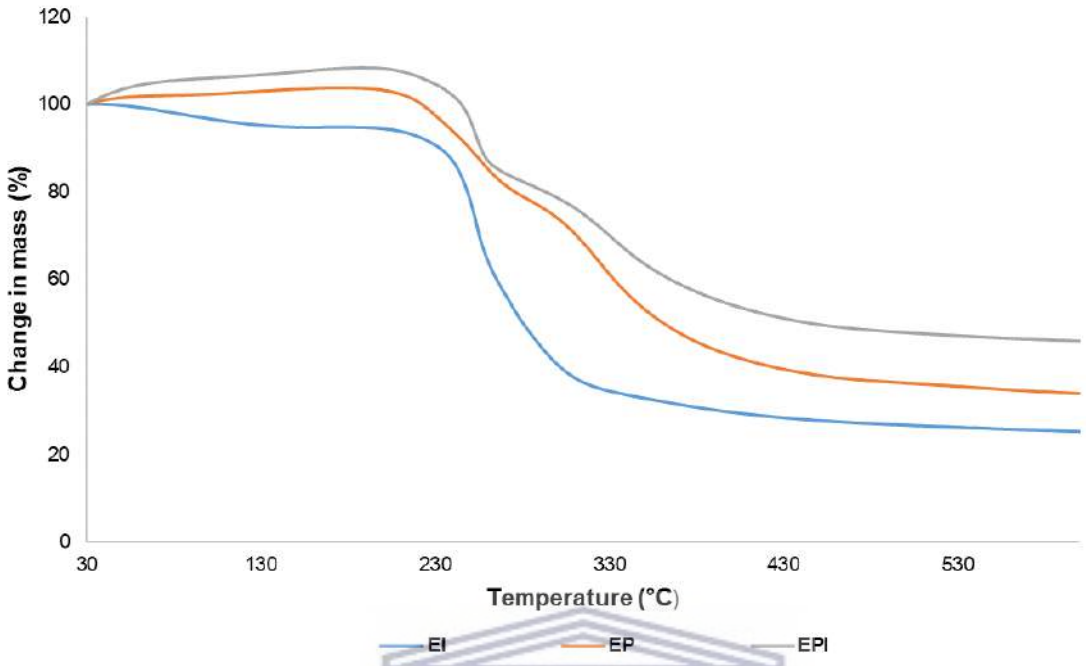

Figure 5.4: Overlay of TGA thermograms for the physical mixtures of EI, EP and EPI. TGA data was collected over a heating range of 30 – 600°C.

5.2.2 Fourier transform infrared spectroscopy

FT-IR spectroscopy is a commonly used technique applied to explore molecular conformations, detect alterations in the vibrational properties of a compound which can be brought into correlation with the molecular functional groups present in the compound (Ewing & Kazarian, 2018). Chemical interactions between EFV and the excipients have the potential to change the molecular conformation, hydrogen bonding arrangements and crystal packing within the EFV crystalline structure, which could potentially influence other physico-chemical properties of the drug.

EFV shows characteristic absorbance bands at 3315.3, 2251.6, 1745.2, 1601.4, and 1319.7 cm^{-1}, respectively attributed to N-H stretching, aromatic C-H stretching, C=O stretching, C=C stretching, and C-O-C stretching (**Figure 5.5**). The obtained EFV spectrum is in accordance to what has been previously reported in literature (Fandaruff et al., 2014 (b)), confirming the solid-state form to be EFV Form I.

IN shows characteristic absorbance bands at 3309.3 cm^{-1} and 1020 cm^{-1} which relate to the O-H groups in the IN structure, as a function of its carbohydrate nature, and the C-O and C-C stretching vibrations of the IN pyranose ring (Fernandes et al., 2016; Apolinário et al., 2017). The spectrum

collected for PPI show characteristic bands at 3282.4, 2931.8, 1631.3, 1517.5, 1391.6, 1155 and 1063 cm^{-1}, respectively attributed to –OH contraction, C-H stretching, C=O stretching and the combination of N-H bending and C-N stretching in amide II and in amide III (Lan et al., 2019).

FT-IR spectroscopy was also used to confirm the compatibility of EFV with IN and PPI (**Figure 5.6**). No significant peak shifts or appearance of new peaks were observed in any of the physical mixtures of EFV and the excipients while characteristic EFV peaks were still observed in all physical mixtures.

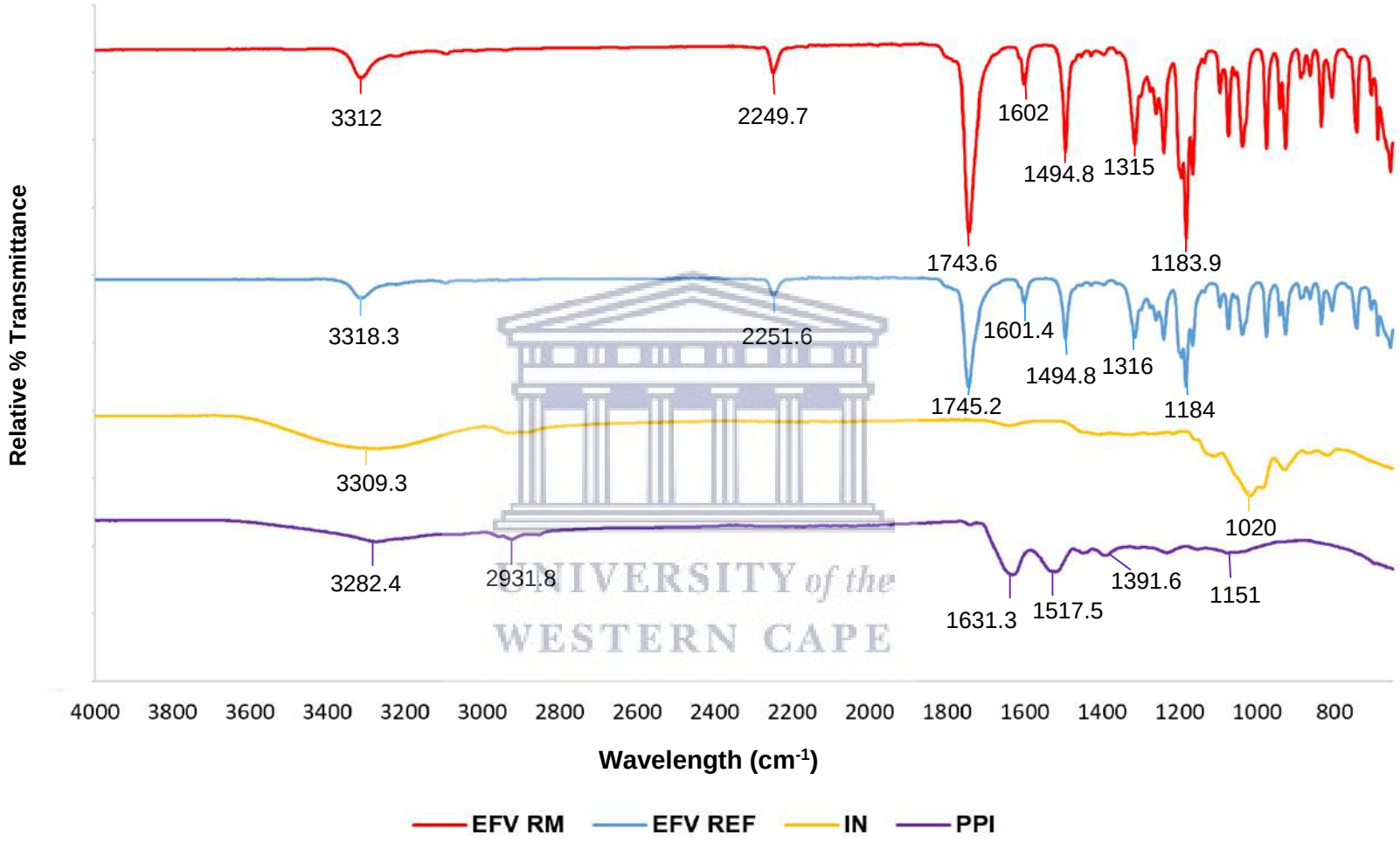

Figure 5.5: An overlay of FT-IR spectra of EFV (EFV RM), EFV REF (WHO reference drug), pure IN and PPI at ambient temperature.

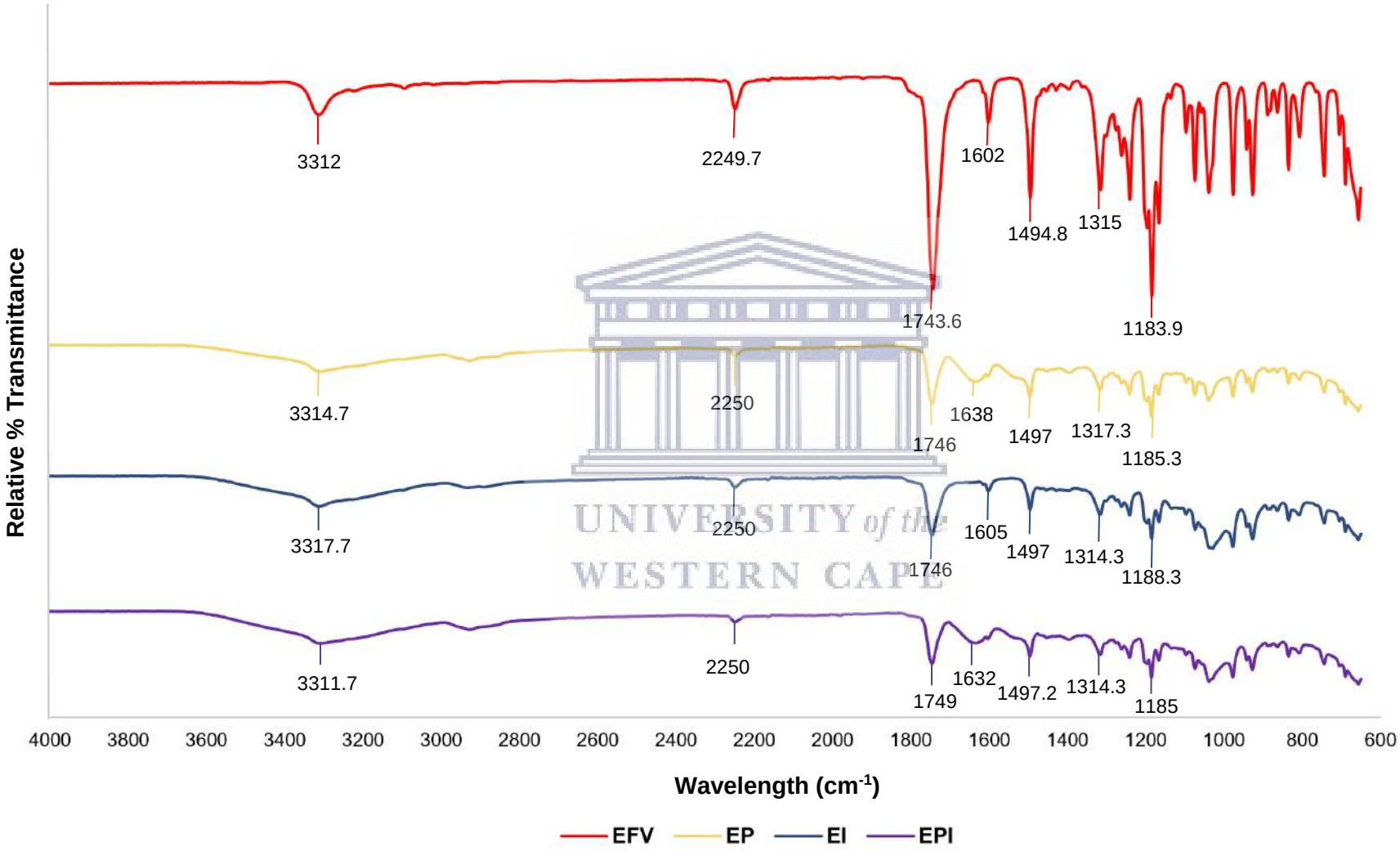

Figure 5.6: An overlay of FT-IR spectra EFV compared to physical mixtures of EI, EP and EPI collected at ambient temperature.

5.2.3 Crystallinity, amorphicity and morphology of investigated compounds

Since one part of this study involved the microencapsulation of EFV using the technique of spray-drying, it was also important to ascertain the morphology of the EFV, PPI, IN before any spray-drying process. This informed on particle morphology of each of the three compounds before any modification of particle morphology and it also enabled the identification of successful EFV encapsulation. Furthermore, knowledge of the specific habit (i.e. crystalline or amorphous) of an API is important when developing a drug formulation since it is a well-known fact that the solid-state form of an API significantly influences all physico-chemical properties of an API but also processes to be used during dosage form manufacturing (**Chapter 2**, **Section 2.2.1.2**).

SEM analysis revealed the typical organised stacked plate-like crystalline morphology of EFV Form I (**Figure 5.7**). The solid-state form of EFV was confirmed to be crystalline using PXRD and consistent with Form I as reported by Wardhana et al. (2020) (**Figure 5.10**). The particle morphology of IN and PPI was also investigated using SEM and solid-state habits of both which were confirmed to be amorphous using PXRD (**Figures 5.8 – 5.10**). IN particles exhibited a smooth spherical morphology while PPI particles exhibited a more wrinkled appearance. This was in agreement with what has been reported in literature (Ronkart et al., 2007; Tamnak et al., 2016). It was also visually observed that there exists considerable particle size distribution between the PPI powder particles.

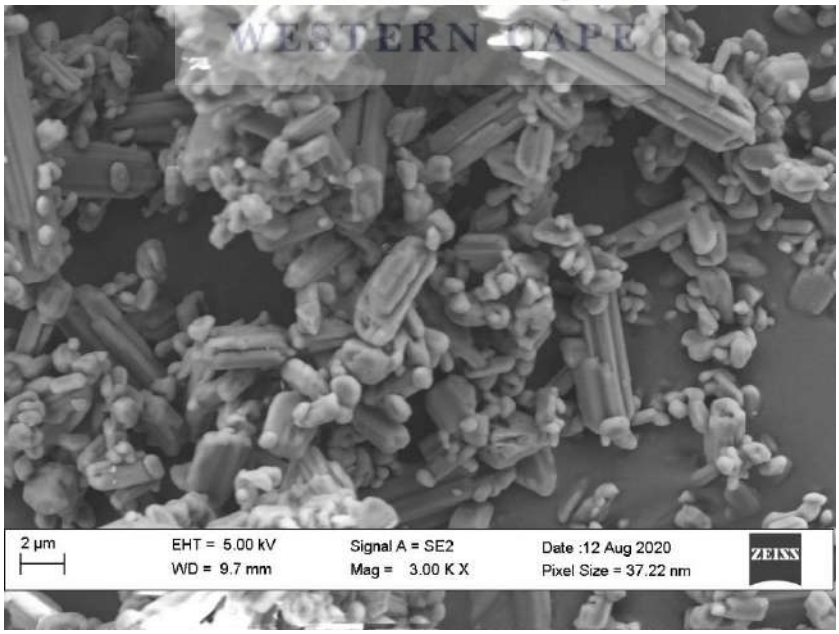

Figure 5.7: Scanning electron microscope (SEM) image for EFV captured at 3, 000 X magnification.

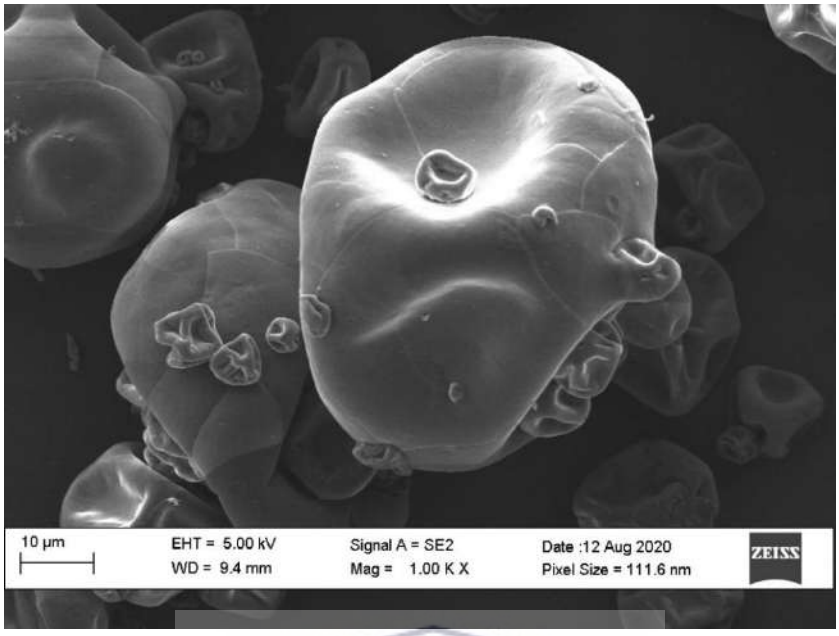

Figure 5.8: Scanning electron microscope (SEM) image for PPI captured at 1000 X magnification.

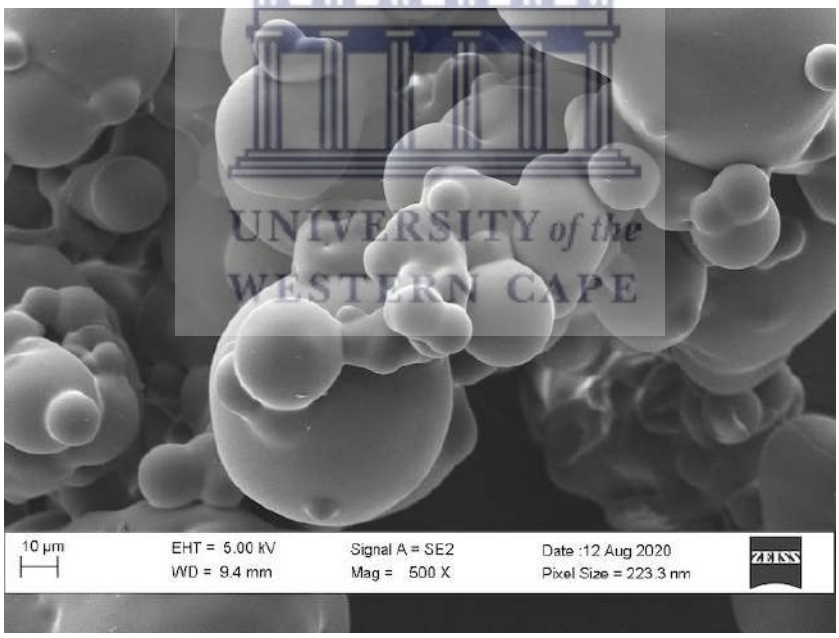

Figure 5.9: Scanning electron microscope (SEM) image for IN captured at 500 X magnification.

Figure 5.11 shows the PXRD profiles for the physical mixture EI, EP and EPI. The crystalline nature of EFV is still detectable in all the physical mixtures. The disappearance of some EFV characteristic peaks can be attributed to the light grinding method used to prepare the physical mixtures or the mere dilution of the amount of EFV in the sample due to a higher ratio of PPI and IN in relation to EFV and is not necessarily attributed to the effect of the excipients.

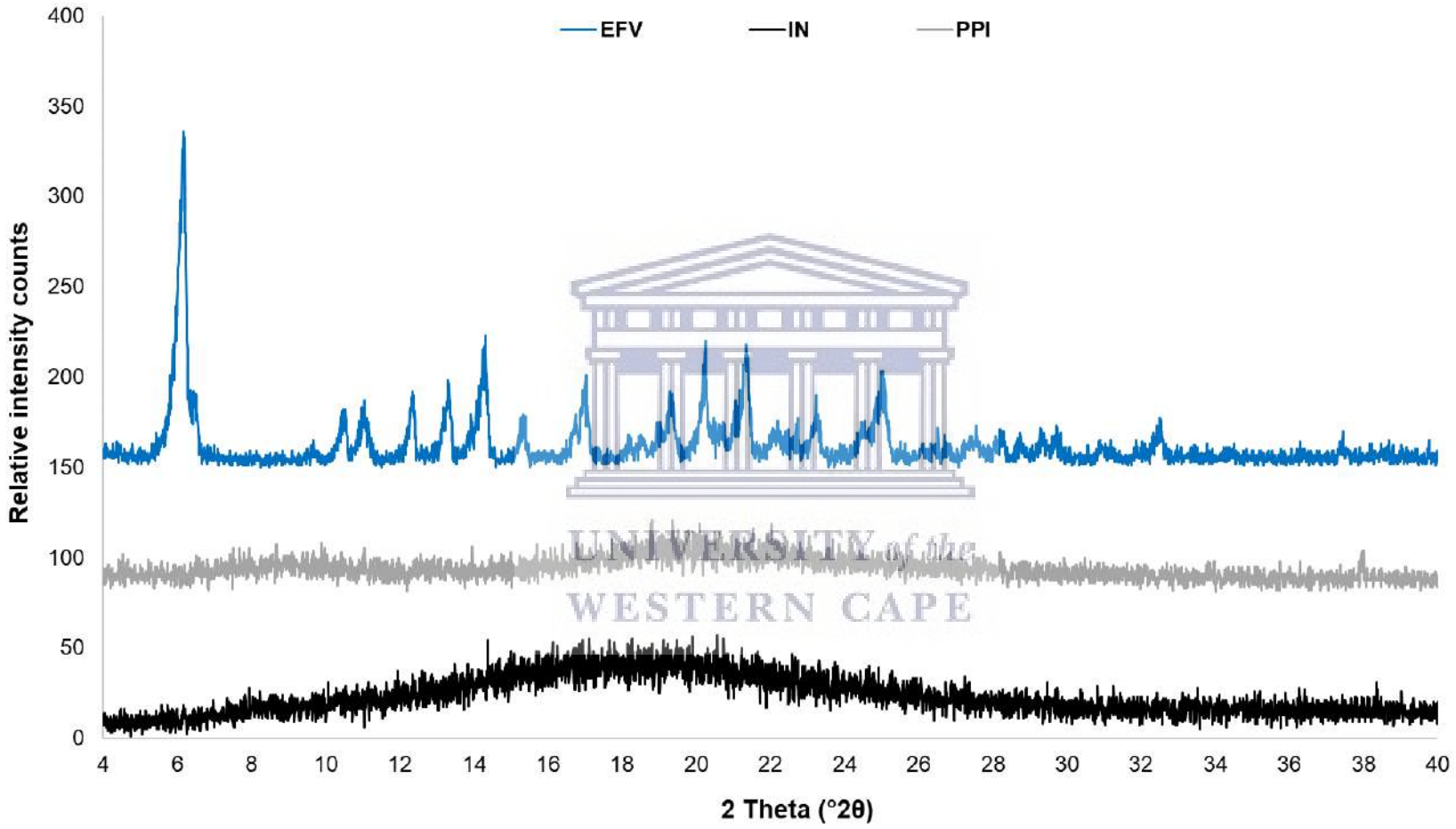

Figure 5.10: Overlay of PXRD patterns obtained for the raw materials EFV, IN and PPI.

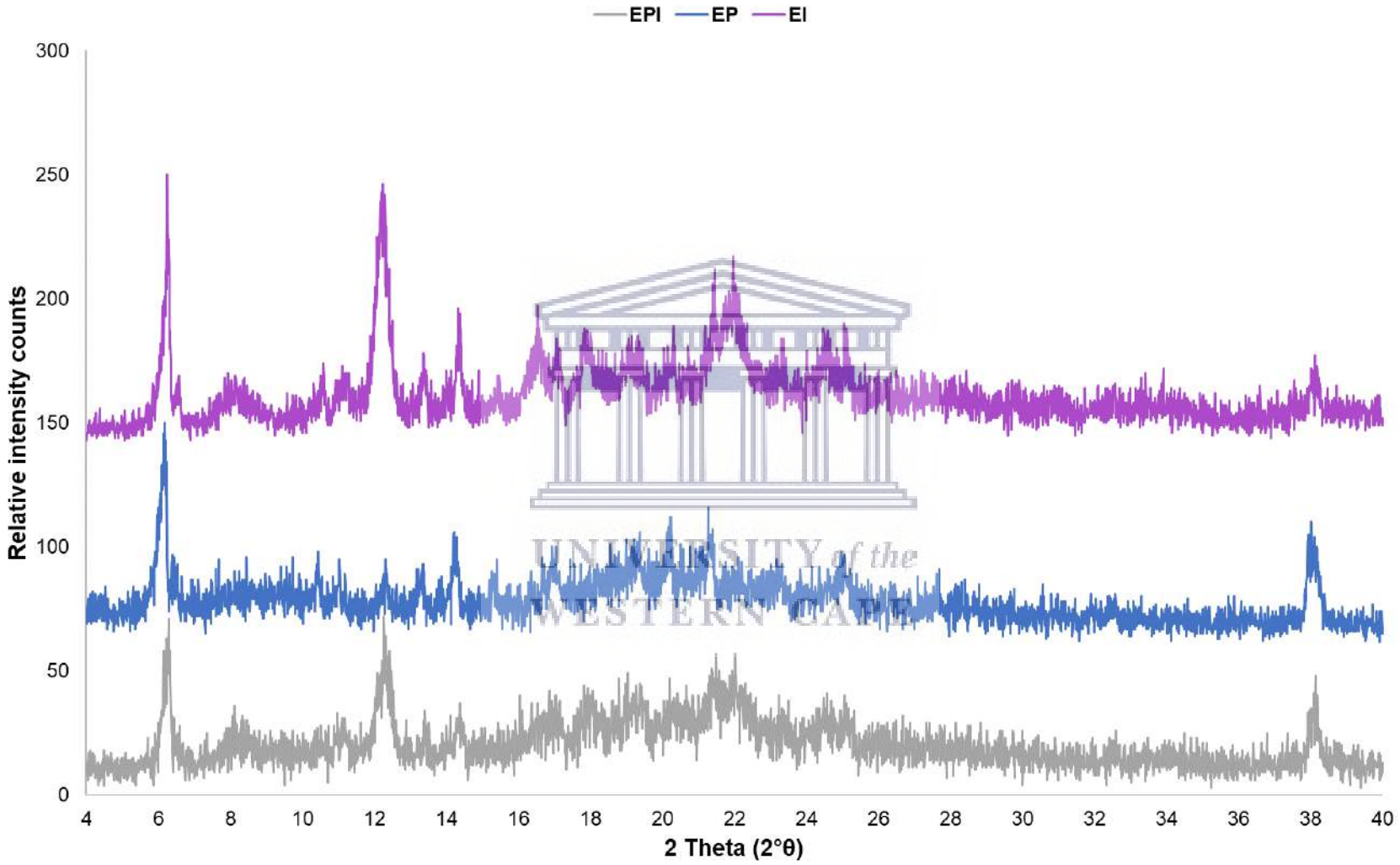

Figure 5.11: Overlay of PXRD patterns obtained for the physical mixtures of EFV with IN and/or PPI.

5.2.4 *In vitro* equilibrium solubility

The solubility of a drug compound is a critical determining factor for the dissolution and bioavailability of the drug. Low aqueous solubility is often associated with low drug bioavailability and suboptimal therapeutic outcomes (Pouton, 2006; Kawabata et al., 2011). There are many examples in literature where the solubility of EFV has successfully been improved *via* particle size reduction or supramolecular modifications such as co-crystal formation, complex formation, and solid dispersions (Alves et al., 2014; Rajurkar et al., 2015; Sathigari et al., 2009; Taneja et al., 2016). These techniques often involve complex, expensive, and time-consuming processing steps.

Since this study investigated the potential to microencapsulate EFV using two different microencapsulation techniques it was imperative to investigate the solubility of EFV in combination with PPI and IN. The rationale for this was based on the fact that the spray-drying method could only utilise aqueous solutions of EFV in combination with the microencapsulants, due to equipment limitations. Thus, it was important to ascertain the level of solubility that would be obtained with the combination of the three compounds.

The aqueous solubility of EFV was quantified to be very low in all biologically relevant media, ranging from pH 1.2 – 7.2 values (**Table 5.1**). Based on the pKa of EFV (pKa = 10.2), pH-dependent solubility is expected with the greatest solubility (0.0036 ± 0.0005 mg/mL) observed at pH 4.5 while the lowest EFV solubility (0.0014 ± 0.00001 mg/mL) was observed in distilled water. Compared to the solubility of EFV alone, the combination EI showed a non-significant 0.08 – 0.28-fold decrease in the aqueous solubility of EFV, except in distilled water, where there was a significant increase ($p = 0.00085$; $p<0.05$) (**Table 5.1**). In contrast, the combination EP showed a significant solubility improvement in a range of 4.44 – 13.54-fold across the entire range of biological pH values as well as in distilled water. The large standard deviation observed in distilled water for the combination EP can be attributed to the poor aqueous solubility of EFV which is associated with a small analytical response leading to high quantification variation. The combination EPI showed a significant solubility improvement in the range of 2.33 – 7.80-fold. However, this solubility improvement seen in the triple combination is significantly lower than the solubility improvement seen in the combination EP with the exception of pH 7.2 (**Figure 5.12**).

Table 5.1: Solubility values (in mg/mL) of efavirenz (EFV), EFV and IN (EI), EFV and PPI (EP) and EFV, PPI and IN (EPI) and the fold change in EFV solubility with respect to that of only EFV in distilled water and buffer solutions.

	Distilled water		pH 1.2		pH 4.5		pH 6.8		pH 7.2	
	Solubility+ (mg/mL)	Fold Increase	Solubility+ (mg/mL)	Fold Increase	Solubility+ (mg/mL)	Fold Increase	Solubility+ (mg/mL)	Fold Increase	Solubility+ (mg/mL)	Fold Increase
EFV	0.0014	-	0.0028	-	0.0036	-	0.0032	-	0.0025	-
EI	0.0030	1.14*	0.0025	- 0.11	0.0033	-0.08	0.0025	-0.22	0.0018	-0.28
EP	0.0203	13.5*	0.0407	13.54*	0.0198	4.50*	0.0174	4.44*	0.0184	6.36*
EPI	0.011	6.86*	0.017	5.07*	0.012	2.33*	0.013	3.07*	0.022	7.80*

* indicates statistical significance with p< 0.05

+refer to Figure 5.12 for standard deviation

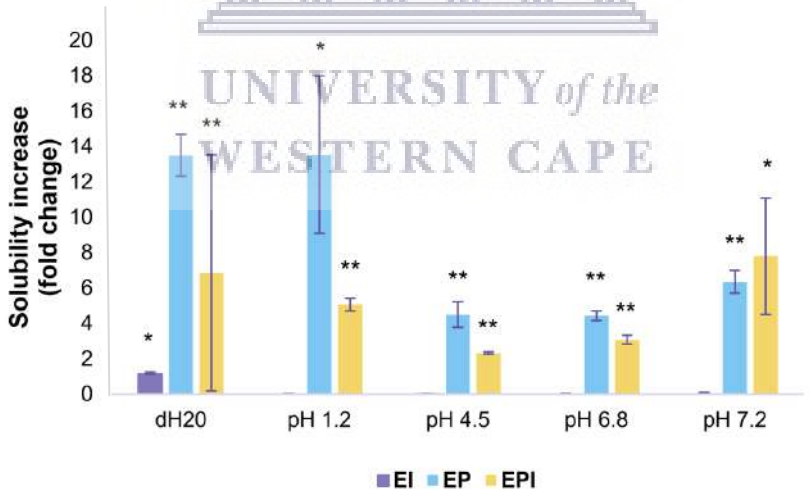

Figure 5.12: Fold change in the aqueous solubility of EFV as a result of the addition of IN and PPI to EFV. * indicates p-value < 0.05; ** indicates p-value < 0.005. Error bars show standard deviation.

Surfactants are often used in pharmaceutical formulations to improve the solubility of drugs by increasing the wettability of these drugs. Two commonly used surfactants, SLS and Tween® 20, were also investigated for their ability to improve EFV solubility when in combination with PPI and IN. EFV solubility in buffered solutions prepared with 1% w/v SLS showed a 30 – 640-fold improvement compared to the solubility determined in bio-relevant media, without the addition of any surfactants (**Table 5.2**). The greatest solubility increases were observed in distilled water (640-fold) and in pH 4.5 buffered solution (240-fold). The addition of Tween® 20 was also associated with a significant solubility improvement compared to the solutions with no surfactant or other excipients added (**Table 5.2**). EFV solubility in 1% v/v Tween® 20 showed 179 - 713 -fold improvement compared to the solubility in buffer-only solutions. The greatest solubility increase was seen in distilled water (713-fold) while the smallest increase was seen in pH 1.2 (179-fold). The degree of solubility improvement increases with increasing pH (**Figure 5.13**). For both SLS and Tween® 20 solutions, the greatest solubility increase was noted in distilled water. This could potentially relate to the interference or competition by the ions present in the buffered solutions. It is possible that the salt ions that are present in the buffered solutions compete for either water molecules or surfactant molecules, thereby reducing their effect on EFV solubility. The degree of solubility improvement imposed by Tween® 20 is greater across the entire pH range when compared to SLS (**Figure 5.13**).

Since Tween® 20 showed greater solubilisation of EFV, the solubility effect thereof on EI, EP and EPI was also investigated to elucidate if a similar trend could be observed as in the buffer-only solutions. EI showed a decrease in EFV solubility in distilled water, pH 6.8 and pH 7.2 while at pH 4.5 no change in solubility was seen in pH 1.2 as a 0.2-fold increase was observed (**Table 5.3**). Similar to the behaviour seen in buffer-only solutions, the combination EP showed significant improvements in solubility across the range of pH values (**Figure 5.14**). Interestingly, however, the combination EPI showed very different behaviour in the 1% v/v Tween® 20 solutions when compared to the buffer-only solutions. In the Tween® 20 solutions, and in the presence of both IN and PPI, the solubility of EFV decreased in all media except pH 4.5 buffered solution. This is in total contrast to the increased solubility seen in buffer-only solutions.

In the combination EP, there was a significant decrease in EFV solubility with decreasing amounts of PPI added (**Table 5.4**). When comparing EFV solubility in the presence of 6 mg/mL PPI (EP (A)) to that with 2 mg/mL PPI, a significant solubility decrease ($p < 0.01$) between 0.8-fold and 0.98-fold was noted across the entire pH range. Similarly, when the amount of PPI was reduced to 1 mg/mL a significant decrease ($p < 0.001$) in solubility ranging between 0.88-fold and 0.9-fold

was noted across the pH range (**Table 5.4, Figure 5.15**). There were no significant EFV solubility differences between solutions containing 2 mg/mL and 1 mg/mL PPI. In the combination EPI, a significant decrease ($p < 0.01$) in EFV solubility was noted with increasing amounts of IN compared to the solubility in the presence of 10 mg/mL (A). There was no significant difference in EFV solubility between solutions containing 12 mg/mL IN and 24 mg/mL IN (**Table 5.5**, **Figure 5.16**).

Overall, it can be said that combining EFV with IN does not significantly affect drug solubility while the combination of EFV with PPI results in increased drug solubility. However, the ability and efficiency of PPI to improve EFV solubility are concentration-dependent and not pH-dependent. Thus the improved solubility can be directly linked to the effect of the excipient and not attributed to the physico-chemical properties (pKa) of EFV. The exact mechanism involved is not clear but it is hypothesised that the quaternary structure of the protein can refold to a degree and that this refolding can result in the protein "wrapping" around the EFV drug molecules. This potentially results in an altered surface interaction between the EFV and water molecules. Proteins are known to have both hydrophilic and hydrophobic regions and therefore the hydrophilic regions associate with the water molecules thus attracting more water into the system. From the solubility data, it became apparent that the wettability of EFV might be improved by the combination thereof with PPI. The equilibrium solubility results were therefore supplemented with the investigation of the wettability of EFV, EI and EPI and for this investigation, two methods were employed, namely: dynamic vapour sorption analysis and contact angle measurements.

Table 5.2: Solubility values (in mg/mL) of EFV in buffered media prepared with distilled water, 1% w/v SLS solutions and 1% v/v Tween® 20 solutions, and the fold increase in EFV solubility relative to that of EFV in the distilled water and normal buffers.

	Distilled water		pH 1.2		pH 4.5		pH 6.8		pH 7.2	
	Solubility+ (mg/mL)	Fold increase	Solubility+ (mg/mL)	Fold increase	Solubility+ (mg/mL)	Fold increase	Solubility+ (mg/mL)	Fold increase	Solubility+ (mg/mL)	Fold increase
Distilled water	0.0014	-	0.0028	-	0.0036	-	0.0032	-	0.0025	-
1% w/v SLS	0.897	640*	0.103	37*	0.868	240*	0.171	53*	0.189	76*
1% v/v Tween®	1.00	713*	0.50	179*	0.66	182*	0.76	238*	1.12	448*

* indicates statistical significance with $p < 0.05$ +refer to Figure 5.13 for standard deviation

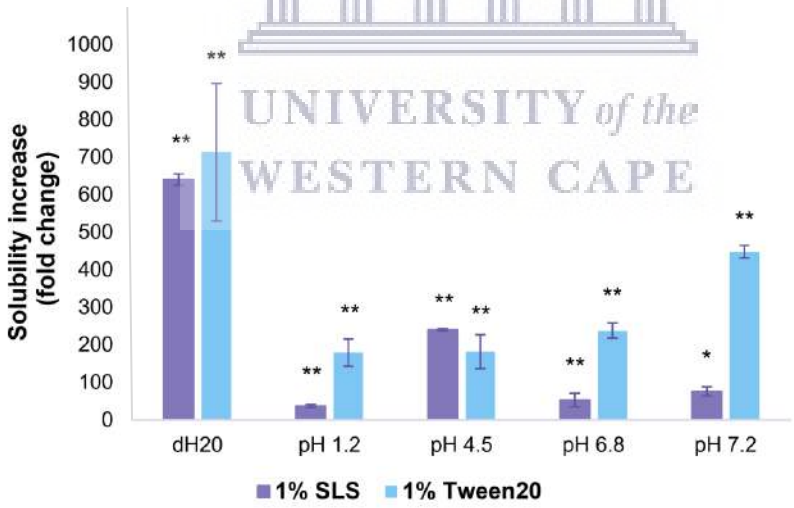

Figure 5.13: Fold increase in aqueous EFV solubility as a result of the use of surfactants 1% w/v SLS and 1% v/v Tween® 20.
* indicates p-value < 0.05; ** indicates p-value < 0.005. Error bars show standard deviation.

Table 5.3: Solubility values (in mg/mL) of EFV, EI, EP and EPI in buffered media prepared with 1% v/v Tween® 20 solutions, and the fold increase in EFV solubility relative to that of EFV only in the 1% v/v Tween® 20 solution.

	Distilled water		pH 1.2		pH 4.5		pH 6.8		pH 7.2	
	Solubility+ (mg/mL)	Fold increase	Solubility+ (mg/mL)	Fold increase	Solubility+ (mg/mL)	Fold increase	Solubility+ (mg/mL)	Fold increase	Solubility+ (mg/mL)	Fold increase
EFV	1.00	-	0.50	-	0.66	-	0.76	-	1.12	-
EI	0.92	-0.08	0.60	0.2	0.66	0	0.36	-0.5*	0.85	-0.24
EP	2.30	1.3*	2.12	3.2*	1.87	1.83*	1.10	0.4*	1.61	0.4*
EPI	0.42	-0.6	0.29	-0.4*	0.99	0.5	0.40	-0.5*	0.12	-0.9*

* Indicates statistical significance with $p < 0.05$ +refer to Figure 5.14 for standard deviation

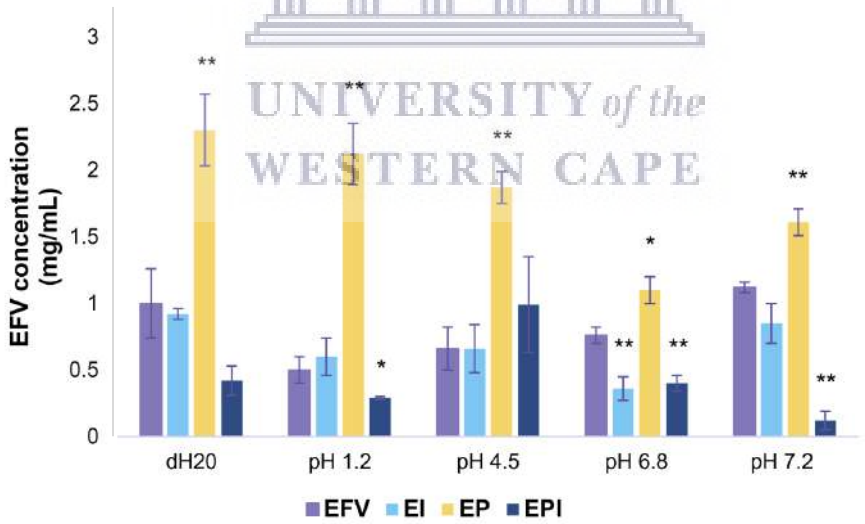

Figure 5.14: The effect of surfactant Tween® 20 on the aqueous solubility of EFV given as drug concentration (mg/mL) values measured at all bio-relevant pH values. * indicates p-value < 0.05; ** indicates p-value < 0.005. Error bars show standard deviation.

Table 5.4: Solubility values (in mg/mL) of EFV as a function of the PPI concentration added and the relative fold change in EFV solubility compared to the solubility in the presence of 6 mg/mL PPI solids.

	Distilled water		pH 1.2		pH 4.5		pH 6.8		pH 7.2	
	Solubility[+] (mg/mL)	Fold increase	Solubility[+] (mg/mL)	Fold increase	Solubility[+] (mg/mL)	Fold increase	Solubility[+] (mg/mL)	Fold increase	Solubility[+] (mg/mL)	Fold increase
EP (A) (6 mg/mL)	0.0203	-	0.0407	-	0.0198	-	0.0174	-	0.0184	-
EP (B) (2 mg/mL)	0.0027	-0.87*	0.001	-0.98*	0.0008	-0.96*	0.001	-0.94*	0.0019	-0.90*
EP (C) (1 mg/mL)	0.0024	-0.88*	0.001	-0.98*	0.001	-0.95*	0.0004	-0.98*	0.0004	-0.98*

*Indicates statistical significance with p > 0.05 [+]refer to Figure 5.15 for standard deviation

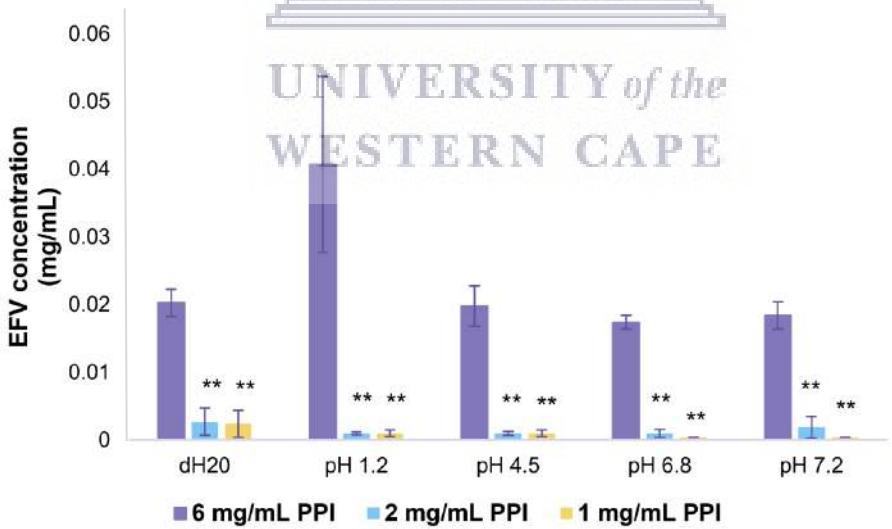

Figure 5.15: The effect that the concentration of added PPI have on the solubility of EFV (mg/mL). * indicates p-value < 0.05; ** indicates p-value < 0.005. Error bars show standard deviation.

Table 5.5: Solubility values (in mg/mL) of EFV as a function of the amount of IN added and the relative fold change in EFV solubility compared to the solubility in the presence of 10 mg/mL IN in the combination EFV, IN and PPI.

	Distilled water		pH 1.2		pH 4.5		pH 6.8		pH 7.2	
	Solubility⁺ (mg/mL)	**Fold increase**	**Solubility⁺ (mg/mL)**	**Fold increase**	**Solubility⁺ (mg/mL)**	**Fold increase**	**Solubility⁺ (mg/mL)**	**Fold increase**	**Solubility⁺ (mg/mL)**	**Fold increase**
EPI (A) (10 mg/mL)	0.011	-	0.017	-	0.012	-	0.013	-	0.022	-
EPI (B) (12 mg/mL)	0.0013	-0.88*	0.001	-0.94*	0.001	-0.92*	0.0001	-0.99*	0.0004	-0.98*
EPI (C) (24 mg/mL)	0.0016	-0.85*	0.001	-0.94*	0.0006	-0.95*	0.0004	-0.97*	0.0003	-0.99*

*Indicates statistical significance with p > 0.05 ⁺refer to Figure 5.16 for standard deviation

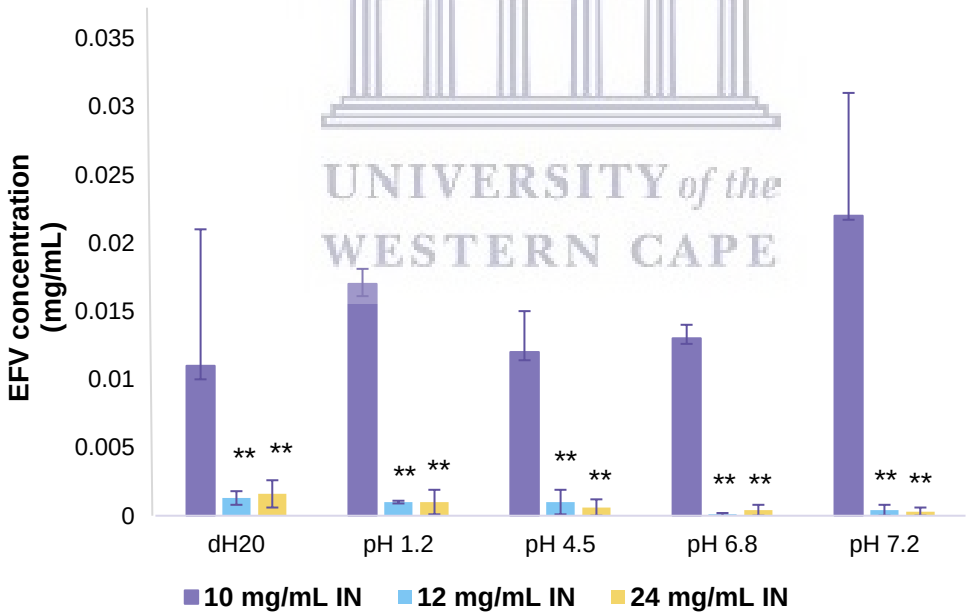

Figure 5.16: The effect that the amount of added IN solids have on the solubility of EFV (mg/mL). * indicates p-value < 0.05; ** indicates p-value < 0.005. Error bars show standard deviation.

5.2.5 Dynamic vapour sorption behaviour and powder contact angle analysis

Based on the equilibrium results as well as the physico-chemical properties, specifically, the morphology of EFV, PPI and IN, determining the wettability or ability of the compounds to attract water further corroborates the observed EFV solubility behaviour. Two recognised techniques for determining the wettability of compounds are water vapour adsorption and powder contact angle. Few correlations exist between the techniques and each provides valuable information in its own right. The results generated from the two techniques are not quantitatively but rather qualitatively comparable, to determine the relative, rather than absolute wettability of dry powders (Muster & Prestidge, 2005).

Contact angle measurements were conducted to inform the wettability of the dry powders in an effort to understand the observed solubility profiles. The greatest contact angles were observed for dry EPI (A) and EPI (C) powder whilst the smallest contact angles (which could not be measured due to instantaneous absorption of the water drop into the powder) was observed for the dry PPI and IN powder (**Table 5.6**). For this study, we focused on the comparison to EFV only to gain comparative information on the relative wettability of the powders. The combination, EI, exhibited a greater contact angle compared to EFV, suggesting poorer wettability. The combinations EP (A) and EP (B) exhibited smaller contact angles compared to EFV, suggesting better wettability of these powder mixtures. In contrast, the combination EP (C) exhibited a greater contact angle compared to EFV, suggesting poorer wettability. All three EPI combinations exhibited greater contact angles compared to EFV, suggesting poorer wettability of these powder mixtures. However, it is worthy to take into consideration the large standard deviation associated with the EFV contact angle measurements. When the largest contact angle recorded for EFV, 128.9°, is considered it can be said that EFV did exhibit the greatest contact angle of all powders tested thereby suggesting that EFV also exhibits the least wettability of all the powders. Further, it was concluded that all powder combinations containing IN and/or PPI exhibited smaller contact angles compared to EFV and therefore does exhibit an improved wettability.

Dynamic vapour sorption (DVS) analyses were performed in complement to the contact angle measurements. EFV exhibited a Type IV moisture sorption isotherm suggesting that vapour uptake is low at low vapour pressure followed by monolayer-multilayer adsorption (Muttakin et al., 2018). From the vapour sorption data, EFV showed the smallest weight change (<0.1%) when exposed to increasing %RH conditions (**Figure 5.17**). PPI exhibited a typical Type V adsorption isotherm thus suggesting that initial moisture uptake is low followed by a rapid rise, ascribed to

the hydrophilic nature of the PPI (Muttakin et al., 2018). In comparison with EFV and IN, PPI showed the greatest humidity-related weight change of ≈ 5%. IN exhibited the second biggest humidity related weight change of ≈ 3% with a typical Type III isotherm (Muttakin et al., 2018), thus suggesting that vapour uptake is low at low relative humidity levels but with a sharp increase in adsorption activity should the relative humidity rise above 75% RH. All physical mixtures of EFV with IN and/or PPI were associated with greater RH-dependent weight changes compared to EFV only, suggesting improved wettability of the powder mixtures. Additionally, it was observed that the weight change of the powder in response to increasing %RH is directly proportional to the relative amount of PPI, with the greatest relative weight change seen in the powder containing the largest amount of PPI (EP (A); **Figure 5.17).** All three EPI mixtures, containing the same amounts of PPI, adsorbed similar amounts of vapour while all three EPI mixtures were associated with greater vapour uptake compared to EP samples (EPI (A), (B) and (C); **Figure 5.17**).

It was observed from the DVS data (**Figure 5.17**) and contact angle measurements (**Table 5.6**) that PPI improves the wettability of EFV. It is known that the PPI contains some dietary fibers such as cellulose. Cellulose fibers are well known for their ability to enhance drug solubility (Wan et al., 2012; Li et al., 2013). It may be that the cellulose fibers reduce the surface tension of EFV thereby improving its wettability and subsequently also its solubility. Furthermore, the isoelectric point (p*I*) for pea proteins is reported in the range 4.3 to 4.5, with greater protein solubility observed at pH values further away from the p*I* (Doan & Ghosh, 2019). This could explain why the biggest EFV solubility improvement for EP solutions was seen at pH 1.2 and the lowest solubility improvement at pH 4.5. The same pattern was observed in 1% v/v Tween® 20 solutions (**Table 5.3**, **Figure 5.14**). It was also noted that the amount of PPI added to the solubility mixture has a significant impact on the EFV solubility, illustrating the need for optimisation of the API:excipient ratios during dosage form pre-formulation and formulation. The addition of 6 g/mL PPI resulted in the greatest solubility improvement. The possibility that a greater EFV solubility can be achieved by adding more PPI exists. This possibility was investigated but the processing of the sample for HPLC quantification through centrifugation and filtering proved to be challenging.

Table 5.6: Right- and left contact angle measurements obtained with the static sessile drop test performed on dry powders.

Powder description	Right contact angle (°)	Left contact angle (°)	Observation	Wettability characterisation
EFV	100.7 ± 22.36	100.7 ± 22.36	Drop stays	>90° - Non-wetting
PPI	-	-	Drop disappears within 3s	Perfect wetting
IN	-	-	Drop disappears within 3s	Perfect wetting
EI	105.6 ± 4.96	105.6 ± 4.96	Drop stays	>90° - Non-wetting
EP (A)	96.9 ± 0.47	96.9 ± 0.47	Drop absorbed t>30 s	Good wetting
EP (B)	90.6 ± 8.13	90.6 ± 8.13	Drop absorbed t>30 s	Good wetting
EP (C)	113 ± 3.87	113 ± 3.87	Drop stays	>90° - Non-wetting
EPI (A)	117.1 ± 5.51	117.1 ± 5.51	Drop stays	>90° - Non-wetting
EPI (B)	105.3 ± 3.67	105.3 ± 3.67	Drop stays	>90° - Non-wetting
EPI (C)	114.6 ± 3.2	114.6 ± 3.2	Drop stays	>90° - Non-wetting

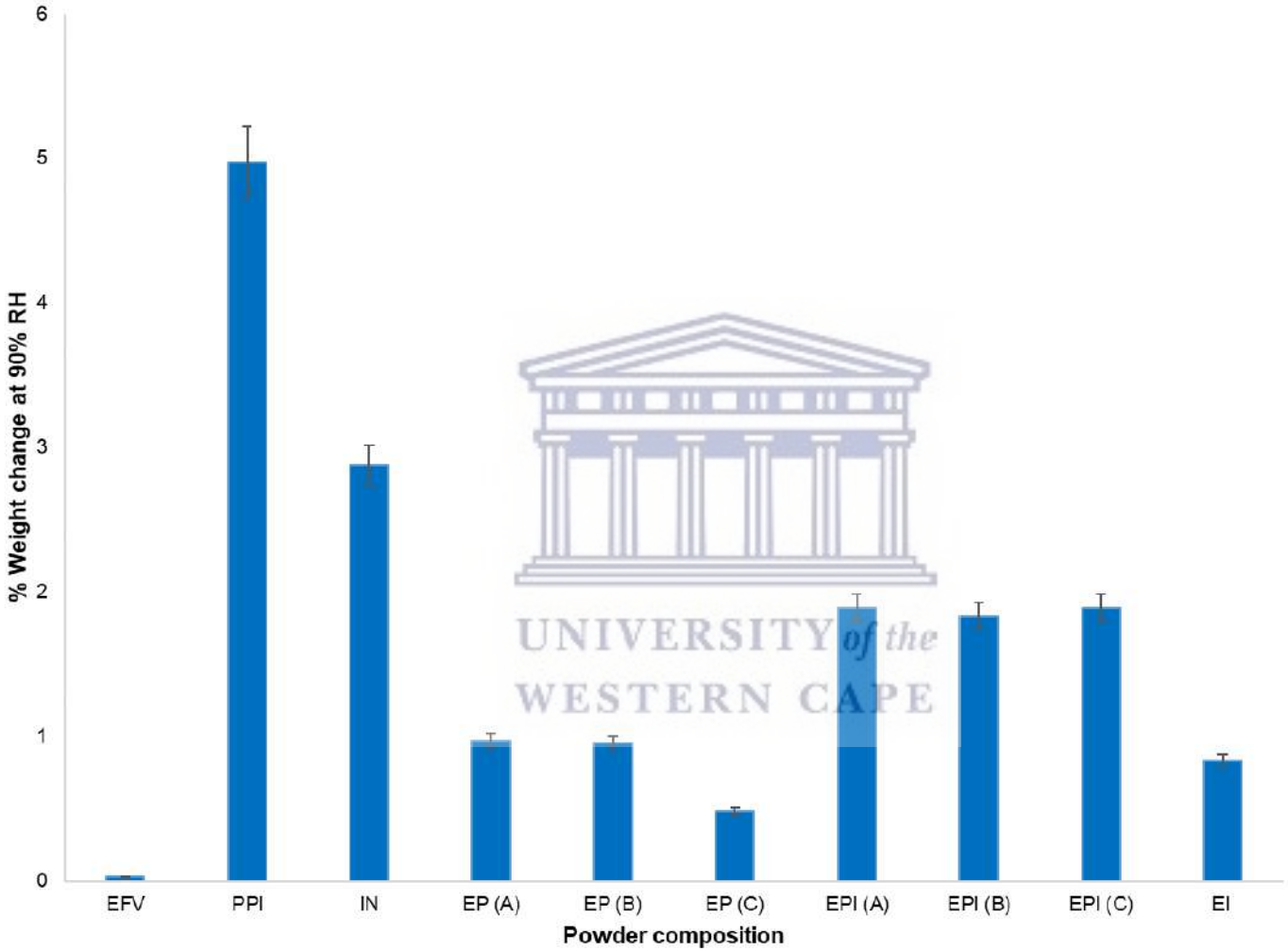

Figure 5.17: Percentage weight (%) change of powders observed after exposure to 0 - 90% relative humidity (RH) during dynamic vapour sorption analyses. Powders of EFV, PPI and IN as well as physical mixtures of EFV and PPI (EP A - C), EFV, PPI and IN (EPI A - C) and also EFV and IN (EI) were analysed isothermally over a range of 0 – 90% RH. Only the data collected at 90% RH are shown here. Error bars show standard deviation

5.3 Conclusion

Here, the physico-chemical properties of EFV and proposed excipients PPI and IN were described. The results presented here further suggested that EFV is compatible with the naturally sourced excipients, PPI and IN. As is the case with EFV, many active pharmaceutical agents (>40%) are poorly water-soluble and are often the source of formulation-related difficulties (Merisko-Liversidge & Liversidge, 2008). Here, we explored the potential use of natural excipients, PPI and IN, to improve the solubility of the poorly water-soluble ARV, EFV as well as to inform towards potential pitfalls that could be expected during the microencapsulation process. The results showed that PPI can be used to improve the solubility of EFV significantly without the use of harmful surfactants. The compatibility of EFV with both IN and PPI as excipients together with their cost-efficient nature motivated the further exploration into the microencapsulation of EFV with the use of IN and PPI. The PPI mediated improved EFV solubility observed here, held good promise for achieving good homogeneity in the spray-drying feed solution and ultimately good content uniformity in the spray-dried powder. Degradation profiles observed for the physical mixtures EP, EI and EPI further suggested the potential that the utilisation of PPI and IN as encapsulants would provide some protection against EFV thermal degradation. In the following chapters, the microencapsulation of EFV through two different technologies will be explored in conjunction with the excipients characterised here.

5.4 References

Alves, L.D.S., de La Roca Soares, M.F., de Albuquerque, C.T., da Silva, É.R., Vieira, A.C.C., Fontes, D.A.F., Figueirêdo, C.B.M., Soares Sobrinho, J.L., Rolim Neto, P.J. 2014. Solid dispersion of efavirenz in PVP K-30 by conventional solvent and kneading methods. *Carbohydrate Polymers*. 104(1):166–174. DOI: 10.1016/j.carbpol.2014.01.027.

Apolinário, A.C., de Carvalho, E.M., de Lima Damasceno, B.P.G., da Silva, P.C.D., Converti, A., Pessoa, A. & da Silva, J.A. 2017. Extraction, isolation and characterization of inulin from Agave sisalana boles. *Industrial Crops and Products*. 108:355–362. DOI: 10.1016/j.indcrop.2017.06.045.

Doan, C.D. & Ghosh, S. 2019. Formation and stability of pea proteins nanoparticles using ethanol-induced desolvation. *Nanomaterials*. 9(7). DOI: 10.3390/nano9070949.

Ewing, A. V. & Kazarian, S.G. 2018. Recent advances in the applications of vibrational spectroscopic imaging and mapping to pharmaceutical formulations. *Spectrochimica Acta - Part A: Molecular and Biomolecular Spectroscopy*. 197:10–29. DOI: 10.1016/j.saa.2017.12.055.

Fandaruff, C., Araya-Sibaja, A.M., Pereira, R.N., Hoffmeister, C.R.D., Rocha, H.V.A. & Silva, M.A.S. 2014a. Thermal behavior and decomposition kinetics of efavirenz under isothermal and non-isothermal conditions. *Journal of Thermal Analysis and Calorimetry*. 115(3):2351–2356. DOI: 10.1007/s10973-013-3306-x.

Fandaruff, C., Rauber, G.S., Araya-Sibaja, A.M., Pereira, R.N., De Campos, C.E.M., Rocha, H.V.A., Monti, G.A., Malaspina, T., Silva, M.A.S., Cuffini, S.L. 2014b. Polymorphism of anti-HIV drug efavirenz: Investigations on thermodynamic and dissolution properties. *Crystal Growth and Design*. 14(10):4968–4975. DOI: 10.1021/cg500509c.

Fernandes, R.V., Botrel, D.A., Silva, E.K., Borges, S.V., de Oliveira, C.R., Yoshida, M.I., **Feitosa, J.P. & de Paula, R.C.M.** 2016. Cashew gum and inulin: New alternative for ginger essential oil microencapsulation. *Carbohydrate Polymers*. 153:133–142. DOI: 10.1016/j.carbpol.2016.07.096.

Rajurkar, V.G., Sunil, N.A. & Ghawate, V. 2015. Tablet Formulation and Enhancement of Aqueous Solubility of Efavirenz by Solvent Evaporation Co-Crystal Technique. *Medicinal Chemistry*. 08(02). DOI: 10.4172/2161-0444.1000002.

Kawabata, Y., Wada, K., Nakatani, M., Yamada, S. & Onoue, S. 2011. Formulation design for poorly water-soluble drugs based on biopharmaceutics classification system: Basic approaches and practical applications. *International Journal of Pharmaceutics*. 420(1):1–10. DOI: 10.1016/j.ijpharm.2011.08.032.

Lan, Y., Chen, B. & Rao, J. 2018. Pea protein isolate–high methoxyl pectin soluble complexes for improving pea protein functionality: Effect of pH, biopolymer ratio and concentrations. *Food Hydrocolloids*. 80:245–253. DOI: 10.1016/j.foodhyd.2018.02.021.

Lan, Y., Xu, M., Ohm, J.B., Chen, B. & Rao, J. 2019. Solid dispersion-based spray-drying improves solubility and mitigates beany flavour of pea protein isolate. *Food Chemistry*. 278:665–673. DOI: 10.1016/j.foodchem.2018.11.074.

Li, B., Konecke, S., Wegiel, L.A., Taylor, L.S. & Edgar, K.J. 2013. Both solubility and chemical stability of curcumin are enhanced by solid dispersion in cellulose derivative matrices. *Carbohydrate Polymers*. 98(1):1108–1116. DOI: 10.1016/j.carbpol.2013.07.017.

Merisko-Liversidge, E.M. & Liversidge, G.G. 2008. Drug Nanoparticles: Formulating Poorly Water-Soluble Compounds. *Toxicologic Pathology*. 36(1):43–48. DOI: 10.1177/0192623307310946.

Muster, T.H., Prestidge, C.A., Hayes, R.A. 2005. Water adsorption kinetics and contact angles of pharmaceutical powders. *Journal of Pharmaceutical Sciences*. 176(4):253–266. DOI: 10.1002/jps.20296.

Muttakin, M., Mitra, S., Thu, K., Ito, K. & Saha, B. 2018. Theoretical framework to evaluate minimum desorption temperature for IUPAC classified adsorption isotherms. *International Journal of Heat and Mass Transfer*. 122:795-805. DOI:10.1016/j.ijheatmasstransfer.2018.01.107

Pouton, C.W. 2006. Formulation of poorly water-soluble drugs for oral administration: Physicochemical and physiological issues and the lipid formulation classification system. *European Journal of Pharmaceutical Sciences*. 29(3-4):278–287. DOI: 10.1016/j.ejps.2006.04.016.

Ronkart, S.N., Deroanne, C., Paquot, M., Fougnies, C., Lambrechts, J.C. & Blecker, C.S. 2007. Characterization of the physical state of spray-dried inulin. *Food Biophysics*. 2(2–3):83–92. DOI: 10.1007/s11483-007-9034-7.

Sathigari, S., Chadha, G., Lee, Y.H.P., Wright, N., Parsons, D.L., Rangari, V.K., Fasina, O. & Babu, R.J. 2009. Physicochemical characterization of efavirenz-cyclodextrin inclusion complexes. *AAPS PharmSciTech*. 10(1):81–87. DOI: 10.1208/s12249-008-9180-3.

Shand, P.J., Ya, H., Pietrasik, Z. & Wanasundara, P.K.J.P.D. 2007. Physicochemical and textural properties of heat-induced pea protein isolate gels. *Food Chemistry*. 102(4):1119–1130. DOI: 10.1016/j.foodchem.2006.06.060.

Tamnak, S., Mirhosseini, H., Tan, C.P., Ghazali, H.M. & Muhammad, K. 2016. Physicochemical properties, rheological behavior and morphology of pectin-pea protein isolate mixtures and conjugates in aqueous system and oil in water emulsion. *Food Hydrocolloids*. 56:405–416. DOI: 10.1016/j.foodhyd.2015.12.033.

Taneja, S., Shilpi, S. & Khatri, K. 2016. Formulation and optimization of efavirenz nanosuspensions using the precipitation-ultrasonication technique for solubility enhancement. *Artificial Cells, Nanomedicine and Biotechnology*. 44(3):978–984. DOI: 10.3109/21691401.2015.1008505.

Vitez, I.M., Newman, A.W., Davidovich, M. & Kiesnowski, C. 1998. The evolution of hot-stage microscopy to aid solid-state characterizations of pharmaceutical solids. *Thermochimica Acta*. 324(1–2):187–196. DOI: 10.1016/s0040-6031(98)00535-8.

Wan, S., Sun, Y., Qi, X. & Tan, F. 2012. Improved bioavailability of poorly water-soluble drug curcumin in cellulose acetate solid dispersion. *AAPS PharmSciTech*. 13(1):159–166. DOI: 10.1208/s12249-011-9732-9.

Wardhana, Y.W., Hardian, A., Chaerunisa, A.Y., Suendo, V. & Soewandhi, S.N. 2020. Kinetic estimation of solid state transition during isothermal and grinding processes among efavirenz polymorphs. *Heliyon*. 6(5):e03876. DOI: 10.1016/j.heliyon.2020.e03876.

CHAPTER 6

Investigating microencapsulation through spray-drying to facilitate taste-masking

6.1 Introduction

Microencapsulation is a well-known technique often employed in the taste-masking of poorly palatable substances (Bansode et al., 2010). As discussed in Chapter 2 (**Section 2.5**) – within the pharmaceutical context – microencapsulation involves the encapsulation of an active drug component while forming an outer, protective layer or wall around it. Spray-drying is often used to achieve microencapsulation of pharmaceutical drugs. Advantages of using spray-drying as a method of microencapsulation include ease of scaling up and the benefit of taste-masking as a result of the modified drug release owing to the process of drug encapsulation (Desai & Park, 2005). Since the active drug component is encapsulated within a shell, the drug molecules will ideally not be able to interact with the taste receptors on the tongue, thereby reducing a taste response (Al-kasmi et al., 2017). This strategy is particularly valuable for poorly palatable drugs such as EFV. Literature contains some examples of studies where spray-drying of EFV has been done and a few of these examples are outlined in the following paragraphs.

Verma et al., (2020) prepared a drug resin complex with EFV using the ion-exchange resin Tulsion® through the process of spray-drying to achieve taste-masking of EFV. High encapsulation efficiency (37 – 84%) of EFV was achieved and EFV release from the drug-resin complexes was deemed low enough for successful taste-masking to be concluded. These ion-exchange resin complexes are relatively expensive to manufacture and limited safety data exists with regards to their use in paediatric patients (Trofimiuk, Wasilewska & Winnicka, 2019). To improve the solubility, dissolution, and stability of EFV, Lavra et al., (2017) prepared spray-dried EFV-Soluplus® particles. High process yield (>70%) and high drug loading (>80%) were achieved under these conditions and EFV solubility was markedly improved through the production of spray-dried solid dispersions.

Costa et al., (2019) performed a very similar experiment to Lavra et al., (2017) where they prepared spray-dried amorphous solid dispersions of EFV and Soluplus®. The purpose of their study was only to characterise API-polymer solubility through the determination of a temperature-composition phase diagram obtained through DSC analysis. Again the production of spray-dried EFV solid dispersions proved successful in improving EFV solubility. The examples discussed here illustrate the value of utilising spray-drying technologies to improve EFV properties and show that spray-drying of EFV is an achievable goal. This study served as an exploration into the microencapsulation of EFV with the purpose of taste-masking using naturally occurring excipients with a low toxicity profile as well as nutritional benefits. Since the ultimate envisioned pharmaceutical product is intended for children that often also present with malnutrition it was imperative to use wall-forming materials that could potentially

offer a level of nutrition. Further to this, the choice of the two wall-formers was based on previous studies involving microencapsulation utilising PPI and IN, individually, as suitable microencapsulants (Nesterenko et al., 2014; Pauck et al., 2017; Miller et al., 2018).

During an extensive literature review, significant evidence was found where PPI was used in microencapsulation either through coacervation or spray-drying processes and mostly involving the combination of PPI with polysaccharides such as maltodextrin, gum arabic, pectin, or sodium alginate (Ducel et al., 2004; Pereira et al., 2009; Gharsalloui et al., 2010). Guided by literature the rationale was followed to combine PPI with the fructan-type polysaccharide that shows to be indigestible to humans, thus having a negligible effect on blood glucose. IN is considered a natural dietary fibre with prebiotic functionality that also shows safety in infant nutrition (Kolida and Gibson, 2007; Closa-Monasterolo et al., 2013).

In this chapter, the microencapsulation of EFV through spray-drying will be discussed within an exploratory framework. Due to the exploratory nature of the study, the spray-drying of EFV was investigated in two stages. During the first stage, a buffered aqueous solvent system was used and during the second stage, an ethanol-based solvent system was used. Overall, the potential of using spray-drying for EFV microencapsulation to potentially achieve taste-masking will be illustrated.

6.2 Spray-drying using buffered aqueous solvent

6.2.1 Choice of solvent system

Moving into the experimental design space it became apparent that information linked to the physico-chemical properties of the identified materials is critical. Since the viscosity of the feed solution had been identified as an important process parameter, as discussed in Chapter 2, **section 2.5.1**, and the initial focus was placed on determining the aqueous solubility of PPI before commencing the spray-drying optimisation process. This was due to observing that PPI doesn't dissolve completely in aqueous solutions but rather that slurries are formed, being attributed to a portion of the PPI consisting of insoluble dietary fibres thus the PPI doesn't consist purely of protein. Initially, the solubility of the protein component of PPI was investigated in pH 1.2, 4.5, 6.8, and 7.2, with solubility in pH 1.2 proving to be the highest and the lowest at pH 4.5 (**Table 6.1**). This observation is in accordance with reports in literature that the isoelectric point (*pI*) for pea proteins are in the range 4.3 - 4.5, with greater protein solubility observed at pH values further away from the *pI* (Gharsallaoui et al., 2009; Lan, Chen & Rao, 2018; Doan & Ghosh, 2019). Based on just this data we could have attempted spray-drying with a feed solution consisting of PPI:IN: EFV dispersed in aqueous buffer pH 1.2, however, this was not possible due to equipment limitations. These limitations included the

use of acid-resistant tubing and a specialised spraying nozzle with the ability to withstand low pH levels. EFV solubility was also investigated in varying pH buffered solutions (**Chapter 5**) and based on the combined results presented in **Table 6.1** it was decided to move forward using pH 6.8 as spray-drying feed solvent. Initially, spray-drying was attempted with only the wall forming materials to determine the best PPI:IN ratio based on percentage solids concentration in the feed solution, the optimal temperature at which the feed solution should be maintained and ultimately percentage powder yield. To achieve this, slurries consisting of PPI:IN (varying ratios and concentrations) in pH 6.8 aqueous buffer solution were spray-dried and the obtained results are discussed in subsequent paragraphs as part of the optimisation process.

Table 6.1: The solubility of PPI and EFV in bio-relevant buffered solutions:

pH of aqueous solution	Dissolved protein concentration (mg/mL) at 25°C (±SD)	EFV solubility (mg/mL) at 37.5°C (±SD)
dH_2O	0.575 (± 0.025)	0.0014 (± 0.0001)
1.2	0.965 (± 0.029)	0.0028 (± 0.0003)
4.5	0.110 (± 0.014)	0.0036 (± 0.0003)
6.8	0.291 (± 0.043)	0.0032 (± 0.0008)
7.2	0.843 (± 0.088)	0.0025 (± 0.0002)

6.2.2 Optimisation of spray-drying equipment parameters

The second step was to determine optimal feed preparations which will allow effective spraying, droplet drying, and particle collection. It should be noted that the spray-drying optimisation studies were performed by the Plant Bioactives Group, Agricultural Research Council, Nietvoorbij, Stellenbosch, South Africa. **Table 6.2** outlines the different process optimisation trials that were executed. The feed preparations prepared during the process optimisation stage did not contain EFV and were slurries of a 1:1 (w/w) ratio of PPI:IN. The slurry consistency was due to the insoluble fibres which formed part of PPI and therefore constant magnetic stirring had to be employed to enable a constant homogenous slurry feed to be pumped to the spray nozzle inlet. Without stirring, the particulate matter in the feed preparation would settle at the bottom of the container and lead to eventual clogging of the tubing system.

During the trials, it was observed that a feed preparation temperature of 60°C instead of 35°C improved the viscosity characteristics of the feed preparation, as no clogging of the spray nozzle occurred in Trial 6 (T6) (75% PPI content) (**Table 6.2**). In comparison, at 35°C, the feed preparation with 75% PPI content (T4) resulted in irreversible clogging of the nozzle. Although T6 could be completed, the yield was low (30.5%) because of poor separation of the particles from the air stream, and their resultant accumulation in the spray cylinder. Direct comparison

of T2 and T5, in which only the feed preparation temperatures differed, indicated an improvement in powder yield with higher temperature. However, the yields were relatively low in both cases. T2 and T5 also had the highest feed concentration (20 %w/w) which resulted in powder accumulation in the drying chamber rather in the glass collection vessel. This is typically associated with inadequate drying of the sprayed particles in the drying chamber thereby reducing the yields. These trial investigations allowed the following conclusions: the feed preparation should be stirred constantly and maintained at 60°C, higher feed concentrations were associated with lower powder yield and thus it is deemed best to keep the solids concentration in the feed preparations below 20% w/w and feed preparation should not exceed 50% w/w PPI content.

Table 6.2: Spray-drying trials for PPI: IN combinations as part of the initial optimisation stage.

	Spray-drying feed preparation					Spray-dried powder	
Trial	**Mass of PPI (g)**	**Mass of IN (g)**	**Dissolution buffer at pH 6.8 (mL)**	**Solids concentration (%)**	**Temperature (°C)**	**Moisture content (%)**	**Yield (%)**
1	25	25	500	10	35	6.02	60.4
2	50	50	500	20	35	3.02	31.6
3	37.5	37.5	500	15	35	4.85	52.0
4	56.25	18.75	500	15	35	4.65	-
5	30	30	300	20	60	4.32	40.2
6	45	15	400	15	60	3.93	30.5

6.2.2.1 Characterisation of the spray-dried powders (T1 - T6)

The spray-dried powders were subjected to thermal analysis to elucidate the effect of the spray-drying process on the thermal properties and thermal stability of the raw materials PPI and IN. From the DSC thermograms shown in **Figure 6.1,** no endotherms were observed between 30 – 180°C for T1 – 6. This corresponds to the thermograms of pure PPI and IN compounds (**Chapter 5, Figure 5.3**). Further, since these trials didn't include EFV yet, the characteristic EFV endotherm at ~140°C was not expected to be observed.

TGA analysis revealed very similar results for T1 – T6, with all thermograms indicating 2 major thermal events within the temperature range of 30 – 600°C (**Figure 6.2**). The onset of degradation for T1 – T6 was confirmed to range between 171 – 180°C. T1 exhibited the lowest onset of degradation temperature (171.2°C) while T5 exhibited the highest onset of degradation temperature (179.59°C).

Overall, the thermal properties of T1 – T6 did not significantly differ and it can be concluded that the differences in feed preparation did not have any significant impact on the thermal behaviour of the produced powders. However, it is worthy to point out that the thermal properties of the spray-dried powders were different compared to that of the pure wall forming agents PPI and IN. Therefore, it can be said that the spray-drying process does impart a degree of unique properties to the produced powders.

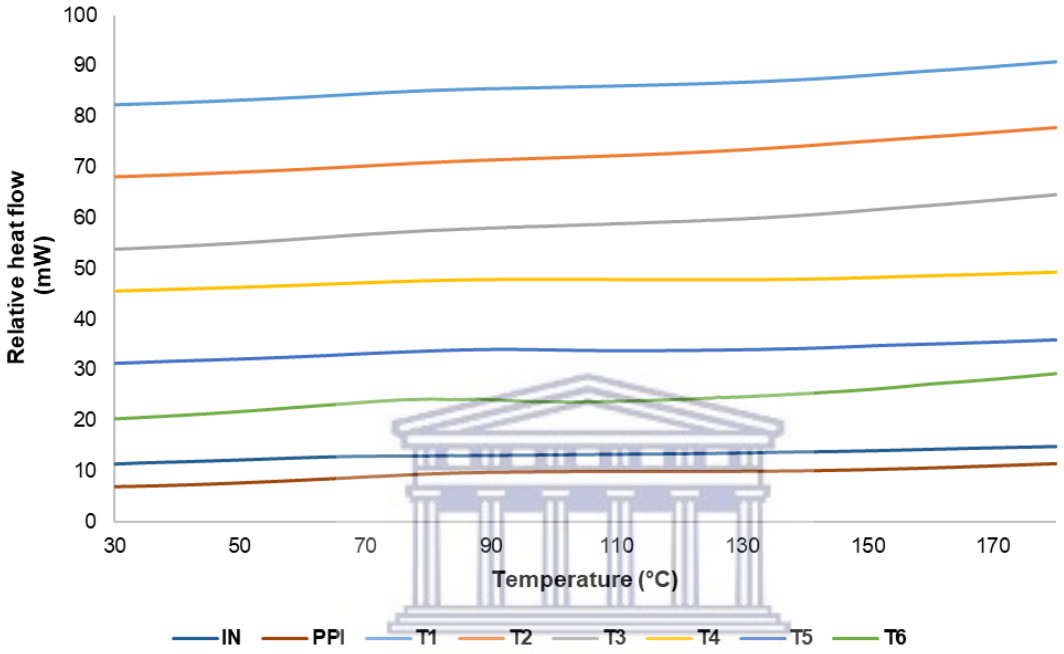

Figure 6.1: Overlay of DSC thermograms for spray-dried trials T1 – T6, collected across a heating range of 30 – 180°C.

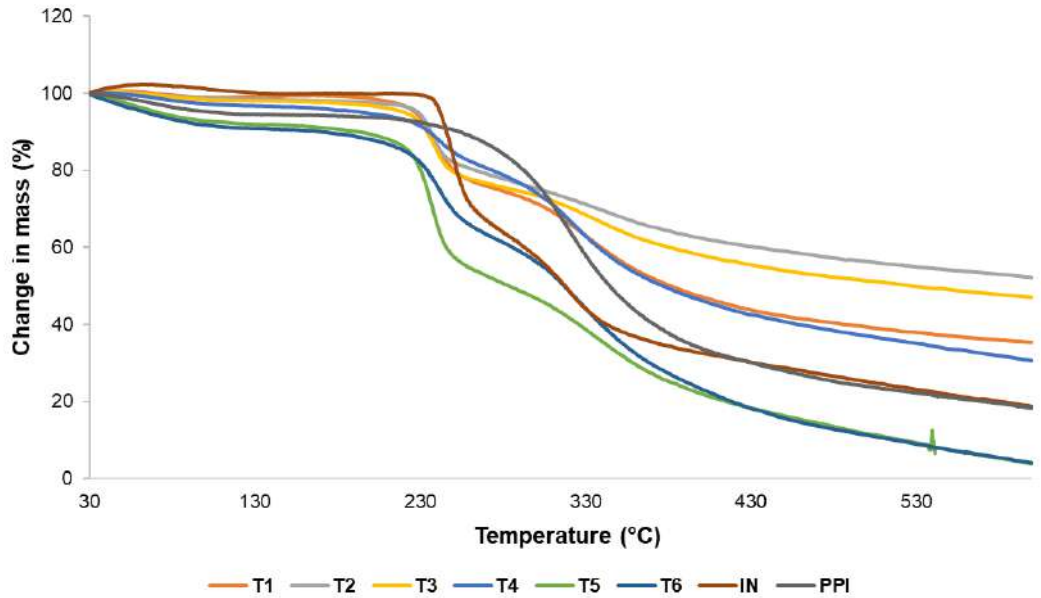

Figure 6.2: Overlay of TGA thermograms for spray-dried powders, T1 – T6, collected across a heating range of 30 – 600°C.

The FT-IR spectra obtained for T1 – T6 was compared to the FT-IR spectra of pure IN and PPI as shown in **Chapter 5** (**Figure 5.7**). IN shows a characteristic absorbance band at 3309.3 cm^{-1} which is related to the O-H groups in the IN structure (Fernandes et al., 2016). The spectrum collected from the PPI show characteristic bands at 3282.4, 2931.8, 1631.3, 1517.5, 1391.6, 1155 and 1063 cm^{-1} attributed to –OH contraction, C-H stretching, C=O stretching and the combination of N-H bending and C-N stretching in amide II and amide III, respectively (Lan et al., 2019). The FT-IR spectra of T1 – T6 show characteristic bands at 3299 cm^{-1}, corresponding to the O-H groups present in both PPI and IN, at 1631 – 1665 cm^{-1}, relating to C=O stretching from the PPI fraction and lastly at 1015 – 1035 cm^{-1} relating to the C-O stretching vibration also from the PPI fraction (**Figure 6.3**). The overlay of the FT-IR spectra of T1 – T6 shows the characteristic PPI absorbance band at 1552 cm^{-1} as was observed for pure PPI, but the intensity of this band is significantly less compared to pure PPI. Overall, the FT-IR spectra of T1 – T6 show characteristic absorbance bands of both PPI and IN, suggesting that no molecular interactions occurred between PPI and IN as a result of the spray-drying process.

Morphologically, the microspheres produced through spray-drying had a wrinkled semi-spherical appearance and most microspheres appeared to be connected to at least one other microsphere (**Figure 6.4**). T1 and T3 microspheres exhibited a more spherical appearance compared to the other trials. However, no trial was able to produce spherical, disconnected microspheres.

The solid-state nature of spray-dried trials T1 – T6 were also investigated with PXRD and the diffractograms collected were subsequently compared to those collected for PPI and IN (**Figure 6.5**). PXRD revealed an amorphous habit for T1 – T6 samples. T1 – T3 exhibited some diffraction at 12°, 17°, 18° and 22 °2θ. This suggests that these samples contained a very small and negligible fraction of crystallinity and this may be an effect of the salt used to prepare the pH 6.8 aqueous buffer used as the solvent. The crystallisation of substances as a result of spray-drying at high temperatures has been reported in literature (Islam & Langrish, 2010; Qiu et al., 2015).

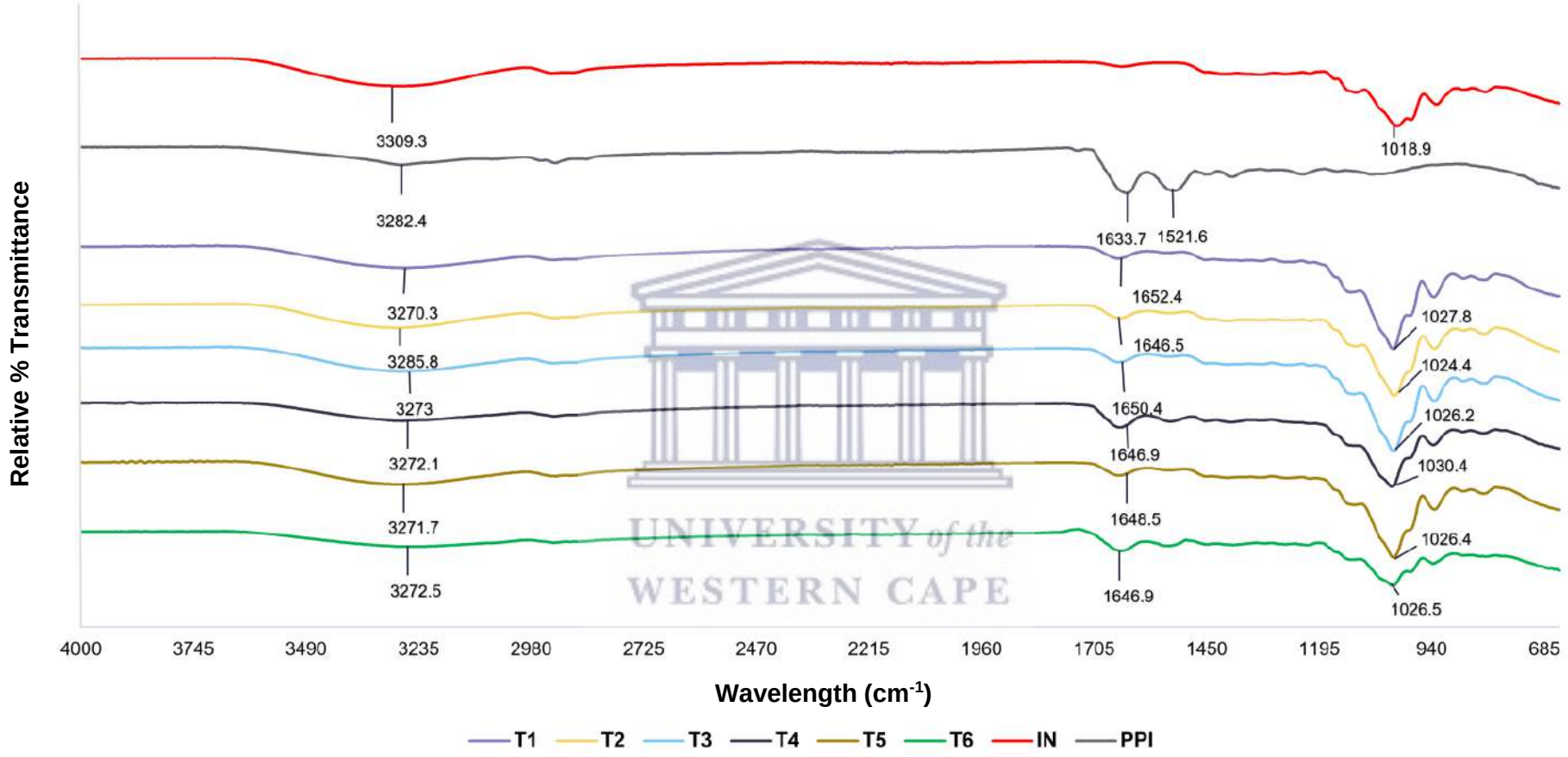

Figure 6.3: Overlay of FT-IR spectra for PPI, IN and spray-dried powders T1 – T6 collected at ambient temperature.

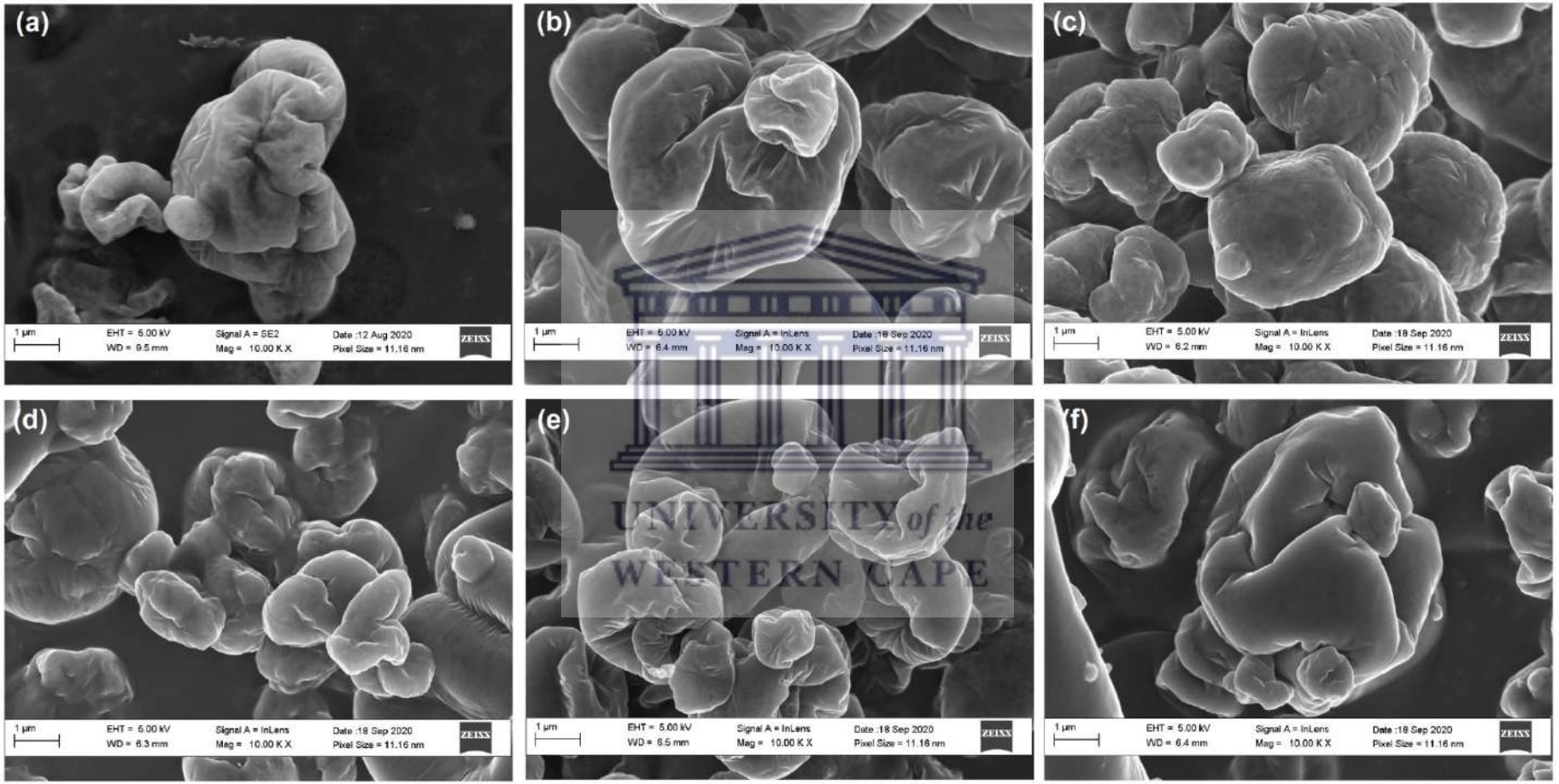

Figure 6.4: Scanning electron micrograph (SEM) micrographs of spray-dried trials T1 – T6 (a – f) captured at 10, 000 X magnification.

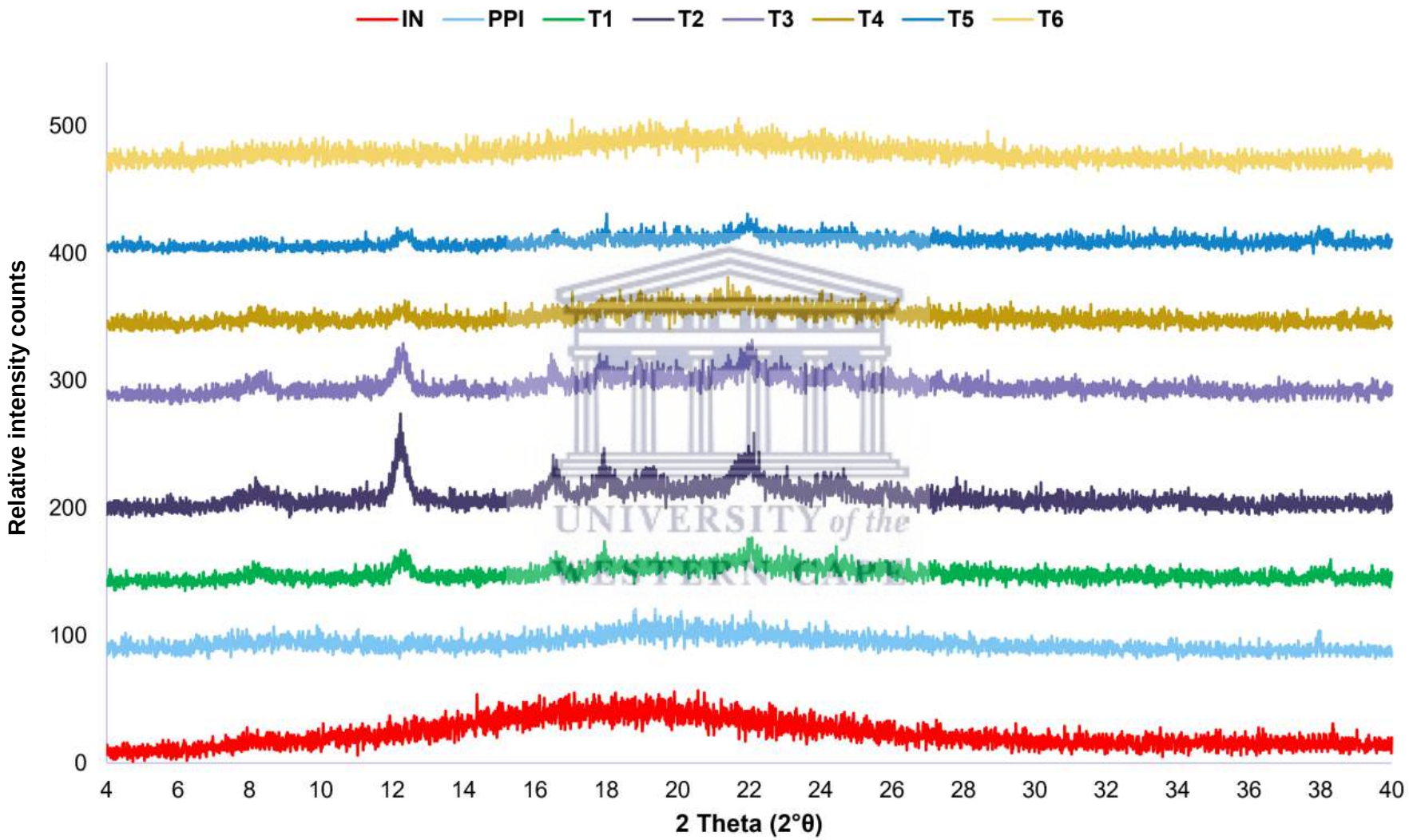

Figure 6.5: Overlay of PXRD patterns of PPI, IN and spray-dried powders T1 – T6.

6.2.3 Optimisation of the spray-drying procedure for microencapsulation of EFV

Based on the data collected from T1 – T6, further trials where EFV was included were attempted. The best performing trial from the initial optimisation phase was T1 as it was associated with the highest yield. The feed preparation for subsequent trials was prepared in accordance with T1 with the exception of using 60°C to prepare and maintain the feed solution before spray-drying. Based on the poor aqueous solubility of EFV, the addition of the surfactants SLS and Tween® 20 was investigated as part of the optimisation process. These surfactants have proven to increase the aqueous solubility of EFV significantly (**Chapter 5**) and it was expected that the efficiency of EFV encapsulation may be linked to drug solubility. Therefore the aim was to achieve the highest possible solubility of EFV in the feed solution. Another alternative that was explored was to firstly solubilise EFV in a lipophilic substance such as a generally regarded as safe oil phase. Followed by the emulsification of the oil phase in the aqueous buffered slurry consisting of PPI and IN. This resulted in the choice of olive oil as an oil phase to allow investigation of this concept. The optimisation of the spray-drying procedure for encapsulating EFV was therefore performed in three phases. In the first phase, EFV was solubilised using SLS in the second and third phases olive oil and Tween® 20 were used, respectively as solubilising agents.

6.2.3.1 Spray-drying optimisation using SLS as EFV solubility enhancer

The use of SLS surfactant in T7 – T9 resulted in low powder yields, ranging between 28 – 33%. It was therefore deduced that either the addition of SLS or EFV reduced the spray-dried powder yield. In order to investigate this further T10 served as a control trial for EFV microencapsulation, containing only EFV without the addition of any solubilisation agents. The powder yield of T10 was 55.58%, rendering it higher than T7 – T9, and it was therefore concluded that the addition of SLS had a detrimental effect on the spray-drying process. This was ascribed to the change in the feed solution viscosity when SLS is introduced into the slurry. Although viscosity was not quantitatively determined, it was observed that the PPI fibres tended to sediment out of the solution and did not want to solubilise at all. This resulted in a visibly less viscous solution. In retrospect, the determination of the feed solution viscosity in each case would have proven helpful in making more conclusive deductions.

Table 6.3: Spray-drying trials for EFV dispersed in a carrier matrix containing PPI and IN.

	Spray-drying feed preparation (60°C)						Spray-dried powder	
Trial	**Mass of EFV (g)**	**Mass of PPI (g)**	**Mass of IN (g)**	**Mass of SLS (g)**	**Aqueous buffer (pH 6.8) (mL)**	**Solids concentration (%)**	**Moisture content (%)**	**Yield (%)**
7	8	15.8	15.8	0.4	400	10	5.72	32.57
8	12	13.8	13.8	0.4	400	10	3.91	31.64
9	8	15.95	15.95	0.1	400	10	5.07	28.17
10	8	16	16	-	400	10	2.18	55.58

6.2.3.2 Characterisation of spray-dried powders (T7 – T10)

With regards to the spray-dried trials performed with EFV dispersed into a PPI and IN containing matrix, characterisation of the produced powders was done with the aim to compare the powder properties to that of pure EFV as well as to perform relative comparisons between the different trials. Visually and at ambient conditions, no significant differences between T7 – T10 were observed. All powders presented as off-white powders with similar textural properties.

i. Thermal properties of spray-dried powders (T7 – T10)

The thermal properties of T7 – T10 were studied using HSM, TGA and DSC. The HSM micrographs are shown in Appendix A (**Figure A3**). From the TGA thermograms collected for T7 – T10, three weight loss events were identified and these are shown in **Table 6.4**. The successful loading of EFV into the spray-dried powder during T7 – T10 was confirmed through the observation of a characteristic melting endotherm at 138.24°C – 138.68°C (ΔH = 2.65 J/g), corresponding to the known melting point of EFV (**Figure 6.6**). Whether or not the EFV was encapsulated during T7 – T10 could not be confirmed through thermal analysis and was further investigated using PXRD and SEM analysis which are described in the following sections.

Overall, there were not any major differences between the TGA thermograms of T7–T10. From the DSC thermograms shown in **Figure 6.6,** a single endotherm was observed in each trial between 135 – 141°C for T7–T10. This corresponds to the DSC thermogram of pure EFV

(**Chapter 5, Figure 5.1**). The observation of a single endotherm in this range is expected for T7 – T10 since these trials were done with the addition of EFV. The characteristic EFV endotherm at ~140°C observed for T7 – T10 is therefore an indication that EFV was successfully loaded into the produced microcapsules. The differences in heat of fusion observed for T7 – T10 can be attributed to the amount of sample analysed in each case. Alternatively, some of the EFV molecules may be molecularly dispersed within the amorphous PPI and IN. This could mean that less EFV is detected during thermal analysis as a result of the amorphous nature or the masking of EFV by PPI and IN. The obtained powders were further evaluated in terms of morphology using SEM and by determining the percentage encapsulation, drug content uniformity, and drug release behaviour. These results are discussed in detail in **sections 6.2.3.5 - 6.2.3.7**.

Table 6.4: Major weight loss steps identified from the collected TGA thermograms for PPI, IN, EFV and T7 – T10.

Sample	Onset temperature (°C)	Percentage weight loss (%)
PPI	30.00	6.45
	257.00	27.00
IN	222.00	17.10
	246.45	25.23
	315.00	8.41
EFV	225.00	91.95
T7	241.34	27.57
	333.61	5.31
T8	239.56	35.44
	331.15	2.69
T9	67.23	5.16
	240.45	30.82
	334.02	3.97
T10	239.23	26.51
	26.51	4.10

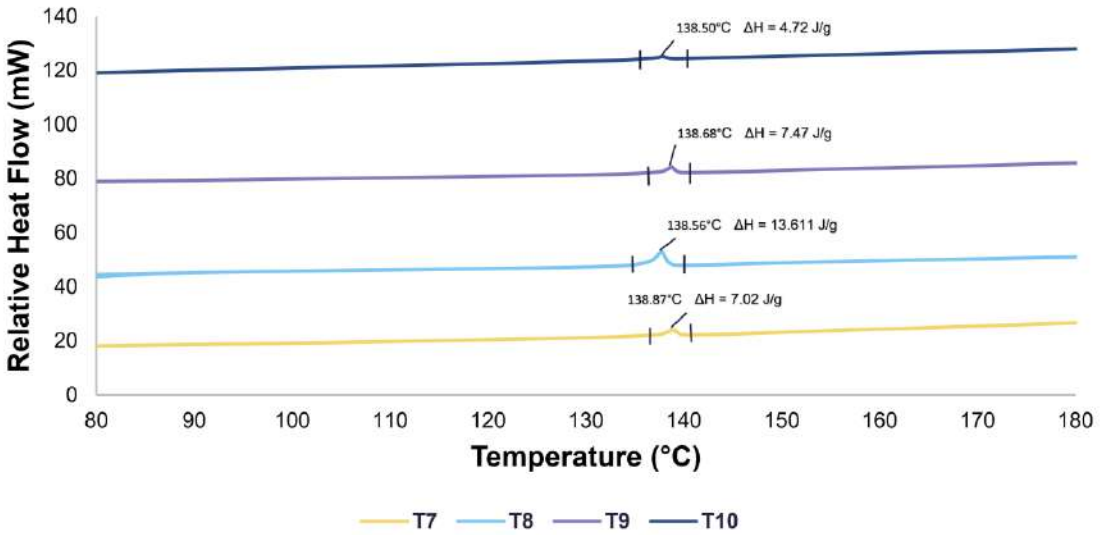

Figure 6.6: Overlay of DSC thermograms for spray-dried powders T7-T10.

ii. Fourier-transform infrared spectroscopy

As already discussed in Chapter 5, **section 5.2.2,** EFV shows characteristic absorbance bands at 3315.3, 2251.6, 1745.2, 1601.4, and 1319.7 cm^{-1}, respectively attributed to N-H stretching, aromatic C-H stretching, C=O stretching, C=C stretching, and C-O-C stretching. During FT-IR analyses of T7 – T10 focus was placed on EFV absorbance peaks and any potential shifts in the absorbance bands which could indicate that some form of interaction occurred between EFV, IN and PPI.

The FT-IR profiles of T7 – T10 proved very similar with no significant changes observed between the different trials (**Figure 6.7**). All trials showed a broad absorbance band between 3298 – 3311 cm^{-1} relating to the –OH groups of PPI and IN and thus associated with the water content of both compounds. The broad nature of this absorbance band possibly masks the N-H stretching vibration of EFV, expected around 3315 cm^{-1}. T7 – T10 further exhibited absorbance bands at 2249 cm^{-1} and 1746 – 1749 cm^{-1}, respectively attributed to the C-H stretching and C=O stretching vibrations of EFV. Absorbance bands at 1495 – 1497 cm^{-1}, 1317 cm^{-1} and 1028 cm^{-1} observed in T7 – T10 relate to the N-H bending vibrations of the amide II associated with PPI, C-O-C stretching vibrations of the EFV fraction and C-O/C-C stretching vibrations of the IN fraction, respectively. Overall, the FT-IR spectra of T7 – T10 show characteristic absorbance bands of EFV, PPI and IN and suggest that no molecular interactions occurred between EFV, PPI and IN as a result of the spray-drying process.

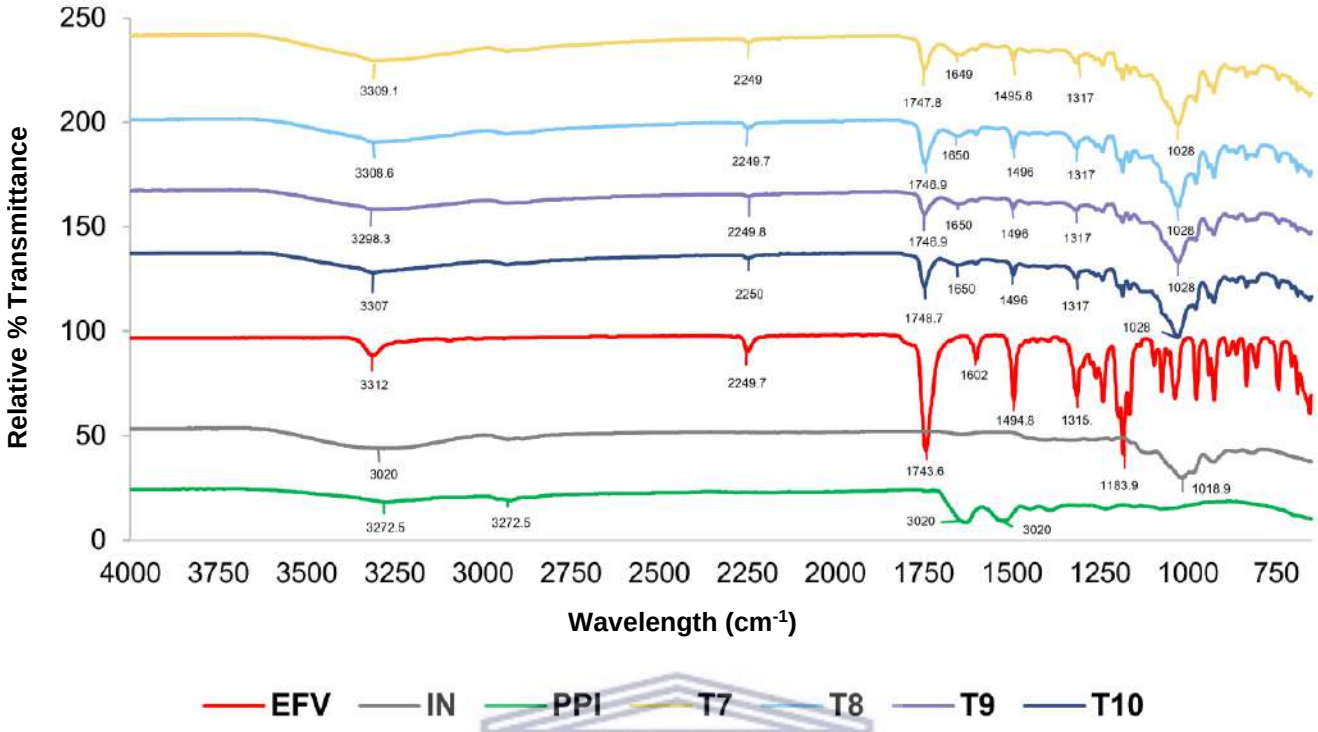

Figure 6.7: Overlay of FT-IR spectra for EFV, IN, PPI and spray-dried powders T7 – T10.

iii. Crystallinity and morphology of spray-dried powders T7 - T10

PXRD confirmed that T7 – T10 were for the most part amorphous (**Figure 6.8**). However, T7 – T10 all exhibited low-intensity diffraction at 6.17 °2θ which is attributed to the characteristic diffraction peak of EFV, suggesting that a small fraction of the samples exhibited crystalline properties, thus leading to the question of whether complete encapsulation of EFV was obtained. The peaks seen in some of the trials around 38° 2θ can be contributed solely to the use of a smaller sample holder during PXRD analysis which resulted in X-ray diffraction from the edges of the holder. The disappearance of some characteristic EFV crystalline peaks T7 – T10 could be attributed to drug masking by PPI and IN or the conversion of EFV to an amorphous state or a partial amorphous state.

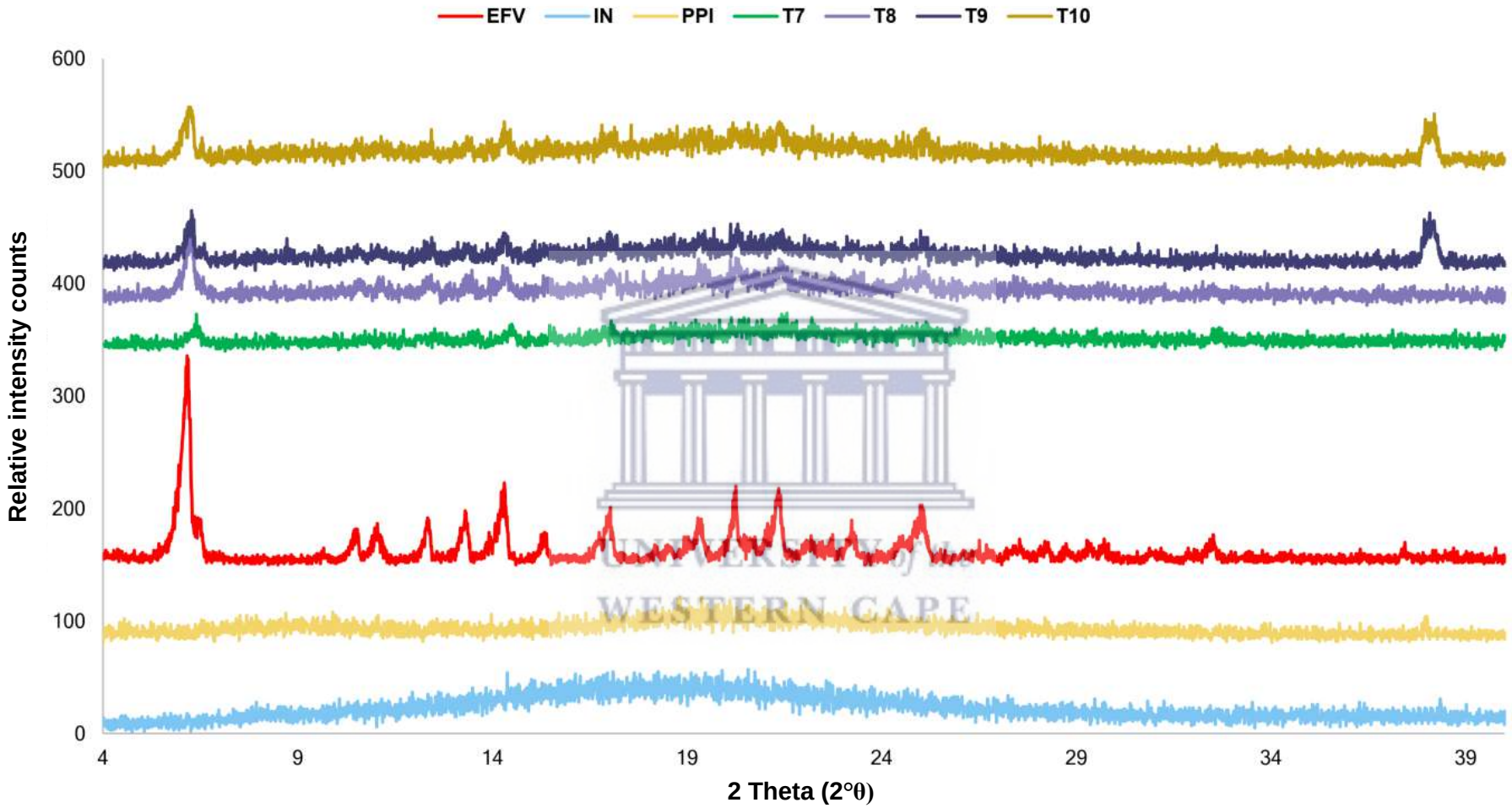

Figure 6.8: Overlay of PXRD patterns of PPI, IN and spray-dried powders T7 – T10.

6.2.4 Spray-drying optimisation using olive oil as EFV solubility enhancer

From T7 – T10, it became apparent that the formation of a homogenous feed solution in which EFV is significantly solubilised is important for efficient spray-drying, powder yields, and drug content. In this regard, the addition of olive oil to the feed solution was investigated as a potential way to improve the solubility of EFV and potentially resulting in a suitable emulsion, thus facilitating effective spray-drying. This resulted in T14 (**Table 6.5**) to which 4.0 g of EFV was added, based on preliminary solubility determination of EFV in olive oil. During spray-drying of this feed preparation, extensive deposition of particles occurred on the drying chamber wall and the cyclone separator (**Figure 6.9 (a)**), while a negligible amount of powder particles ultimately reached the glass collection vessel (**Figure 6.9 (b)**), despite the aspirator pump set to full capacity.

Table 6.5: Spray-drying trials for EFV dispersed in a carrier matrix containing PPI, IN and olive oil.

Trial	Spray-drying feed preparation (60°C)						Spray-dried powder	
	Mass of EFV (g)	Mass of PPI (g)	Mass of IN (g)	Mass of olive oil (g)	Mass of SLS (g)	Mass of Tween® 20 (g)	Moisture content (%)	Yield (%)
14	8	14	14	4.0	-	-	nd	nd
15	8	15.8	15.8	0.4	-	-	4.91	12.13
16	-	17.8	17.8	4.0	-	0.4	nd	nd
17	-	17.8	17.8	4.0	0.4	-	nd	nd

Greasy powder depositions were found on the spray cylinder wall, while the depositions in the cyclone separator and air filter inlet were less greasy but more sticky. It was also noted that the colour of the deposits was different, either suggesting physical separation or other factors (moisture content, particle morphology, agglomeration) at play. The tan colour of the wall deposit in the spray chamber was similar to that of the PPI, while the white was similar to that of IN and EFV. This allowed the conclusion that the concentration of olive oil was too high thus leading to the formation of greasy deposits that couldn't be characterised as a free-flowing powder. Subsequently, the olive oil content was reduced in T15 but a similar pattern of particle deposition was observed as for T14, albeit to a lesser extent. Powder with a moisture content

of 4.91% was collected and although a higher yield was obtained than with T14, it was still lower, compared to previous trials.

Figure 6.9: Picture showing the lack of powder collection in the collection vessel and complete covering of the drying chamber and cyclone glass with clear distinct separation of the individual feed preparation constituents, as obtained with T14 (Used with permission from the ARC).

To address the problems encountered during T14 and T15, surfactants, either SLS or Tween® 20 were added to the feed mixture in an attempt to create a stable emulsion, which would allow for more homogenous dispersion of the constituents, without relying simply on high-speed magnetic stirring to achieve this goal. EFV was not included in T16 and T17 as to first establish the potential of the feed preparation protocol for an oil-in-water emulsion. The oil-in-water emulsion was quickly added to the dry ingredients, and the feed mixture was stirred throughout the spray-drying process at a temperature of 60°C. The outlet air temperature was maintained at 90 – 100°C throughout the spray-drying process. The addition of a surfactant had an obvious effect on the appearance of the oil-in-water mixture. Magnetic stirring of the mixture after the addition of 1%w/v Tween® 20 (**Figure 6.10**) resulted in a more homogenous distribution of the oil throughout the mixture. The addition of SLS at 1%w/v had the same effect. Despite the addition of Tween® 20 or SLS as surfactants, the outcome of the spray-drying process also resulted in no powder reaching the collection vessel, and extensive deposition of practically all of the solid feed constituents was noted along the inner walls of the spray cylinder, cyclone separator and air filter inlet (similar to Figure 6.7 (a)). Upon dismantling of the system for cleaning, dry crusted material was recovered from the inside of the spray cylinder by tapping the outside walls.

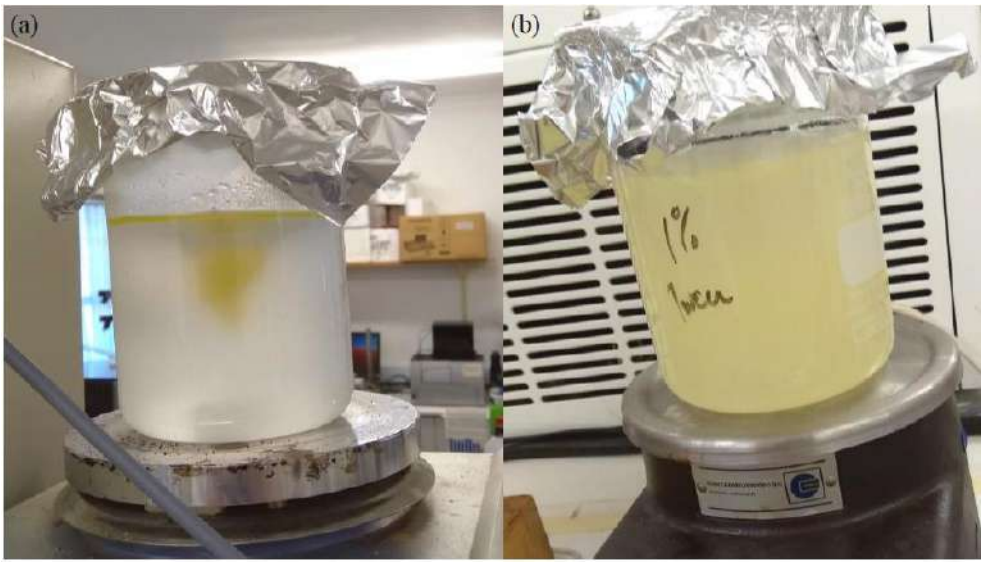

Figure 6.10: Magnetic stirring at 60°C of mixture comprising (a) 4 g olive oil in 400 mL aqueous buffer (pH 6.8), without surfactant, and (b) 4 g olive oil in 400 mL buffer with 0.4 g Tween® 20 added as surfactant.

From these trials, it was thus concluded that a more oil-like substance, although solubilising a significant concentration of EFV is not suitable to be incorporated into the feed preparation. Since most of the powder yield for T14 – T17 could not be collected successfully from the collection vessel these trials were not investigated further.

6.2.5 Spray-drying optimisation using Tween® 20 as EFV solubility enhancer

Based on the obtained results the next objective was to investigate the effect of Tween® 20 on the spray-drying of a feed mixture containing EFV, PPI and IN (**Table 6.6**). Spray-drying of the feed preparation containing 4 g of Tween® 20 (T18) resulted in poor process efficiency, with no powder collected in the collection vessel and extensive wall deposition (**Figure 6.11**). When the amount of Tween® 20 in the feed was decreased (T19 and T20), spray-dried powder with low moisture content was retrieved from the collection vessel, although yields were still comparatively low (< 44%). **Figure 6.11** depicts the major difference in the pattern of wall deposition being that higher amounts of particles were deposited on the inside of the cyclone separator when the Tween® 20 content was higher (T18) than for T19. The cyclone separator was relatively free of wall depositions upon completion of T19.

Table 6.6: Spray-drying trials for EFV dispersed in a carrier suspension consisting of PPI, IN and Tween® 20.

	Spray-drying feed preparation (60°C)					Spray-dried powder	
Trial	**Mass of EFV (g)**	**Mass of PPI (g)**	**Mass of IN (g)**	**Mass of Tween® 20 (g)**	**Aqueous buffer (pH 6.8) (mL)**	**Moisture content (%)**	**Yield (%)**
18	8	14	14	4.0	400	nd	nd
19	8	15.8	15.8	0.4	400	1.93	43.43
20	8	15.9	15.9	0.2	400	2.01	28.63
21	8	15.6	15.6	0.8	400	1.75	14.75

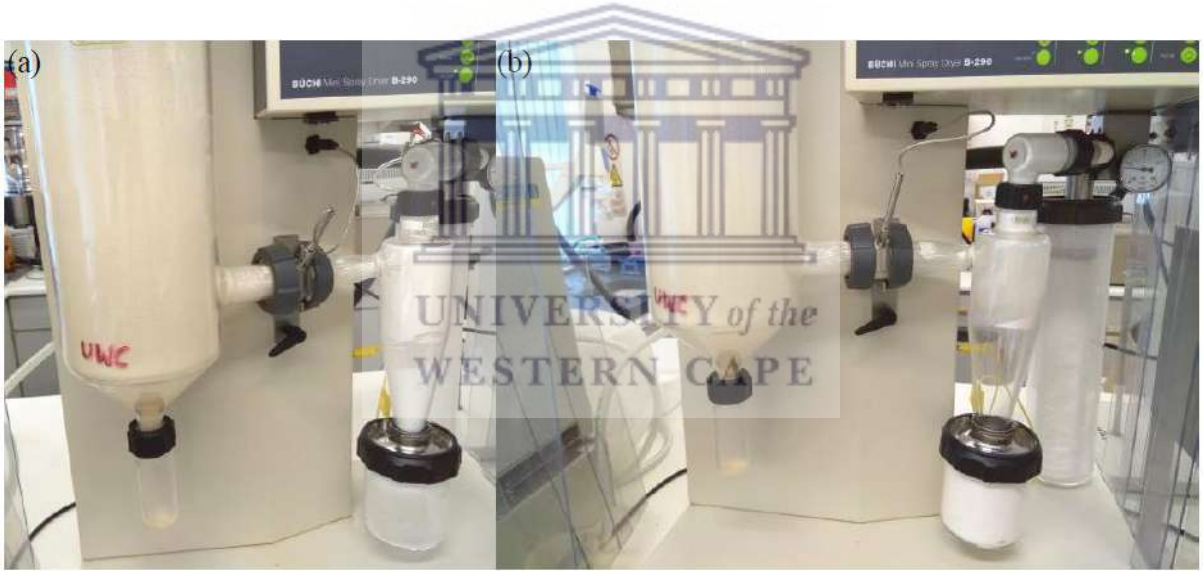

Figure 6.11: Spray-dryer pictured upon completion of (a) T18 and (b) T19.

6.2.5.1 Characterisation of produced spray-dried powders (T19 – T21)

i. Thermal properties of spray-dried powders T19 – T21

Overall, there was not any major differences between the TGA thermograms of T19 – 21. The TGA thermograms collected for T19 – T21 exhibited two major thermal events at 237.99°C - 240.93°C and 340.78°C - 326.57°C, respectively accounting for 24.73% - 29.84% and 2.794% - 5.67% - weight loss (**Figure 6.12**). The successful loading of EFV during T19 – T21 was confirmed by the observation of the characteristic EFV melting endotherm respectively identified at 138.48°C (ΔH = 4.604 J/g), 138.44°C (ΔH = 5.609 J/g) and 135.21°C (ΔH = 1.367 J/g) (**Figure 6.13**). This corresponds to the DSC thermogram of pure EFV (**Chapter 5,**

Figure 5.3). The observation of a single endotherm in this range is expected for T19 – T21 since these trials included EFV. The characteristic EFV endotherm at ~140°C observed for T19 – T21 is therefore an indication that EFV was successfully loaded into the produced microcapsules. To further evaluate the efficiency of the encapsulation process the microcapsules were further investigated utilising SEM and the determination of percentage encapsulation, drug uniformity, and *in vitro* dissolution studies. This is discussed in paragraph (**iii**) of this section as well as **section 6.2.3.6**.

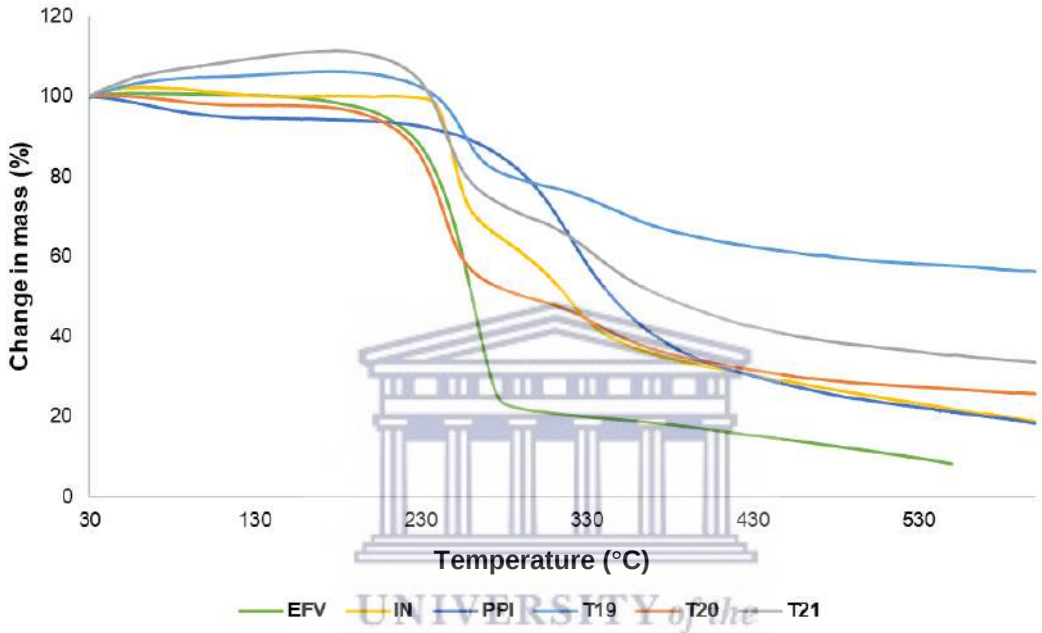

Figure 6.12: Overlay of TGA thermograms for EFV, PPI, IN and spray-dried powders collected from T19 – T21.

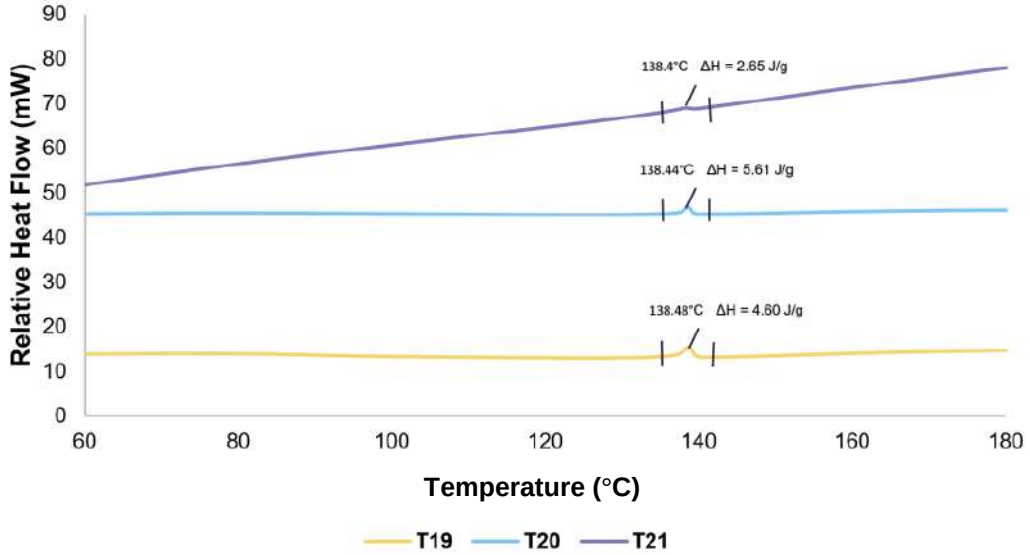

Figure 6.13: Overlay of DSC thermograms of spray-dried trials T19 – T21.

ii. Fourier transform infrared spectroscopic analysis of T19 – T21

The FT-IR spectra of T19 – T21 proved very similar with no significant changes observed between the different trials (**Figure 6.14**). All trials showed a broad absorbance between 3298 – 3311 cm^{-1} relating to the –OH groups attributed to PPI and IN and thus associated with the water content of both compounds. The broad nature of this absorbance band possibly masks the N-H stretching vibration of EFV, expected around 3315 cm^{-1}. T19–T21 further exhibited absorbance bands at 2249 cm^{-1} and 1746 – 1749 cm^{-1}, respectively attributed to the C-H stretching and C=O stretching vibrations of EFV. Absorbance bands at 1495 – 1497 cm^{-1}, 1317 cm^{-1} and 1028 cm^{-1} observed in T19 – T21 relate to the N-H bending vibrations in amide II of the PPI fraction, C-O-C stretching vibrations of the EFV fraction and C-O/C-C stretching vibrations of the IN fraction, respectively. Overall, the FT-IR spectra of T19 – T21 show characteristic absorbance bands of EFV, PPI and IN and suggest that no molecular interactions occurred between EFV, PPI and IN as a result of the spray-drying process.

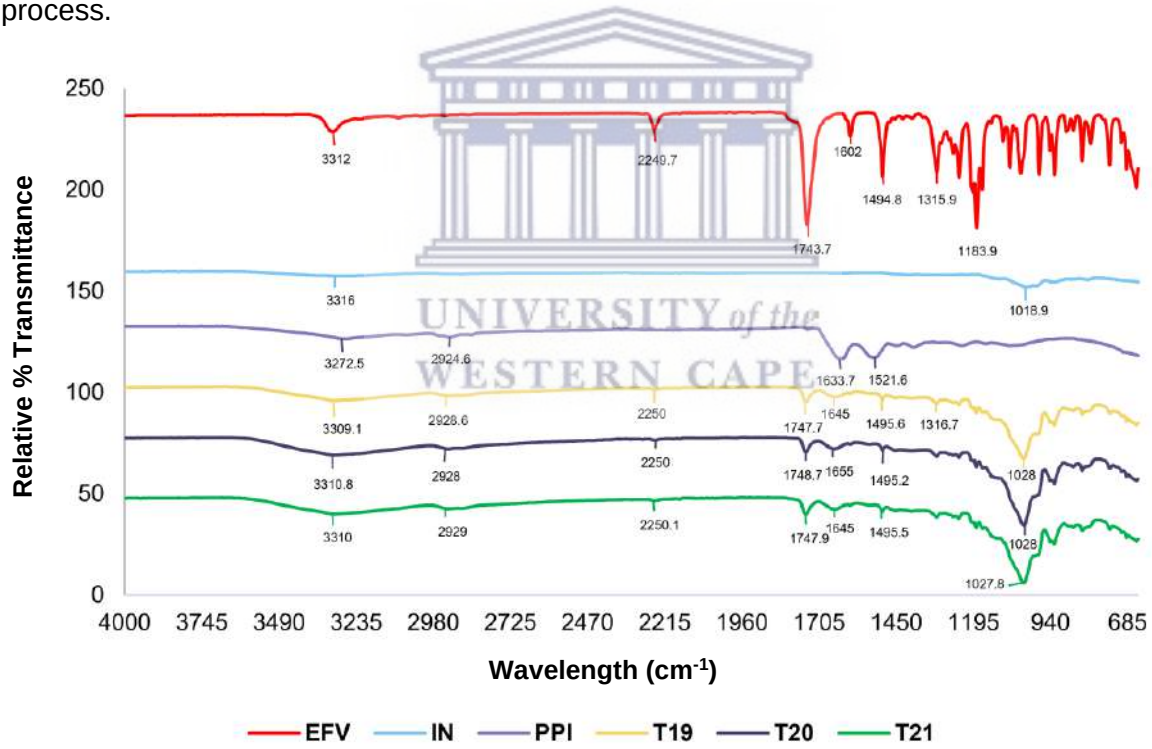

Figure 6.14: Overlay of FT-IR spectra collected for EFV, IN, PPI and spray-dried powders T19 – T21, collected at ambient temperature.

iii. Crystallinity and morphology of T19 – T21

PXRD confirmed that T19 – T21 were for the most part amorphous (**Figure 6.15**). However, just as with T7 – T10 the characteristic diffraction peak of EFV at 6.17 °2θ was observed in T19, T20 and T21. It was therefore hypothesised that incomplete microencapsulation is a possibility since the sample manipulation for PXRD analysis did not involve any vigorous

grinding which could potentially lead to rupturing of the produced microcapsules. Further investigation into the microencapsulation efficiency was thus warranted for these trials. The peak observed at 38.4 °2θ for T20 can be contributed solely to the use of a smaller sample holder during PXRD analysis which resulted in X-ray diffraction off the edges of the holder. The smaller sample holder was used for this sample due to the small amount of powder collected during the trial. The disappearance of some characteristic EFV crystalline peaks T19 – T21 could be attributed to drug masking by PPI and IN or the conversion of EFV to an amorphous state or a partial amorphous state.

SEM micrographs were only collected of T10, T19 and T21. This was because, during these trials produced a sufficient amount of product that could be collected for analysis. SEM micrographs depict the rod-like EFV particles (**Figure 6.16(a)**) in comparison with the general spherical particle shape of T10, T19 and T21. SEM analysis showed the incomplete microencapsulation associated with T10 (**Figure 6.16(b)**) with rod-like EFV particles protruding from the spherical particles. Protrusion of EFV particles was also apparent from the particles associated with T19, but to a much lesser extent (**Figure 6.16(c)**). This observation suggests that a greater degree of EFV encapsulation was achieved with T19, whilst in comparison T21 did not show any protruding EFV particles. The presence of rod-like EFV particles protruding from the spherical particles could be the effect of EFV instability. It is therefore possible that the quantity of EFV molecules protruding from particles is not an indication of the degree of encapsulation achieved, but rather indicates the conversion of amorphous EFV to a more stable crystalline form. The time between the production of the spray-dried powders and the SEM analysis could very well have had an effect on EFV stability. Due to the COVID-19 pandemic and SEM equipment problems, samples were not analysed immediately after production and storage times for the different trials were not the same. Different storage times could have resulted in varying fractions of EFV converting from amorphous to crystalline thereby accounting for the differing quantities of protruding EFV particles. The surface morphology of T21 showed an almost fused, uniform mass and it was not possible to distinguish individual particles (**Figure 6.16(d)**). These results correlate to the PXRD patterns (**Figure 6.8 and 6.15**).

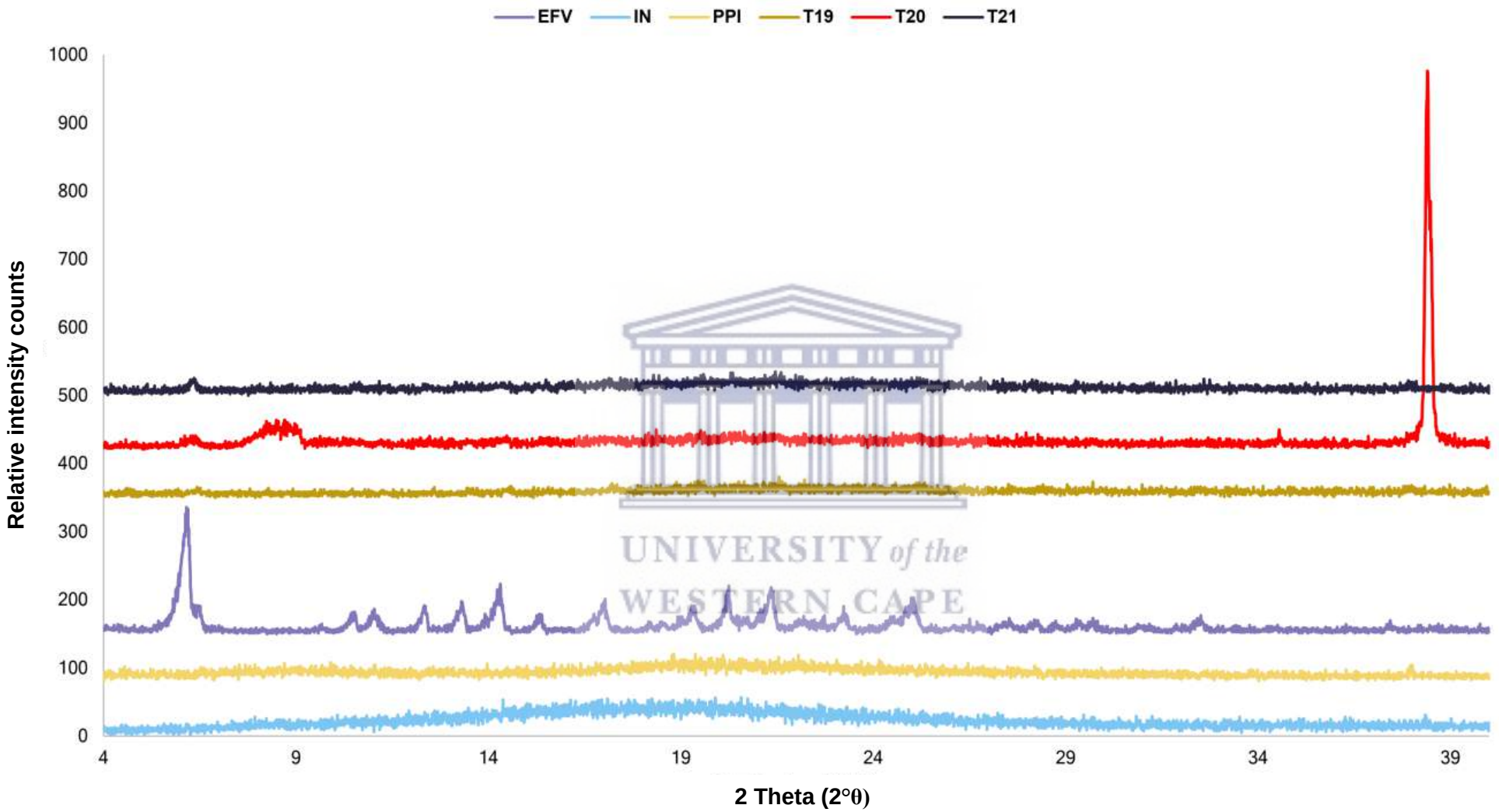

Figure 6.15: Overlay of PXRD patterns obtained for EFV, PPI, IN and spray-dried trials T19 – T21.

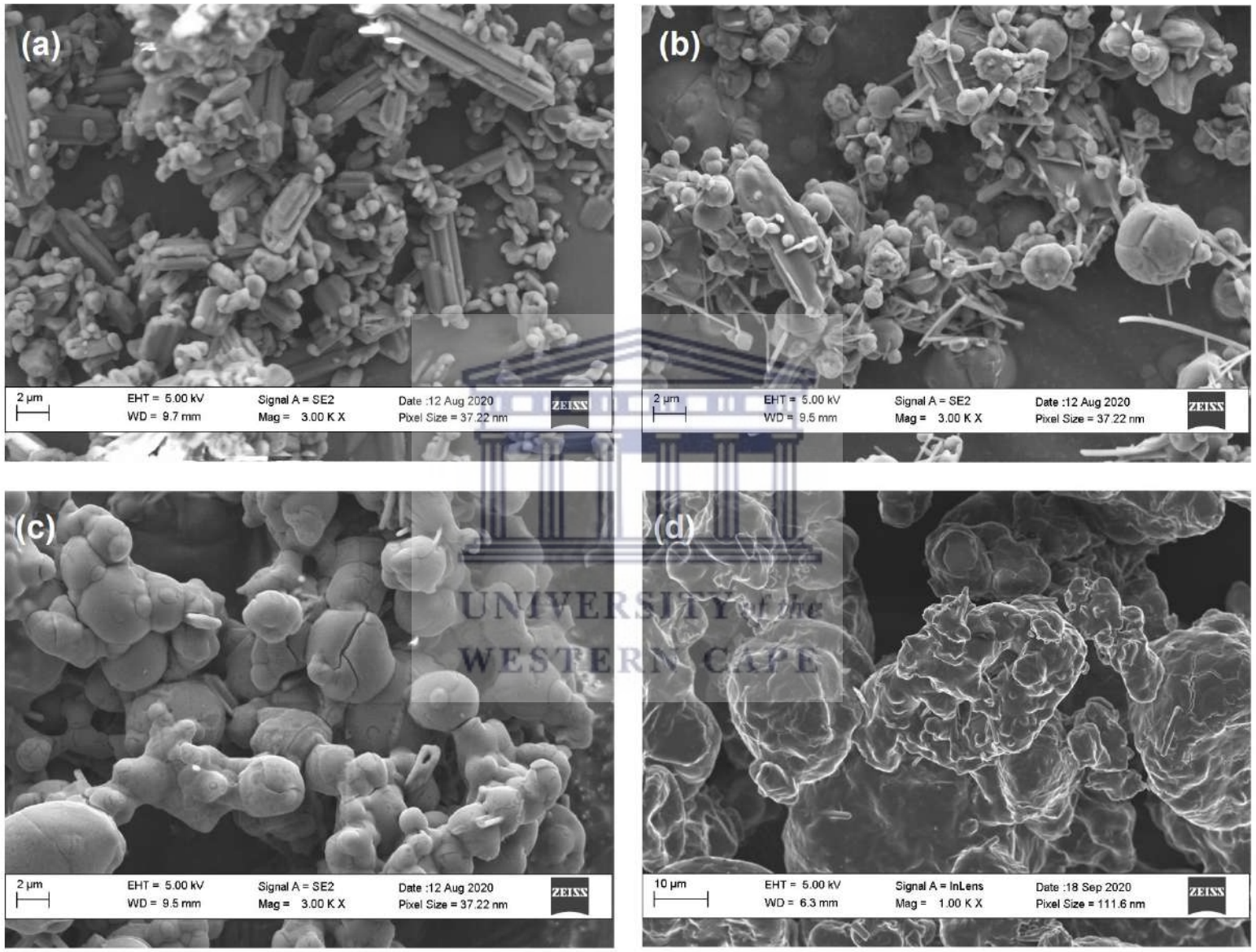

Figure 6.16: Scanning electron microscope (SEM) micrographs of EFV (a) and spray-dried powders T10 (b) and T19 (c) captured at 3, 000 X magnification and T21 (d) captured at 1, 000 X magnification.

6.2.6 EFV drug content, percentage drug loading and content uniformity of trials T7 – T21

The EFV drug content of the produced spray-dried powders was determined in order to evaluate the efficiency of the process and also to inform the practicality of the powders as solid oral dosage forms. Drug loading achieved during T7 – T21 ranged between 55.64 – 85.28% with T8 and T21 exhibiting the highest EFV content and T19 exhibiting the lowest EFV drug content (**Table 6.7**).

Table 6.7: EFV drug content, the achieved drug loading % and EFV content uniformity of spray-dried powders from T7 – T21.

Trial	% Drug loading	Content uniformity at top (%)	Content uniformity in middle (%)	Content uniformity at bottom (%)
7	76.91	92.65	102.67	104.68
8	57.54	111.73	88.41	99.87
9	57.36	102.45	98.16	99.40
10	61.06	82.65	108.11	109.24
19	55.64	105.96	96.22	97.82
20	56.67	85.09	108.81	106.10
21	85.28	108.62	111.09	76.29

*%Drug loading and drug content uniformity was calculated using *Equations 4.2* and *4.3* as described in **section 4.3.6**

The high EFV content of T8 can be related to the higher EFV loading during the preparation of spray-drying feed solutions (**Table 6.7**). T8 was prepared with 50% more EFV than any of the other trials. Considering this, it is clear that the amount of EFV loaded into the feed solutions can influence the final EFV content of the powders. The high EFV content of T21 can be related to the effect of Tween® 20 on the solubility of EFV as well as the improved homogeneity of the feed solution (**Table 6.7, Figure 6.10**). The improvement of EFV solubility by Tween® 20 was fully discussed in **Chapter 5, section 5.2.4**.

T7–T21 were all associated with relatively high effective drug loading percentages ranging between 55 – 86%. This means that a significant fraction of the EFV added into the initial feed solutions was retained in the final powder. Drug loading efficiencies can have considerable consequences for the economic aspects of production and manufacturing and therefore it is a critical process parameter for consideration when optimising process parameters. Drug loading efficiencies do not appear to be linked to the use of SLS in feed solutions since T10, which contains no surfactant, exhibited a higher drug loading percentage compared to

T7 – T9. The results do however demonstrate that the drug loading efficiency of EFV microspheres was affected by the concentration of Tween® 20. When comparing T19 – T21 it is apparent that a higher Tween® 20 concentration is associated with a higher drug loading efficiency. The difference in the effect of SLS and Tween® 20 may relate to the chemical nature of the compounds. Tween® 20 was used in this study, which could have increased the viscosity of the feed solution. Increased viscosity of feed solutions, within limits, has been reported to increase the drug encapsulation efficiencies during spray-drying (Desai & Park, 2005). The increased viscosity of the solution could prevent the too rapid drying of the atomised droplets after spraying thus allowing droplets to dry more uniformly and subsequently allowing complete microcapsule formation. The use of natural polymers such as chitin, chitosan, or sodium alginate could potentially further increase the EFV drug loading into the spray-dried microspheres by increasing the viscosity of the feed solution.

Content uniformity in the powders was determined to evaluate the uniform distribution of EFV within the powder. This is important for the therapeutic efficiency and safety of such a dosage form. Drug content uniformity for all trials, except T10 and T21, was acceptable with drug content at different sampling locations ranging between 85 – 112% complying with the quality control standards outlined in the USP (U.S. Pharmacopoeial Convention, 2011). T21 exhibited the largest variation in drug content for EFV drug content (76.29 – 115.09%), illustrating a significant variation in EFV content within the sample that could have negative implications for the therapeutic efficiency and safety of the product. This large variation in the drug content is relatively unexpected as the feed solution for T21 did appear the most homogenous in nature of all the trails. The initial homogeneity of the solution can therefore not be the causing factor of this large EFV content variation. It is possible that some degree of separation occurred during storage resulting in the observed content variation.

6.3 Evaluation of *in vitro* drug release as an indication of potential taste-masking

As part of the study, it was imperative to test the release of EFV from spray-dried samples (T7 – T21) in a pH 6.8 dissolution medium to inform whether the potential of taste-masking could be achieved through this particular process microencapsulation. A preliminary study was carried out at first (n = 1) using only one dissolution vessel to simply inform the best performing trials. The 3 best performing trials were selected based on drug release in pH 6.8 as well as the safety of excipients in the paediatric population. In this regard, T19 and T21 were immediately selected as the lowest drug release was associated with these trials. T7 and T9 exhibited the next lowest drug release, however, these trials were prepared with SLS and so trace amounts of SLS would have been present in the final powders. SLS is known to be a

mucosal irritant and therefore its use in a paediatric formulation will prove problematic (Neppelberg et al., 2007; Ahlfors, Dahl & Lyberg, 2011). With T8 and T10 exhibiting very similar dissolution performance in pH 6.8 the decision was made to continue with T10 as the preparation of T10 did not include SLS as with T8. *In vitro* drug release associated with T10, T19 and T21 were determined as per the method described in Chapter 4, **section 4.3.11**.

Drug release from T10, T19 and T21 was higher compared to EFV raw material (**Figure 6.17**). This initially raised concern with regards to the achieved taste-masking through spray-drying. Subsequently, the decision was made to also perform an *in vitro* dissolution assessment of Stocrin® film-coated tablets, an on-the-market drug formulation of EFV, in a pH 6.8 media. This provided promising results into the relative taste-masking of the microspheres. T10, T19 and T21 all exhibited at least 10-fold lower drug release in pH 6.8 medium compared to Stocrin® film-coated tablets (**Figure 6.18**). The significantly lower drug release of EFV from spray-dried microcapsules suggests that at least some level of taste-masking could be possible. An alternative explanation could be related to the SLS content of Stocrin® tablets. Given that Stocrin® tablets contain a small amount of SLS it may very well explain the higher drug release observed. Nevertheless, if a patient was to consume a crushed dose of Stocrin® tablets, they will likely experience some degree of mucosal irritation and potentially the well-known bitter taste associated with Stocrin® tablets.

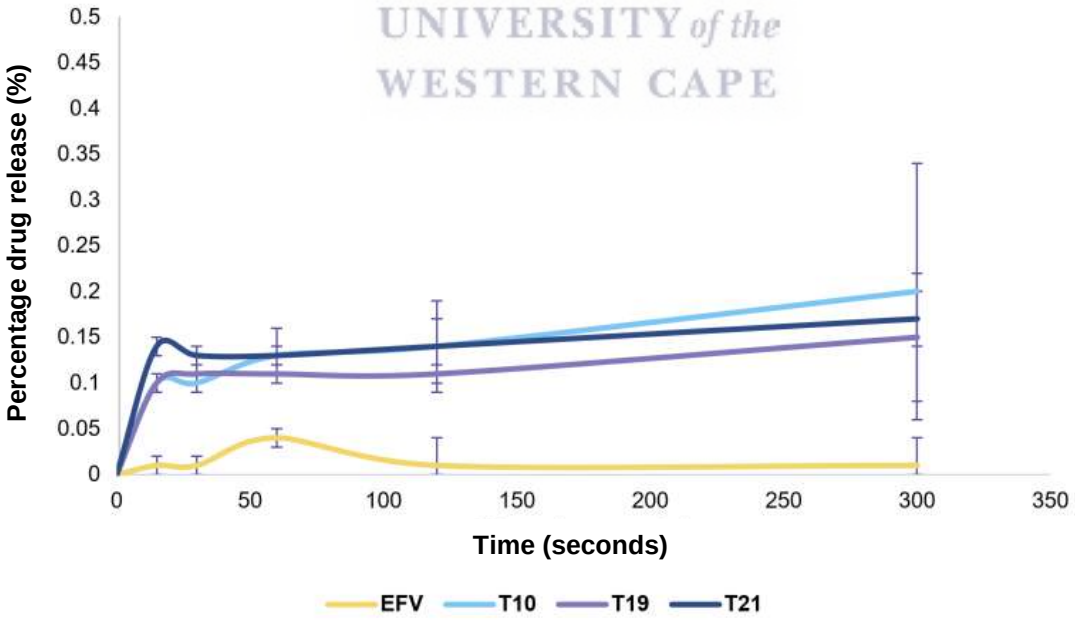

Figure 6.17: The percentage drug dissolution for EFV raw material and the EFV loaded microspheres produced during T10, T19 and T21 in pH 6.8 media maintained at 37.5°C. Error bars show standard deviation.

Because different pharmaceutical drugs have different taste intensities and taste profiles the % drug release threshold for each drug is different. It is therefore not accurate to use the reported thresholds of other drugs for interpreting EFV data. Unfortunately, no drug release threshold for evaluating taste masking of EFV dosage forms has been reported in the literature. Despite this, the results obtained here for spray-dried EFV microspheres do present promising properties related to taste-masking. Other strategies for evaluating taste-masking do exist. These include the use of electronic tongue systems and human taste panels. The economic and ethical factors related to such studies make it difficult to completely evaluate the achieved taste-masking. The results obtained from *in vitro* dissolutions studies remain predictive and not absolute with regards to taste-masking evaluation.

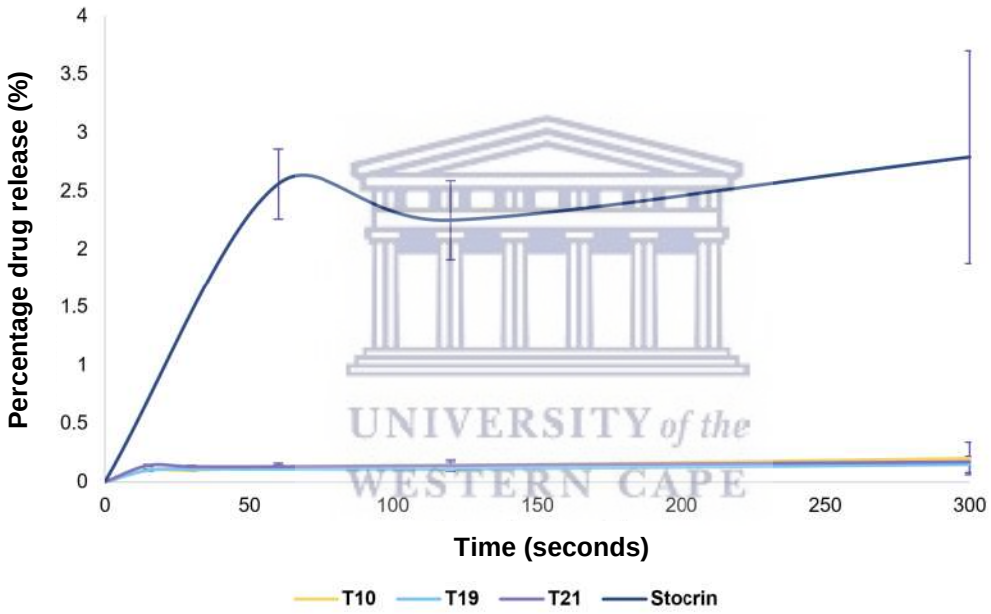

Figure 6.18: The percentage drug dissolution for Stocrin® film-coated tablets compared to the EFV-loaded microspheres produced during trials T10, T19 and T21 in pH 6.8 media maintained at 37.5°C. Error bars show standard deviation.

From the results obtained it appears that there is some correlation between the drug loading and the maximum drug release. This is prevalent with T21 as this trial showed both the highest drug loading and the highest maximum drug release in pH 6.8. However, the observed trend could also be an effect of the Tween® 20 in the formulation since Tween® 20 has been proven to facilitate the solubilisation of EFV (**Chapter 5**, **section 5.2.4**). This could also explain why T19 exhibited higher drug release despite being associated with lower drug loading compared to T10. Despite the highest degree of physical EFV encapsulation being observed for T21, the drug release for T21 was not the lowest as might be expected from a higher degree of encapsulation. This illustrates that improved physical encapsulation does not necessarily

correspond to delayed dissolution thus not unequivocally providing the possibility of effective taste-masking. Dissolution of poorly soluble drugs is known to be solubility limited and so it is possible that the low drug release observed in the dissolution profiles can be attributed to low EFV solubility in pH 6.8 media (Aulton, 2017).

6.4 Investigation of EFV spray-drying using ethanol as feed solution solvent

It should be highlighted that this part of the study originated after the University of the Western Cape, School of Pharmacy was able to procure a suitable spray-dryer.

6.4.1 Choice of solvent system

EFV is known to be freely soluble in ethanol (Avachat & Parpani, 2015) and therefore the choice of ethanol for the solvent system was based on the high solubility of EFV in ethanol and the acceptable viscosity of the prepared feed solution. Since the research is aimed at contributing to paediatric drug development the use of 100% ethanol was not the ideal option. So a short observation experiment was conducted to determine the lowest ethanol: water ratio that resulted in complete solubilisation of EFV and was found to be a 50% v/v ethanol solution. Subsequent spray-drying trials were carried out using 50% v/v ethanol solutions for feed preparation.

Table 6.8: Spray-drying trials for EFV dispersed in an ethanol-based carrier matrix containing PPI and IN.

	Spray-drying feed preparation				Process	Spray-dried powder	
Trial	**Mass of EFV (g)**	**Mass of PPI (g)**	**Mass of IN (g)**	**Solvent 50% v/v EtOH (mL)**	**Inlet temperature (°C)**	**Moisture content (%)**	**Yield (%)**
22	8	16	16	400	185	7.83	5.55
23	9	18	18	450	190	4.19	26.6

6.4.2 Optimisation of the process parameters for using an ethanol-based solvent system

The feed preparations for T22 and T23 were prepared based on the optimisation conducted earlier in this study (**Table 6.8**). The only change that was made to the original optimised feed preparation was the solvent system being changed to 50% v/v ethanol and with the omission

of any surfactants. Due to the change in the solvent system, some process parameters were changed. The inlet temperature was changed to accommodate the boiling point of the 50% v/v ethanol solution and subsequently, nitrogen gas was used rather than compressed air to create an inert spraying environment.

6.4.3 Characterisation of the spray-dried powder produced

i. Thermal properties of T22 and T23

TGA analysis was used to confirm the onset of degradation at a temperature of 193.19°C (**Figure A5**). Between 200 – 250°C the sample colour darkened progressively as the temperature increased. The TGA thermogram was also used to identify a major thermal event at 237.91°C that accounted for a 24.39% weight loss. This further confirms the degradation of the sample at temperatures higher than 193.19°C. At the end of the TGA run, at 600°C, 37.8% of the sample remained. The successful loading of EFV during T22 was confirmed by the observation of the characteristic EFV melting endotherm at 138.4°C (**Figure 6.19**).

This was confirmed with TGA analysis, where the TGA thermogram was used to confirm the onset of degradation at a temperature of 191.21°C (**Figure A5**). Between 191 – 220°C the sample colour darkened progressively as the temperature increased. The TGA thermogram was also used to identify a major thermal event at 236.91°C that accounted for a 32.4% weight loss. This further confirms the degradation of the sample at temperatures higher than 191.21°C. The successful loading of EFV during T23 was confirmed by the observation of the characteristic EFV melting endotherm at 135.21°C (**Figure 6.19**).

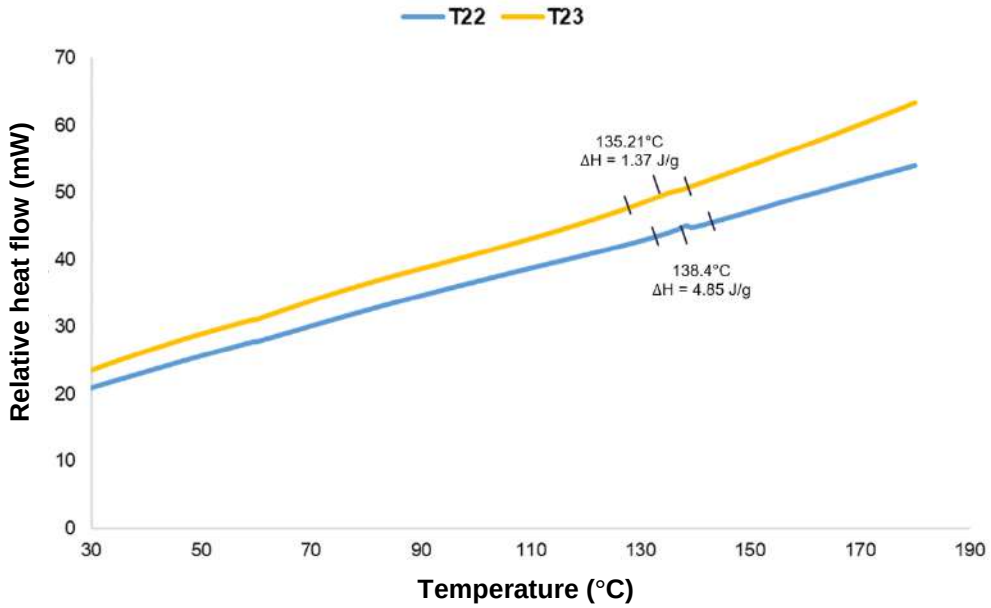

Figure 6.19: Overlay of DSC thermograms of spray-dried powders from T22 and T23.

ii. Fourier transform infrared spectroscopic properties of T22 and T23

T22 and T23 showed a broad absorbance at 3267 cm^{-1} relating to the –OH groups of PPI and IN (**Figure 6.20**) and further to this both trials show characteristic absorbance bands associated with EFV, PPI and IN thus suggesting that no molecular interactions occurred between EFV, PPI and IN as a result of the spray-drying process.

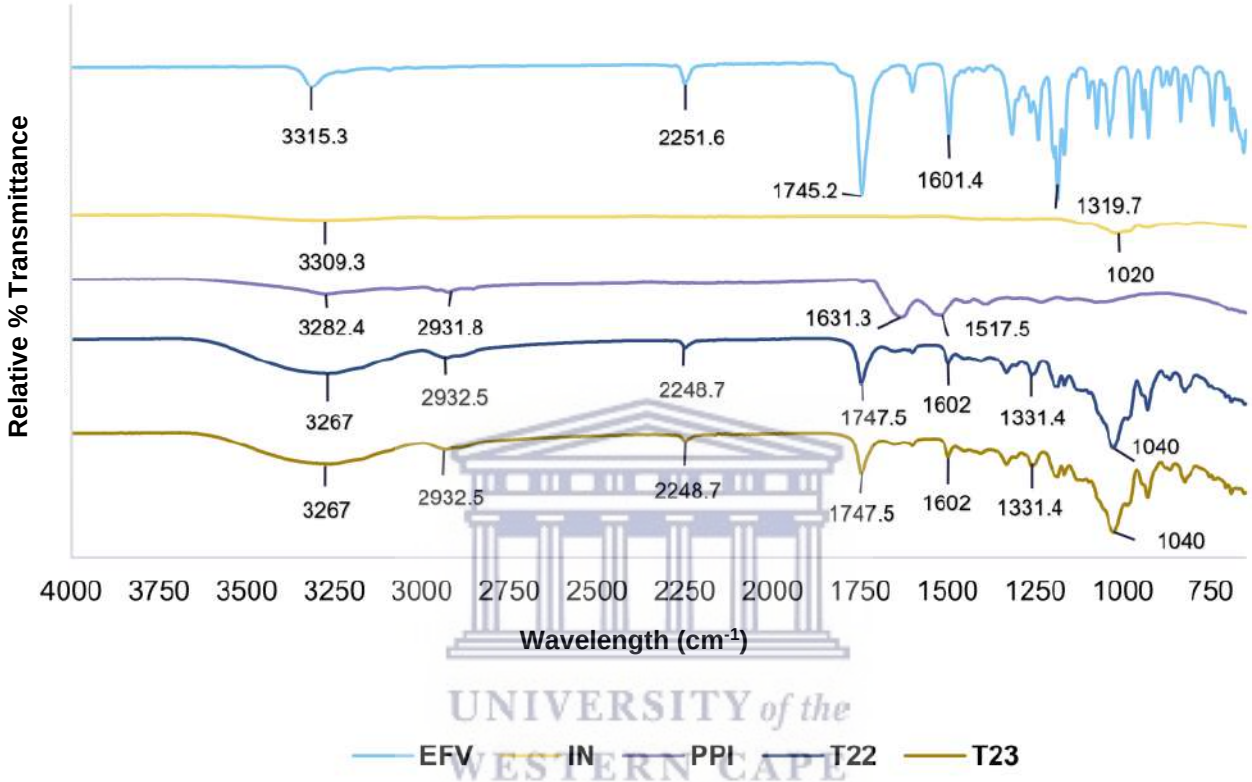

Figure 6.20: Overlay of FT-IR spectra of EFV, PPI, IN, T22 and T23, collected at ambient temperature.

iii. Crystallinity of T22 and T23

The amorphous habit for both T22 and T23 was confirmed using PXRD. T23 exhibited low-intensity diffraction peak at 6.17 °2θ, which is characteristic of EFV, suggesting that complete microencapsulation of EFV during this trial was possibly not achieved (**Figure 6.21**). The peak seen in T23 around 38°2θ can again be contributed to the use of a smaller sample holder.

iv. EFV drug loading and content uniformity in spray-dried powders obtained from T22 and T23

The EFV drug content was determined for spray-dried T23 but not for T22 since T22 was associated with a very low yield rendering extensive analysis of the sample difficult. The drug content uniformity achieved in T23 was 92 – 108% acceptable and 98.6% drug loading was achieved (**Table 6.9**). Drug content uniformity was acceptable indicating a relatively

homogenous distribution of EFV throughout the sample. Compared to T7 – T21 the drug content and drug loading achieved in T23 was markedly higher. This shows that the use of a 50% v/v ethanol solution for the spray-drying feed reduces the loss of EFV during processing making the spray-drying process more effective and economic. The complete solubilisation of EFV within the feed solution could very likely have been the driving factor behind the high drug content and % drug loading achieved here.

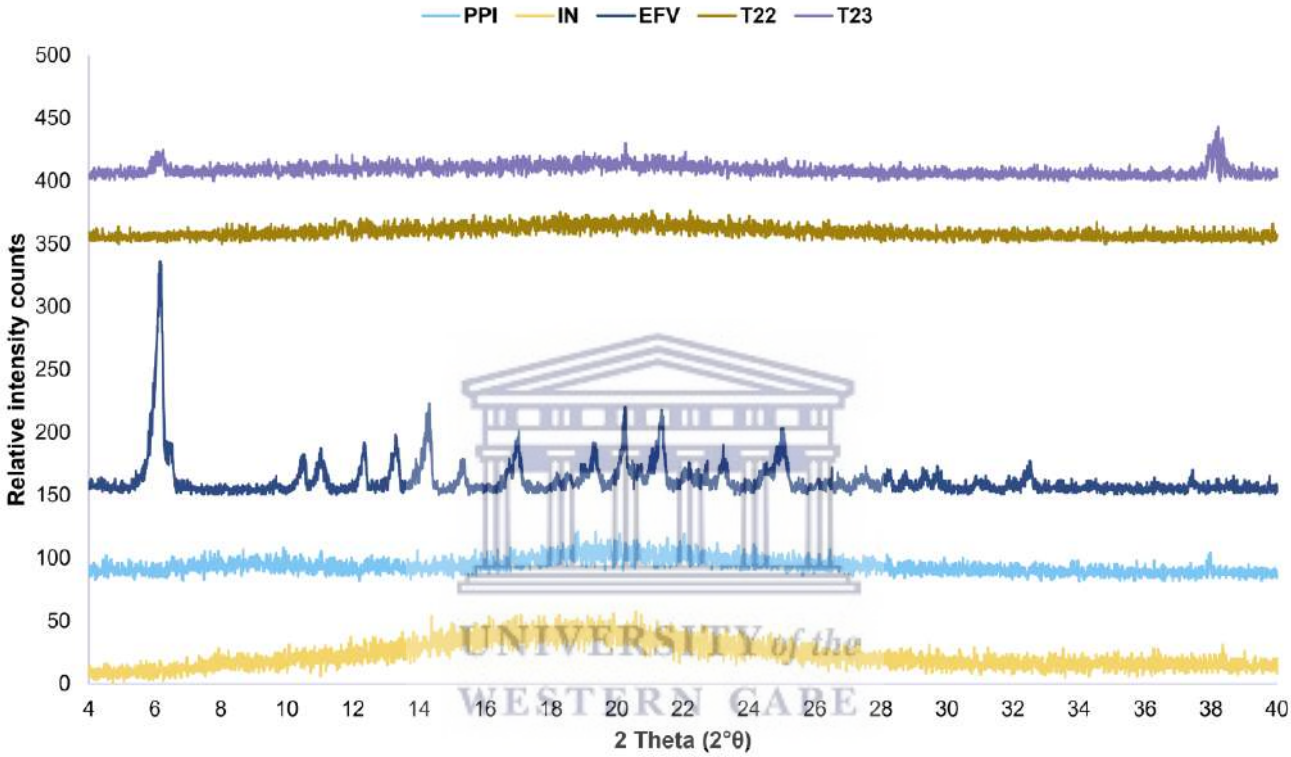

Figure 6.21: Overlay of PXRD diffractogram patterns for EFV, PPI, IN and T22 and T23.

Table 6.9: EFV drug content, the achieved drug loading % and EFV content uniformity of spray-dried powder from T23.

Trial	% Drug loading	Content uniformity at top (%)	Content uniformity in middle (%)	Content uniformity at bottom (%)
23	98.6	92.56	99.71	107.73

v. Evaluation of *in vitro* drug release of T23 as an indication of potential taste-masking

The EFV drug release from the spray-dried microspheres produced during T23 was notably higher than the drug release from any of the other spray-drying powder trials. Further, drug release from T23 was also higher than drug release from Stocrin® (**Figure 6.22**). Dissolution of EFV when T23 was subjected to pH 6.8 media proved more than two-fold higher than EFV dissolution from Stocrin®. These results could suggest that the attempt at taste-masking was unsuccessful for T23. Alternatively, the greater dissolution observed could be an effect of the amorphous nature of EFV in the T23 particles. It can further be concluded that the use of an ethanol-based solvent system for the preparation of EFV microspheres through spray-drying is not the ideal process design for achieving taste-masking.

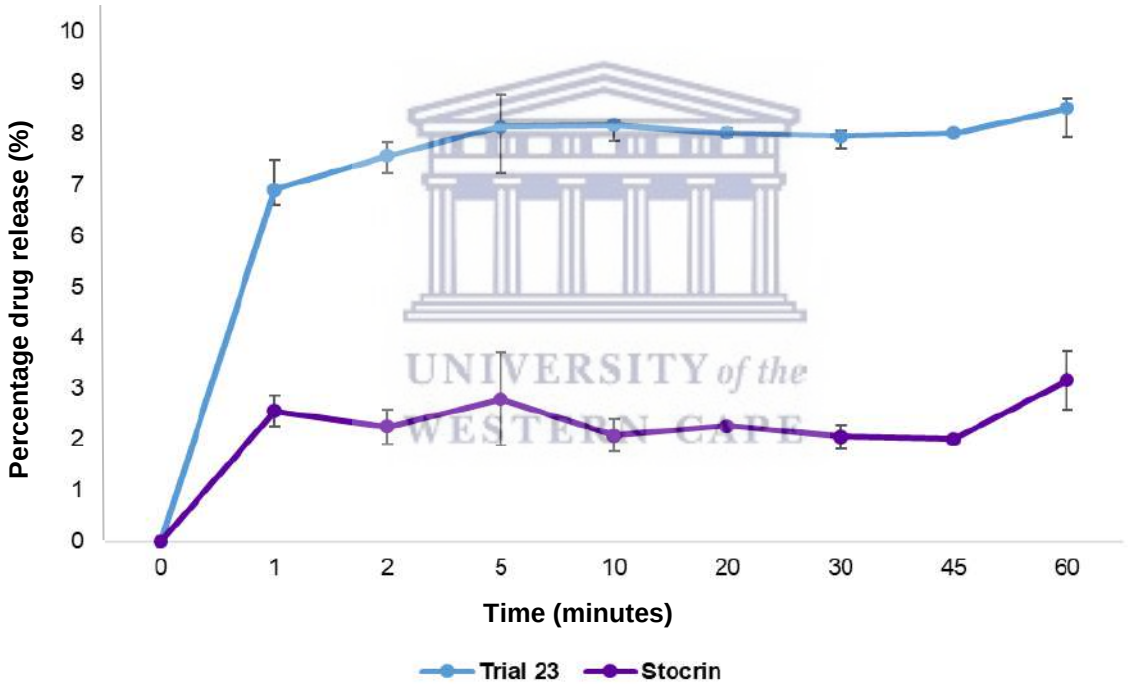

Figure 6.22: The percentage drug dissolution for spray-dried T23 and Stocrin® in pH 6.8 media maintained at 37.5°C. Error bars show standard deviation.

6.4.4 Recommendations and comments

The use of an ethanol-based solvent system for spray-drying EFV comes with advantages such as high drug loading, high drug uniformity and simple, unproblematic processing, and manufacturing steps. Here, the yield of such trials proved very low and therefore the economic aspect of this approach renders the strategy currently non-pursuable. Further, taste-masking of EFV was not successful with this strategy. The release of EFV from the produced microspheres could potentially be retarded by the addition of another natural polymer or by

increasing the concentration of the IN in the feed solution. This may simultaneously increase the viscosity of the feed solution and reduce the solubility of EFV in a pH 6.8 media. The reduced EFV solubility is likely to retard drug dissolution since EFV drug dissolution is thought to be solution limited. Here, particle size and SEM analyses were not performed for T23 but such analyses could provide valuable insight into the higher dissolution rate of T23 compared to marketed drugs.

Recommendations for future work:

- Increase and optimise IN concentration in feed solution
- Investigate the use of a different/additional polymer such as cellulose or chitosan

6.5 Comparison of EFV raw material to spray-dried EFV

In order to better understand the effect of spray-drying on the active ingredient, EFV was spray-dried without the excipients PPI and IN. Spray-drying of EFV (EFV SD) was done using the same process parameters as T7 – T10. The yield was extremely low and the process subsequently delivered a very small amount of product. Analyses that could have been done with the small sample amount will be discussed here. For all analysis, the EFV SD results were compared to those obtained from EFV raw material.

6.5.1 Thermal properties of spray-dried EFV

According to the TGA thermograms obtained, the thermal degradation of EFV SD was delayed compared to EFV (**Table 6.10**). This is evident from the delayed onset of degradation as well as the shift of the major thermal degradation event to a higher temperature. This suggests that the spray-drying process may confer improved thermal stability to EFV and may hold the potential to offer longer shelf life. The melting endotherm for EFV SD was slightly lower compared to EFV and was also associated with a slightly lower heat of fusion. The lower heat of fusion observed for the EFV melting event in EFV SD was small enough to be attributed to the difference in the amount of sample used for analysis. Enhanced thermal stability of active ingredients upon spray-drying has previously been reported in literature (Tupuna et al., 2018; Wang et al., 2020).

Table 6.10: Comparison of the thermal properties of EFV and EFV SD.

Property analysed	EFV	EFV SD
Onset of degradation (°C)	163	169
Major thermal degradation event (°C)	260.41	266.63
Melting endotherm (°C; ΔH)	140.19; 44.55	139.84; 40.72

6.5.2 Fourier transform infrared spectroscopic properties of spray-dried EFV

No major differences in the FT-IR spectral profiles were observed between EFV and EFV SD (**Figure 6.23**). Very small differences in the peak wavelengths were observed for EFV SD compared to EFV. These differences can however be considered insignificant and therefore negligible. This suggests that no changes in the molecular conformation or bond polarity occur as a result of the spray-drying process.

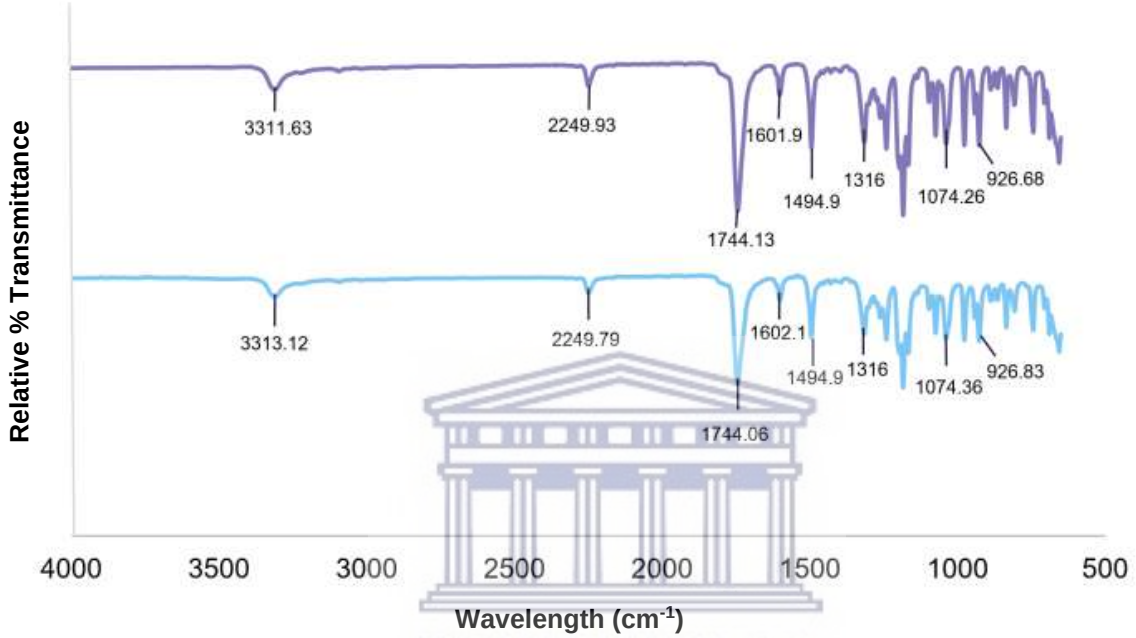

Figure 6.23: Overlay of FT-IR spectra of EFV raw material (top) and spray-dried EFV (bottom), collected at ambient temperature.

6.5.3 Solubility and *in vitro* dissolution assessment of spray-dried EFV

The equilibrium solubility of spray-dried EFV was assessed in distilled water, pH 1.2, pH 4.5, pH 6.8 and pH 7.2 media and subsequently compared to the solubility profile of EFV. **Figure 6.24** shows that there is a significant improvement in EFV solubility upon spray-drying. This suggests that the spray-drying process results in improved EFV solubility. The observation of similar DSC endotherms and FT-IR peaks suggest that the EFV SD sample did not exhibit significantly different crystalline properties compared to EFV. The results can suggest that the improved solubility of EFV SD may be related to the reduction in particle size achieved through spray-drying.

However, the drug dissolution rate of EFV SD was not significantly different from EFV (**Figure 6.25**). This suggests that the spray-drying process does not significantly influence the dissolution of EFV. The dissolution method used may very likely not have been sensitive enough to detect and quantify the solubility difference between EFV SD and EFV.

Overall it can be said that the process of spray-drying improves the thermal stability and solubility of EFV, but does not significantly impact the dissolution behaviour of EFV.

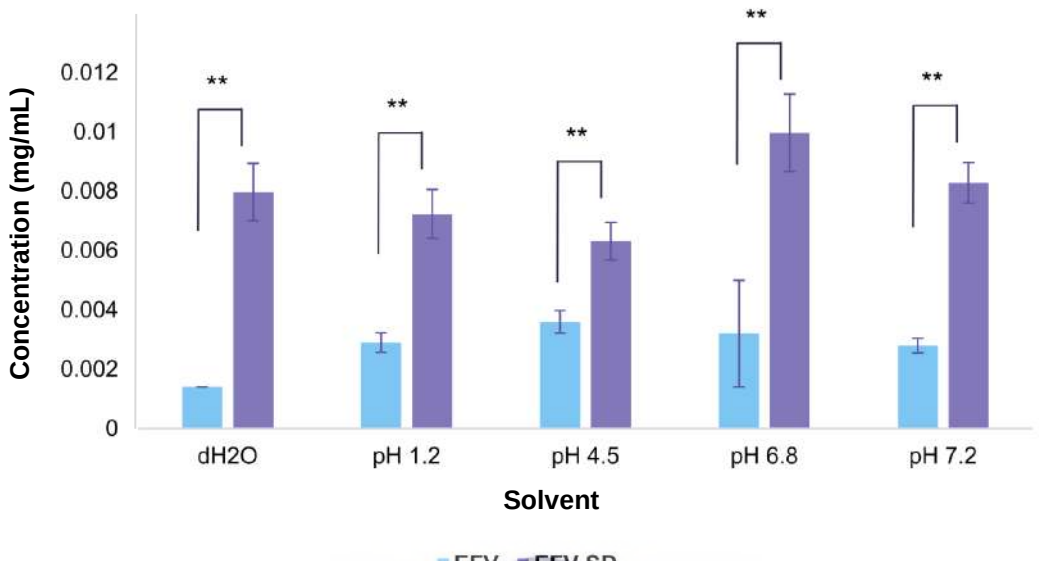

Figure 6.24: The equilibrium solubility of spray-dried EFV (EFV SD) relative to EFV raw material in distilled water (dH2O) and pH 1.2 – 7.2 buffered solutions determined at 37.5°C. ** indicates $p < 0.005$.

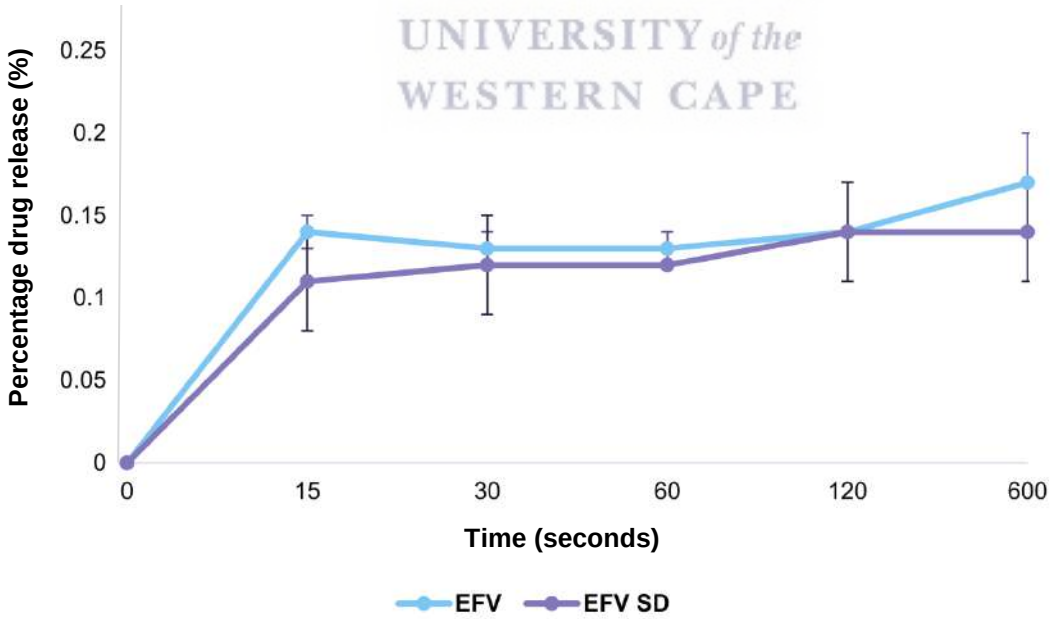

Figure 6.25: The percentage drug dissolution for EFV and EFV SD in pH 6.8 media maintained at 37.5°C. Error bars show standard deviation.

6.6 Preliminary stability investigation

As part of a pre-formulation study and especially since very little is known about PPI and IN as excipients for pharmaceutical formulations, it was important to investigate how these microencapsulants will react when stored at typical ICH stability conditions (International Conference of Harmonisation, 2009). This will provide valuable information in terms of further processing into a finished pharmaceutical product an thus the stability investigation consisted of exposing EFV, PPI, IN, T10, T19 to the storage condition of 40°C ± 2 °C / 75% ± 2 % relative humidity (%RH), which is the most severe or harshest storage conditions according to ICH stability testing guidelines (International Conference of Harmonisation, 2009). It should be noted this was only a preliminary stability study and was thus only conducted for a period of 2 months. This period is not sufficiently long to inform shelf-life requirements but valuable information was collected to inform further pre-formulation strategies involving the spray-dried microcapsules. Further to this, it must also be noted that at the time when this investigation started T23 was not yet available since this was linked to the procurement of a suitable spray-drier.

6.6.1 Stability investigation of individual compounds and physical powder mixtures

Preliminary stability testing was done on pure EFV, PPI, IN, physical mixtures and selected spray-dried formulations. As outlined in Chapter 4, **section 4.3.12**, four different storage conditions were tested under the conditions 40°C / 75% RH for 2 months and 30°C / 65% RH for 2 months.

Visual recordings of the open container for all samples subjected to the stability storage conditions were made over the period of 2 months and were used to identify any obvious visual abnormalities or changes that occurred compared to the initial sample. Visually, the EFV powder remained stable with no colour or bulk property changes noted over 2 months. Some changes were noted in the pure PPI sample stored in an open container. The powder colour changed from a light beige to a dark beige-yellow over 2 months (**Figure 6.26)**. It was also observed that the powder became hardened with a brittle texture. Overall, the visual observations made over 2 months suggest that the physical stability of the PPI is compromised to some degree, however, no degradation was identifiable from DSC, TGA, and FT-IR (**Table 6.11**; **Figure A7**). The evaluation of the potency of EFV over the 2 months indicated significant degradation (16% ± 1.9%) of EFV in the open container and 1% ± 1% for EFV stored in the plastic bottle packaging. From the visual observations made over 2 months, it was noted that IN undergoes significant visual and bulk property changes upon exposure to 40°C/75% RH. Changes became apparent as soon as one month after the initiation of the stability study.

Initially, IN presented as a fine white powder (**Figure 6.26**). After one month IN presented as a hard, toffee-like solid which presented with challenges for analysing the sample using FT-IR, TGA, and DSC. Subsequently, pure IN samples were not analysed for physical stability. With regards to the EFV excipient mixtures, no obvious visual changes were noted during the 2 months (**Figure 6.26**). As a result of exposure to high relative humidity, the moisture content of all physical mixtures did increase over two months (**Table 6.11**) but this increase was not considered to be significant.

The potency of EFV within the excipient mixtures remained unchanged after the first month for all packaging types except for the EI sample, stored in an open container, which exhibited a notable 10% ± 5.7% reduction in EFV potency (**Table 6.11**). The most significant decrease in EFV potency due to exposure to elevated temperature and relative humidity was observed with the EI and EP samples stored in open containers for the 2 months, with a quantified 16% ± 5% and 16% ± 2.5% decrease in the drug potency, respectively. This corresponds to the potency decrease observed with pure EFV. This data was indicative of the fact that irrespective of the combination of EFV with the two microencapsulants EFV will degrade upon exposure to elevated temperature and humidity and that protection through storage in a container, even a container that doesn't necessarily seal tightly is imperative.

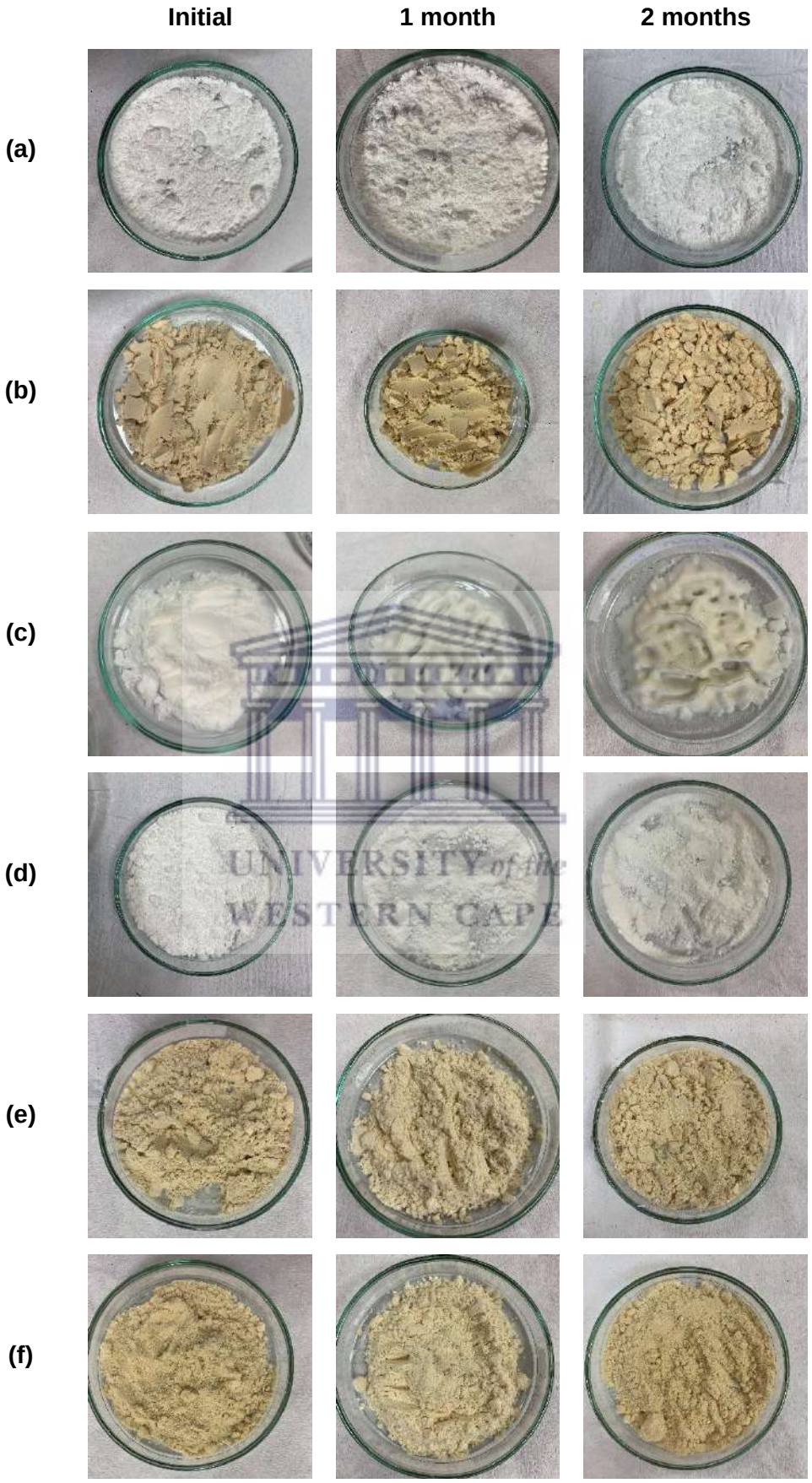

Figure 6.26: Visual observations of (a) EFV, (b) PPI, (c) IN, (d) EI, (e) EP and (f) EPI stored at 40 ± 0.5°C and 75 ± 2% RH for a period of 2 months when stored in open containers.

Table 6.11: Moisture content (%), melting point (°C), degradation temperature (°C) and drug potency (%) determined over a 2 month period after exposure to 40°C and 75%RH conditions for individual components EFV, PPI, IN and physical combinations EP, EI and EPI.

	Moisture content (%)			Melting point (°C)			Degradation temperature (°C)			Drug potency (%)		
EFV												
	Initial	**30 d**	**60 d**	**Initial**	**30 d**	**60 d**	**Initial**	**30 d**	**60 d**	**Initial**	**30 d**	**60 d**
Open container	0.94	0.88	0.78	140.19	139.90	139.53	260.41	261.90	264.53	100.00	100.00	84.02
Plastic bag	0.94	0.94	0.93	140.19	139.89	139.55	260.41	262.82	262.03	100.00	100.00	100.00
Plastic bottle	0.94	0.64	0.88	140.19	139.38	139.28	260.41	266.52	263.69	100.00	100.00	99.84
Paper bag	0.94	0.85	1.80	140.19	139.97	140.18	260.41	250.46	262.50	100.00	100.00	100.00
PPI												
Open container	5.73	7.46	7.19	N/A	N/A	N/A	313.40	311.43	315.89	N/A	N/A	N/A
Plastic bag	5.73	7.63	7.20	N/A	N/A	N/A	313.40	323.20	318.50	N/A	N/A	N/A
Plastic bottle	5.73	7.36	7.61	N/A	N/A	N/A	313.40	320.50	318.18	N/A	N/A	N/A
Paper bag	5.73	7.50	7.70	N/A	N/A	N/A	313.40	321.78	323.70	N/A	N/A	N/A
IN (not analysed) Refer to Figure 6.27 and paragraph 6.6.1												
EP												
Open container	4.88	7.14	7.14	139.78	139.62	138.87	250.27	223.78	250.69	100.00	100.00	94.83
							320.58	317.13	323.30			
Plastic bag	4.88	6.73	6.50	139.78	139.92	139.97	250.27	223.30	247.02	100.00	100.00	94.80
							320.58	315.60	319.57			
Plastic bottle	4.88	6.75	6.92	139.78	139.22	138.57	250.27	222.91	249.23	100.00	100.00	100.00
							320.58	317.55	326.92			
Paper bag	4.88	6.67	2.70	139.78	139.31	139.44	250.27	232.07	222.61	100.00	100.00	100.00
							320.58	319.02	327.17			

Table 6.10 continued: Moisture content (%), melting point (°C), degradation temperature (°C) and drug potency (%) determined over a 2 month period after exposure to 40°C and 75%RH conditions.

	Moisture content (%)			Melting point (°C)			Degradation temperature (°C)			Drug potency (%)		
	Initial	**30 d**	**60 d**	**Initial**	**30 d**	**60 d**	**Initial**	**30 d**	**60 d**	**Initial**	**30 d**	**60 d**
EI												
Open container	5.26	5.93	5.23	139.60	139.70	139.30	244.55	246.37	247.22	100.00	100.00	99.47
Plastic bag	5.26	5.40	5.92	139.60	139.21	139.09	244.55	248.88	241.93	100.00	100.00	99.52
Plastic bottle	5.26	5.98	5.71	139.60	139.80	138.88	244.55	247.21	244.09	100.00	100.00	100.00
Paper bag	5.26	5.29	6.67	139.60	139.59	139.02	244.55	246.19	242.08	100.00	100.00	100.00
EPI												
Open container	5.13	5.88	5.63	139.22	139.60	139.34	248.93 327.25	245.80 327.18	242.62 321.50	100.00	100.00	97.01
Plastic bag	5.13	6.56	6.43	139.22	139.28	139.07	248.93 327.25	242.73 326.02	242.43 326.61	100.00	100.00	100.00
Plastic bottle	5.13	6.84	6.86	139.22	139.16	139.15	248.93 327.25	243.70 326.52	243.94 328.51	100.00	100.00	98.33
Paper bag	5.13	7.06	7.25	139.22	139.31	139.21	248.93 327.25	245.19 325.55	242.30 324.82	100.00	100.00	100.00

6.6.2 Stability investigation of spray-dried powders stored at 40°C/75% RH

Throughout the stability study, visual changes were observed in the spray-dried powders. For T10 the colour changed from an off-white to a slightly darker cream-yellow colour (**Figure 6.27**). As a result of caking, the bulk properties of the powder also changed from a soft powder exhibiting acceptable flowability to a hard and clumpy powder. T19 exhibited a colour change from an off-white to a darker brown colour. Initially, the sample exhibited a typical powder appearance but caking occurred and the powder changed to a very hard solid. The observed changes in the colour and texture of the samples were attributed to the presence of the IN and PPI, based on the observations in **section 6.6.1**. Both IN and PPI are prone to absorb moisture as discussed in Chapter 5 (**section 5.2.5**). This could potentially mean that IN solubilises partially as a result of the absorbed moisture and subsequently mixes with the EFV and PPI resulting in the whole mass solidifying. These significant visual changes may be related to the potential incompatibility between EFV, PPI and IN as discussed in Chapter 5.

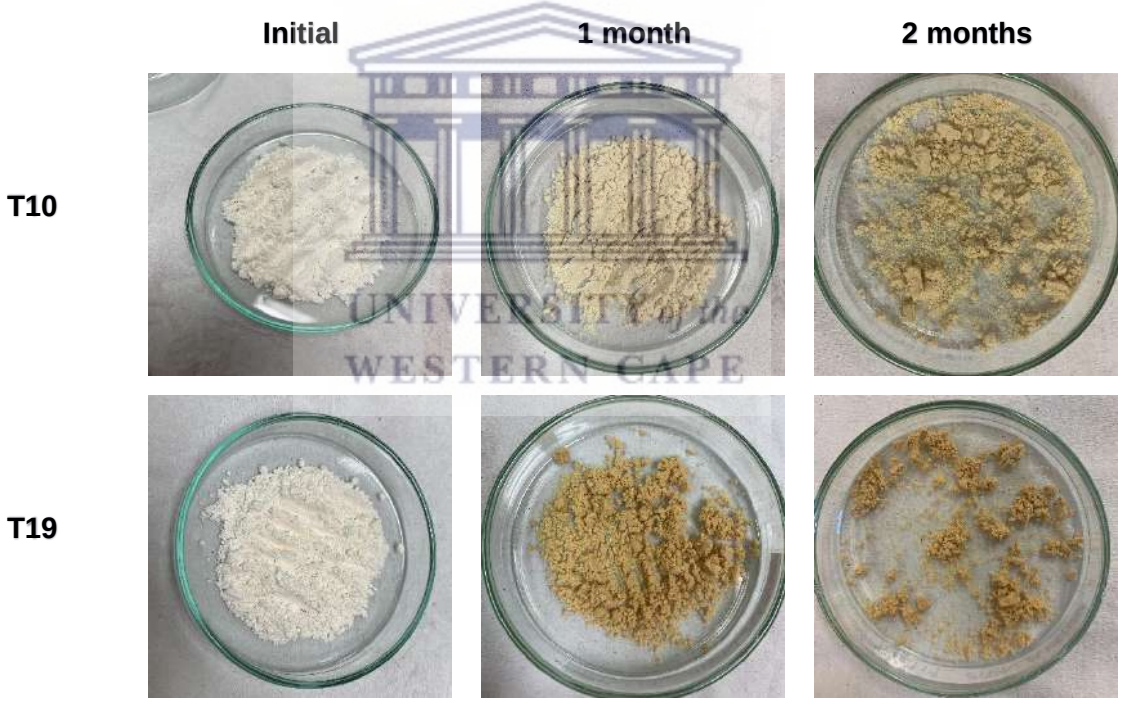

Figure 6.27: Visual observations of two selected spray-dried trials stored at 40 ± 0.5°C and 75 ± 2% RH for a period of 2 months.

During the stability study, the melting point of EFV in the spray-dried powders remained unchanged thus indicating that no solid-state transformation occurred (**Table 6.12**). The moisture content of the spray-dried powders increased during the testing period (**Table 6.12**). In terms of EFV potency, T10 proved to be highly stable across the 2 months whilst T19 showed a decrease in potency for the sample stored in an open container (15% ± 2.2%) and

the plastic bottle a (21% ± 5.8%). It was this T19 sample that showed the highest degree of degradation of 20% after 2 months of storage.

Table 6.12: Moisture content (%), melting point (°C), degradation temperature (°C) and drug potency (%) determined over a 2 month period after exposure to 40°C and 75%RH conditions for spray-dried powders T10 and T19.

	Moisture content (%)			Melting point (°C)			Degradation temperatures (°C)			Drug potency (%)		
T10												
	Initial	**30 d**	**60 d**	**Initial**	**30 d**	**60 d**	**Initial**	**30 d**	**60 d**	**Initial**	**30 d**	**60 d**
Open container	2.18	8.22	7.32	138.50	139.23	139.27	239.23	241.29	239.08	100.00	100.00	100.00
							325.70	329.68	323.30			
Plastic bag	2.18	7.63	7.03	138.50	139.23	139.68	239.23	244.24	240.20	100.00	100.00	100.00
							325.70	323.05	328.65			
Plastic bottle	2.18	5.77	5.74	138.50	138.27	139.10	239.23	240.43	240.81	100.00	100.00	100.00
							325.70	320.32	328.80			
Paper bag	2.18	6.80	6.96	138.50	139.00	139.78	239.23	241.72	238.76	100.00	100.00	94.55
							325.70	333.91	323.50			
T19												
Open container	1.93	4.55	5.91	138.48	138.96	139.53	240.93	240.08	236.79	100.00	88.41	85.21
							340.78	330.92	339.52			
Plastic bag	1.93	3.74	3.03	138.48	138.78	140.01	240.93	238.92	238.96	100.00	100.00	86.74
							340.78	337.00	330.37			
Plastic bottle	1.93	1.36	1.99	138.48	139.31	138.76	240.93	240.08	237.61	100.00	88.22	79.81
							340.78	330.92	335.70			
Paper bag	1.93	3.05	3.76	138.48	138.47	139.43	240.93	236.34	236.95	100.00	100.00	84.64
							340.78	338.01	334.98			

6.6.3 Stability evaluation of individual compounds, T19 and T23 at 30°C/65% RH

Based on the preliminary 2-month stability study it was decided to investigate the stability for another two months but at a less harsh ICH stability condition. Furthermore, based on the stability that T10 exhibited as well as the fact that these investigations are only preliminary it was decided to not include T10 in this study but to add the T23 sample since no preliminary data were available for this trial, yet. Likewise, it was deemed necessary to evaluate the stability of T19 at 30°C/65% RH due to its chemical instability at 40°C/75% RH storage conditions. Trial 23 stability was also evaluated at 30°C/65% RH and for the sake of making accurate comparisons all three raw materials were again included for stability evaluation at 30°C/65% RH. The samples stored in sealed paper bags at 40°C/75% RH exhibited the best overall stability and therefore the storage of samples in paper bags at 30°C/65% RH was again evaluated. Open containers were again included to prove the most extreme exposure to the environment. A third, additional storage condition, namely a sealed glass polytop, was included for 30°C/65% RH stability evaluation.

Visually, the EFV powder remained stable with no obvious changes in the bulk properties were noted during the 2 months. Similar to what was observed under the conditions 40°C/75% RH some visual changes were noted in the pure PPI and IN samples stored at 30°C/65% RH. For PPI, the powder colour changed from an off-white to a dark cream-yellow. (**Figure 6.28**). It was also observed that the powder became hardened with a brittle texture. It was noted that IN undergoes significant visual and textural changes. Initially, IN presented as a fine white powder and after one month of exposure in the stability chamber IN presented as a hard, toffee-like solid (**Figure 6.28**). A colour change from an off-white to a darker brown colour was observed for T19. Initially, the powder had a soft and light texture but changed to a very hard solid. For T23 visual changes were observed where the colour of the sample changed from an off-white to cream-yellow and the texture changed from a fine powder to a hard and clumpy powder (**Figure 6.28**). From a visual perspective, it did not appear that T19 and T23 remained physically stable over the 2 months.

Upon exposure to 30°C/65% RH conditions, the moisture content of EFV increased significantly for EFV stored in the open container (**Table 6.13**). For the EFV samples stored in a glass polytop and a sealed paper bag, the moisture content decreased over the 2 months. The moisture content increased for all PPI samples over a 2 months with the greatest moisture increase observed for the sample stored in the paper bag (**Table 6.13**). For the IN samples, moisture increases were observed for all three storage containers. For both T19 and T23 moisture increases in for observed for the samples as a result of the exposure to 30°C/65% RH conditions. Moisture uptake by the sample can again be partially attributed to

the amorphous nature of the powders after spray-drying. After 2 months, the T19 sample stored in a glass polytop exhibited the lowest moisture content and after 2 months, the T23 sample stored in a sealed paper bag exhibited the lowest moisture content.

Figure 6.28: Photographs taken for the visual observations of raw materials (a) EFV, (b) PPI, (c) IN and spray-dried powders from (d) T19 and (e) T23 stored in open containers at 30°C/65% RH for a period of 2 months.

Table 6.13: Moisture content (%), melting point (°C), degradation temperature (°C) and drug potency (%) determined over a 2 month period after exposure to 30°C and 65%RH conditions for EFV, PPI, IN and spray-dried powders T19 and T23.

EFV						
	Moisture content (%)			**Drug potency (%)**		
Time	**Initial**	**30 d**	**60 d**	**Initial**	**30 d**	**60 d**
Open container	0.94	0.00	1.82	100.00	90.45	79.66
Glass polytop	0.94	0.79	0.75	100.00	88.97	83.43
Paper bag	0.94	0.74	2.26	100.00	94.39	84.80
PPI						
Open container	5.73	6.09	7.99	-	-	-
Glass polytop	5.73	6.35	6.71	-	-	-
Paper bag	5.73	7.12	8.46	-	-	-
IN						
Open container	3.25	3.20	4.68	-	-	-
Glass polytop	3.25	3.93	3.80	-	-	-
Paper bag	3.25	3.44	3.80	-	-	-
T19						
Open container	3.90	6.09	6.23	100.00	84.91	73.17
Glass polytop	3.90	5.26	6.09	100.00	95.35	88.73
Paper bag	3.90	1.73	5.08	100.00	87.12	62.23
T23						
Open container	4.19	7.05	6.54	100.00	99.18	93.89
Glass polytop	4.19	5.26	6.05	100.00	100.00	100.00
Paper bag	4.19	6.75	4.67	100.00	100.00	100.00

A decline in the drug potency of EFV raw material was observed from 1 month after exposure to 30°C/65% RH conditions. This was unexpected since no reduction in drug potency was observed for EFV raw material when stored at 40°C and 75% RH. The EFV samples stored in paper bags exhibited the smallest reduction in drug potency suggesting that EFV remains most stable in this packaging. On the other hand, the EFV sample stored in an open container exhibited the greatest reduction in EFV potency suggesting that EFV is least stable when stored in an open container. For spray-dried T19 the drug potency of EFV stored at 30°C/65% RH exhibited a decline over 2 months for all storage containers, with the sample stored in a sealed glass polytop being associated with the smallest reduction in EFV activity (**Table 6.13**). In comparison to T19, spray-dried T23 exhibited a smaller reduction in EFV potency suggesting that EFV drug stability is greater in T23.

Overall, both the spray-dried trials exhibited adequate physical stability but T23 exhibited significantly greater chemical stability compared to T19 under the conditions of 30°C and 65% RH. The instability of the spray-dried powder powders may be linked to their amorphous nature (Shetty et al., 2018). The amorphous nature of spray-dried powders, in general, has been linked to physical instability. This is attributed to moisture absorption by the amorphous powders in humid conditions which can result in particle agglomeration, as seen here. This type of particle agglomeration has previously been reported for spray-dried powders upon storage at high humidity conditions (Chiou & Langrish, 2007; Shetty et al., 2018). The use of hydrophobic amino acids, such as leucine, as excipients have proven helpful in preventing moisture-induced sample deterioration and reducing particle-particle and particle-moisture interactions (Li et al., 2017; Shetty et al., 2020). With regards to the instability of T19, the addition of the surfactant Tween® 20 should also be considered. It has been reported that although surfactants keep air–liquid interface sensitive molecules away from the surface they may consequently also produce a coat with a low glass transition temperature on the surface. This may cause high cohesive forces between particles resulting in agglomeration and physical instability (Vehring, 2008). The use of surfactant Tween® 80 in formulations containing proteins has been reported to stimulate aggregation and oxidation of proteins during storage with the rate of oxidation being directly proportional to storage temperature (Wang, Wang & Wang, 2008). Tween® 20 also contains residual peroxides, as does Tween® 80 and therefore similar effects can be expected for formulations containing proteins and Tween® 20. The aggregation of the protein fraction coupled with the low glass transition temperature on the particle could create an unstable environment where chemical degradation is triggered.

6.7 Conclusions and recommendations

Here, microencapsulation of EFV through spray-drying was explored. The use of natural excipients PPI and IN as encapsulating agents proved relatively successful. However, the resulting powders did not consist of microspheres in the true sense but rather presented with a more agglomerated/fused nature when EFV was added. FT-IR and DSC results showed that EFV was successfully loaded into the spray-dried powders and that the amount of EFV present in the powders was sufficient for detection. The use of an aqueous buffered solution for the preparation of the spray-drying feed solution produced an EFV containing powder with adequate taste-masked properties. EFV drug release from T10, T19 and T21 proved significantly lower compared to the marketed product Stocrin® film-coated tablets, suggesting that these formulations could potentially be associated with better palatability compared to the marketed product that is manipulated (crushed and ground) to enable children to take a daily EFV dose. On the other hand, the use of an ethanol-based solution for the preparation of the feed solution did not produce powders with a sufficient decrease in drug release in a pH 6.8 environment. The downfall related to the spray-drying strategy was the overall stability of the resulting powders. Visually the powders underwent significant changes in terms of bulk properties, to such a degree that the powders would not maintain physical integrity for even 1 month upon exposure to either 40°C/75% RH or 30°C/65% RH conditions. One of the limiting factors in this study was the inability to perform protein analysis. Future work could include the characterisation and analysis of the protein fraction used particularly in order to better understand the stability of the spray-dried powders. Further consideration is required regarding suitable packaging in order to achieve maximum stability of PPI and IN. The packaging options tested here were not sealed particularly tight and so it is possible that the use of a more protective container with better sealing can eliminate the stability problems observed here.

The use of individually sealed, small sachets also present economic advantages and provide easy dose flexibility with the possibility of using different sizes of paper bags for different age/weight groups. Based on the results obtained here it is also suggested that dehumidifying desiccants are added to the packaging of spray-dried powders.

Future work may include investigating the use of hydrophobic amino acids like leucine as an additional excipient. This will ideally help improve the physical stability of the spray-dried powders by reducing the particle surface energy (Shetty et al., 2018). It is possible that improved physical stability will also improve the chemical stability of the powders.

6.8 References

Ahlfors, E.E., Dahl, J.E. & Lyberg, T. 2011. The development of T cell-dominated inflammatory responses induced by sodium lauryl sulphate in mouse oral mucosa. *Archives of Oral Biology*. 57(6):796–804. DOI: 10.1016/j.archoralbio.2011.11.005.

Al-kasmi, B., Bashir, M.H.D., Bashimam, M. & El-zein, H. 2017. Mechanical microencapsulation: The best technique in taste masking for the manufacturing scale - Effect of polymer encapsulation on drug targeting. *Journal of Controlled Release*. 260:134–141. DOI: 10.1016/j.jconrel.2017.06.002.

Aulton, M. 2017. Dissolution and Solubility. In: *Pharmaceutics: The Science of Dosage Form Design*. Fifth ed. M. Aulton & K. Taylor, Eds. London: Elsevier. 18–35.

Avachat, A.M. & Parpani, S.S. 2015. Formulation and development of bicontinuous nanostructured liquid crystalline particles of efavirenz. *Colloids and Surfaces B: Biointerfaces*. 126:87–97. DOI: 10.1016/j.colsurfb.2014.12.014.

Bansode, S.S., Banarjee, S.K., Gaikwad, D.D., Jadhav, S.L. & Thorat, R.M. 2010. Microencapsulation: A review. *International Journal of Pharmaceutical Sciences Review and Research*. 1(2):38–43.

Chiou, D. & Langrish, T.A.G. 2007. Crystallization of amorphous components in spray-dried powders. *Drying Technology*. 25(9):1427–1435. DOI: 10.1080/07373930701536718.

Closa-Monasterolo, R., Gispert-Llaurado, M., Luque, V., Ferre, N., Rubio-Torrents, C., Zaragoza-Jordana, M. & Escribano, J. 2013. Safety and efficacy of inulin and oligofructose supplementation in infant formula: Results from a randomized clinical trial. *Clinical Nutrition*. 32(6):918-927. DOI: 10.1016/j.clnu.2013.02.009

Costa, B.L.A., Sauceau, M., Del Confetto, S., Sescousse, R. & Ré, M.I. 2019. Determination of drug-polymer solubility from supersaturated spray-dried amorphous solid dispersions: A case study with Efavirenz and Soluplus®. *European Journal of Pharmaceutics and Biopharmaceutics*. 142(April):300–306. DOI: 10.1016/j.ejpb.2019.06.028.

Desai, K.G.H. & Park, H.J. 2005. Preparation and characterization of drug-loaded chitosan-tripolyphosphate microspheres by spray drying. *Drug Development Research*. 64(2):114–128. DOI: 10.1002/ddr.10416.

Doan, C.D. & Ghosh, S. 2019. Formation and stability of pea proteins nanoparticles using ethanol-induced desolvation. *Nanomaterials*. 9(7). DOI: 10.3390/nano9070949.

Ducel, V., Richard, J., Popineau, Y. & Boury, F. 2004. Adsorption Kinetics and Rheological Interfacial Properties of Plant Proteins at the Oil−Water Interface. *Biomacromolecules*. 5(6): 2088-2093. DOI: 10.1021/bm049739h

Fernandes, R.V. de B., Botrel, D.A., Silva, E.K., Borges, S.V., Oliveira, C.R. de, Yoshida, M.I., Feitosa, J.P. de A. & de Paula, R.C.M. 2016. Cashew gum and inulin: New alternative for ginger essential oil microencapsulation. *Carbohydrate Polymers*. 153:133–142. DOI: 10.1016/j.carbpol.2016.07.096.

Gharsallaoui, A., Cases, E., Chambin, O. & Saurel, R. 2009. Interfacial and emulsifying characteristics of acid-treated pea protein. *Food Biophysics*. 4(4):273–280. DOI: 10.1007/s11483-009-9125-8.

Gharsallaoui, A., Yamauchi, K., Chambin, O., Cases, E. & Saurel, R. 2010. Effect of high methoxyl pectin on pea protein in aqueous solution and at oil/water interface. *Carbohydrate Polymers*. 80(3):817-827. DOI: 10.1016/j.carbpol.2009.12.038

International Conference of Harmonisation. 2009. *International conference on harmonisation of technical requirements for registration of pharmaceuticals for human use*. V. 8. Available: https://www.ich.org/ [Accessed:2021, April 15].

Islam, M.I.U. & Langrish, T.A.G. 2010. An investigation into lactose crystallization under high temperature conditions during spray drying. *Food Research International*. 43(1):46–56. DOI: 10.1016/j.foodres.2009.08.010.

Kolida, S. & Gibson, G. 2007. Prebiotic Capacity of Inulin-Type Fructans. *The Journal of Nutrition*. 137(11):2503S-2506S. DOI: 10.1093/jn/137.11.2503s

Lan, Y., Chen, B. & Rao, J. 2018. Pea protein isolate–high methoxyl pectin soluble complexes for improving pea protein functionality: Effect of pH, biopolymer ratio and concentrations. *Food Hydrocolloids*. 80:245–253. DOI: 10.1016/j.foodhyd.2018.02.021.

Lan, Y., Xu, M., Ohm, J.B., Chen, B. & Rao, J. 2019. Solid dispersion-based spray-drying improves solubility and mitigates beany flavour of pea protein isolate. *Food Chemistry*. 278(October 2018):665–673. DOI: 10.1016/j.foodchem.2018.11.074.

Lavra, Z.M.M., Pereira de Santana, D. & Ré, M.I. 2017. Solubility and dissolution performances of spray-dried solid dispersion of Efavirenz in Soluplus. *Drug Development and Industrial Pharmacy*. 43(1):42–54. DOI: 10.1080/03639045.2016.1205598.

Li, L., Leung, S., Gengenbach, T., Yu, J., Gao, G., Tang, P., Zhou, Q. & Chan, H. 2017. Investigation of L-leucine in reducing the moisture-induced deterioration of spray-dried salbutamol sulfate power for inhalation. *International Journal of Pharmaceutics*. 530(1-2):30-39. DOI: 10.1016/j.ijpharm.2017.07.033

Miller, N., De Beer, D., Aucamp, M., Malherbe, C.J. & Joubert, E. 2018. Inulin as microencapsulating agent improves physicochemical properties of spray-dried aspalathin-rich green rooibos (Aspalathus linearis) extract with α-glucosidase inhibitory activity. *Journal of Functional Foods*. 48(April):400–409. DOI: 10.1016/j.jff.2018.07.028.

Neppelberg, E., Costea, D.E., Vintermyr, O.K. & Christine, A. 2007. Dual effects of sodium lauryl sulphate on human oral epithelial structure. *Experimental Dermatology*. 16(8):574–579. DOI: 10.1111/j.1600-0625.2007.00567.x.

Nesterenko, A., Alric, I., Violleau, F., Silvestre, F. & Durrieu, V. 2014. The effect of vegetable protein modifications on the microencapsulation process. *Food Hydrocolloids*. 41:95–102. DOI: 10.1016/j.foodhyd.2014.03.017.

Pauck, C., De Beer, D., Aucamp, M., Liebenberg, W., Stieger, N., Human, C. & Joubert, E. 2017. LWT - Food Science and Technology Inulin suitable as reduced-kilojoule carrier for production of microencapsulated spray-dried green Cyclopia subternata (honeybush) extract. *LWT - Food Science and Technology*. 75:631–639. DOI: 10.1016/j.lwt.2016.10.018.

Pereira, H., Saraiva, K., Carvalho, L., Andrade, L., Pedrosa, C. & Pierucci, A. 2009. Legumes seeds protein isolates in the production of ascorbic acid microparticles. *Food Research International*. 42(1):115-121. DOI: 10.1016/j.foodres.2008.10.008

Qiu, H., Stepanov, V., Di Stasio, A.R., Surapaneni, A. & Lee, W.Y. 2015. Investigation of

the crystallization of RDX during spray drying. *Powder Technology*. 274:333–337. DOI: 10.1016/j.powtec.2015.01.032.

Shetty, N., Park, H., Zemlyanov, D., Mangal, S., Bhujbal, S. & Zhou, Q. 2018. Influence of excipients on physical and aerosolization stability of spray dried high-dose powder formulations for inhalation. *International Journal of Pharmaceutics*. 544(1):222–234. DOI: 10.1016/j.ijpharm.2018.04.034.

Shetty, N., Cipolla, D., Park, H. & Zhou, Q.T. 2020. Physical stability of dry powder inhaler formulations. *Expert Opinion on Drug Delivery*. 17(1):77–96. DOI: 10.1080/17425247.2020.1702643.

Trofimiuk, M., Wasilewska, K. & Winnicka, K. 2019. How to modify drug release in paediatric dosage forms? Novel technologies and modern approaches with regard to children's population. *International Journal of Molecular Sciences*. 20(3200). DOI: 10.3390/ijms20133200.

Tupuna, D.S., Paese, K., Guterres, S.S., Jablonski, A., Flôres, S.H. & Rios, A. de O. 2018. Encapsulation efficiency and thermal stability of norbixin microencapsulated by spray-drying using different combinations of wall materials. *Industrial Crops and Products*. 111(December 2017):846–855. DOI: 10.1016/j.indcrop.2017.12.001.

U.S. Pharmacopoeial Convention. 2011. *(905) Uniformity of Dosage Units. Stage 6 Harmonization.* Available: https://www.usp.org/sites/default/files/usp/document/harmonization/gen-method/q0304_stage_6_monograph_25_feb_2011.pdf.

Vehring, R. 2008. Pharmaceutical particle engineering via spray drying. *Pharmaceutical Research*. 25(5):999–1022. DOI: 10.1007/s11095-007-9475-1.

Verma, U., Mujumdar, A. & Naik, J. 2020. Preparation of Efavirenz resinate by spray drying using response surface methodology and its physicochemical characterization for taste masking. *Drying Technology*. 38(5–6):793–805. DOI: 10.1080/07373937.2019.1590845.

Wang, W., Wang, Y.J. & Wang, D.Q. 2008. Dual effects of Tween 80 on protein stability. *International Journal of Pharmaceutics*. 347(1–2):31–38. DOI: 10.1016/j.ijpharm.2007.06.042.

Wang, Y., Hao, F., Lu, W., Suo, X., Bellenger, E., Fu, N., Jeantet, R. & Chen, X.D. 2020. Enhanced thermal stability of lactic acid bacteria during spray drying by intracellular accumulation of calcium. *Journal of Food Engineering*. 279:109975. DOI: 10.1016/j.jfoodeng.2020.109975.

CHAPTER 7

Efavirenz microencapsulation through ionic gelation

7.1 Introduction

EFV is known for its very low aqueous solubility (<0.001 mg/mL), rendering it the ideal candidate drug for formulation into calcium alginate beads. Alginates have protective functionality as they are known to protect the mucous membrane of the upper gastrointestinal tract from the irritation of chemicals (Arica et al., 2005). Therefore, drug-loaded alginate beads might provide this advantage for ARVs, such as EFV, which are associated with mucosal irritation. Since the main objective of this project was to explore microencapsulation of EFV to impart taste-masking, this property of alginates rendered its potential use in formulation worthy of investigation.

Two different formulations were attempted, one with the addition of IN together with EFV into the alginate matrix and one with only EFV dissolved into the alginate matrix. The beads were evaluated for moisture content, size, weight, drug content and encapsulation efficiency, surface morphology by light microscopy, crystallinity by powder x-ray diffraction (PXRD), swelling, and *in vitro* drug release in both acidic and alkaline media.

7.2 Results and discussion

7.2.1 Physico-chemical characterisation of calcium alginate beads

7.2.1.1 Thermal properties

Microencapsulation of EFV *via* ionic gelation was explored in addition to spray-drying. As described in **Chapter 4, section 4.3.7**, EFV-loaded calcium alginate beads were prepared through ionic gelation by dropping an EFV-SA solution into $CaCl_2$. After drying the beads were subjected to physico-chemical characterisation.

The thermal behaviour of the dried empty and EFV-loaded alginate beads was investigated using HSM, TGA, and DSC as discussed in **Chapter 5**. HSM was used qualitatively to observe any thermal events such as phase changes for the characterisation of the alginate beads. First, pure sodium alginate (SA) was analysed, followed by the empty and loaded alginate beads. The results obtained for pure EFV and IN at an earlier stage (**Chapter 5**) were also compared to the results obtained here. The comparison of these results was used to characterise the interaction between the materials and to characterise the thermal profile of the synthesised alginate beads. This visual HSM data was used in conjunction with the quantitative results obtained from TGA and DSC analyses. The HSM results are presented in Appendix A.

TGA was used to characterise and quantify any changes in the thermal stability of the compounds. The quantitative data gained from the TGA is in the form of percentage mass loss experienced by the sample during heating. First, the pure components were analysed and then used as a reference for the comparison of the prepared alginate beads. To determine significant mass loss events over time, the first derivative was calculated using the Pyris™ Software.

Figure 7.1 and Table 7.1 show the weight loss events identified for SA, IN, EFV, and the prepared calcium alginate beads. The HSM and TGA results correspond to the thermal properties of SA previously described in literature (Soares et al., 2004).

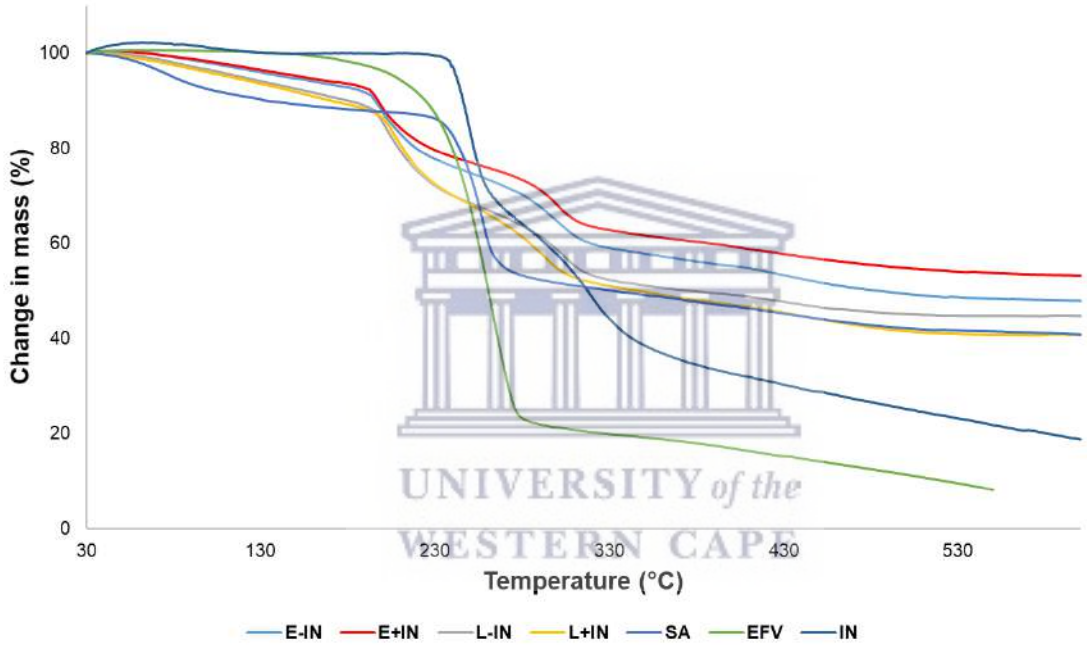

Figure 7.1: Overlay of TGA thermograms of sodium alginate (SA), inulin (IN), efavirenz (EFV), empty beads (E) and EFV loaded beads (L), both with (+IN) and without IN (-IN) collected at a heating range of 30 – 600°C.

As shown in **Figure 7.1**, the E+IN and E-IN beads presented with similar TGA thermograms. It is noteworthy to mention that a residue of 53.19% for E+IN and 48.01% for E-IN beads remained at the end of the experiment at 600°C. This high residue amount can be attributed to a change in the chemical nature of SA, which can be expected as a result of the cross-linking reaction that led to the formation of the alginate beads. Interestingly, the E+IN and E-IN beads showed onset of degradation at a lower temperature but with a higher mass percentage remaining that didn't degrade before the end of the heating run at 600°C. The higher residue mass that remained at the end of the TGA run at 600°C could be attributed to increased stability achieved through the crosslinking process.

The TGA thermograms for the loaded formulations also exhibited similar thermal profiles. A residue of 40.48% for L+IN beads and 44.68% for L-IN beads remained at the end of the experiment at 600°C. The TGA analysis for the loaded alginate beads delivered similar results as the empty beads. This suggests that the presence of EFV does not affect the stability of the alginate matrix.

Table 7.1: Major weight loss steps identified from the collected TGA thermograms for SA, IN, EFV and E-IN, E+IN, L-IN and L+IN beads.

Sample	Onset temperature (°C)	Percentage weight loss (%)
SA	30.00	12.69
	253.77	31.22
	300.00	15.09
IN	222.00	17.10
	246.45	25.23
	315.00	8.41
EFV	225.00	91.95
E-IN	70.00	8.65
	197.79	10.99
	298.82	5.25
E+IN	70.00	7.06
	195.05	10.01
	298.44	6.58
L-IN	70.00	11.16
	199.05	12.36
	303.34	4.48
L+IN	70.00	11.69
	203.84	11.56
	292.55	4.10

The DSC thermograms for pure EFV, pure SA, and the four alginate bead preparations were collected across the temperature range of 30 – 180°C and are shown in **Figure 7.2**. Pure EFV exhibits a single sharp endothermic peak at 140.19°C with ΔH = 44.32 J/g as described and discussed in **Chapter 5.3.1**. The DSC thermograms for pure SA and the four bead preparations did not exhibit any endo- or exothermic peaks. The absence of the characteristic EFV endotherm from the DSC analysis of the EFV-loaded beads at ~139°C could potentially suggest the encapsulation of EFV within the alginate matrix (**Figure 7.2**). Alternatively the disappearance of the melting endotherm could be indicative of EFV encapsulation on a molecular level thereby forming a solid solution that masks the individual EFV melting event. Lastly, the absence of the EFV melting endotherm could also suggest that very small amounts of EFV is present in the bead matrix. This is the most unlikely explanation since high drug loading was achieved. Whether or not complete encapsulation of EFV was achieved may require further analysis but regardless, the absence of the EFV melting endotherm could in the very least suggest that EFV is not located on the exterior surface of the alginate bead. This may have promise with regards to taste-masking. According to literature, SA exhibits an exothermic event around 250°C relating to its thermal degradation, as was seen during HSM analysis (Soares et al., 2004; Pongjanyakul & Puttipipatkhachorn, 2007). Here, the DSC experiment was only run to 190°C as to comply with DSC protocol at UWC of not exceeding the degradation temperature for any single component, thus not allowing the observation of the degradation through DSC analysis.

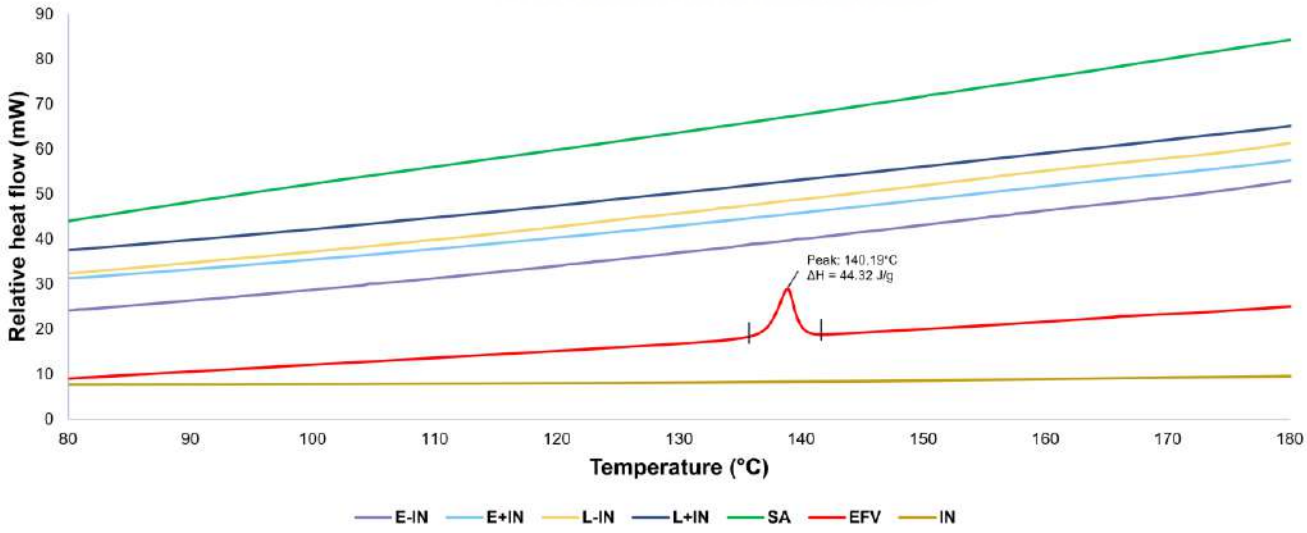

Figure 7.2: Overlay of DSC thermograms of EFV, SA, empty beads prepared with IN (E +IN), loaded beads prepared with IN (L +IN), unloaded beads prepared without IN (E –IN) and

loaded beads prepared without IN (L -IN) collected at a heating range of 30 – 190°C with only the range of 80 – 180°C depicted.

7.2.1.2 Fourier transform infrared spectroscopy

The FT-IR spectra of SA, EFV, E-IN, E+IN, L-IN, and L+IN are shown in **Figure 7.3**. The spectrum obtained for SA exhibited a broad peak at around 3227 cm^{-1} which is attributed to -OH stretching while characteristic peaks at 1596 cm^{-1} and 1407 cm^{-1} were attributed to $-COO^-$ symmetrical and asymmetrical stretching vibrations. These observations are in accordance with what has been previously reported in literature (Borba et al., 2016; Li et al., 2016). The spectra for E+IN, E-IN, L+IN, and L-IN beads showed a very broad absorbance peak at around 3300 cm^{-1} that could be attributed to the presence of water in the bead structures, as also observed from TGA (**Figure 7.1**). For all the empty and loaded beads, the spectra also showed a slight shift of the asymmetrical stretching vibration of the carboxyl group to a slightly higher wavenumber at around 1413 – 1418 cm^{-1} which can be attributed to the crosslinking of Ca^{2+}-ions to the $-COO^-$ group (Li et al., 2016). EFV shows characteristic absorbance bands at 3315.3, 2251.6, 1745.2, 1601.4, and 1319.7 cm^{-1} respectively attributed to N-H stretching, aromatic C-H stretching, C=O stretching, C=C stretching, and C-O-C stretching. These characteristic peaks were, however, completely absent in the FT-IR spectra obtained with the drug-loaded alginate beads, therefore suggesting encapsulation of EFV. However, FT-IR exhibits very high penetrating capabilities and should be able to detect EFV within the alginate matrix. Considering this, it is possible that the gelling process could have resulted in molecular interactions between the SA, IN and EFV. These molecular interaction could change the orientation of certain EFV functional groups thereby resulting in either no detection, as a result of masking by the other excipients, or detection of weak intensity. Lastly, it is also possible that the absence of characteristic EFV peaks could mean that no EFV is present in the alginate beads. Therefore, it was important to confirm the presence of EFV in the beads through drug content determination.

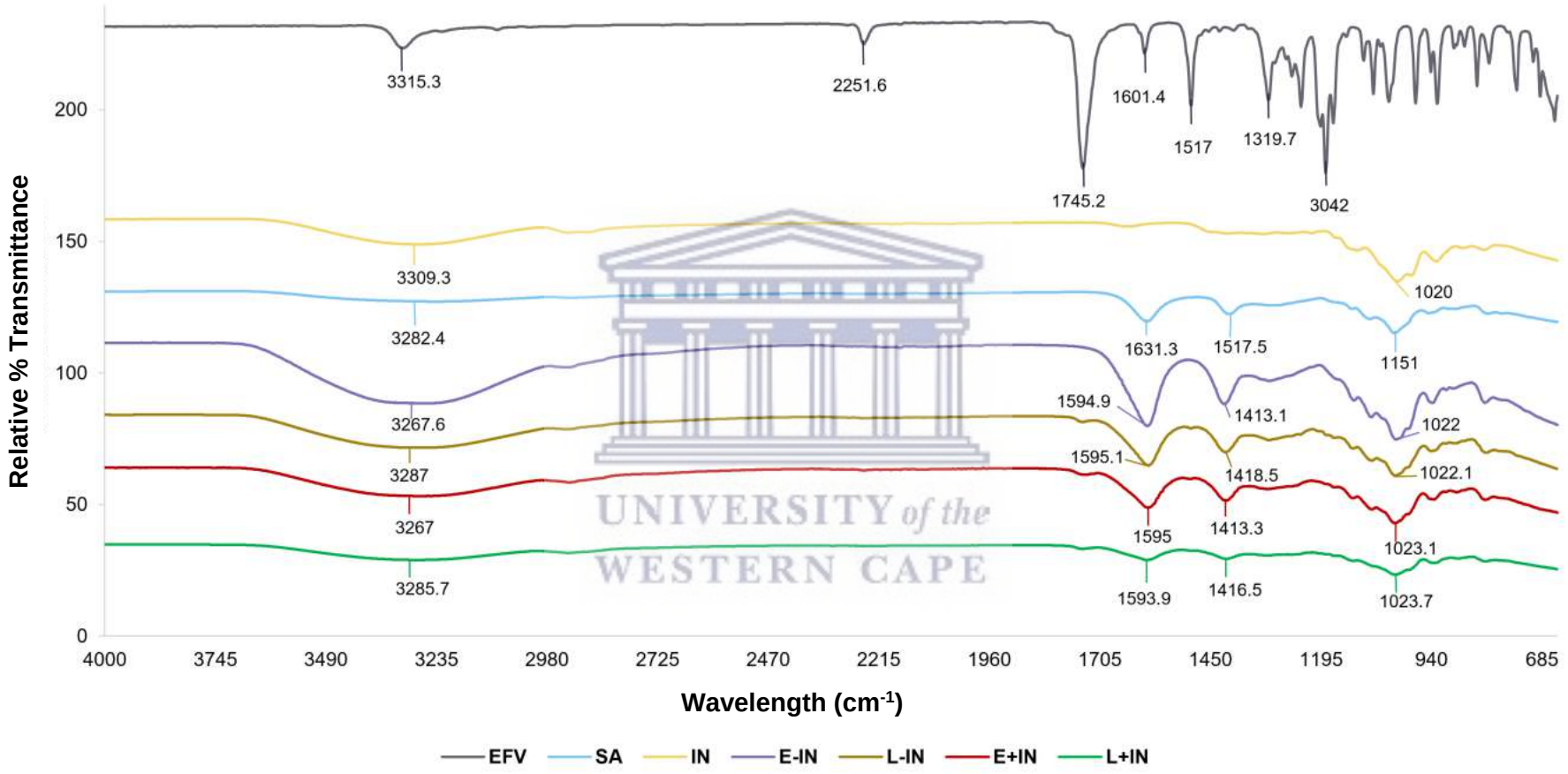

Figure 7.3: An overlay of FT-IR spectra of EFV, sodium alginate (SA), empty beads without IN (E–IN), loaded beads without IN (L–IN), empty beads with IN (E+IN) and loaded beads with IN (L+IN), collected at ambient temperature.

7.2.1.3 Weight, moisture content and swelling behaviour of beads

The mean bead weight for each batch is shown in **Table 7.2**. It is important to note that the term wet refers to the state of the beads immediately after preparation while the term dry refers to beads after 120 h of ambient temperature drying. The average wet weight of the empty beads was higher compared to their loaded counterparts, while the average wet weight of the –IN beads was also higher compared to the +IN beads. The E-IN beads exhibited the highest wet and dry average weight. The L+IN beads exhibited the lowest average weight when wet while the empty counterparts exhibited the lowest average weight when dry. The moisture content of dry beads was also investigated to better understand the observed weight differences. The moisture content of the dry beads was in the range 7.10 – 11.69% with the EFV loaded beads exhibiting greater moisture content compared to empty beads. EFV may have an impact on the water absorption ability of the alginate beads (**Table 7.2**). Alginates can absorb a large amount of water due to their hygroscopic nature which may be affected by the mixing of EFV.

Table 7.2: Weight of calcium-alginate beads directly after production (wet) and after 120 h (dry), as well as the moisture content of the dry beads as a percentage.

Batch	Weight when wet (mg ± SD, n=4)	Weight when dry (mg ± SD, n = 4)	Moisture content when dry (%)
E-IN	27.6 ± 2.4	1.05 ± 0.04	8.65
L-IN	23.5 ± 6.1	0.80 ± 0.02	11.16
E+IN	27.1 ± 2.1	0.75 ± 0.04	7.10
L+IN	21.3 ± 2.0	0.90 ± 0.01	11.69

It is known that drug release from alginate matrices is mainly facilitated by swelling and erosion. The swelling behaviour of the beads was investigated in order to understand drug release from the beads (Tønnesen & Karlsen, 2002; Bajpai & Sharma, 2004). Here, the degree of swelling was determined by measuring the weight change of the beads when placed in an aqueous environment with pH values ranging from 1.2 – 7.2. The swelling behaviour of the beads is depicted in **Figure 7.4**. As would happen in a biological system, the beads were first placed in a pH 6.8 environment to mimic the behaviour of the beads in the oral cavity. The results obtained showed that regardless of the formulation, all beads were associated with swelling in a pH 6.8 buffer environment. Within the first 5 min between 27% - 59% swelling was observed with the greatest degree of swelling observed for the L-IN beads. The maximum swelling ratio observed in pH 6.8 was 141.58 – 290.80% w/w within 30 min with the greatest maximum swelling observed for the L+IN beads. EFV loaded beads exhibited a greater average percentage swelling (%) compared to empty counterparts while +IN beads exhibited a greater average swelling % than the –IN beads. The beads were subsequently transferred

to pH 1.2 buffered media and underwent a gradual reduction in weight over a period of 120 minutes with an average total weight reduction of 100.63%. The smallest weight reduction and the greatest weight reduction were observed for E-IN (46.53%) and L+IN (145.98%), respectively.

Thereafter, the beads were transferred to a pH 4.5 environment for 120 minutes. Here, a maximum average swelling ratio of 40.88% for all bead types was observed over a period of 120 min. The greatest swelling ratio observed in pH 4.5 was 72.22% for E+IN beads, followed by 40.59% for E-IN beads. The smallest swelling ratio was observed for L+IN beads with a swelling ratio of 21.84% achieved. Overall, empty beads showed greater swelling in pH 4.5 compared to loaded beads.

Finally, the beads were transferred to a pH 7.2 medium. Complete erosion and disintegration of the beads occurred within 30 – 60 min for all formulations. All beads types initially swelled within the first 10 minutes, after which a steady decrease in weight was noted, attributed to erosion and disintegration rather than shrinking of the beads. All beads were completely disintegrated by 60 min.

Overall, the SA beads exhibited pH-dependent swelling with the lowest swelling ratio in pH 1.2 and the highest in pH 7.2 and pH 6.8. Loaded beads were generally associated with a greater degree of swelling in all media, except for in pH 4.5, where empty beads exhibited a greater degree of swelling compared to their loaded counterparts.

This pH-dependent swelling behaviour can be explained by the chemical nature of alginates as well as the mechanism of cross-linking involved. Since alginates have a pKa of 3.4, the carboxylic acid groups exist in an unionised form (-COOH) at pH-values below this pKa while existing in an ionised form ($-COO^-$) at pH-values above the pKa. It can therefore be concluded that alginates are rather insoluble at pH values below 3.4 and that they are increasingly soluble at pH values above 3.4 with greater solubility seen in alkaline solutions. This is because when the carboxylic acid group is ionised (at pH > 3.4) it results in increased electrostatic repulsion causing the polymer chain to expand and swell. This partly explains why the greatest degree of swelling was observed at pH 7.2, while the smallest degree of swelling was observed at pH 1.2. However, even though alginates show pH-dependent solubility, the Ca^{2+}-induced cross-linking imposes stability to the alginate structure in aqueous media. It can therefore be concluded that the pKa of alginates are not the sole determining factor for the swelling behaviour observed. A second process namely, ion-exchange, plays a significant role in the observed swelling behaviours. Bajpai and Sharma, (2004) also showed that the swelling of alginate beads is directly correlated to the presence and quantity of Na^+-ions present in the

liquid media. They further showed that the release of Ca^{2+}-ions was also associated with the swelling of beads. It was concluded that ion-exchange between Na^{+}- and Ca^{2+}-ions is the main factor responsible for the swelling of alginate beads. This is because the Na^{+}-ions are not able to bind the $-COO^{-}$-ion groups as strongly, resulting in weaker cross-linking, higher water uptake and subsequent swelling.

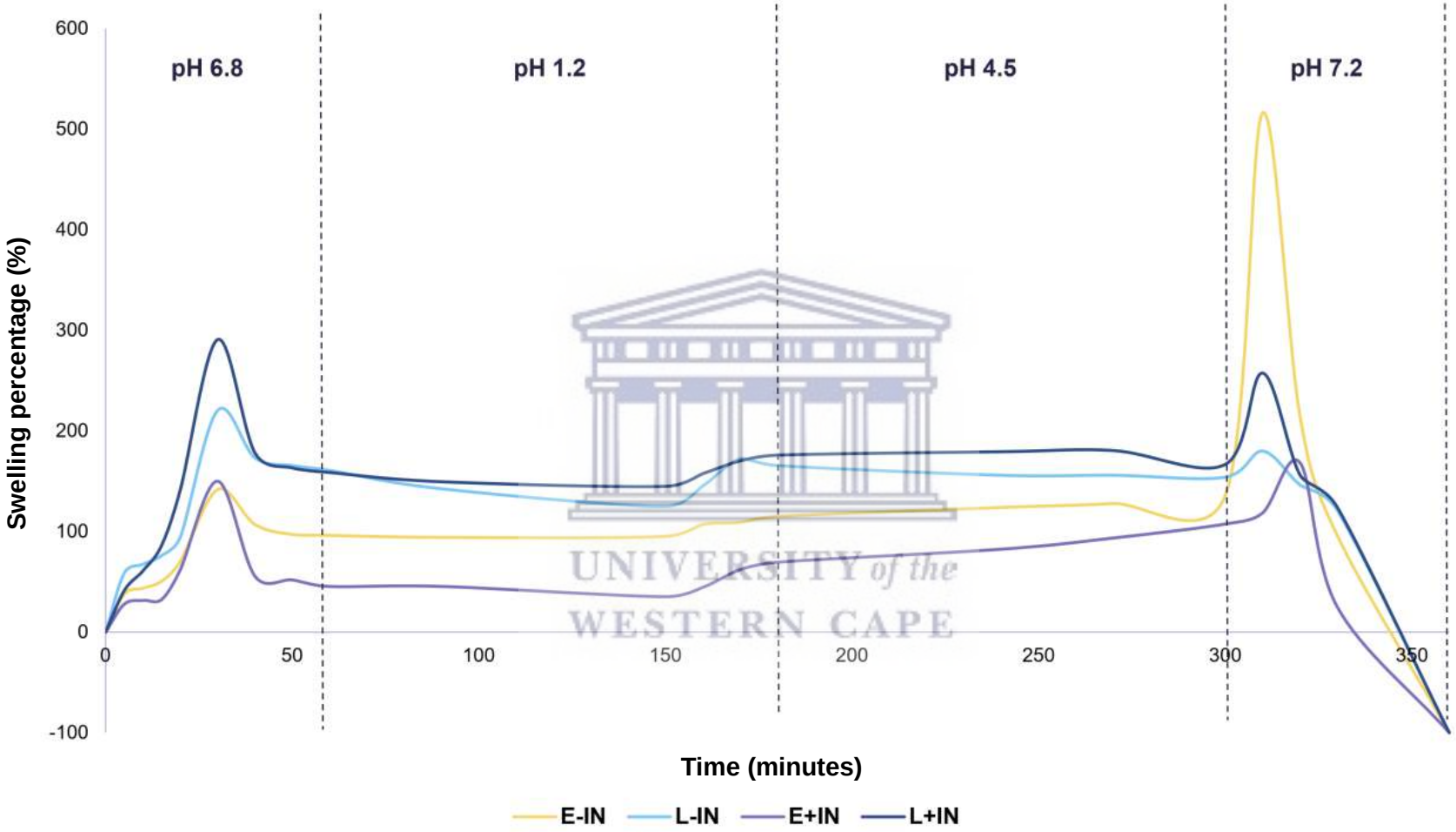

Figure 7.4: Swelling profiles of alginate beads as determined by placing dried beads in GIT-related pH aqueous solutions (pH 1.2 – 7.2) in a consecutive manner that mimics the transition of a compound through the GIT. Swelling percentages are given as a function of the original dry weight of the beads before the start of the study.

7.2.1.4 Morphology of beads

The morphology of synthesised alginate beads was analysed using optical microscopy to characterise the morphology of the alginate beads as well as to determine if there were any morphological differences between the formulations. The beads were evaluated for diameter and degree of symmetry. **Figure 7.5** shows that the synthesised beads were spherical in nature directly after synthesis with a high degree of symmetry.

The mean particle sizes of the obtained beads are shown in **Table 7.3**. The mean wet size of the alginate beads was in the range of 637.02 ± 16.37 – 672.86 ± 16.11 µm. The drug-loaded beads were on average smaller when wet compared to their empty counterparts, while the +IN beads were on average smaller compared to the –IN beads.

Upon drying of the beads the morphology changed significantly with beads becoming less spherical and less symmetrical (**Figure 7.5; Table 7.4**). The dried beads appeared more irregular in shape compared to the wet beads while EFV loaded beads appeared slightly more spherical than the empty beads. The irregular shape observed in the dried beads can be attributed to the partial collapse or restructuring of the polymer network during dehydration (Pasparakis & Bouropoulos, 2006). All beads underwent a substantial size reduction during the process of air drying. The mean particle size of the beads after drying was in the range of 227.53 ± 16.53 – 281.63 ± 19.01 µm. The E-IN beads exhibited the highest wet and dry average size. The L+IN beads exhibited the smallest average size when wet while the empty counterparts exhibited the smallest average size when dry. The significant weight reduction experienced by the beads and the final moisture content of the dry beads supports the idea that water was released from the matrix.

From the bead sizing data, it is evident that the EFV-loaded beads are on average smaller than their empty counterparts when wet. This could be attributed to the manner in which EFV interacts with the calcium alginate matrix. It is possible that the EFV molecules occupy the spaces in the alginate matrix in a manner that prevents water molecules to be captured in the cross-linked matrix, with EFV molecules filling the spaces in the cross-linked matrix and repelling water from the matrix. This is opposed to the empty beads where water molecules are the only occupants of the spaces within the alginate matrix. Despite water molecules being smaller than EFV molecules, it is possibly a cumulative effect of water molecules attracting more water molecules leading to the matrix spaces being occupied by clusters of water molecules. This is opposed to a single or a small amount of EFV molecules in the loaded

beads. This could potentially explain the difference in the size of the beads as well as the moisture content differences seen between the EFV-loaded beads and empty beads.

No obvious pattern was observed regarding the difference in the average size or weight between +IN and -IN beads. This suggests that the inclusion of IN into the bead matrix does not significantly impact the physical characteristics of the formed beads. It is however worthy to note that the pattern observed with regards to the weight and size of beads were the same, suggesting that a high level of correlation exists between the size and weight of the beads.

Table 7.3: Particle size of calcium-alginate beads directly after production (wet) and after 120 h (dry).

Batch	Particle size when wet (µm ± SD, n=4)	Particle size when dry (µm ± SD, n = 4)
E-IN	672.86 ± 16.11	281.63 ± 19.01
L-IN	649.99 ± 10.44	239.64 ± 12.68
E+IN	660.27 ± 26.34	227.53 ± 16.53
L+IN	637.02 ± 16.37	256.44 ± 20.37

PXRD analysis was performed on the pure substances as well as the produced calcium alginate beads. As discussed in **Chapter 5**, the solid-state of EFV was confirmed to be crystalline while the solid-states of IN and SA were confirmed to be amorphous. The irregular and broad peak in their PXRD profiles around 7.4 – 9.2 2°θ observed for E-IN, E+IN and L-IN beads can be attributed to the sample holder used during analysis (**Figure 7.6**). The packing of the beads onto the sample holder was not uniform, resulting in small sections of the sample holder being exposed and subsequently resulting in the observance of a diffraction peak. Overall, no significant differences in terms of solid-state were observed between the bead types.

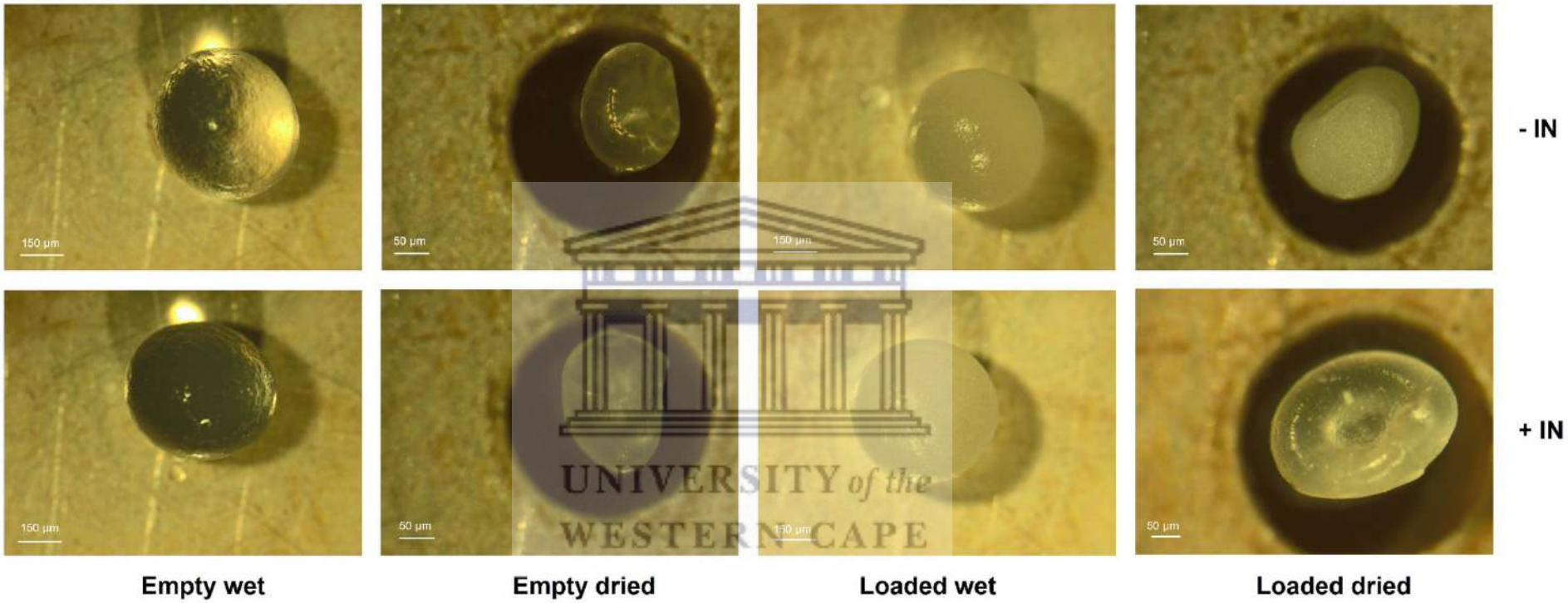

Figure 7.5: Micrographs showing the wet and dry beads of each formulation to illustrate the morphology of the beads.

Table 7.4: Degree of symmetry measured as a similarity between three measured diameters per bead.

Formulation	Degree of symmetry (n=3; ±SD)	
	Wet beads	Dried beads
L+IN	1.03 ± 0.03	1.11 ± 0.11
L- IN	1.02 ± 0.02	1.20 ± 0.04

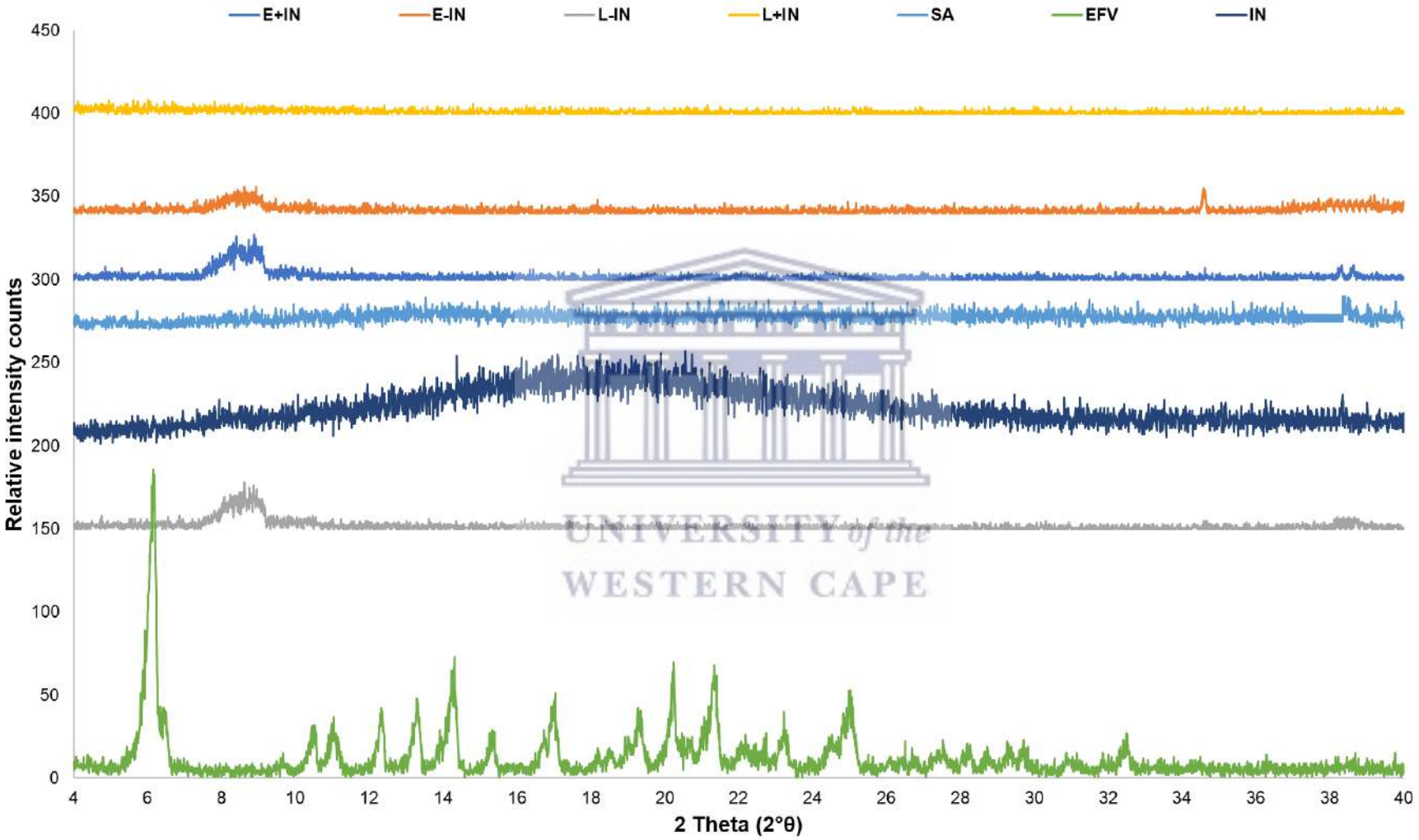

Figure 7.6: Overlay of PXRD patterns of pure EFV, sodium alginate (SA), IN and the prepared calcium alginate beads collected at ambient temperature.

7.2.2 Determining the drug loading and encapsulation efficiency

The drug loading achieved through the production of EFV-loaded alginate beads was found to be in the range of 52 – 75%, as shown in **Table 7.5**. Higher drug loading was achieved for beads prepared without IN compared to those prepared with IN.

The achieved drug loading percentages were used to determine the mass of beads required for an effective dose to be delivered. To do this, **Equation 7.1** was used.

$$mass\ beads\ required\ for\ 100\ mg\ dose = \frac{100+\%DL}{100} \times 100 \qquad \textit{Equation 7.1}$$

Table 7.5: The composition of the drug/polymer and curing solutions with the achieved drug loading and encapsulation efficiencies achieved for both formulations.

Formulation	Sodium alginate (% w/v)	Curing solution	Drug loading (%)	Encapsulation Efficiency (%)
L+IN	2 (+1% IN)	$CaCl_2$	55.91 ± 3.17	99.29
L-IN	2	$CaCl_2$ (+1% IN)	68.41 ± 6.22	99.51

Drug loading into the alginate beads determines the number/mass of beads required to achieve an adequate dose. The % drug loading achieved here was relatively high at 55.91 ± 3.17% for L+IN beads and 68.41 ± 6.22% for L-IN beads. Almeida and Almeida, (2004) achieved similar drug loading (55.1 – 71.4%) with another poorly soluble pharmaceutical agent, pindolol. The achieved drug loading % in the present study was used to determine the mass of beads that would be required to achieve typical dosages (**Equation 7.1**). For L+IN beads, 178.57 mg and for L-IN, 147.06 mg of dried beads are required per 100 mg EFV dose needed.

The extremely high encapsulation efficiency achieved here (**Table 7.5**) may be due to the extremely low solubility of EFV in the aqueous calcium chloride solution. The low solubility prevents drug migration and partitioning from the alginate solution during bead preparation. Almeida and Almeida (2004) also achieved high encapsulation efficiencies (≥80% w/w) (Almeida & Almeida, 2004). It is possible that the lower solubility of EFV compared to the pindolol drug used by Almeida and Almeida (2004) could explain the higher encapsulation efficiency achieved here. High encapsulation efficiencies were achieved for both formulations (**Table 7.4**). For the L-IN beads, only a slightly higher encapsulation efficiency of 99.51% was achieved as opposed to the 99.29% achieved with the L+IN beads.

7.2.3 *In vitro* drug release studies

As described in **section 4.3.11**, drug dissolution studies were used to evaluate the amount of drug that gets released from the alginate beads and that would effectively be available for potential absorption in the GIT by going into solution. Drug release was first evaluated in distilled water and pH 6.8 medium separately and then drug release in pH 1.2 and pH 7.2 media was evaluated in a consecutive manner where beads were transferred from pH 1.2 directly to pH 7.2 medium.

The drug release rate from the loaded alginate beads in distilled water and pH 6.8 was evaluated over a period of 60 min. This was to accurately mimic drug release when beads might be mixed in a glass of water or when administered directly into the mouth cavity. Overall, the two formulations exhibited similar EFV release profiles in both distilled water and pH 6.8 media. In both dissolution media, drug dissolution commenced immediately with 7.72 – 7.89% drug release observed within the first 1 minute in distilled water (**Figure 7.7 – 7.8**). The maximum amount of drug released in distilled water over a period of 60 min was 8.27% and 8.42% for beads prepared with IN and without IN, respectively. In the pH 6.8 medium similar released drug concentrations of 8.42% and 8.02% for +IN and -IN were respectively quantified.

Drug release in pH 1.2 medium was studied over a period of 120 min, immediately followed by 120 min in pH 7.2 medium, this was to mimic drug release in the gastrointestinal tract (**Figure 7.7 – 7.8**). Drug release in pH 7.2 was determined with the consideration of the amount of drug already released in pH 1.2. Drug dissolution started immediately in pH 1.2 for both formulations and stabilised after 5 min. For both the L+IN and L-IN beads, a maximum drug release concentration of ± 8.00% across the 120 min was achieved. Overall, the drug release in distilled water, pH 6.8 and pH 1.2 were very similar for the two EFV-loaded bead formulations. However, in pH 7.2 the drug dissolution was significantly different for the two formulations. For the L-IN beads, the maximum drug dissolution in pH 7.2 was between 10 – 11%. The L+IN beads exhibited complete drug dissolution in pH 7.2 after 20 min (**Figure 7.7 (b)**). In contrast, the L-IN beads only exhibited maximum drug dissolution of 11.31% within 120 minutes (**Figure 7.8 (b)**).

The high degree of drug dissolution from the drug-loaded beads, observed in the first minute for all media, provides some insight into the potential mode of drug release from the calcium-alginate beads. The observed drug dissolution after 1 minute ranged between 7.72 – 12.52% (**Figure 7.7 – 7.8**). These values correspond to EFV concentrations of 0.0085 – 0.015 mg/mL. When compared to the inherent aqueous solubility of EFV as reported

in **Chapter 6**, the EFV solubility achieved here is significantly higher than what was achieved with pure EFV. This may be attributed to the properties of alginates. It has been reported that alginates can enhance the solubility and dissolution rate of drugs through improved wettability (Tønnesen & Karlsen, 2002; Gutsche, Krause & Kranz, 2008), however, this was only observed in drug-alginate matrices and not cross-linked alginate structures. This can potentially explain why the dissolution of EFV was to such a degree that exceeds the normal EFV aqueous solubility. Although in low concentrations, rapid release of EFV in all media can potentially mean that the EFV entrapment within the alginate bead is of rather weak strength and upon exposure to an aqueous medium the migration of EFV molecules out of the alginate beads may be an obvious response.

As already mentioned, alginate beads are known to be stable in acidic environments and associated with swelling and degradation in alkaline environments (Tønnesen & Karlsen, 2002; Li et al., 2016). Additionally, Patel, Sher and Pawar, (2006) found that in the case of metronidazole loaded into calcium-alginate beads, drug release from calcium alginate beads was governed by drug solubility in an acidic medium while in a basic medium drug release tends to be controlled by the gel properties, specifically the swelling behaviour. Taking this into account, together with the possibility of alginate-mediated solubility improvement of EFV the higher initial drug dissolution observed in pH 1.2 compared to distilled water and pH 6.8 could be explained. The solubility improvement of EFV as a result of the presence of the alginate matrix may impact the drug dissolution in pH 1.2 to a greater degree since the solubility of EFV is assumed to be the major determining factor of dissolution in this acidic environment.

The highest drug dissolution was observed in pH 7.2 media. Considering the observations made by Patel, Sher and Pawar (2004), this high drug release can be attributed to the swelling and complete disintegration of the beads. From the swelling study (**Figure 7.4**) the complete disintegration of the beads occurred between 30 – 40 min after immersion in a pH 7.2 environment. The maximum drug dissolution was observed in pH 7.2 after 45 min for the L+IN beads (75%) and after 120 minutes for L-IN beads (11.2%). The timing difference between the maximum drug dissolution and complete bead disintegration could suggest that the complete erosion of the matrix is not a necessary step for drug dissolution. The partial erosion of the alginate matrix together with the diffusion of EFV and the effect of the solubilized alginate matrix on the EFV solubility most likely act synergistically to ultimately result in the high degree of dissolution. However, the diffusion of EFV was likely the major factor contributing to the drug dissolution while disintegration only contributed to a small degree. This is supported by the fact that the L-IN only achieved 11.2% drug dissolution in pH 7.2 despite having completely

disintegrated. The difference in drug release between the two formulations is not completely understood and investigation into this phenomenon in a future study may be valuable.

The drug release data represented here has to be considered only partial. Given the data that was collected the best possible discussions and predications were made. The interrogation and interpretation of this data may change significantly if the absolute value of EFV was quantified during dissolution. This could have been done by first obtaining a sample from the dissolution vessel, diluting it with methanol or ACN and subsequently analysed it using HPLC. This will allow for the quantification of the absolute amount of EFV released by the EFV-loaded alginate beads. It would be very valuable to compare the absolute amount of EFV released to the amount of EFV in solution. It will only then be able to make more reliable conclusions on the potential of EFV-loaded alginate beads. Future studies and experiments should consider this.

Table 7.6: Weight change percentage (%) undergone by alginate beads during dissolution experiments at different pH conditions.

	Percentage weight change (%)				
	Distilled water	**pH 6.8** 37.5°C	**pH 6.8** 40°C	**pH 1.2**	**pH 7.2**
L-IN	63.01 ± 10.88	1284.71 ± 39.18	1371.84 ± 110.25	74.29 ± 1.08	-
L+IN	49.82 ± 4.14	1263.37 ± 151.12	1179.71 ± 73.02	46.81 ± 2.63	-

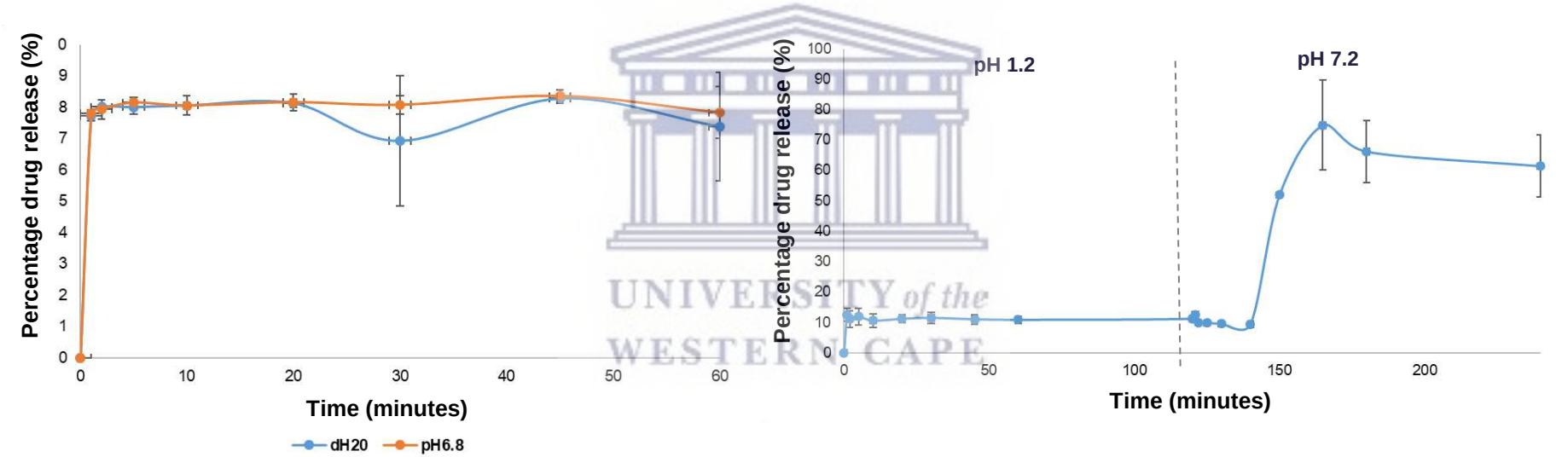

(a) **(b)**

- indicates the complete disintegration and erosion of the calcium-alginate beads

Figure 7.7: The percentage drug dissolution of L+IN beads in (a) distilled water and pH 6.8 media and (b) pH 1.2 and pH 7.2 at 37.5°C. Error bars show standard deviation.

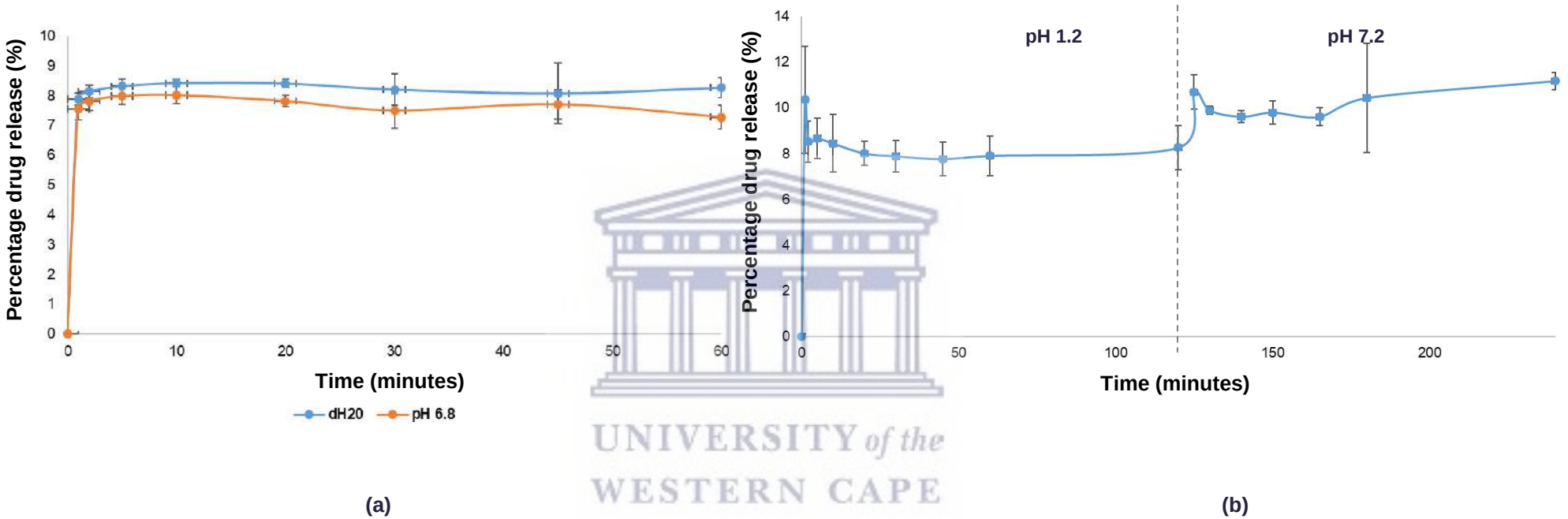

Figure 7.8: The percentage drug dissolution of L-IN beads in (a) distilled water and pH 6.8 media and (b) pH 1.2 and pH 7.2 at 37.5°C. Error bars show standard deviation.

The L+IN showed slightly higher drug release in all media except in distilled water where similar dissolution profiles were achieved. This behaviour does not appear to be linked to the swelling of the beads as no strong linkage was found between the swelling and composition of the prepared beads (**Figure 7.4**). It is possible that this difference in drug release can rather be attributed to the diffusion and solubilisation of EFV. It has previously been reported that the dissolution profile of poorly soluble drugs has been improved by the addition of IN. Structurally, the hydroxyl groups of IN can interact with water molecules giving IN some potential surfactant activity (Fares, Salem & Khanfar, 2011). However, as reported in **Chapter 5**, the solubility study done for EFV revealed that IN does not significantly improve EFV solubility. It is possible that the combination of IN with the alginate acts synergistically to enhance EFV solubility and dissolution.

It is worthy to point out that the dissolutions in pH 1.2 and pH 7.2 were carried out consecutively, with the same beads being transferred to pH 7.2 media after 2 h in pH 1.2 media. It has been reported that highly acidic environments can induce the hydrolysis of alginates into the more soluble and lower molecular weight form of alginic acids. This conversion means that there is a reduction in the mechanical strength of the beads (Tønnesen & Karlsen, 2002; Bajpai & Sharma, 2004). It is, therefore, possible that this reduction in mechanical strength may have occurred to some degree in a pH 1.2 media, and then on subsequent transfer to a pH 7.2 media, the swelling, degradation, and drug release occurred in a much shorter time span than what might have been anticipated (Bajpai & Sharma, 2004). The swelling behaviour of the beads together with the drug dissolution profiles suggests that this may well be the case here.

To evaluate the effect of drug administration with a warm drink or food sources on the drug release, the drug dissolution in pH 6.8 at 40°C ± 1°C was also investigated. Both formulations showed higher drug dissolution in 40°C compared to 37.5°C (**Figure 7.9**). The L+IN exhibited maximum drug dissolution of 15.25% ± 2.74% at 40°C compared to the 8.35% ± 0.21% at 37.5°C. Similarly, the L-IN beads also exhibited significantly higher drug dissolution of 11.46% ± 0.6% in 40°C compared to the 8.02% ± 0.28% exhibited in 37.5%.

The results depicted in **Figure 7.9** suggest that the higher temperature facilitates more rapid drug dissolution. It is possible that the higher temperature allows the alginate gel matrix to relax to some degree, thereby resulting in more rapid diffusion of EFV out of the alginate matrix. This has important implications for the taste-masking of the formulation. Considering that the aim of this study was to produce a taste-masked EFV formulation for the paediatric

population, drug administration with food and drink substances is expected in some cases. This means that drug administration might involve elevated temperatures in some cases for example when administering the drug with warm porridge. The results obtained here illustrate that elevated temperatures result in an increased dissolution rate and subsequently compromise taste-masking.

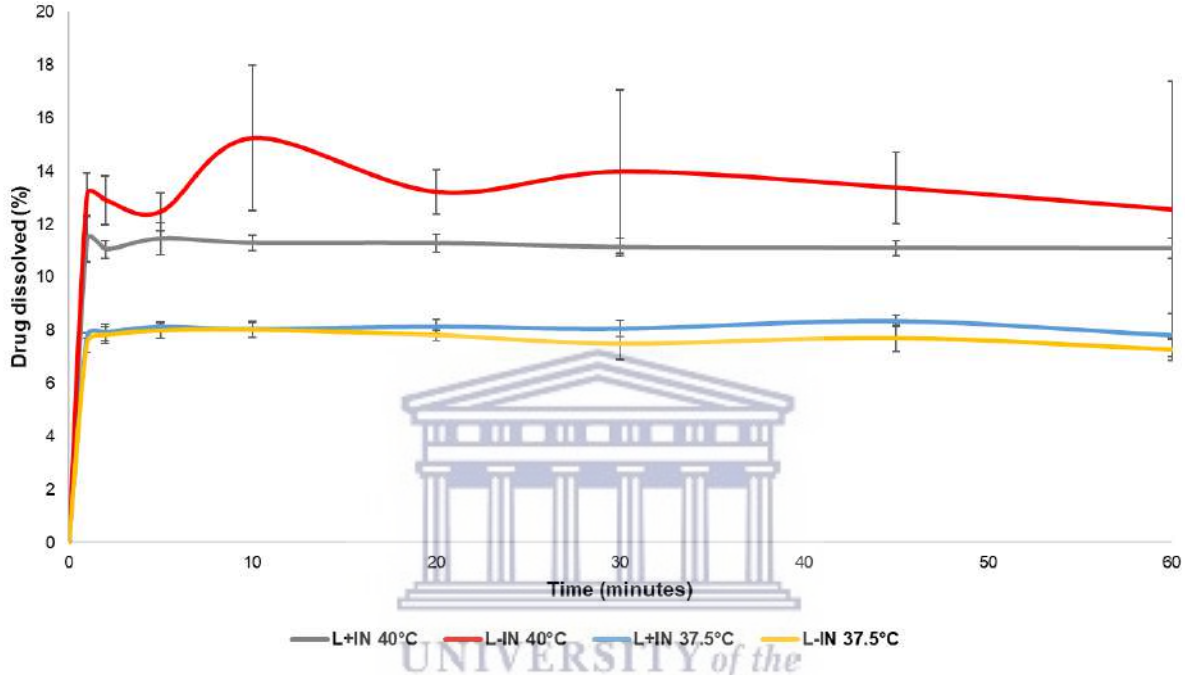

Figure 7.9: The percentage drug dissolution of the two EFV-loaded alginate bead formulations in pH 6.8 media at 37.5°C and 40°C. Errors bars show standard deviation.

For accurate comparisons to be made regarding the achieved taste-masking efficiency, the marketed product, Stocrin® film-coated tablets were also subjected to dissolution in a pH 6.8 media for a 60 minute period. Stocrin® tablets were crushed to a powder before dissolution, as a caregiver to a paediatric patient may do. The prepared EFV-loaded alginate beads exhibited a greater degree of drug dissolution compared to the marketed product (**Figure 7.10**).

Overall, the drug release profiles together with the swelling behaviour of the beads suggest that maximum drug release will occur in the lower duodenum and small intestine. A small amount of drug release occurs in pH 6.8 media, suggesting that some drug release will occur in the oral cavity. These results suggest that sufficient taste-masking was not achieved. This is especially prevalent when the drug release of the formulated EFV-loaded beads is compared to the release of the on-the-market product. Formulated EFV-loaded beads are

associated with significantly higher drug release levels compared to Stocrin® in pH 6.8, suggesting that the formulated EFV beads will potentially be associated with a higher degree of the bitter taste. It is however unclear how the alginate matrix will impact the interaction of the released EFV molecules with the taste receptors in the oral cavity. It is possible that the EFV molecules are associated with a layer of dissolved alginate which may reduce the experience of the bitter taste. But alas, it is not possible to evaluate this *in vitro* and ultimately a human taste panel would provide the ultimate verdict.

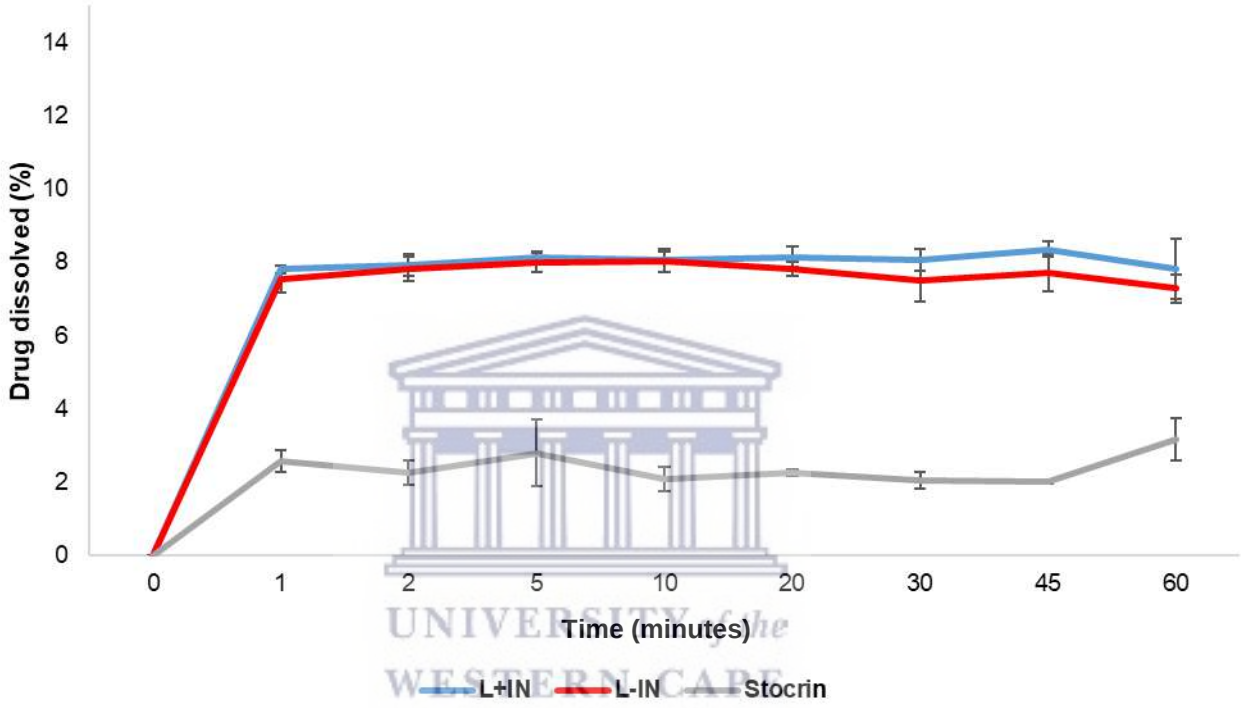

Figure 7.10: The percentage drug dissolution in pH 6.8 over a period of 60 minutes for the prepared EFV-loaded beads and Stocrin®. Errors bars show standard deviation.

Interestingly, in a previous study, it was discovered that the ability of dry calcium–alginate beads to swell in water is lower when coated with chitosan. This was attributed to greater physical entanglement of the polymer chains which resulted in greater resistance to swelling (Pasparakis & Bouropoulos, 2006). The application of this strategy to the EFV-loaded calcium-alginate beads produced here may have a positive effect on taste-masking efficiency. The coating of calcium-alginate beads has been demonstrated to be associated with delayed drug diffusion in multiple studies (Okhamafe, Amsden & Goosen, 1996; Anal & Stevens, 2005; Patel et al., 2016). By coating the produced EFV-loaded calcium alginate beads with chitosan it could reduce swelling in a pH 6.8 environment and therefore also reduce the drug release and dissolution rate while potentially achieving better taste-masking.

7.2.4 Preliminary stability studies

The analytical techniques employed during stability studies of the formulated alginate beads were FT-IR, moisture analysis, particle size, and weight and finally drug content. Only EFV-loaded beads were subjected to a preliminary stability evaluation through the exposure of the beads to 30°C and 65% RH conditions for 60 days.

The FT-IR spectra shown in **Figure 7.11** showed no significant peak shifts or molecular rearrangements in the prepared alginate beads after 60 days. The intensity of some peaks did however change over the period of 60 days. For the L-IN beads, the peak intensity decreased over the period of 60 days while peak intensity increased for the L+IN beads. These differences may be correlated to the moisture content which suggests that L+IN beads take up more water compared to L-IN beads.

The average weight of the prepared alginate beads showed an insignificant increase of 0.1 ± 0.02 mg for L+IN and 0.3 ± 0.05 mg for L-IN. Although the size of the beads did not significantly change within the 60 day period, the moisture content of the beads did increase slightly and corresponded to a slight increase in particle weight over 60 days (**Table 7.7**). The drug content of the beads was determined after 60 days and compared to the initial drug content for comparison. The drug content of both L-IN beads and L+IN beads remained relatively unchanged upon exposure to 30°C/65% RH conditions over a period of 60 days.

Table 7.7: Physical and chemical properties of EFV-loaded alginate beads exposed to accelerated stability conditions of 30°C and 65% RH in an open container.

	Moisture content (% ± SD)		**Size (µm ± SD)**		**Drug content (% ± SD)**	
	0 days	**60 days**	**0 days**	**60 days**	**0 days**	**60 days**
L+IN	11.69 ± 0.52	13.51 ± 0.13	248.48 ± 15.6	247.87 ± 10.4	55.74 ± 1.44	54.61 ± 2.05
L-IN	7.10 ± 0.44	8.58 ± 0.37	233.30 ± 0.47	236.73 ± 8.00	60.52 ± 3.23	60.62 ± 5.97

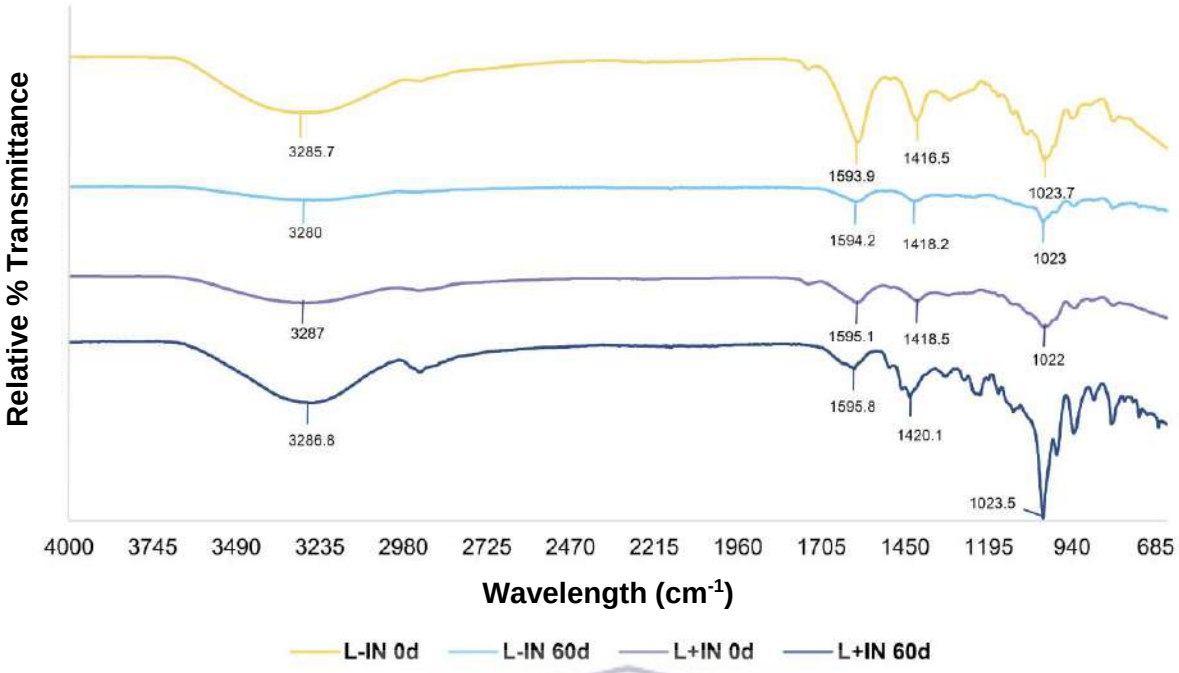

Figure 7.11: FT-IR spectra of the prepared alginate beads exposed to conditions of 30°C and 65% RH over a period of 60 days.

From the results obtained through the preliminary stability study under the conditions of 30°C ± 0.5°C; 65 ± 5% RH, it can be concluded that the prepared EFV loaded alginate beads remain both physically and chemically stable for at least 60 days. Over the 60 days, no significant molecular rearrangements occurred suggesting that the EFV gel matrix composition remained relatively unchanged. The slight increase in the average particle weight together with the slight increase in moisture content points to the absorption of a small amount of water over 60 days. This is not surprising, since alginates are known to be hydration candidates as a result of intermolecular bonding with water molecules to their hydroxyl and carboxyl functional groups (Tønnesen & Karlsen, 2002). It is likely that the time period of exposure to 30°C ± 65% RH and the amount of water content in the dried beads are directly linked. It can be expected that the moisture content of the beads will increase over time under these conditions and the lack of stability data for a longer period of time is deemed a limitation of this specific part of the study which should be further explored in the potential future studies.

7.3 Conclusions and recommendations

Here, calcium-alginate microspheres of EFV were prepared by a single ionic gelation method. High drug loading (55 – 68%) and high encapsulation efficiency (>90%) were obtained by this method. The drug release from the microspheres was affected by the pH of the dissolution

medium as well as EFV solubility. FT-IR and DSC studies did not reveal any significant drug-excipient interactions and confirmed that EFV was encapsulated within the calcium-alginate matrix. The drug release and dissolution profile of the EFV-loaded beads suggest that maximum drug release will occur in the lower duodenum and small intestine. Taste-masking of EFV through the production of the beads was deemed unsuccessful due to the high degree of drug dissolution observed in pH 6.8. It is however crucial for future studies to quantify the absolute amount of EFV released from the alginate beads as well as the effect of SA on EFV solubility to make better conclusions. Further, it could be strongly considered to perform X-ray photoelectron spectroscopy (XPS) on the EFV-loaded alginate beads to determine if EFV is present on the surface of the alginate beads. This will provide more conclusive evidence of the success of EFV encapsulation. This can also be coupled to nuclear magnetic resonance spectroscopy (NMR) for more robust results and subsequent conclusions.

Overall, EFV-loaded calcium-alginate beads have some advantageous properties as an oral dosage form. The physical and morphological nature of this formulation holds great advantage to children due to the ease of dose scale-up. As a result of the dynamic and variable nature of the target paediatric population, it would be ideal if the packaging of this formulation is done as a function of 100 mg dosages. Where each sachet would contain beads equivalent to 100 mg EFV. This would simplify the scale-up as children get older while still ensuring adequate dosing without complicating the manufacturing and processing involved. It is not yet ideal for the paediatric population specifically due to the fact that sufficient taste-masking was not achieved. Future work may involve investigating the coating of the EFV-loaded calcium alginate beads as a method to delay the diffusion and release of EFV, especially into a pH 6.8 environment. This may ultimately lead to improved taste-masking, which coupled with the other good properties of the formulation will render it potentially marketable.

The final formulation may also benefit from the addition of PPI. This is motivated by the effect of PPI on EFV solubility, as discussed in **Chapter 5**. The solubility improvement mediated by PPI may further assist the dissolution of EFV released from the beads. This will be particularly relevant in pH 1.2 (stomach) where the degree of EFV solubility improvement in combination with PPI is the greatest. This will simply mean that a greater percentage of the released drug will solubilise thereby potentially increasing the bioavailability of EFV.

7.4 References

Almeida, P. & Almeida, A. 2004. Cross-linked alginate-gelatine beads: a new matrix for controlled release of pindolol. *Journal of Controlled Release*. 97(3):431–439. DOI: 10.1016/j.conrel.2004.03.015.

Anal, A.K. & Stevens, W.F. 2005. Chitosan – alginate multilayer beads for controlled release of ampicillin. *International Journal of Pharmaceutics*. 290:45–54. DOI: 10.1016/j.ijpharm.2004.11.015.

Arica, B., Çaliş, S., Atilla, P., Durlu, N.T., Çakar, N., Kaş, H.S. & Hincal, A.A. 2005. In vitro and in vivo studies of ibuprofen-loaded biodegradable alginate beads. *Journal of Microencapsulation*. 22(2):153–165. DOI: 10.1080/02652040400026319.

Bajpai, S.K. & Sharma, S. 2004. Investigation of swelling/degradation behaviour of alginate beads crosslinked with Ca2+ and Ba2+ ions. *Reactive and Functional Polymers*. 59(2):129–140. DOI: 10.1016/j.reactfunctpolym.2004.01.002.

Borba, P.A.A., Pinotti, M., De Campos, C.E.M., Pezzini, B.R. & Stulzer, H.K. 2016. Sodium alginate as a potential carrier in solid dispersion formulations to enhance dissolution rate and apparent water solubility of BCS II drugs. *Carbohydrate Polymers*. 137:350–359. DOI: 10.1016/j.carbpol.2015.10.070.

Fares, M.M., Salem, M.S. & Khanfar, M. 2011. Inulin and poly(acrylic acid) grafted inulin for dissolution enhancement and preliminary controlled release of poorly water-soluble Irbesartan drug. *International Journal of Pharmaceutics*. 410(1–2):206–211. DOI: 10.1016/j.ijpharm.2011.03.029.

Gutsche, S., Krause, M. & Kranz, H. 2008. Strategies to overcome pH-dependent solubility of weakly basic drugs by using different types of alginates. *Drug Development and Industrial Pharmacy*. 34(12):1277–1284. DOI: 10.1080/03639040802032895.

Li, J., Kim, S.Y., Chen, X. & Park, H.J. 2016. Calcium-alginate beads loaded with gallic acid: Preparation and characterization. *LWT - Food Science and Technology*. 68:667–673. DOI: 10.1016/j.lwt.2016.01.012.

Okhamafe, A.O., Amsden, B. & Goosen, M.F.A. 1996. Modulation of protein release from chitosan-alginate microcapsules using the pH-sensitive polymer hydroxypropyl methylcellulose acetate succinate. *Journal of Microencapsulation*. 13(5):497–508. DOI: 10.3109/02652049609026035.

Pasparakis, G. & Bouropoulos, N. 2006. Swelling studies and in vitro release of verapamil from calcium alginate and calcium alginate – chitosan beads. *International Journal of Pharmaceutics*. 323:34–42. DOI: 10.1016/j.ijpharm.2006.05.054.

Patel, N., Lalwani, D., Gollmer, S., Injeti, E., Sari, Y. & Nesamony, J. 2016. Development and evaluation of a calcium alginate based oral ceftriaxone sodium formulation. *Progress in Biomaterials*. 5(2):117–133. DOI: 10.1007/s40204-016-0051-9.

Patel, Y.L., Sher, P. & Pawar, A.P. 2006. The Effect of Drug Concentration and Curing Time on Processing and Properties of Calcium Alginate Beads Containing Metronidazole by Response Surface Methodology. *AAPS PharmSciTech*. 7(4):E1-E7. DOI: 10.1208/pt070486.

Pongjanyakul, T. & Puttipipatkhachorn, S. 2007. Xanthan-alginate composite gel beads:

Molecular interaction and in vitro characterization. *International Journal of Pharmaceutics*. 331(1):61–71. DOI: 10.1016/j.ijpharm.2006.09.011.

Soares, J.P., Santos, J.E., Chierice, G.O. & Cavalheiro, E.T.G. 2004. Thermal behavior of alginic acid and its sodium salt. *Ecletica Quimica*. 29(2):53–56. DOI: 10.1590/S0100-46702004000200009.

Tønnesen, H.H. & Karlsen, J. 2002. Alginate in Drug Delivery Systems Alginate in Drug Delivery Systems. *Drug Development and Industrial Pharmacy*. 28(6):621–630. DOI: 10.1081/DDC-120003853.

CONCLUSIONS

This thesis started out by providing the context and challenges with regards to the treatment of paediatric HIV-infected patients. The challenges of providing acceptable dosage forms, specifically aimed at treating children has been highlighted. The non-nucleoside reverse transcriptase inhibitor, efavirenz, was explored as a model ARV for taste-masking purposes where two microencapsulation techniques, spray-drying, and ionic gelation was utilised in an attempt to achieve this goal.

The potential use of natural excipients, PPI and IN, to improve the solubility of the poorly water-soluble ARV was explored. The results showed that PPI can be used to improve the solubility of EFV significantly without the use of harmful surfactants. Next, the microencapsulation of EFV through spray-drying was investigated. The use of natural excipients PPI and IN as encapsulating agents proved relatively successful. FT-IR and DSC results showed that EFV was successfully loaded into the spray-dried powders. The use of an aqueous buffered solution for the preparation of the spray-drying feed solution produced an EFV containing powder with adequate taste-masked properties since EFV drug release proved significantly lower compared to the marketed product Stocrin® film-coated tablets. The use of an ethanol based solution for the preparation of the feed solution did not however produce powders with adequate taste-masking. The most significant downfall related to the spray-drying strategy was the overall stability of powders. Visually the powders underwent significant changes to such a degree that the powders would not maintain physical integrity for even 1 month upon exposure to either 40°C/75% RH or 30°C/65% RH conditions.

Further, calcium-alginate microspheres of EFV were prepared by a single ionic gelation method. High drug loading and high encapsulation efficiency was obtained by this method. The drug release from the microspheres was affected by the pH of the dissolution medium as well as EFV solubility. FT-IR and DSC studies suggest that EFV was encapsulated within the calcium-alginate matrix. Unfortunately, taste-masking of EFV through the production of the beads was deemed unsuccessful due to the high degree of drug dissolution observed in pH 6.8. Despite this, the physical and morphological nature of this formulation holds great advantage to children due to the ease of dose scale up. Future work may involve investigating the coating of the EFV loaded calcium alginate beads as a method to delay the diffusion and release of EFV, especially into a pH 6.8 environment. This may ultimately lead to improved taste-masking, which coupled with the other good properties of the formulation will render it potentially marketable. It is also worthy to acknowledge the limitation of this study with regards to analysis of SA solutions which was not possible at UWC due to equipment limitations. Given the chemical nature and viscosity of SA, the solubility of EFV in SA solutions could not be investigated. Future work may potentially include investigating the effect of SA on EFV

solubility. As mentioned in section 7.3, it will be beneficial to perform X-ray photoelectron spectroscopy (XPS) on the EFV-loaded alginate beads to determine if EFV is present on the surface of the alginate beads. This will provide more conclusive evidence of the success of EFV encapsulation. This can also be coupled to nuclear magnetic resonance spectroscopy (NMR) for more robust results and subsequent conclusions.

APPENDIX A

Supplementary figures

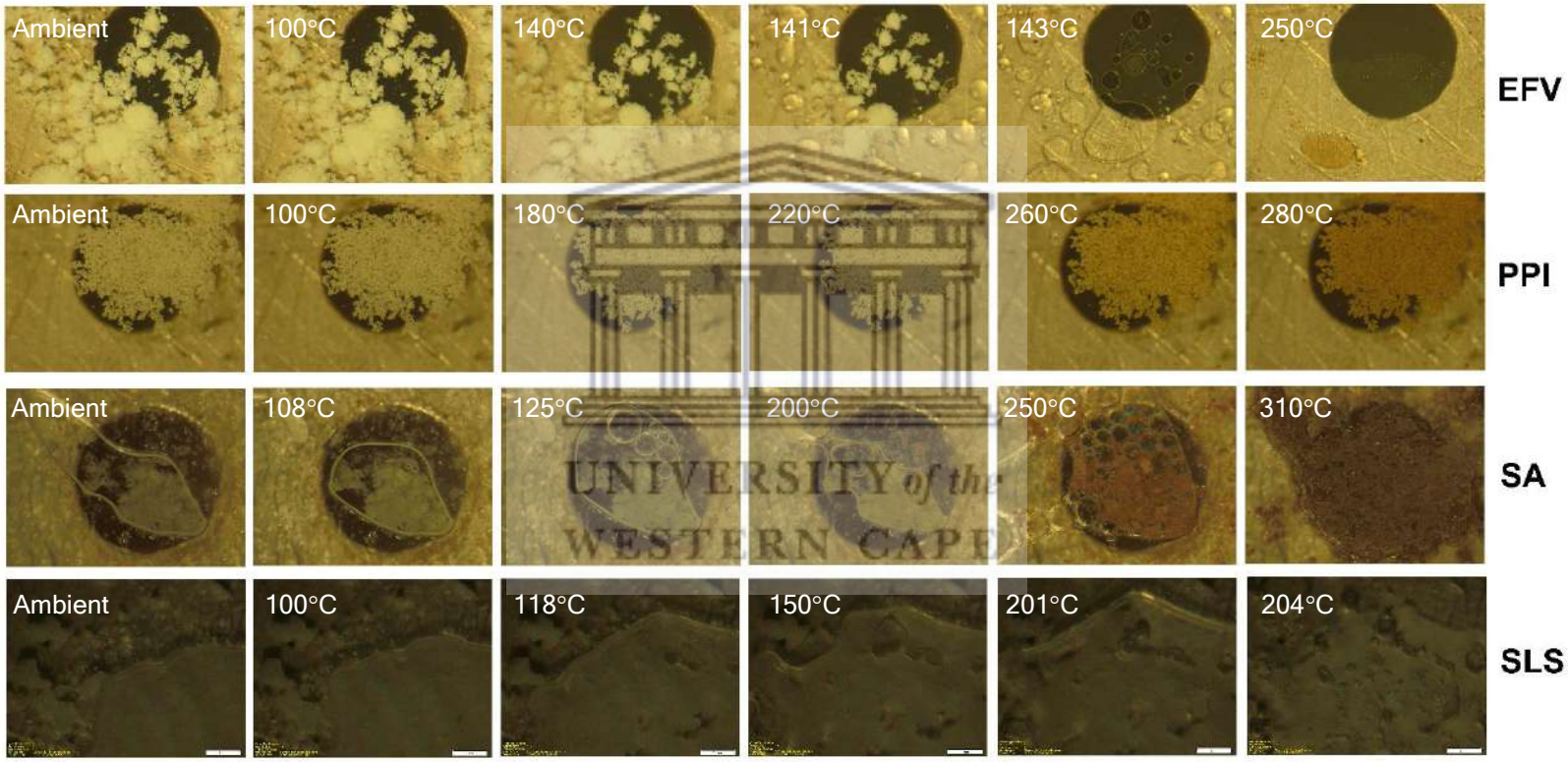

Figure A1: HSM micrographs showing the thermal behaviour of the raw materials EFV, SA, PPI and SLS. Data was collected over a range of 25 – 300°C, with only significant thermal events photographed and depicted here.

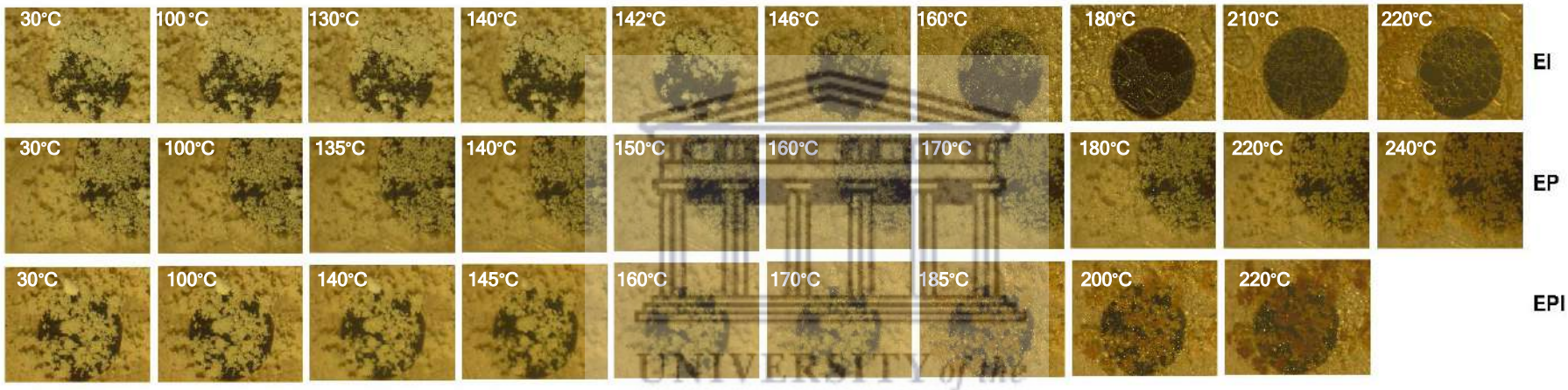

Figure A2: HSM micrographs showing the thermal behaviour of the physical combinations of EFV and IN (EI), EFV and PPI (EP) and finally EFV, PPI and IN (EPI). Data was collected over a range of 25 – 300°C, with only significant thermal events photographed and depicted here.

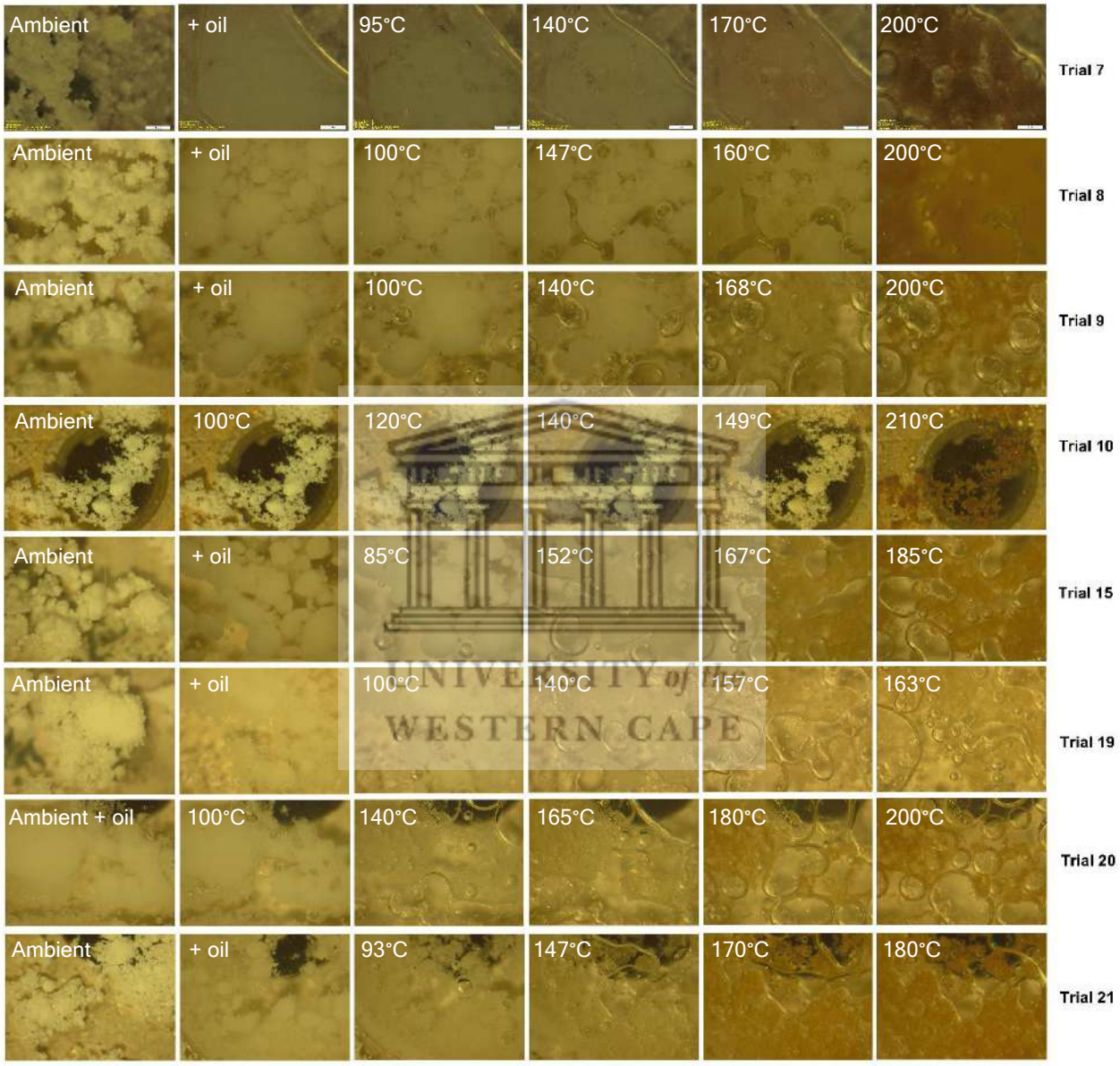

Figure A3: HSM micrographs collected for T7 – T21 over a heating range of 25 - 250°C.

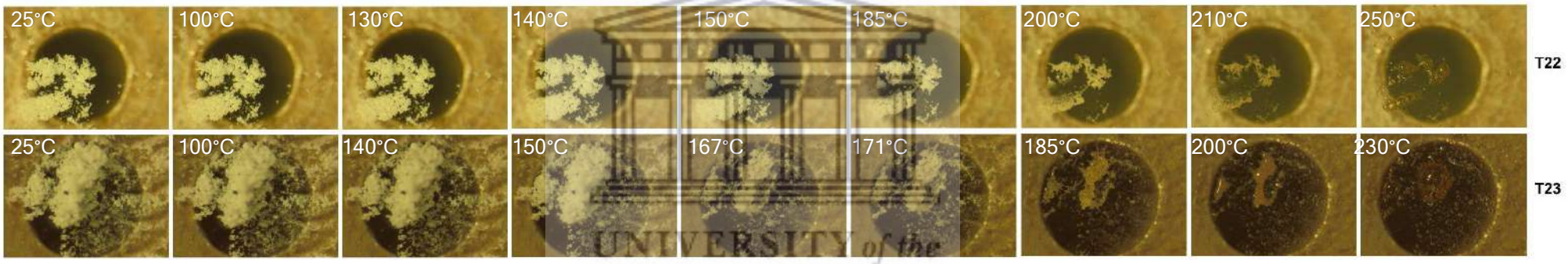

Figure A4: HSM micrographs collected for T22 and T23 over a heating range of 25 - 250°C.

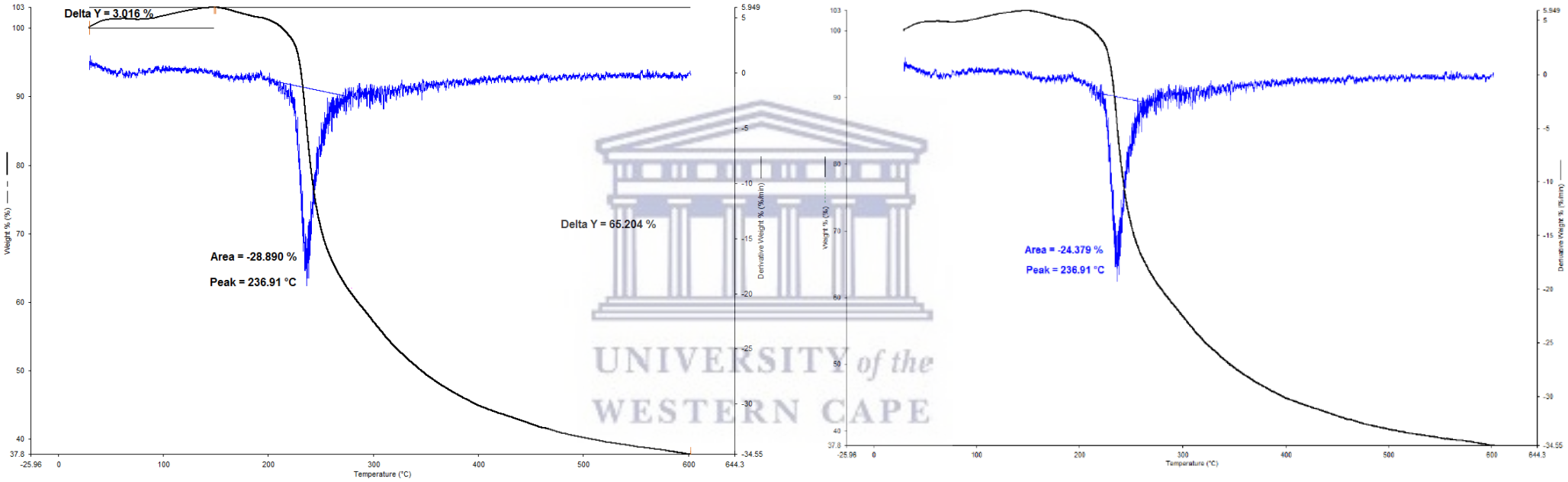

Figure A5: TGA thermograms collected for T22 (left) and T23 (right) across the range 30 – 600°C.

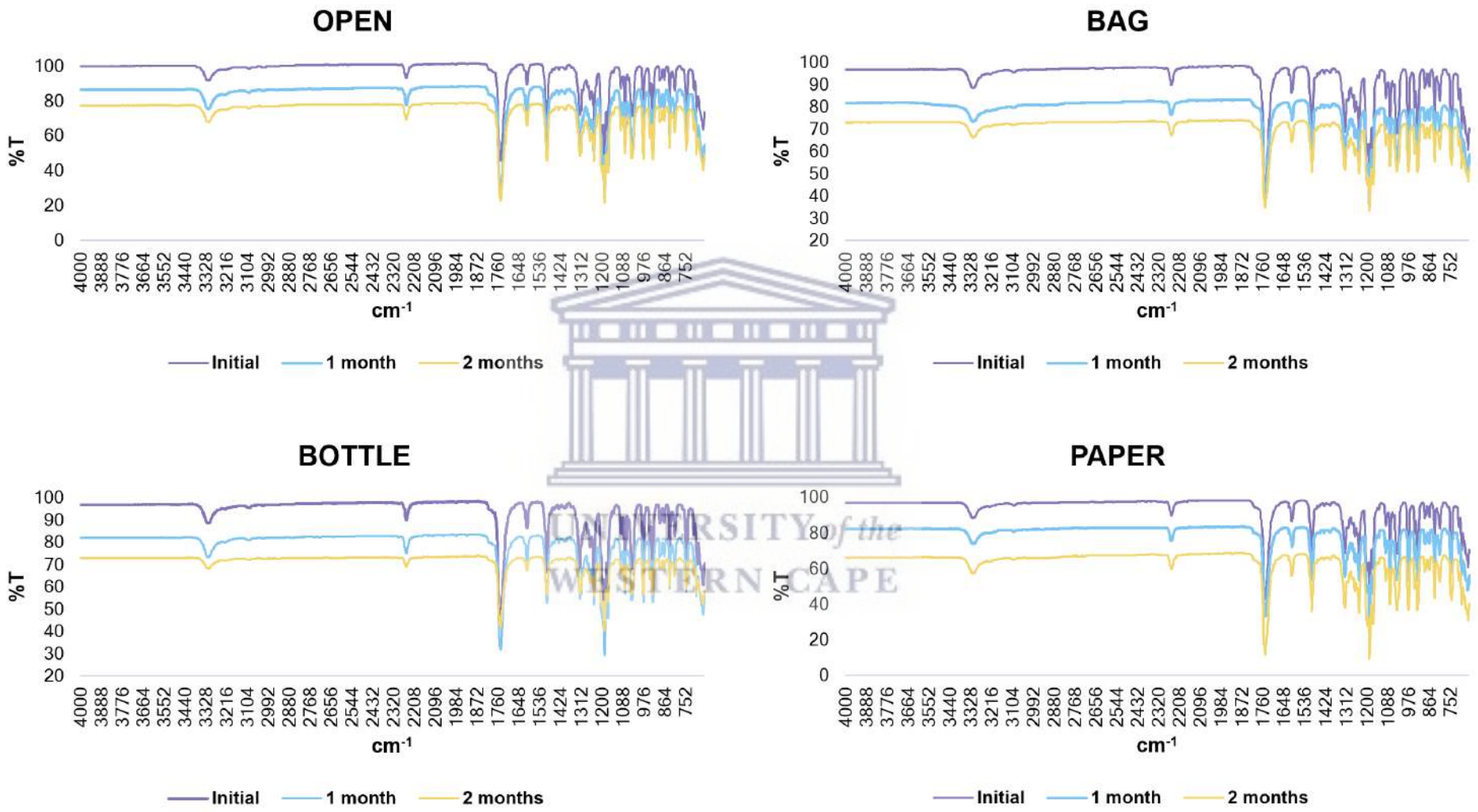

Figure A6: FT-IR spectra of EFV stored for 2 months at accelerated stability conditions of 40°C/75%RH in four different storage conditions.

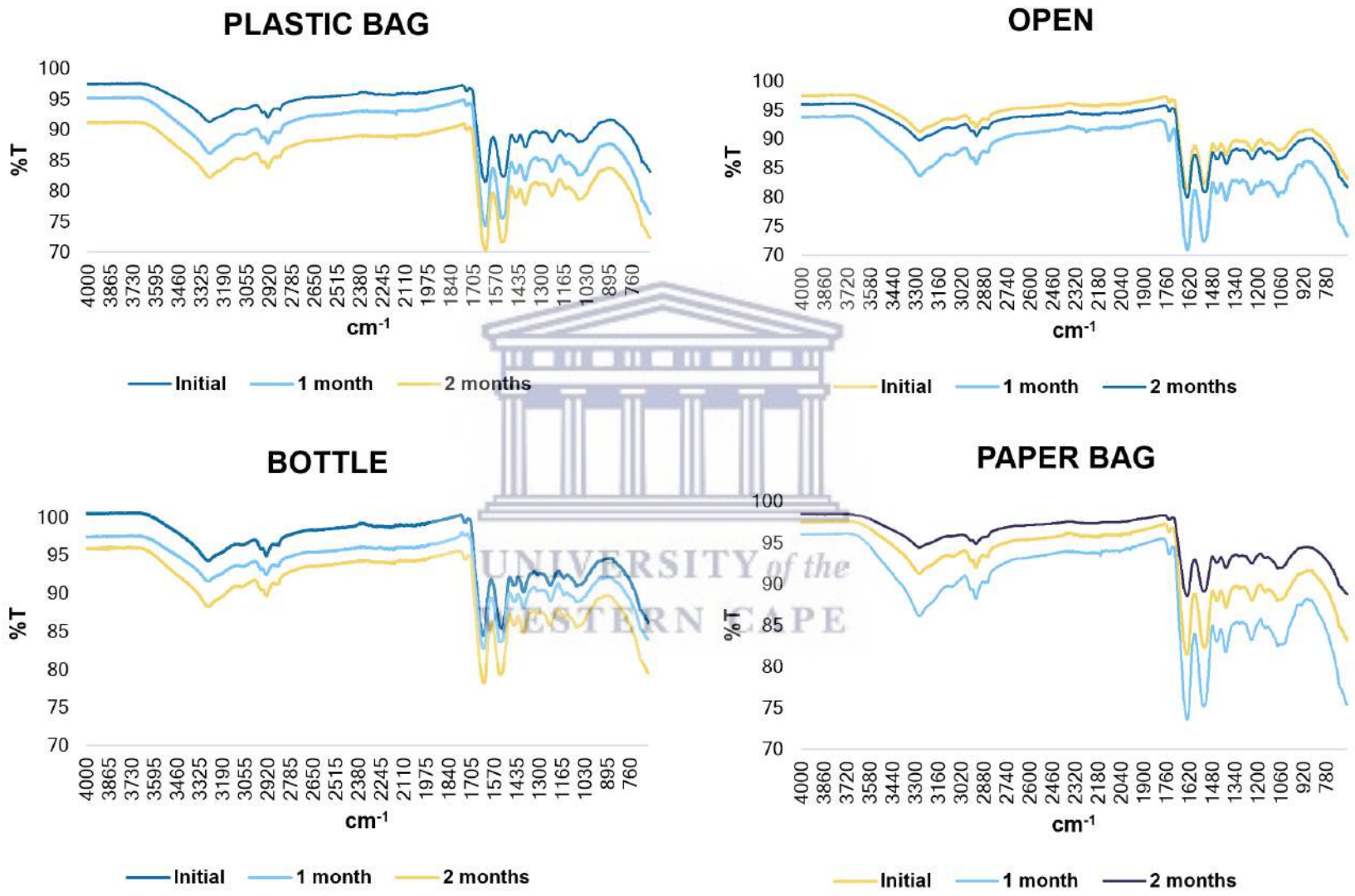

Figure A7: FT-IR spectra of PPI stored for 2 months at accelerated stability conditions of 40°C/75%RH in four different storage conditions.

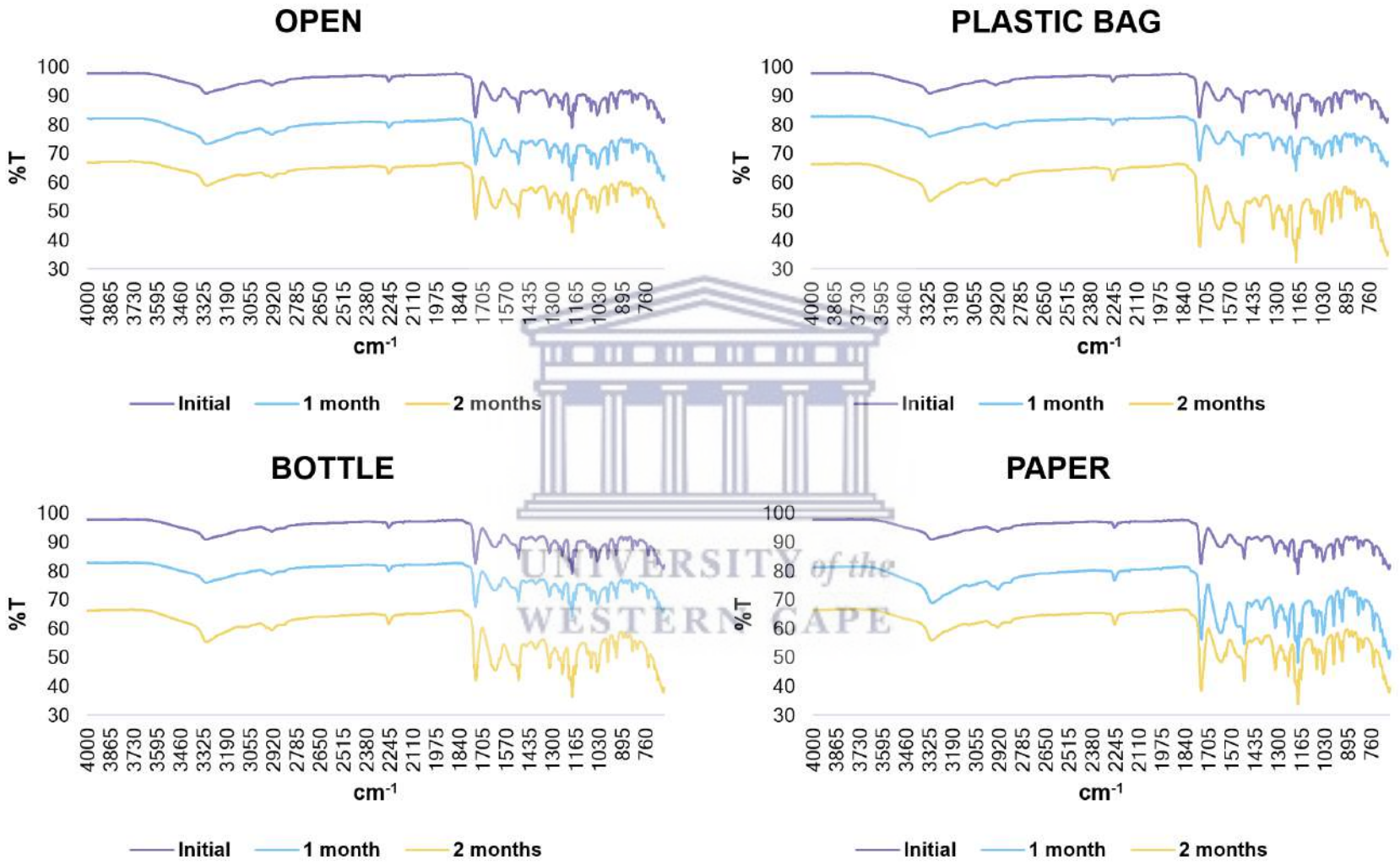

Figure A8: FT-IR spectra of the physical mixture of EP stored for 2 months at accelerated stability conditions of 40°C/75%RH in different storage containers.

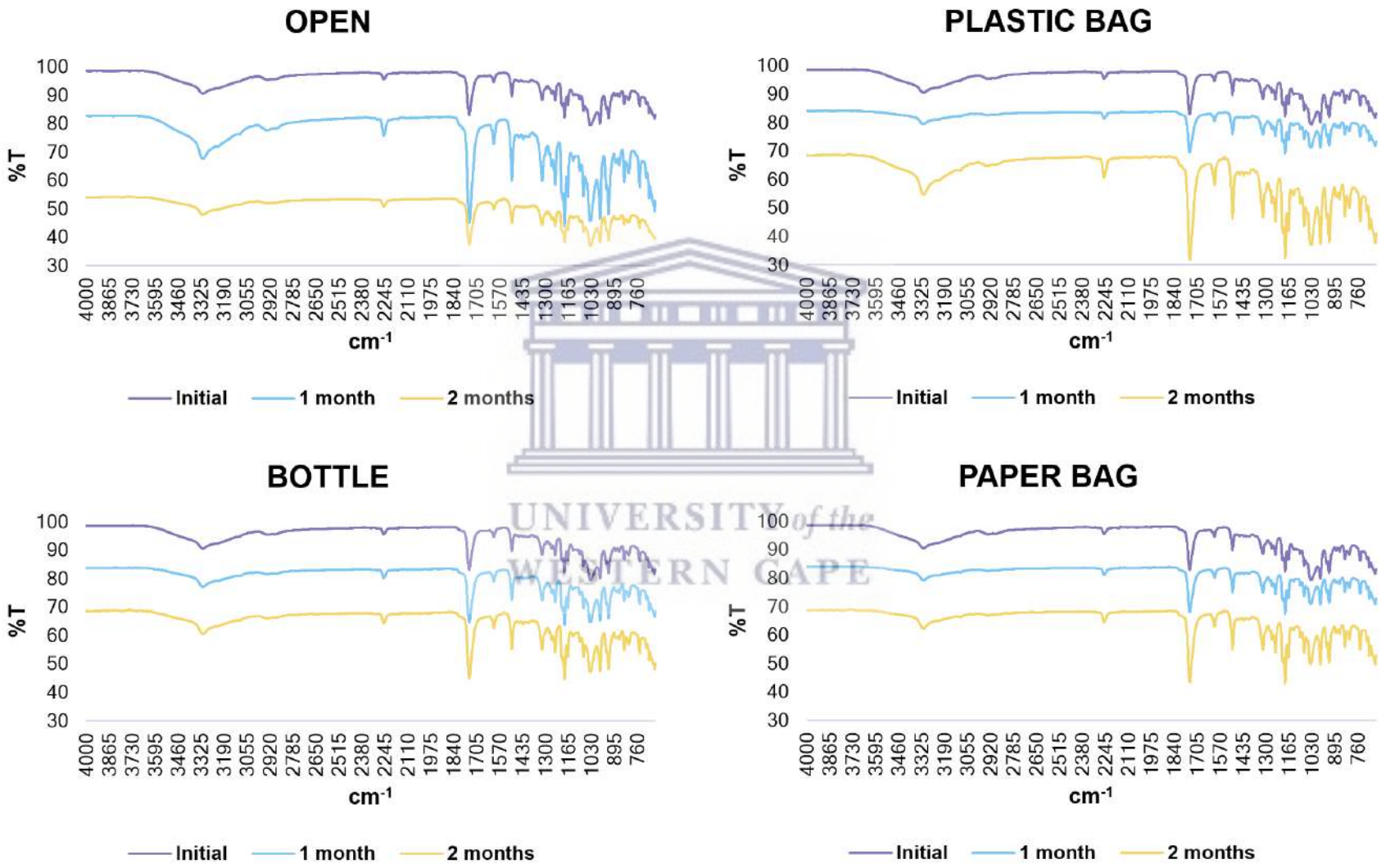

Figure A9: FT-IR spectra of the physical mixture of EI stored for 2 months at accelerated stability conditions of 40°C/75%RH in different storage containers.

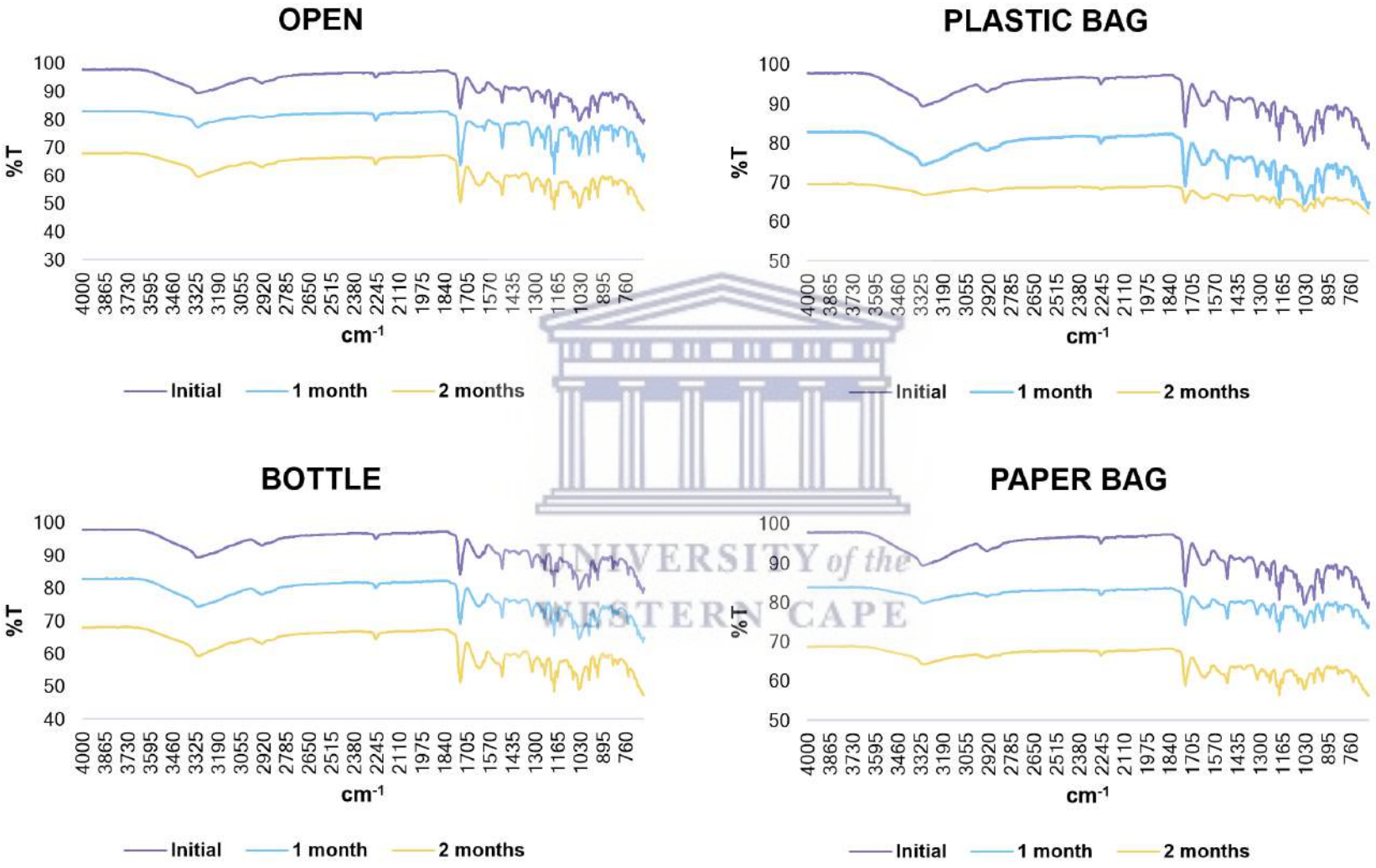

Figure A10: FT-IR spectra of the physical mixture of EPI stored for 2 months at accelerated stability conditions of 40°C/75%RH in different storage containers.

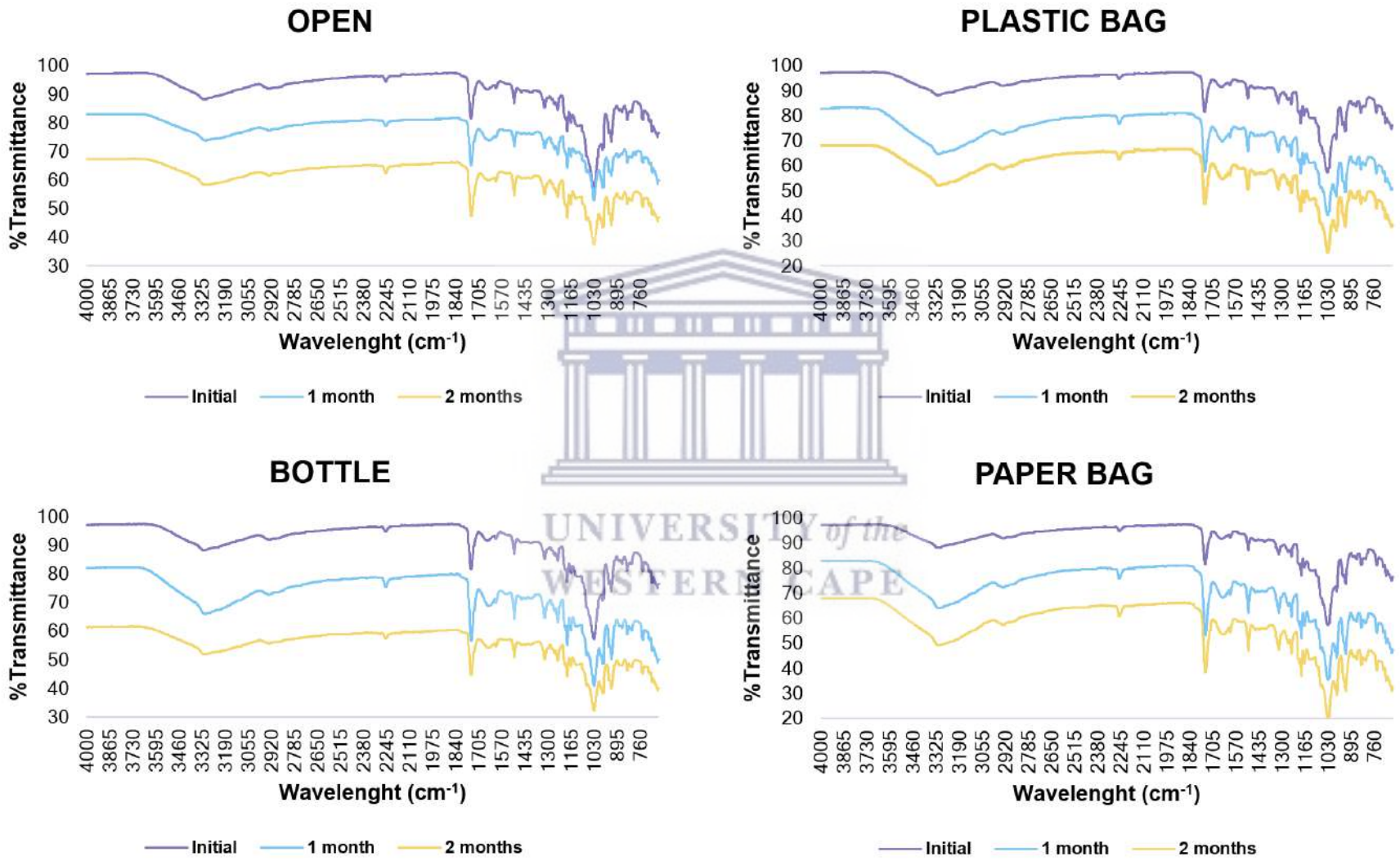

Figure A11: FT-IR spectra of spray-dried powder T10 stored for 2 months at accelerated stability conditions of 40°C/75%RH in different storage containers.

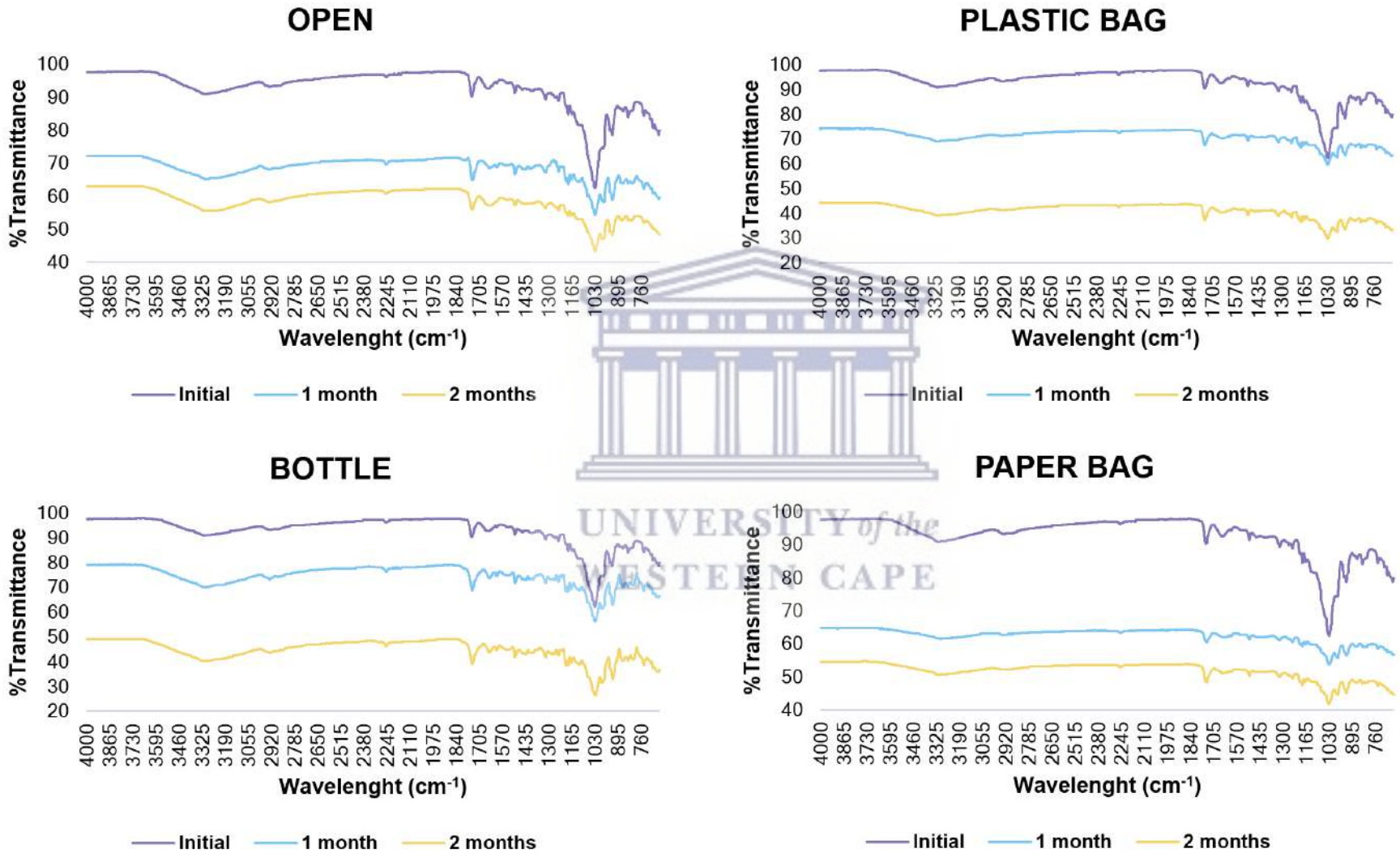

Figure A12: FT-IR spectra of spray-dried powder T19 stored for 2 months at accelerated stability conditions of 40°C/75% RH in different storage containers.

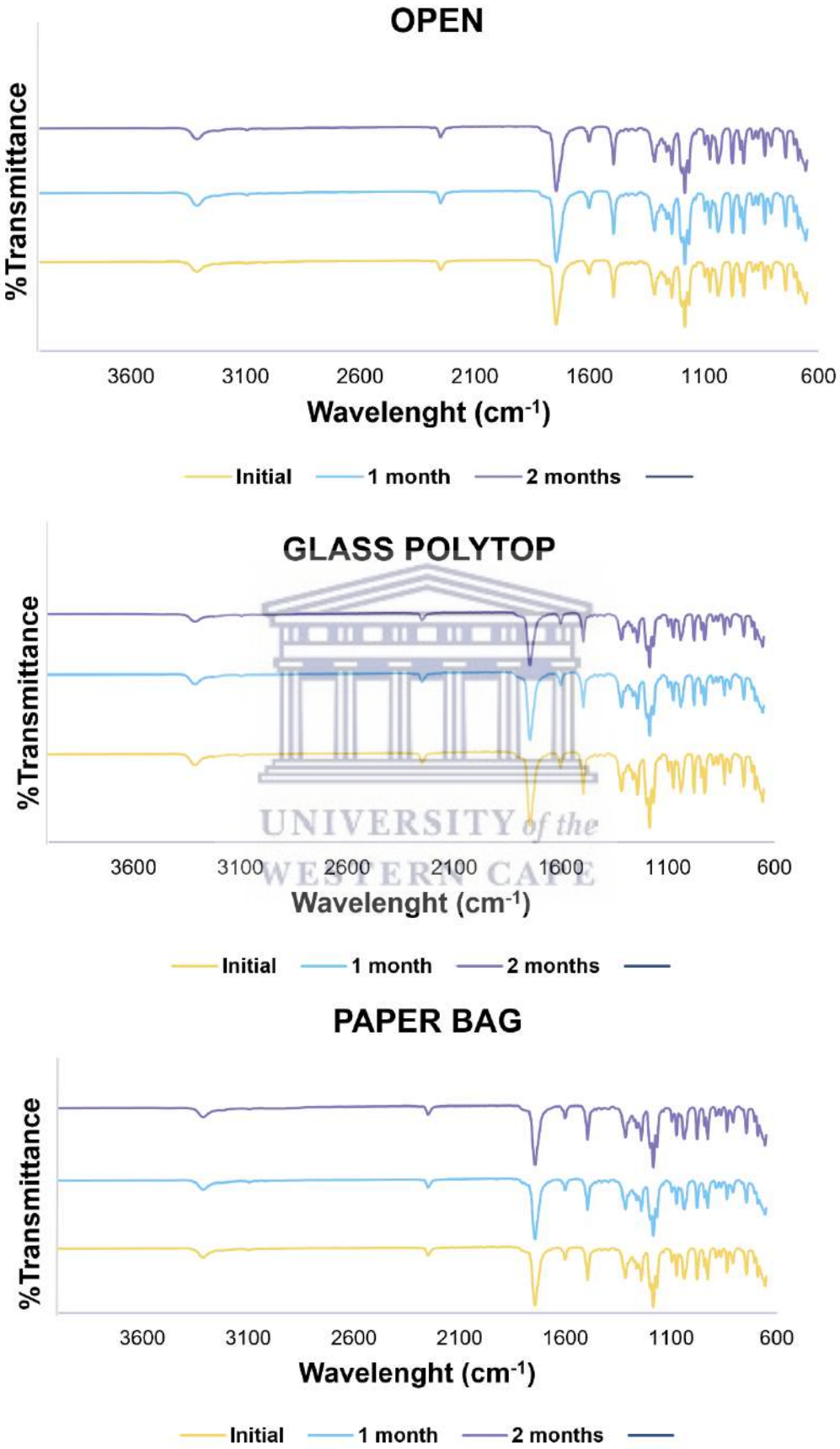

Figure A13: Overlay of FT-IR spectra for EFV raw material stored at 30°C/65% RH in different storage containers over a period of 2 months.

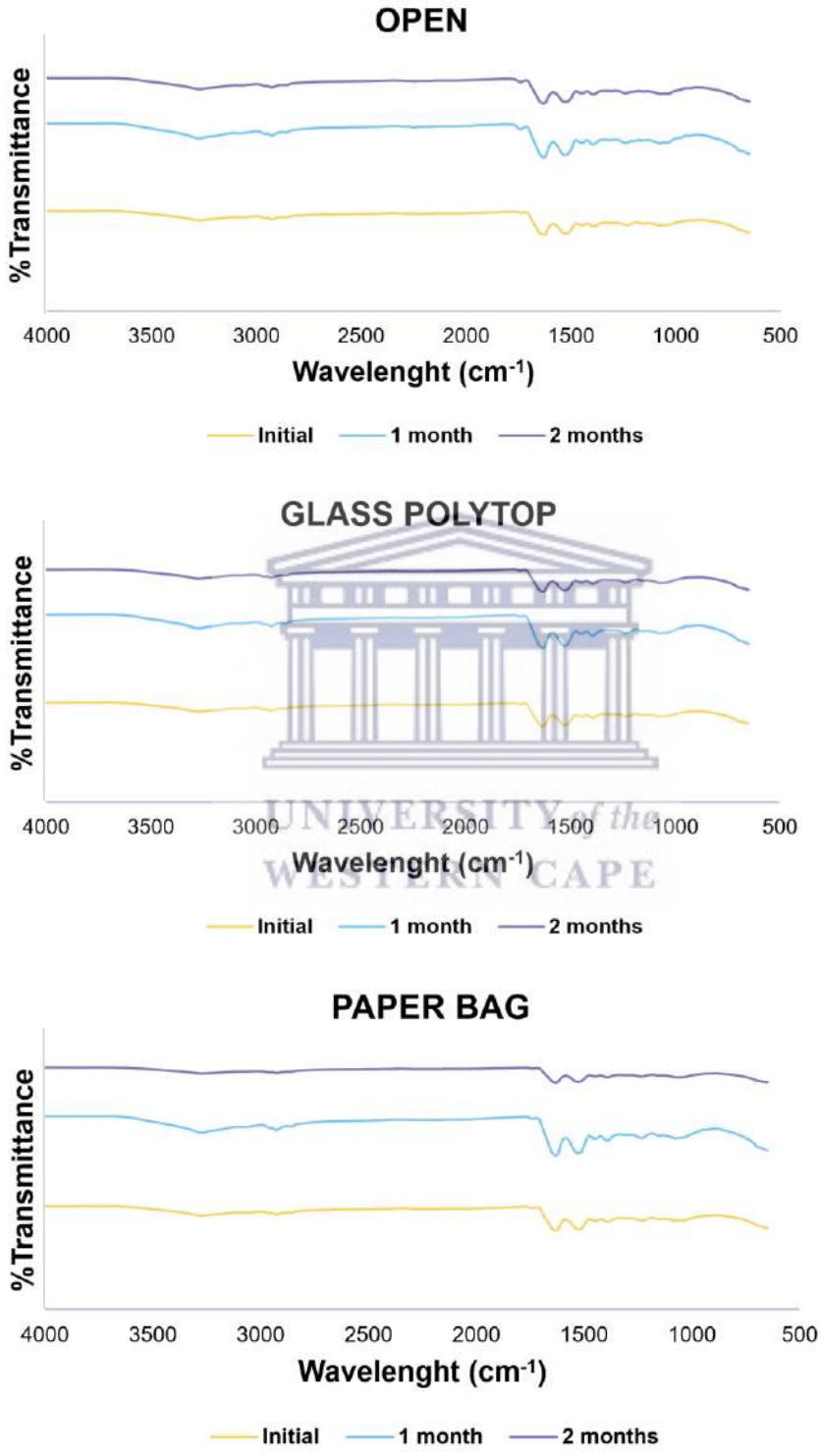

Figure A14: Overlay of FT-IR spectra for PPI raw material stored at 30°C/65% RH in different storage containers over a period of 2 months.

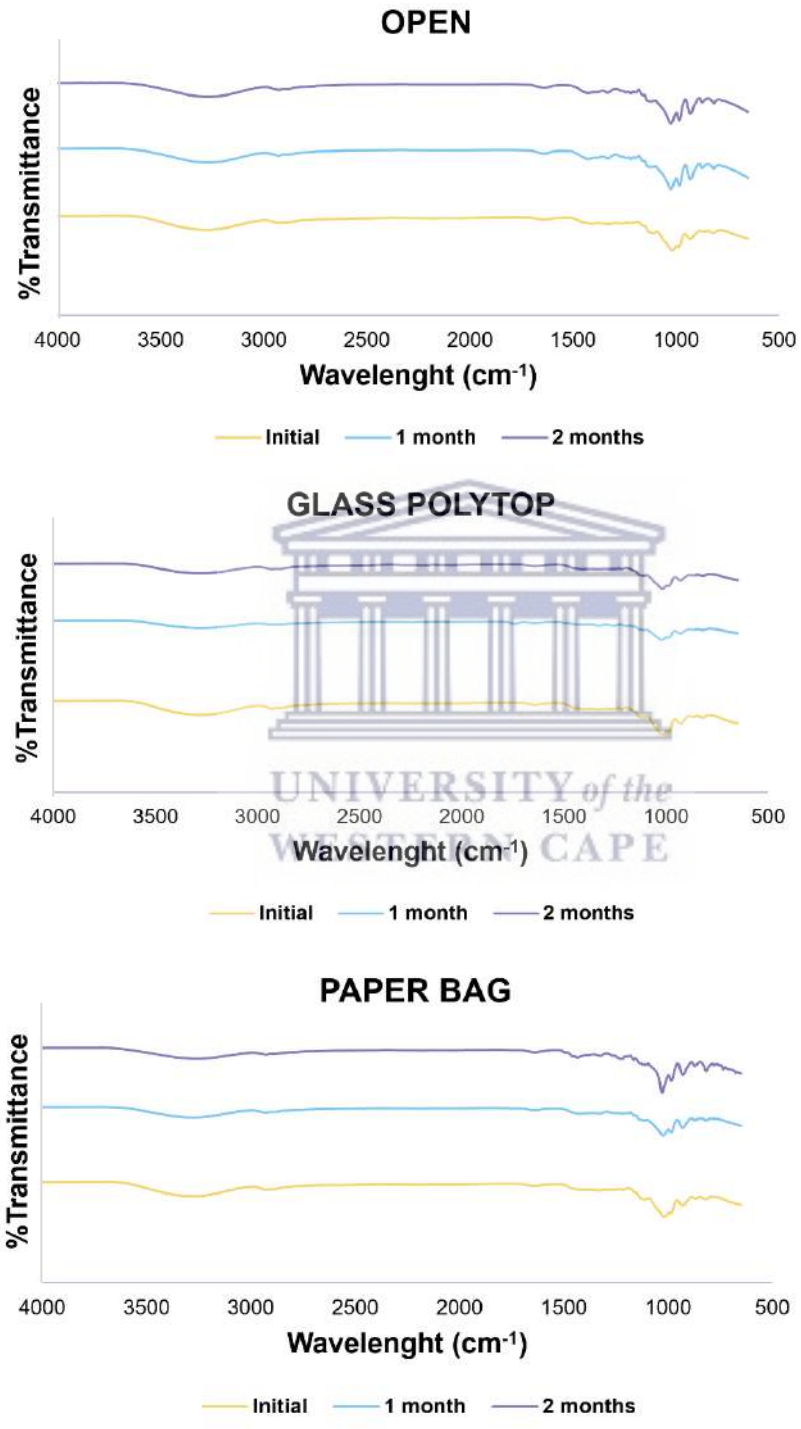

Figure A15: Overlay of FT-IR spectra for IN raw material stored at 30°C/65% RH in different storage containers over a period of 2 months.

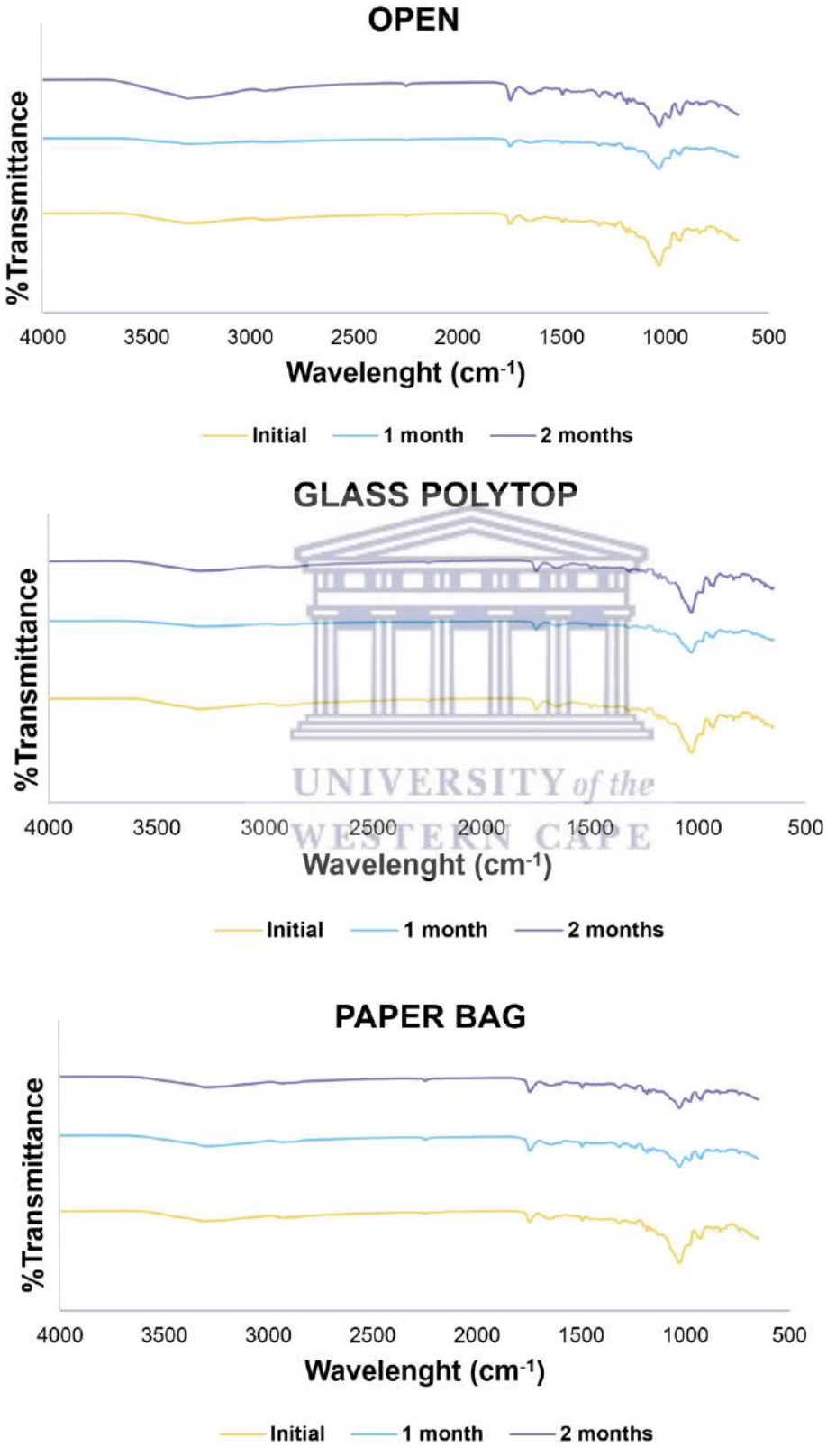

Figure A16: Overlay of FT-IR spectra for spray-dried T19 stored at 30°C/65% RH in different storage containers over a period of 2 months.

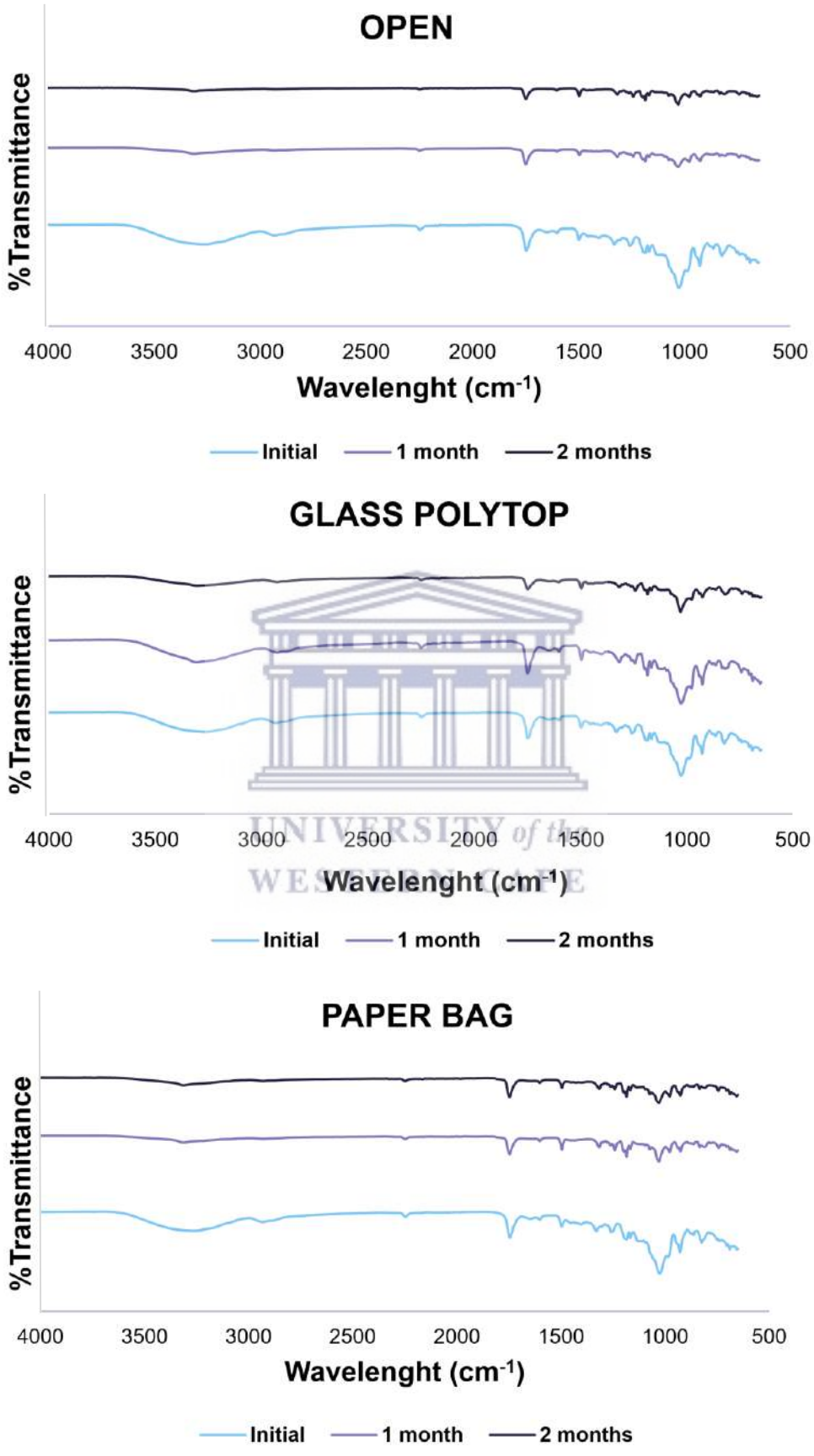

Figure A17: Overlay of FT-IR spectra for spray-dried T23 stored at 30°C/65% RH in different storage containers over a period of 2 months.

Figure A18: HSM micrographs showing the thermal behaviour of pure SA and the prepared alginate beads.

APPENDIX B

Paper submitted to Journal of Drug Delivery Science and Technology

Title: Using natural excipients to enhance the solubility of poorly water-soluble antiretroviral drug, efavirenz.

Authors: Marise Nel[1], Halima Samsodien[1], Marique Elizabeth Aucamp[1*]

Affiliations: [1]School of Pharmacy, Faculty of Science, University of the Western Cape, Cape Town, Bellville, 7353, South Africa

[*]**Corresponding author:** maucamp@uwc.ac.za, +27 219553229

Abstract

The anti-retroviral drug efavirenz (EFV) exhibits poor aqueous solubility which renders pharmaceutical formulation challenging. During a pre-formulation phase, involving spray drying of EFV for pediatric dosage form development, the combination of EFV with two natural excipients, pea protein isolate (PPI) and inulin (IN), was explored. In this study the effect of PPI and IN on the solubility of EFV became apparent, leading to an in-depth investigation. Equilibrium solubility studies were performed for different combinations of EFV, PPI and IN in distilled water and buffered solutions in the presence and absence of commonly used surfactants, Tween® 20 and sodium lauryl sulphate (SLS). In the combination of EFV and PPI, PPI significantly improved EFV solubility while in the combination of EFV and IN, EFV solubility was not affected significantly. In the combination of EFV, PPI and IN, a significant solubility improvement was noted, yet the degree of solubility improvement was less compared to the combination of only EFV and PPI. Further, the effects of PPI and IN on the solubility proves to be concentration related. It was concluded that PPI can be used as a functional excipient to improve EFV solubility, conversely IN can be used as a drug dissolution retardant and finally it was also concluded that it is crucial to optimize the ratio of drug to excipient to ensure optimal pharmaceutical formulation outcomes.

Keywords

Solubility, solubility enhancer, natural excipients, pre-formulation, efavirenz, powder wettability, inulin, pea protein isolate

Manuscript body

1. Introduction

Efavirenz (EFV) is an FDA approved non-nucleoside reverse transcriptase inhibitor with activity against HIV-1 (Adkins and Noble, 1998). EFV is classified as a BCS class II drug because of its low aqueous solubility (< 10 *μ*g/mL) and high membrane permeability (Rakhmanina and van den Anker, 2010). The low solubility of EFV limits the oral absorption and bioavailability of the drug and it renders the formulation of EFV difficult and suboptimal in most cases (Merisko-Liversidge and Liversidge, 2008). Over the last decade a magnitude of research has been done on improving the aqueous solubility of EFV. A few examples reported in literature include the use of nano-suspensions, polymer and cyclodextrin complexation, self-emulsifying drug delivery systems (SEDDS), drug loaded polymeric micelles, hydroxyethylcellulose (HEC) and polyacrylic acid (PAA) hydrogels as well as hot melt extrusion techniques (Chadha et al., 2012; Chiappetta et al., 2010; Mabrouk et al., 2015; Pawar et al., 2016; Reddy et al., 2014; Taneja et al., 2016). Most of these pre-formulation processes yielded EFV solubility improvement ranging 12 – 8250 fold. Despite the success of these processes, they are often complex, time-consuming and expensive. Another commonly used drug solubility enhancement technique is the use of surfactants such as sodium lauryl sulphate (SLS) and Tween® 20. Surfactants have long been used to improve the solubility of various chemical compounds by reducing the interfacial free energy on the surface. However, the chemical nature of surfactants have been associated with adverse effects (Rosen and Kunjappu, 2012). In recent years, focus has shifted to using more naturally occurring substances rather than harsh chemical ingredients as pharmaceutical excipients. Using natural ingredients as pharmaceutical excipients have many benefits over synthetic ones since they are biocompatible, biodegradable, cost-effective, available in abundance, non-toxic and generally regarded as safe (GRAS) for human consumption (Bhosale et al., 2014; Choudhary and Pawar, 2014). Using naturally-sourced ingredients have particular benefit for pharmaceutical products intended for the pediatric population owing to the safety and regulation of these ingredients. Additionally, natural ingredients also have economic advantages associated with manufacturing which becomes increasingly important when formulating medications for diseases prevalent in low-economic countries.

The effect that naturally sourced excipients, inulin (IN) and pea protein isolate (PPI) have on the solubility of EFV was investigated as part of the spray-drying optimization phase. Here, drug solubility enhancement showed to be a critical process parameter for formulation of an EFV

containing pediatric dosage form. The effect that IN and PPI exhibited on EFV aqueous solubility was also compared to the effect of two typical surfactants on EFV solubility.

2. Materials and methods

2.1 Materials

The active pharmaceutical ingredient, efavirenz (EFV), batch number IF-EF-190902 and pea protein isolate (PPI), batch number 3700D04034180040 was sourced from DB Fine Chemicals (Pty) Ltd., Rivonia, South Africa. Inulin (IN) with a degree of polymerisation > 10 was purchased from Savannah Fine Chemical (Pty) Ltd, Milnerton, Cape Town, South Africa. The purity of EFV raw material was confirmed in comparison to a World Health Organisation (WHO) reference standard (EFV REF), batch number 2.0, purchased from Stargate Scientific, Johannesburg, South Africa, with a certified purity of 99.8%. Chromatography grade acetonitrile was purchased from Labchem, Johannesburg, South Africa. Analytical grade formic acid, sodium lauryl sulphate (SLS) and Tween® 20 (Polysorbate 20) was purchased from Sigma Aldrich (Germany).

Finally, distilled water was obtained from a Mili-Q Elix® Essential 3 Water Purification System from Merck® (Johannesburg, South Africa) water purification system and ultrapure HPLC water with resistivity of 18.2 $M\Omega.cm^{-1}$ was obtained from a Lasec® (Johannesburg, South Africa) Purite laboratory water system.

2.2 Methods

2.2.1 Preparation of physical mixtures

Physical mixtures of EFV and IN (EI), EFV and PPI (EP) and finally EFV, PPI and IN (EPI) were prepared in the mass ratios of 1:4, 1:4 and 1:4:4, respectively. Compounds were weighed in the defined ratios and lightly grinded with a pestle in a mortar to achieve a homogenous powder mixture. Mixtures were stored in sealed glass containers until further analysis.

2.2.2 Hot stage microscopy (HSM)

During this study thermal events of samples were recorded using a real-time Olympus UC30 (Tokyo, Japan) camera fitted to an Olympus SZX-ILLB200 (Tokyo, Japan) polarised light microscope to which a Linkam THMS600/720 heating stage (Surrey, UK) was attached. The recorded micrographs were analysed using Stream Essentials software® (Olympus, Tokyo, Japan). For all HSM analyses small quantities of samples were place on a microscope slide.

2.2.3 Thermogravimetric analysis (TGA)

TGA analyses were done using a Perkin Elmer 4000 thermogravimetric system (Waltham, USA). Analyses were carried out under a nitrogen purge of 20 ml/min and a heating temperature range of 30 – 600°C using a heating rate of 10°C/min. The same heating program was used for all samples.

2.2.4 Differential scanning calorimetry (DSC)

A DSC 8000 Perkin Elmer instrument (Waltham, USA), incorporating an intra-cooling system was used to carry out all DSC analyses. Samples, weighing 2 – 4 mg, were sealed by crimping the aluminium pans with aluminium lids. The samples were heated at a heating rate of 10°C/min from 30 - 190°C. All analyses were performed under continuous dry nitrogen purging with a flow rate of 20 mL/min.

2.2.5 Fourier transform infrared (FTIR) spectroscopic analysis

FTIR spectra were obtained using a Perkin-Elmer (Waltham, USA) Spectrum 400 spectrometer. For each sample a spectrum was collected within the 650 – 4000 cm^{-1} range by placing a small amount of sample on the metal plate and applying between 50 and 60% force. Spectra were subsequently analysed for the absence or shift in the characteristic peak wave numbers.

2.2.6 Scanning electron microscopy (SEM)

SEM analysis of EFV, IN and PPI were done using an AURIGA Field Emission High-Resolution Scanning Electron Microscope (HRSEM), Zeiss (Germany). Powder samples were mounted onto aluminum stubs using carbon tape. The mounted samples were subsequently coated with a thin layer of gold-palladium. Accelerating voltage of 5 keV and a lament current of 2,359 A was used.

2.2.7 Powder X-ray diffraction (PXRD)

PXRD was used to confirm the solid-state form of EFV, PPI and IN. PXRD data was collected using a Bruker D8 Advance powder X-ray diffractometer (Karlsruhe, Germany). High voltage and current was set to 40 kV and 40 mA. All diffraction runs were performed at ambient temperature using a diffraction range of 4 – 40° 2θ.

2.2.8 Dynamic vapor sorption (DVS) analyses

Water sorption analyses were performed using the Q5000 vapor sorption analyzer (TA instruments, New Castle, USA). The following humidity-temperature program was preset:

temperature was controlled isothermally at 25°C with the first humidity ramp set from 0 – 90% RH. Subsequent desorption and adsorption phases were set to either range from 90 – 10% RH or 10 – 90 % RH, respectively. For each vapor sorption run, not more than 10 mg of sample was added to a metalized quartz sample holder. Each run started with a drying phase at 60°C for 60 min or until the weight fluctuation was less 0.0001%.

2.2.9 Powder contact angle measurements

For assessment of wettability, contact angle measurements were performed in triplicate using the static sessile drop method. A Krüss Drop Shape Analyzer DSA 25 (Hamburg, Germany) was used and all analyses were performed at ambient temperature. Approximately, a spatula tip amount of each powder sample was placed onto a clean microscope slide. A second slide was then placed on top and powder samples were subsequently pressed lightly between the two glass slides to obtain a level and uniform powder bed. A single drop of deionised water (5 μL) was deposited on the powder bed. The right (R) and left (L) contact angle was then measured within 5 seconds of the drop landing on the powder bed surface. Furthermore, the time taken for the water drop to absorb into the powder was also recorded. All measurements were performed in triplicate, three independent water drops and measurements were done on different areas of the same sample. The size of the contact angle and the time taken for the absorption of the water drop is inversely proportional to the degree of powder wettability (Bracco and Holst, 2013).

2.2.10 Equilibrium solubility studies

Equilibrium *in vitro* solubility testing of EFV was done in all bio-relevant media as well as in 1% v/v Tween® 20 and 1% w/v SLS buffer solutions. Aqueous buffered solutions at pH 1.2, 4.5, 6.8, and 7.2 were prepared according to the buffer solutions preparation guidelines as per the International Pharmacopoeia (World Health Organization, 2019). Solubility was done by adding an excess amount of EFV while controlling the amount of PPI to 6 mg/ml, to prevent filter clogging, and IN to 10 mg/ml to prevent gel formation. The combinations that were used in the solubility testing was (a) EFV, (b) EFV and IN (EI), (c) EFV and PPI (EP) and (d) EFV, PPI and IN (EPI). In addition, different concentrations of PPI were tested in the combination EP and different combinations of IN was tested in the combination EPI. For the combination EP the PPI concentrations tested were 6 mg/ml (EP (A)), 2 mg/ml (EP (B)) and 1 mg/ml (EP (C)). For the combination EPI the IN concentrations tested were 10 mg/ml (EPI (A)), 12 mg/ml (EPI (B)) and 24 mg/ml (EPI (C)). All combinations were tested in all relevant media as described above. Samples were agitated using a Grant-bio orbital shaker incubator ES-80 (Cambridge, UK)

maintained at 37.5 ± 0.5°C, set at a shaking speed of 180 rpm for a period of 24 h. Subsequently, samples were filtered using 0.22 μm nylon syringe filters and analyzed using an HPLC method described by Singh et al., (2013). For HPLC analysis a mobile phase consisting of 60% v/v chromatography grade acetonitrile and 40% v/v ultra-pure water containing formic acid (1% v/v) at a flow rate of 1 ml/min was used. A Phenomenex® Kinetex® (Torrance, CA, USA) C_{18}, 150 x 4.6 mm column was used as the stationary phase with a detection wavelength of 264 nm. The concentration EFV was quantified using an Azura® Knauer (Berlin, Germany) HPLC system equipped with an autosampler, quaternary pump, PDA detector and column temperature controller. All solubility measurements were done in triplicate.

2.2.11 Statistical analyses

One-way ANOVA statistical testing was used to calculate statistical significance observed in the solubility values. P values of ≤ 0.05 were considered significant.

3. Results

3.1 Thermal Analysis

HSM is considered the cornerstone of pharmaceutical thermal analyses, providing a visual aid to the interpretation of other common thermal techniques, such as TGA and DSC (Vitez et al., 1998). In this study it was important to ascertain the morphology of the EFV, PPI and IN as well as to confirm the specific solid-sate form of EFV. HSM micrographs (Figure 1 - inset) showed EFV to melt at 140°C and complete degradation was observed at 245°C, which was confirmed through TGA. Onset of degradation of IN and PPI was observed at ≈ 245°C and 313°C, respectively. No change in the degradation profiles were observed in any of the physical mixtures.

DSC analysis of crystalline EFV showed a single sharp endothermic peak at a temperature of 140.19°C with ΔH = 44.32 J/g (Figure 1). This temperature corresponds to the reported melting temperature of EFV Form I in literature (Fandaruff et al., 2014 (a); Wardhana et al., 2020). As depicted in Figure 1 (inset) which provides a zoomed scale section of the thermogram obtained with IN a glass transition temperature of 136.63°C and no other endothermic or exothermic peaks were observed. The melting endotherm of EFV was also observed in the physical mixtures of the drug in combination with the two excipients. DSC analysis of physical mixtures of EI (1:4 ratio), EP (1:4 ratio) and finally EPI (1:4:4 ratio) each showed a single endothermic peak at 139.60°C (ΔH = 6.14 J/g), 139.78°C (ΔH = 6.47 J/g) and 139.22°C (ΔH = 4.42 J/g), respectively thus also confirming that no incompatibility exists between EFV and the two excipients (Figure 2). Differences in the EFV endothermic peak size were solely attributed to the weight dependent decrease in the EFV concentration of EFV in the prepared mixtures.

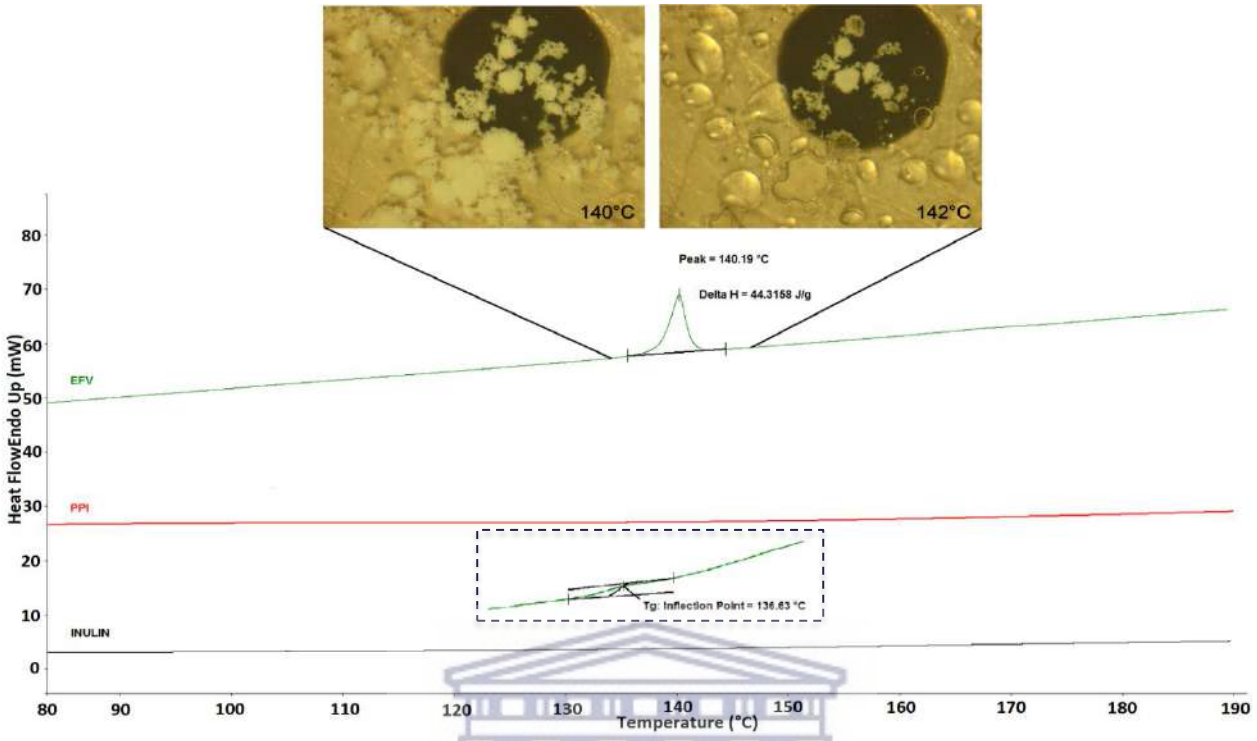

Figure 1: Overlay of DSC thermograms of EFV, PPI and IN collected at a heating range of 30 – 190°C with only the range of 80 – 190°C depicted. HSM micrographs, as an inset, for EFV captured at 140°C and 142°C are depicted as well as an inset depicting the glass transition temperature (T_g) observed for IN.

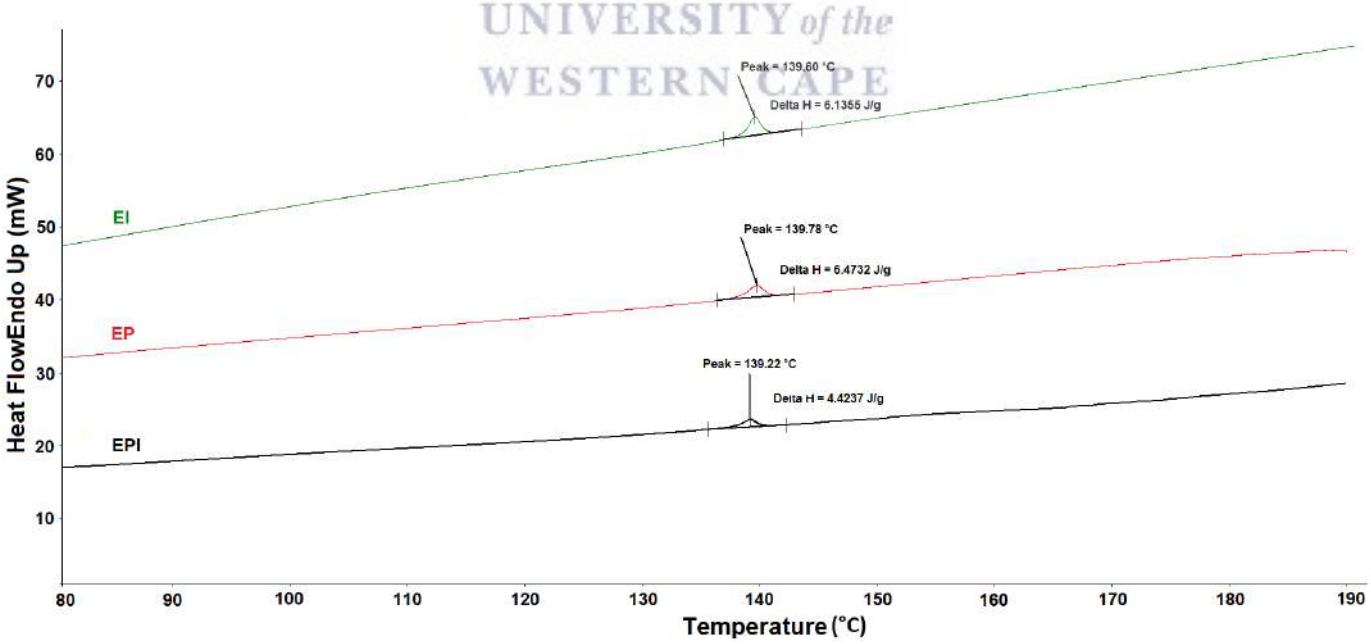

Figure 2: Overlay of DSC thermograms obtained for the physical mixtures of EFV and IN (EI), EFV and PPI (EP) and finally EFV, PPI and IN (EPI). Data collected at a heating range of 30 – 190°C with only the range of 80 – 190°C depicted.

3.2 Fourier transform infrared spectroscopy

FTIR spectroscopy is a commonly used technique applied to explore molecular conformations, detect alterations in the vibrational properties of a compound which can be brought into correlation with the molecular functional groups present in the compound. Chemical interactions between EFV and the excipients have the potential to change the molecular conformation, hydrogen bonding arrangements and crystal packing within the EFV crystalline structure, which could potentially influence other physio-chemical properties of the drug. EFV shows characteristic absorbance bands at 3315.3, 2251.6, 1745.2, 1601.4, and 1319.7 cm^{-1}, respectively attributed to N-H stretching, aromatic C-H stretching, C=O stretching, C=C stretching, and C-O-C stretching (Figure 3a). The obtained EFV spectrum is in accordance to what has been previously reported in literature (Fandaruff et al., 2014 (b)). IN shows a characteristic absorbance band at 3309.3 cm^{-1} which is related to the O-H groups in the IN structure (Fernandes et al., 2016). The spectrum collected from the PPI show characteristic bands at 3282.4, 2931.8, 1631.3, 1517.5, 1391.6, 1155 and 1063 cm^{-1}, respectively attributed to –OH contraction, C-H stretching, C=O stretching and the combination of N-H bending and C-N stretching in amide II and in amide III (Lan et al., 2019). FTIR spectroscopy was also used to confirm the compatibility of EFV with IN and PPI (Figure 3(b)). No significant peak shifts were observed in any of the physical mixtures of EFV and the excipients while characteristic EFV peaks were still observed in all physical mixtures.

3.3 Crystallinity and amorphicity of investigated compounds

Knowledge of the specific habit (i.e. crystalline or amorphous) of an API is crucial when developing a drug formulation. The physicochemical properties of an API is affected by different solid-state forms and therefore knowledge of the specific solid-state in which the API exists is necessary. It is well-known that EFV may exist in different solid-state forms and therefore the specific form had to be identified in order to conclude *in vitro* equilibrium solubility behaviour (Wardhana et al., 2020). SEM analysis revealed the typical organized stacked plate-like crystalline morphology of EFV Form I (Figure 4(a)). The solid state of EFV was confirmed to be crystalline using PXRD and consistent with Form I as reported by Wardhana et al. (2020) (Figure 4(a)). The particle morphology of IN and PPI was also investigated using SEM and solid-state habits of both which were confirmed to be amorphous using PXRD (Figure 4(b) and (c)). IN particles exhibited a smooth spherical morphology while PPI particles exhibited a more wrinkled appearance. This was in agreement with what has been reported in literature (Ronkart et al., 2007; Tamnak et al., 2016). It was also visually observed that there exists considerable particle size distribution between the PPI powder particles.

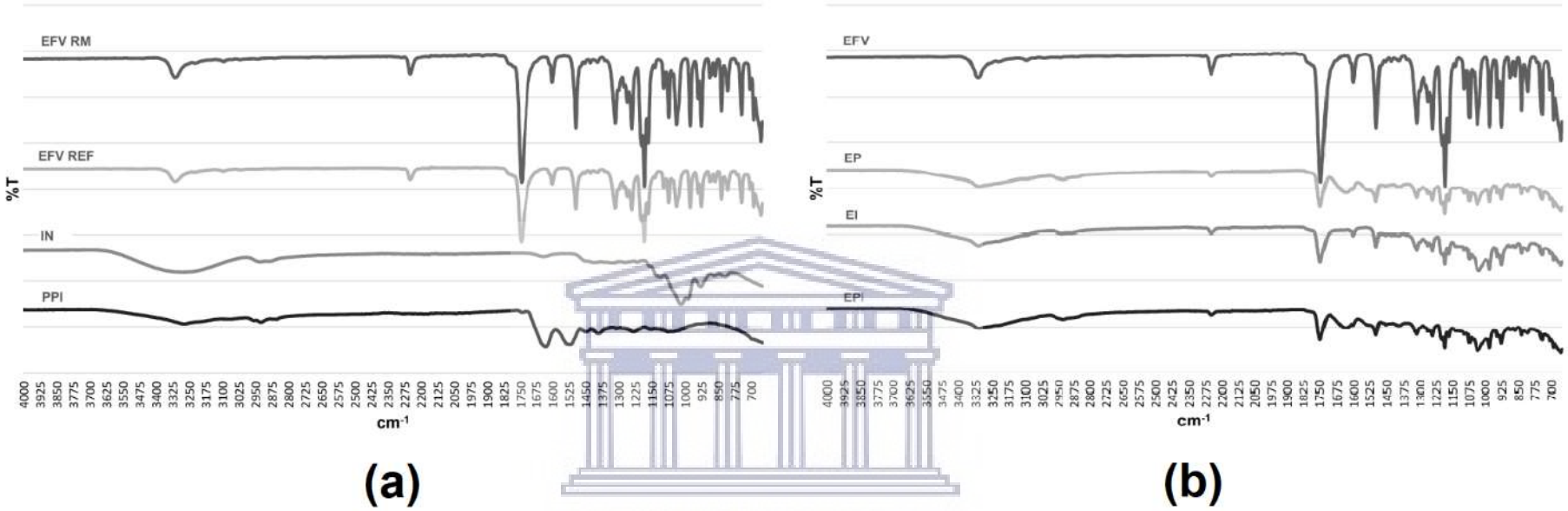

Figure 3: An overlay of FTIR spectra of (a) EFV RM (raw material), EFV REF (WHO reference drug), pure IN and PPI; and (b) EFV compared to physical mixtures of EFV and IN (EI), EFV and PPI (EP) and EFV, IN and PPI (EPI), collected at ambient temperature.

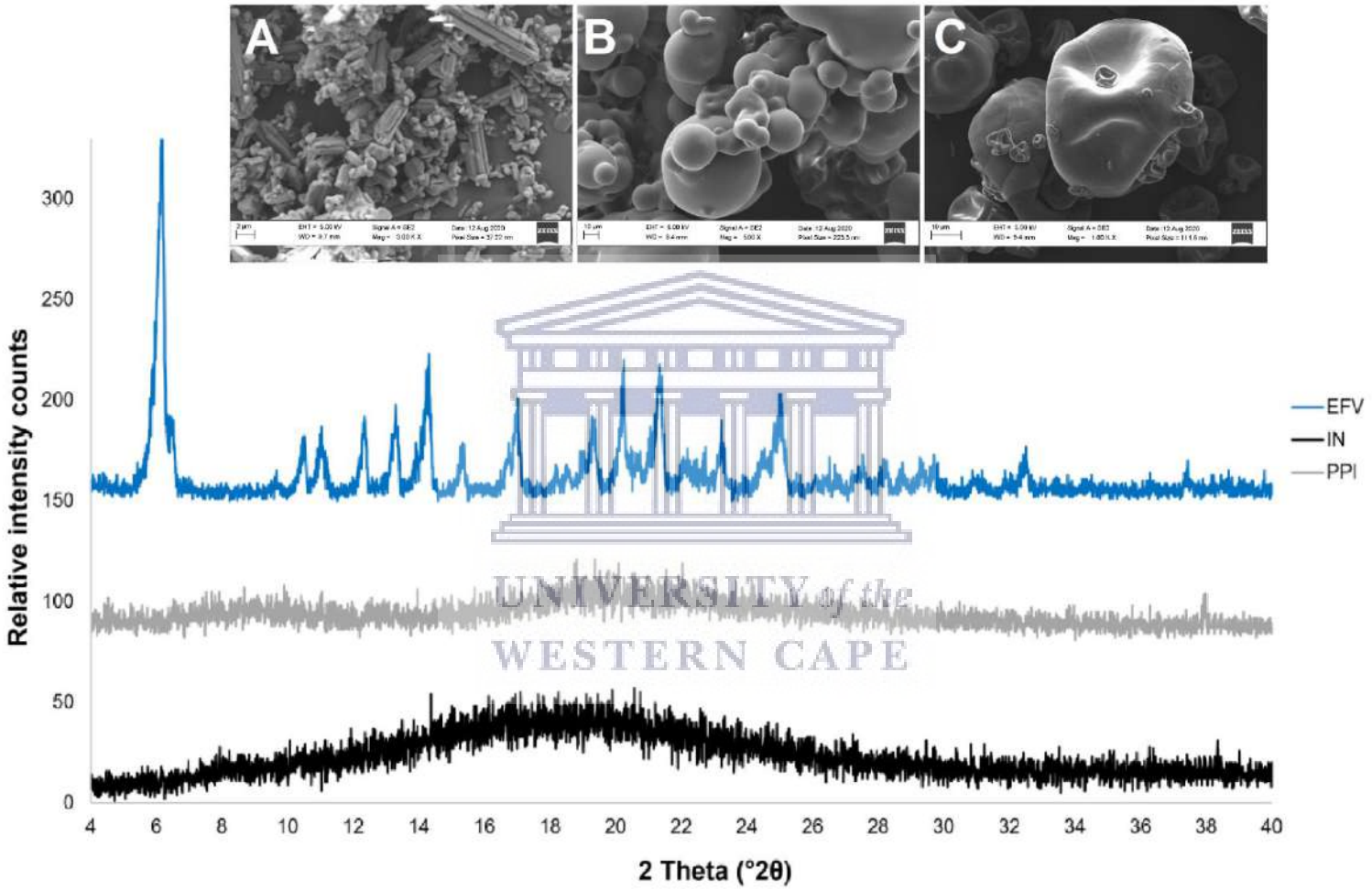

Figure 4: Overlay of PXRD patterns obtained for EFV, IN and PPI with (A) depicting the morphology of EFV observed through scanning electron micrograph (SEM) captured at 3, 000 X magnification, (B) pure IN at 5000 X magnification and (C) PPI at 1000 X magnification.

3.4 *In vitro* equilibrium solubility

One particularly important objective during pre-formulation studies, in particular microencapsulation *via* spray drying, is to optimize drug solubility (Alsenz and Kansy, 2007). The solubility of a compound is influenced by its inherent physicochemical properties. Establishing how the solubility of the drug is affected by proposed excipients can also guide the choice of excipients for optimal drug performance (Basalious et al., 2011; Vogt et al., 2008; Zarmpi et al., 2020). Here, the effect of the naturally-sourced excipients, IN and PPI, were investigated for their ability to enhance the solubility of EFV. This was compared to the effect that typical surfactants have on EFV solubility.

The aqueous solubility of EFV is very low in all biologically relevant media, ranging from pH 1.2 – 7.2 values (Table 1). Based on the pKa of EFV (pKa = 10.2), pH dependent solubility is expected with the greatest solubility (0.0036 ± 0.0005 mg/mL) observed at pH 4.5 while the lowest EFV solubility (0.0014 ± 0.00001 mg/mL) observed in distilled water. Compared to the solubility of EFV alone, the combination EI showed a non-significant 0.08 - 0.28-fold decrease in the aqueous solubility of EFV, except in distilled water, where there was a significant increase ($p = 0.00085$; $p<0.05$) in the aqueous solubility (Table 1). In contrast, the combination EP showed a significant solubility improvement in a range of 4.44 - 13.54-fold increase across the entire range of biological pH values as well as in distilled water. The large standard deviation observed in distilled water for the combination EP can be attributed to the poor aqueous solubility of EFV which is associated with small analytical response leading to high quantification variation. The combination EPI showed a significant solubility improvement in the range of 2.33 - 7.80-fold. However, this solubility improvement seen in the triple combination is significantly lower to the solubility improvement seen in the combination EP with the exception of pH 7.2 (Figure 5).

Surfactants are often used in pharmaceutical formulations to improve the solubility of drugs by increasing the wettability of these drugs. Two commonly used surfactants, SLS and Tween® 20, were also investigated for their ability to improve EFV solubility. EFV solubility in buffered solutions prepared with 1% w/v SLS showed a 30 – 640-fold improvement compared to the solubility determined in bio-relevant media, without the addition of any surfactants (Table 2). The greatest solubility increases were observed in distilled water (640-fold) and in pH 4.5 buffered solution (240-fold). The addition of Tween® 20 was also associated with a significant solubility improvement compared to the solutions with no surfactant or other excipients added (Table 2). EFV solubility in 1% v/v Tween® 20 showed 179 - 713 -fold improvement compared to the solubility in buffer only solutions. The greatest solubility increase was seen in distilled water (713-fold) while

the smallest increase was seen in pH 1.2 (179-fold). The degree of solubility improvement increases with increasing pH (Figure 6). For both SLS and Tween® 20 solutions, the greatest solubility increase was noted in distilled water. The degree of solubility improvement imposed by Tween® 20 is greater across the entire pH range when compared to SLS (Figure 6).

Since Tween® 20 had a greater effect on EFV, the solubility effect on EI, EP and EPI was also investigated to try and elucidate if a similar pattern could be observed as in the buffer only solutions. The combination EI showed a decrease in EFV solubility in distilled water, pH 6.8 and pH 7.2 while at pH 4.5 no change in solubility was seen and at pH 1.2 a 0.2-fold increase was observed (Table 3). Similar to the behavior seen in buffer only solutions, the combination EP showed significant improvements in solubility across the range of pH values (Figure 7). Interestingly however, the combination EPI showed a very different pattern in the 1% v/v Tween® 20 solutions when compared to the buffer only solutions. In the Tween® 20 solutions, and in the presence of both IN and PPI, the solubility of EFV decreased in all media except pH 4.5 buffered solution. This is in total contrast of the increased solubility seen in buffer only solutions.

To establish whether the excipients had a concentration related effect on the solubility of EFV two additional experiments were done. For the combination EP the amount of PPI added was reduced to 2 mg/mL (EP (B)) and then to 1 mg/mL (EP (C)) to evaluate the solubility effect. For the combination EPI the amount of IN added was increased to 12 mg/mL (EPI (B)) and 24 mg/mL (EPI (C)). In the combination EP there was a significant decrease in EFV solubility with decreasing amounts of PPI added (Table 4). When comparing EFV solubility in the presence of 6 mg/ml PPI (EP (A)) to that with 2 mg/mL PPI, a significant solubility decrease between 0.8-fold and 0.98-fold was noted across the entire pH range. Similarly, when the amount of PPI was reduced to 1 mg/ml a significant decrease in solubility ranging between 0.88-fold and 0.9-fold was noted across the pH range (Table 4, Figure 8). There were no significant EFV solubility differences between solutions containing 2 mg/mL and 1 mg/mL PPI. In the combination EPI a significant decrease in EFV solubility was noted with increasing amounts of IN compared to the solubility in the presence of 10 mg/mL (A). There was no significant difference in EFV solubility between solutions containing 12 mg/mL IN and 24 mg/mL IN (Table 5, Figure 9).

Overall, it can be said that combining EFV with IN does not significantly affect drug solubility while the combination of EFV and PPI results in increased drug solubility. However, the ability and efficiency of PPI to improve EFV solubility is dependent on the amount of PPI present in the solution and EFV solubility is not pH dependent. Thus the improved solubility can be directly linked to the effect of the excipient and not attributed to the physicochemical properties (pKa) of EFV.

3.5 Vapour sorption behaviour

Based on the equilibrium results as well as the physicochemical properties, specifically the morphology of EFV, PPI and IN, determining the wettability or ability of the compounds to attract water further corroborates the observed EFV solubility behaviour. Two recognized techniques for determining the wettability of compounds are water adsorption and particle contact angle. Few correlations exist between the techniques and each provide valuable information in its own right. The results generated from the two techniques are not quantitatively comparable but can however be qualitatively compared, to determine the relative, rather than absolute wettability of dry powders (Muster and Prestidge, 2005).

Contact angle measurements were done to inform the wettability of the dry powders in an effort to understand the observed solubility profiles. The greatest contact angles were observed for dry EPI (A) and EPI (C) powder whilst the smallest contact angles (which could not be measured due to instantaneous absorption of the water drop into the powder) was observed for the dry PPI and IN powder (Table 6). For the purpose of this study, we focused on the comparison to EFV only to gain information on the relative wettability of the powders compared to EFV. The combination EI exhibited a greater contact angle compared to EFV, suggesting poorer wettability of EI. The combinations EP (A) and EP (B) exhibited smaller contact angles compared to EFV, suggesting better wettability of these powder mixtures. In contrast, the combination EP (C) exhibited a greater contact angle compared to EFV, suggesting poorer wettability of EP (C). All three EPI combinations exhibited greater contact angles compared to EFV, suggesting poorer wettability of these powder mixtures. However, it is worthy to take into consideration the large standard deviation associated with the EFV contact angle measurements. When the largest contact angle recorded for EFV, 128.9°, is considered it can be said that EFV did exhibit the greatest contact angle of all powders tested thereby suggesting that EFV also exhibits the least wettability of all the powders. Further, it can then also be said that all powder combinations containing IN and/or PPI exhibited smaller contact angles compared to EFV and therefore does exhibit an improved wettability.

Dynamic vapour sorption (DVS) analysis was completed in complement to the contact angle measurements. DVS was performed on EFV, IN and PPI as single compounds as well as on all the physical mixtures in the various ratios used in the solubility studies. EFV exhibited a Type IV moisture sorption isotherm suggesting that vapour uptake is low at low vapour pressure followed by monolayer-multilayer adsorption (Muttakin et al., 2018). From the vapour sorption data EFV showed the smallest weight change (<0.1%) when exposed to increasing %RH conditions (Figure

10). PPI exhibited a typical Type V adsorption isotherm thus suggesting that initial moisture uptake is low followed by a rapid rise, ascribed to the hydrophilic nature of the PPI (Muttakin et al., 2018). In comparison with EFV and IN, PPI showed the greatest humidity related weight change of ≈ 5%. IN exhibited the second biggest humidity related weight change of ≈ 3% with a typical Type III isotherm, thus suggesting that vapour uptake is low at low relative humidity levels but with a sharp increase in adsorption activity should the relative humidity rise above 75% RH. All physical mixtures of EFV with IN and/or PPI was associated with greater RH-dependent weight changes compared to EFV only, suggesting improved wettability of the powder mixtures. Additionally, it was observed that the weight change of the powder in response to increasing %RH is directly proportional to the relative amount of PPI, with the greatest relative weight change seen in the powder containing the largest amount of PPI (EP (A); Figure 10). All three EPI mixtures, containing the same amounts of PPI, adsorbed similar amounts of vapour while all three EPI mixtures were associated with greater vapour uptake compared to EP samples (EPI (A), (B) and (C); Figure 10).

Table 1: Solubility values (in mg/mL) of efavirenz (EFV), EFV and inulin (EI), EFV and pea protein (EP) and EFV, PPI and IN (EPI) and the fold change in EFV solubility with respect to that of only EFV in distilled water and buffer solutions.

	Distilled water		pH 1.2		pH 4.5		pH 6.8		pH 7.2	
	Solubility[+] (mg/mL)	**Fold Increase**	**Solubility[+] (mg/mL)**	**Fold Increase**	**Solubility[+] (mg/mL)**	**Fold Increase**	**Solubility[+] (mg/mL)**	**Fold Increase**	**Solubility[+] (mg/mL)**	**Fold Increase**
EFV	0.0014	-	0.0028	-	0.0036	-	0.0032	-	0.0025	-
EI	0.0030	1.14*	0.0025	- 0.11	0.0033	-0.08	0.0025	-0.22	0.0018	-0.28
EP	0.0203	13.5*	0.0407	13.54*	0.0198	4.50*	0.0174	4.44*	0.0184	6.36*
EPI	0.011	6.86*	0.017	5.07*	0.012	2.33*	0.013	3.07*	0.022	7.80*

* indicates statistical significance with p< 0.05

[+]refer to Figure 5 for standard deviation

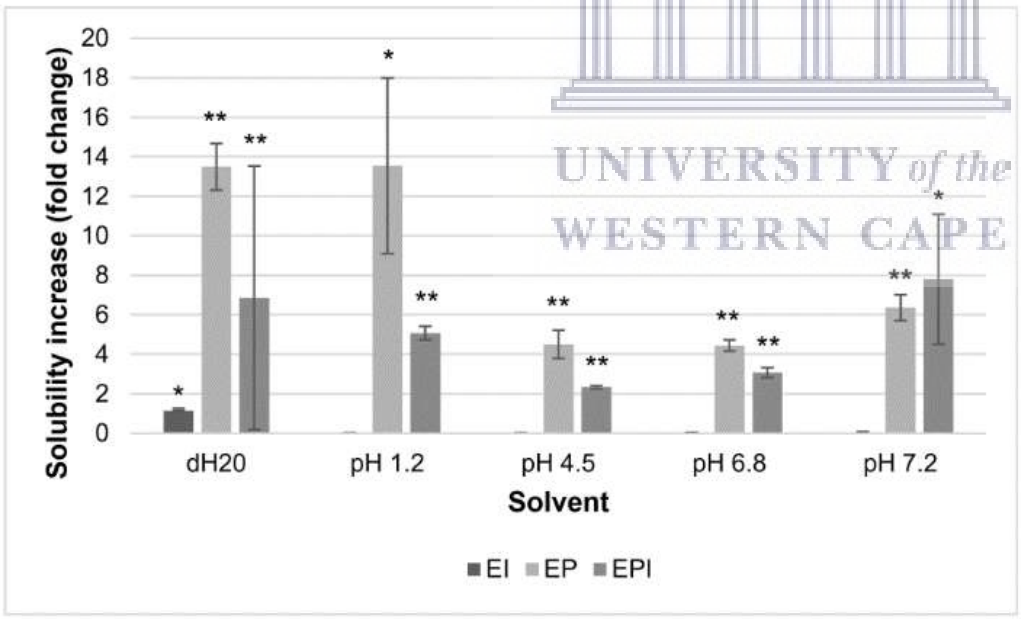

Figure 5: Fold change in the aqueous solubility of EFV as a result of the addition of IN and PPI to EFV. * indicates p value < 0.05; ** indicates p value < 0.005. Error bars show standard deviation.

Table 2: Solubility values (in mg/mL) of EFV in buffered media prepared with distilled water, 1% w/v SLS solutions and 1% v/v Tween® 20 solutions, and the fold increase in EFV solubility relative to that of EFV in the distilled water and normal buffers.

	Distilled water		pH 1.2		pH 4.5		pH 6.8		pH 7.2	
	Solubility [+] (mg/mL)	**Fold increase**	**Solubility [+] (mg/mL)**	**Fold increase**	**Solubility [+] (mg/mL)**	**Fold increase**	**Solubility [+] (mg/mL)**	**Fold increase**	**Solubility [+] (mg/mL)**	**Fold increase**
Distilled water	0.0014	-	0.0028	-	0.0036	-	0.0032	-	0.0025	-
1% w/v SLS	0.897	640*	0.103	37*	0.868	240*	0.171	53*	0.189	76*
1% v/v Tween®	1.00	713*	0.50	179*	0.66	182*	0.76	238*	1.12	448*

* indicates statistical significance with $p < 0.05$ [+]refer to Figure 6 for standard deviation

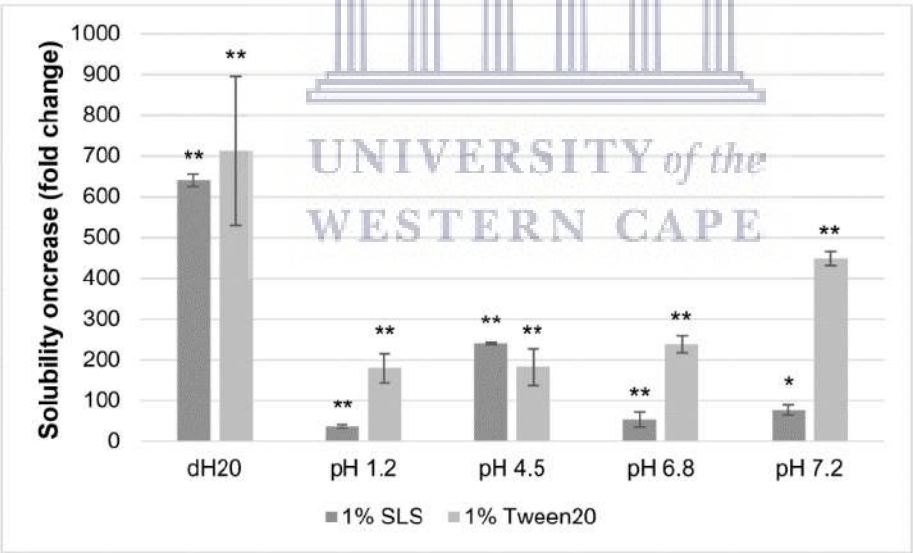

Figure 6: Fold increase in aqueous EFV solubility as a result of the use of surfactants 1% w/v SLS and 1% v/v Tween® 20.

* indicates p value < 0.05; ** indicates p value < 0.005. Error bars show standard deviation.

Table 3: Solubility values (in mg/mL) of EFV, EI, EP and EPI in buffered media prepared with 1% v/v Tween® 20 solutions, and the fold increase in EFV solubility relative to that of EFV only in the 1% v/v Tween® 20 solution.

	Distilled water		pH 1.2		pH 4.5		pH 6.8		pH 7.2	
	Solubility⁺ (mg/mL)	**Fold increase**	**Solubility⁺ (mg/mL)**	**Fold increase**	**Solubility⁺ (mg/mL)**	**Fold increase**	**Solubility⁺ (mg/mL)**	**Fold increase**	**Solubility⁺ (mg/mL)**	**Fold increase**
EFV	1.00	-	0.50	-	0.66	-	0.76	-	1.12	-
EI	0.92	-0.08	0.60	0.2	0.66	0	0.36	-0.5*	0.85	-0.24
EP	2.30	1.3*	2.12	3.2*	1.87	1.83*	1.10	0.4*	1.61	0.4*
EPI	0.42	-0.6	0.29	-0.4*	0.99	0.5	0.40	-0.5*	0.12	-0.9*

* Indicates statistical significance with p > 0.05

⁺refer to Figure 7 for standard deviation

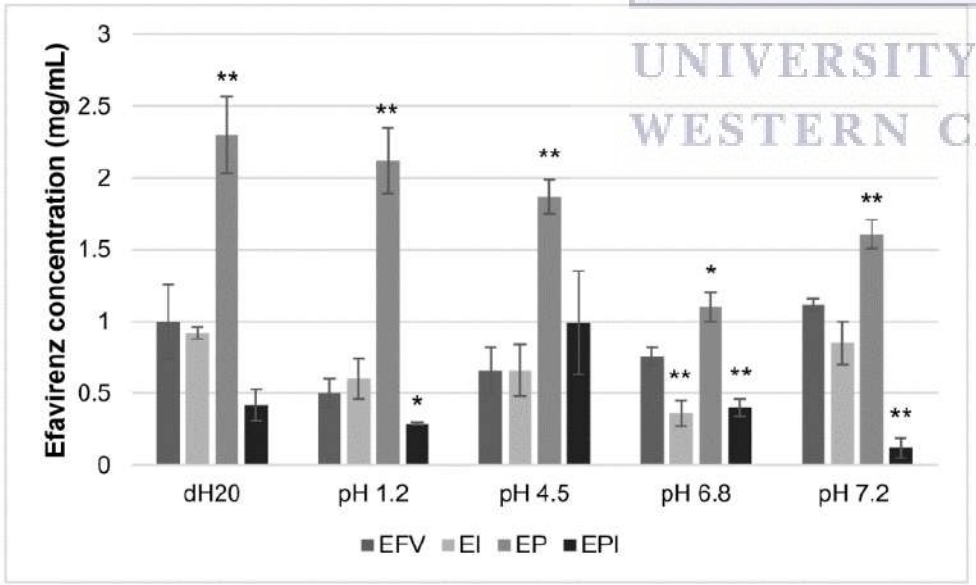

Figure 7: The effect of surfactant Tween® 20 on the aqueous solubility of EFV given as drug concentration (mg/mL) values measured at all bio-relevant pH values. * indicates p value < 0.05; ** indicates p value < 0.005. Error bars show standard deviation.

Table 4: Solubility values (in mg/mL) of EFV as a function of the PPI concentration added and the relative fold change in EFV solubility compared to the solubility in the presence of 6 mg/mL PPI solids.

	Distilled water		pH 1.2		pH 4.5		pH 6.8		pH 7.2	
	Solubility[+] (mg/mL)	**Fold increase**	**Solubility[+] (mg/mL)**	**Fold increase**	**Solubility[+] (mg/mL)**	**Fold increase**	**Solubility[+] (mg/mL)**	**Fold increase**	**Solubility[+] (mg/mL)**	**Fold increase**
EP (A) (6 mg/mL)	0.0203	-	0.0407	-	0.0198	-	0.0174	-	0.0184	-
EP (B) (2 mg/mL)	0.0027	-0.87*	0.001	-0.98*	0.0008	-0.96*	0.001	-0.94*	0.0019	-0.90*
EP (C) (1 mg/mL)	0.0024	-0.88*	0.001	-0.98*	0.001	-0.95*	0.0004	-0.98*	0.0004	-0.98*

*Indicates statistical significance with p > 0.05

[+]refer to Figure 8 for standard deviation

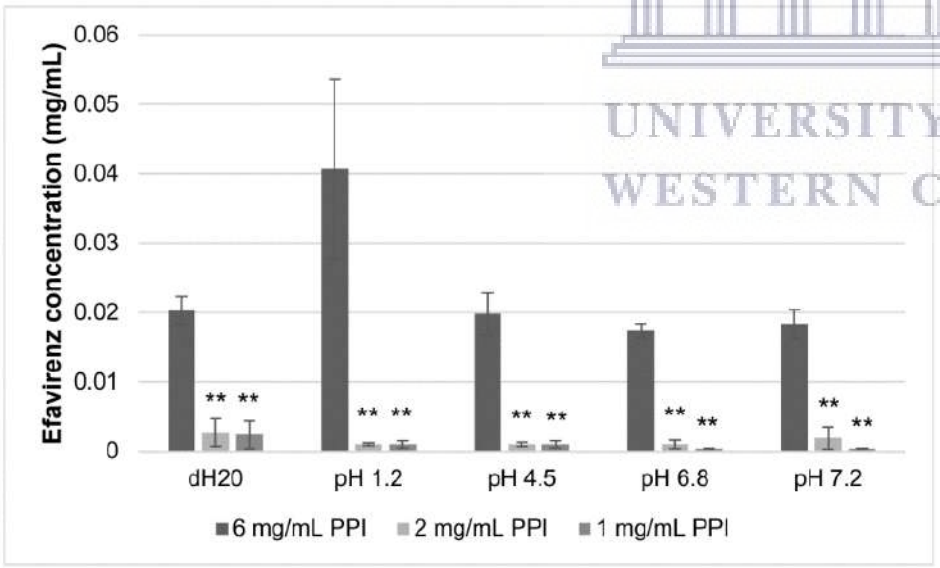

Figure 8: The effect that the concentration of added PPI have on the solubility of EFV (mg/mL). * indicates p value < 0.05; ** indicates p value < 0.005. Error bars show standard deviation.

Table 5: Solubility values (in mg/mL) of EFV as a function of the amount of IN added and the relative fold change in EFV solubility compared to the solubility in the presence of 10 mg/mL IN in the combination EFV, IN and PPI.

	Distilled water		pH 1.2		pH 4.5		pH 6.8		pH 7.2	
	Solubility[+] (mg/mL)	Fold increase	Solubility[+] (mg/mL)	Fold increase	Solubility[+] (mg/mL)	Fold increase	Solubility[+] (mg/mL)	Fold increase	Solubility[+] (mg/mL)	Fold increase
EPI (A) (10 mg/mL)	0.011	-	0.017	-	0.012	-	0.013	-	0.022	-
EPI (B) (12 mg/mL)	0.0013	-0.88*	0.001	-0.94*	0.001	-0.92*	0.0001	-0.99*	0.0004	-0.98*
EPI (C) (24 mg/mL)	0.0016	-0.85*	0.001	-0.94*	0.0006	-0.95*	0.0004	-0.97*	0.0003	-0.99*

*Indicates statistical significance with p > 0.05

[+]refer to Figure 9 for standard deviation

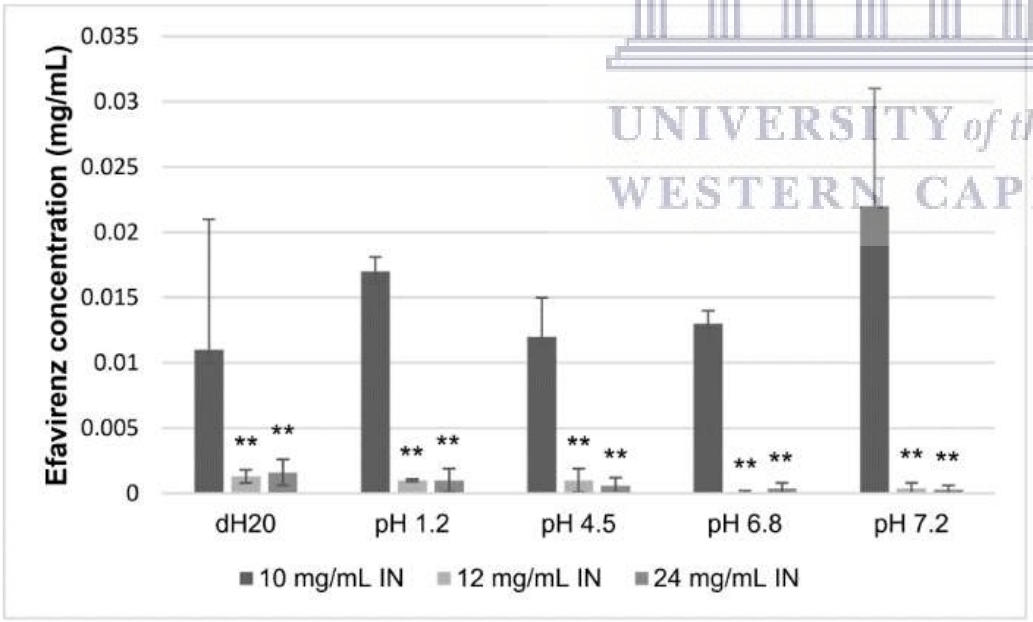

Figure 9: The effect that the amount of added IN solids have on the solubility of EFV (mg/mL). * indicates p value < 0.05; ** indicates p value < 0.005.

Table 6: Right- and left contact angle measurements obtained with the static sessile drop test performed on dry powders.

Powder description	Right contact angle (°)	Left contact angle (°)	Observation	Wettability characterisation
EFV	100.7 ± 22.36	100.7 ± 22.36	Drop stays	>90° - Non-wetting
PPI	-	-	Drop disappears within 3s	Perfect wetting
IN	-	-	Drop disappears within 3s	Perfect wetting
EI	105.6 ± 4.96	105.6 ± 4.96	Drop stays	>90° - Non-wetting
EP (A)	96.9 ± 0.47	96.9 ± 0.47	Drop absorbed t>30 s	Good wetting
EP (B)	90.6 ± 8.13	90.6 ± 8.13	Drop absorbed t>30 s	Good wetting
EP (C)	113 ± 3.87	113 ± 3.87	Drop stays	>90° - Non-wetting
EPI (A)	117.1 ± 5.51	117.1 ± 5.51	Drop stays	>90° - Non-wetting
EPI (B)	105.3 ± 3.67	105.3 ± 3.67	Drop stays	>90° - Non-wetting
EPI (C)	114.6 ± 3.2	114.6 ± 3.2	Drop stays	>90° - Non-wetting

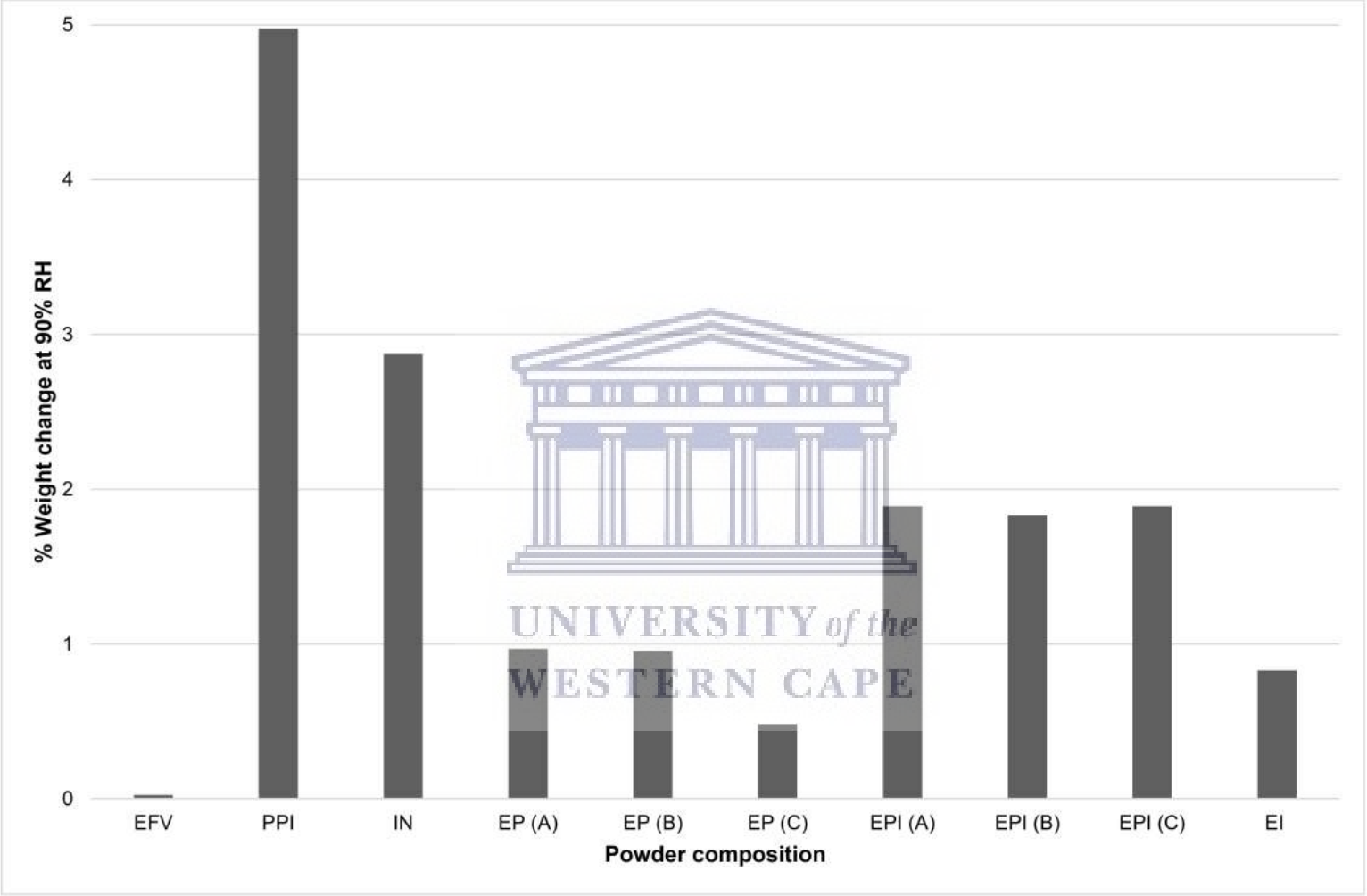

Figure 10: Percentage weight (%) change of powders observed after exposure to 0 - 90% relative humidity (RH) during dynamic vapour sorption analyses. Powders of EFV, PPI and IN as well as physical mixtures of EFV and PPI (EP A - C), EFV, PPI and IN (EPI A - C) and also EFV and IN (EI) were analyzed isothermally over a range of 0 – 90% RH. Only the data collected at 90% RH are shown here.

4. Discussion

The solubility of a drug compound is a critical determining factor for the dissolution and bioavailability of the drug. Low aqueous solubility is often associated with low drug bioavailability and suboptimal therapeutic outcomes (Kawabata et al., 2011; Pouton, 2006). There are many examples in literature where the solubility of EFV has successfully been improved via particle size reduction or supramolecular modifications such as co-crystal formation, complex formation and solid dispersions (Alves et al., 2014; Rajurkar et al., 2015; Sathigari et al., 2009; Taneja et al., 2016). These techniques often involve complex, expensive and time-consuming processing steps. The prospective of simply using excipients to improve drug solubility could mean lower input costs and faster dosage form production which ultimately mean more profit. Besides the financial advantage of using simplified strategies, the use of natural excipients provide an added benefit to drug formulations, especially with the recent "green-trend", even in the pharmaceutical industry.

The aqueous solubility of EFV was extremely low in distilled water and improved in buffered pH solutions (Table 1). The improved EFV solubility observed can potentially be attributed to the ion effect of the buffered solutions. Since EFV has a pKa of 10.2, it could be expected that the solubility of EFV should increase with increasing pH owing to a bigger ionized:unionized species ratio (Figure 5) (Pinto et al., 2014). However, the pattern observed here did not show this and therefore it can be assumed that the observed solubility improvement is not related to the pH of the solution but rather to the addition of the excipients.

IN is a natural polysaccharide that is biologically inert and non-toxic. Structurally, the hydroxyl groups of IN are able to interact with water molecules giving IN some potential surfactant activity. The polymerization degree of IN does influence the physiochemical properties of the polymer (Barclay et al., 2010). In this study the combination EI did significantly improve EFV solubility in distilled water but did not significantly affect the aqueous solubility of EFV in buffered solutions (Table 1; Figure 5). The fact that there was no solubility improvement in the buffered solutions could possibly be attributed to the large degree of polymerization of the IN batch used. Larger IN polymers, with degree of polymerization greater than 10, are known to be associated with limited solubility (Mensink et al., 2015). The same trend was observed in 1% v/v Tween® 20 solutions (Table 3, Figure 6).

The combination EP significantly improves the aqueous solubility of EFV in distilled water as well as in buffered solutions (Table 1, Figure 5). The exact mechanism involved is not clear but we are hypothesizing that the quaternary structure of the protein can refold to a degree and that this refolding can result in the protein "wrapping" around the EFV drug molecules. This potentially results in an altered surface interaction between the EFV and water molecules.

Proteins are known to have both hydrophilic and hydrophobic regions and therefore the hydrophilic regions associate with the water molecules thus attracting more water into the system. This was clearly observed from the DVS data (Figure 10) and contact angle measurements (Table 6) which showed that PPI improves the wettability of EFV. It is known that the PPI contains some dietary fibers such as cellulose. Cellulose fibers are well known for their ability to enhance drug solubility (Li et al., 2013; Wan et al., 2012). It may be that the cellulose fibers reduce the surface tension of EFV thereby improving its wettability and subsequently also its solubility. Furthermore, the isoelectric point (p*I*) for pea proteins are reported in the range 4.3 to 4.5, with greater protein solubility observed at pH values further away from the p*I* (Doan and Ghosh, 2019). This could explain why the biggest EFV solubility improvement for EP solutions was seen at pH 1.2 and the lowest solubility improvement at pH 4.5. The same pattern was observed in 1% v/v Tween® 20 solutions (Table 3, Figure 6). It was also noted that the amount of PPI added to the solubility mixture has a significant impact on the EFV solubility, illustrating the need for optimization of the API : excipient ratios during dosage form pre-formulation and formulation. The addition of 6 mg/mL PPI resulted in the greatest solubility improvement. The possibility that a greater EFV solubility can be achieved by adding more PPI exists. In fact, this possibility was investigated but the processing of the sample for HPLC quantification through centrifugation and filtering proved to be challenging.

The combination EPI also resulted in a significant improvement of the aqueous solubility of EFV, however this solubility improvement was to a lesser degree when compared to the combination of EP only. It seems as if IN has the ability to counteract the ability of PPI to improve the solubility of EFV. This may be due to the interaction between IN and PPI. Polysaccharides, such as inulin, are known to have the ability to help maintain the native conformation of proteins (Barclay et al., 2010). The possibility that the protein conformation is in a way stabilized by IN could mean that the protein can no longer unfold to the same degree and therefore the PPI may be less efficient in improving the solubility of EFV. The contrasting pattern seen in 1% v/v Tween® 20 solutions can be attributed to the fact that surfactants are known to promote the gelling of polymers (Kundu and Kundu, 2001; Prasad et al., 2005). Increased gelling of IN triggered by Tween® 20 could lead to increased stabilization of the protein conformation which inhibits its refolding. Decreased EFV solubility is subsequently achieved due to complete folding restriction and subsequent rigidification of protein quaternary structure.

Particles with high surface energies and subsequently good wettability are expected to exhibit relatively high-water adsorption rates, which should be reflected in higher values of water adsorbed. Muster and Prestidge (2005) observed a general trend of inverse correlation between amount of adsorbed water and the powder contact angle. This trend was not a perfect

one but it provided enough support for at least qualitative comparison of the results from the two techniques. In agreement with this, the general pattern observed here with contact angle of dry powders and relative amounts of water adsorbed provided some explanation of the aqueous solubility behaviour of EFV in combination with the two natural excipients investigated in this study. Since EFV proved to exhibit a high contact angle as well as adsorption of the least amount of water it can be concluded that EFV powder possesses the lowest overall wettability of the powders tested while PPI and IN powders had the best wettability. The lack of observed solubility improvement in the combination of EI correlates to the poor powder wettability, as seen with the large contact angle measurements. The greater water absorption by EI may be explained by other properties of IN, such as its gelling ability. The combinations EP (A) and EP (B) did improve the wettability compared to EFV alone as is evident from the contact angle and DVS results (Table 6, Figure 10). The reduced contact angle and greater degree of vapour uptake for EP (A) links with the improved solubility behaviour of this powder compared to EFV. While EP (B) and EP (C) exhibited no improved solubility, both were associated with higher vapour uptake and EP (B) was associated with reduced contact angle, while EP (C) was not. The smaller amount of PPI utilized in the preparation of EP (B) and EP (C) may have resulted in the powder mixtures not being truly homogenous as the protein amount is simply not enough to be distributed throughout the entire powder sample. Since contact angle measurements are performed on a small amount of dry powder it is possible that any non-perfect homogeneity may result in non-representative results. This may explain why a smaller contact angle was observed for EP (B) but not for EP (C) given that only a small spot of powder determines the contact angle. Further, it seems that there is a concentration related function of PPI when present in a powder mixture with greater amounts of PPI being associated with greater vapour adsorption. EP (B) powder adsorbed slightly less vapour while EP (C) adsorbed significantly less moisture compared to EP (A) linking to the lower solubility seen in these two mixtures. Overall the EPI combinations were associated with greater contact angles, yet exhibited more vapour uptake and greater solubility. Similar vapour adsorption was observed for all three EPI combinations, while EPI (A) exhibited the greatest contact angle. From Figure 10 it can be suggested that the amount of IN present in the reaction mixture does not change the relative amount of vapour adsorbed, but the mere presence of IN does seem to be associated with some degree of vapour uptake as all EPI samples were associated with more vapour sorption compared to EP. The specific vapour adsorption behaviours of these powders, gathered from the DVS isotherm shapes (results not shown), show that vapour adsoprtion by IN is mostly at high %RH conditions while PPI starts adsorbing vapour at lower %RH. This correlates to the relative contributions of IN and PPI to improving solubility of EFV, which is determined at 37.5°C. Overall, some correlations were evident, yet neither contact angle nor vapour sorption analysis exhited a

near perfect correlation with the solubility behaviour observed. Failure to identify correlations between solubility data, contact angle and vapour sorption results could also potentially be attributed to differences in temperature used to conduct the different tests as well as absolute volume of water present in each analysis.

Using *in silico* modelling to predict the three-dimensional interaction between EFV, PPI and IN may provide valuable insight into the mechanism at hand (Piñero et al., 2018). The field of *in silico* modelling is a rapidly evolving one and in the years to come it will provide even more valuable supporting evidence for speculations such as ones made here. Computational approaches could enable fast and cost-effective analysis of drug-excipient interactions (Das et al., 2020). However, the generation of more data like the data presented here is necessary in order to build robust computational systems for future predictions.

5. Conclusion

Many active pharmaceutical agents (> 40%) are poorly water-soluble and are often the source of formulation related difficulties (Merisko-Liversidge and Liversidge, 2008). Here, we explored the potential use of natural excipients, PPI and IN, to improve the solubility of the poorly water-soluble ARV, EFV. The results showed that PPI can be used to improve the solubility of EFV significantly without the use of harmful surfactants. This study was initially conducted as part of a pre-formulation process development phase, but the data generated illustrates the importance of a simple strategy such as adding natural and cost-effective excipients for improving drug solubility.

6. Funding Statement

The authors would like to thank the Royal Society/African Academy of Science (AAS) - FLAIR Fellowship, grant number: FLR\R1\191360 and the National Research Foundation (Grant no. MND190614447631) for funding this research as well as for their support.

7. Conflict of interest statement

The authors report no conflicts of interest regarding this manuscript.

8. Acknowledgements

The authors would like to thank Prof. Baker from SensorLab-UWC for her assistance in performing the contact angle measurements.

9. References

Adkins, J.C., Noble, S., 1998. Efavirenz. Drugs 56, 1055–1064. https://doi.org/10.2165/00003495-199856060-00014.

Alsenz, J., Kansy, M., 2007. High throughput solubility measurement in drug discovery and development. Adv. Drug Deliv. Rev. 59, 546–567. https://doi.org/10.1016/j.addr.2007.05.007.

Alves, L.D.S., De La Roca Soares, M.F., De Albuquerque, C.T., Da Silva, É.R., Vieira, A.C.C., Fontes, D.A.F., Figueirêdo, C.B.M., Soares Sobrinho, J.L., Rolim Neto, P.J., 2014. Solid dispersion of efavirenz in PVP K-30 by conventional solvent and kneading methods.

Carbohydr. Polym. 104, 166–174. https://doi.org/10.1016/j.carbpol.2014.01.027.

Barclay, T., Ginic-Markovic, M., Cooper, P., Petrovsky, N., 2010. Inulin - A versatile polysaccharide with multiple pharmaceutical and food chemical uses. J. Excipients Food Chem. 1, 27–50.

Basalious, E.B., El-Sebaie, W., El-Gazayerly, O., 2011. Application of pharmaceutical QbD for enhancement of the solubility and dissolution of a class II BCS drug using polymeric surfactants and crystallization inhibitors: Development of controlled-release tablets. AAPS PharmSciTech 12, 799–810. https://doi.org/10.1208/s12249-011-9646-6.

Bhosale, R.R., Osmani, R.A.M., Moin, A., 2014. Natural gums and mucilages: A review on multifaceted excipients in pharmaceutical science and research. Int. J. Pharmacogn. Phytochem. Res. 6, 901–912.

Bracco, G., Holst, B., 2013. Contact angle and wetting properties, in: Surface Science Techniques. pp. 3–34. https://doi.org/10.1007/978-3-642-34243-1.

Chadha, R., Arora, P., Bhandari, S., Jain, D.V.S., 2012. Effect of hydrophilic polymer on complexing efficiency of cyclodextrins towards efavirenz-characterization and thermodynamic parameters. J. Incl. Phenom. Macrocycl. Chem. 72, 275–287. https://doi.org/10.1007/s10847-011-9972-z.

Chiappetta, D.A., Hocht, C., Sosnik, A., 2010. A Highly Concentrated and Taste-Improved Aqueous Formulation of Efavirenz for a More Appropriate Pediatric Management of the Anti-HIV Therapy. Curr. HIV Res. 8, 223–231. https://doi.org/10.2174/157016210791111142.

Choudhary, P.D., Pawar, H.A., 2014. Recently Investigated Natural Gums and Mucilages as Pharmaceutical Excipients: An Overview. J. Pharm. 2014, 1–9. https://doi.org/10.1155/2014/204849.

Das, T., Mehta, C.H., Nayak, U.Y., 2020. Multiple approaches for achieving drug solubility: an in silico perspective. Drug Discov. Today 25, 1206–1212. https://doi.org/10.1016/j.drudis.2020.04.016.

Doan, C.D., Ghosh, S., 2019. Formation and stability of pea proteins nanoparticles using ethanol-induced desolvation. Nanomaterials 9. https://doi.org/10.3390/nano9070949.

Fandaruff, C., Araya-Sibaja, A.M., Pereira, R.N., Hoffmeister, C.R.D., Rocha, H.V.A., Silva, M.A.S., 2014. Thermal behavior and decomposition kinetics of efavirenz under isothermal and non-isothermal conditions. J. Therm. Anal. Calorim. 115, 2351–2356. https://doi.org/10.1007/s10973-013-3306-x. (a)

Fandaruff, C, Rauber, G.S., Araya-Sibaja, A.M., Pereira, R.N., De Campos, C.E.M., Rocha, H.V.A., Monti, G.A., Malaspina, T., Silva, M.A.S., Cuffini, S.L., 2014. Polymorphism of anti-HIV drug efavirenz: Investigations on thermodynamic and dissolution properties. Cryst. Growth Des. 14, 4968–4975. https://doi.org/10.1021/cg500509c. (b)

Fares, M.M., Salem, M.S., Khanfar, M., 2011. Inulin and poly(acrylic acid) grafted inulin for dissolution enhancement and preliminary controlled release of poorly water-soluble Irbesartan drug. Int. J. Pharm. 410, 206–211. https://doi.org/10.1016/j.ijpharm.2011.03.029.

Fernandes, R.V. de B., Botrel, D.A., Silva, E.K., Borges, S.V., Oliveira, C.R. de, Yoshida, M.I., Feitosa, J.P. de A., de Paula, R.C.M., 2016. Cashew gum and inulin: New alternative for ginger essential oil microencapsulation. Carbohydr. Polym. 153, 133–142. https://doi.org/10.1016/j.carbpol.2016.07.096.

G Rajurkar, V., Sunil, N.A., Ghawate, V., 2015. Tablet Formulation and Enhancement of Aqueous Solubility of Efavirenz by Solvent Evaporation Co-Crystal Technique. Med. Chem. (Los. Angeles). 08. https://doi.org/10.4172/2161-0444.1000002.

Kawabata, Y., Wada, K., Nakatani, M., Yamada, S., Onoue, S., 2011. Formulation design for poorly water-soluble drugs based on biopharmaceutics classification system: Basic

approaches and practical applications. Int. J. Pharm. 420, 1–10. https://doi.org/10.1016/j.ijpharm.2011.08.032.

Kundu, P.P., Kundu, M., 2001. Effect of salts and surfactant and their doses on the gelation of extremely dilute solutions of methyl cellulose. Polymer (Guildf). 42, 2015–2020. https://doi.org/10.1016/S0032-3861(00)00506-1.

Lan, Y., Xu, M., Ohm, J.B., Chen, B., Rao, J., 2019. Solid dispersion-based spray-drying improves solubility and mitigates beany flavour of pea protein isolate. Food Chem. 278, 665–673. https://doi.org/10.1016/j.foodchem.2018.11.074.

Li, B., Konecke, S., Wegiel, L.A., Taylor, L.S., Edgar, K.J., 2013. Both solubility and chemical stability of curcumin are enhanced by solid dispersion in cellulose derivative matrices. Carbohydr. Polym. 98, 1108–1116. https://doi.org/10.1016/j.carbpol.2013.07.017.

Mabrouk, M., Chejara, D.R., Mulla, J.A.S., Badhe, R. V., Choonara, Y.E., Kumar, P., Du Toit, L.C., Pillay, V., 2015. Design of a novel crosslinked HEC-PAA porous hydrogel composite for dissolution rate and solubility enhancement of efavirenz. Int. J. Pharm. 490, 429–437. https://doi.org/10.1016/j.ijpharm.2015.05.082.

Mensink, M.A., Frijlink, H.W., Van Der Voort Maarschalk, K., Hinrichs, W.L.J., 2015. Inulin, a flexible oligosaccharide. II: Review of its pharmaceutical applications. Carbohydr. Polym. 134, 418–428. https://doi.org/10.1016/j.carbpol.2015.08.022.

Merisko-Liversidge, E.M., Liversidge, G.G., 2008. Drug Nanoparticles: Formulating Poorly Water-Soluble Compounds. Toxicol. Pathol. 36, 43–48. https://doi.org/10.1177/0192623307310946

Muster, T.H., Prestidge, C.A., 2005. Water adsorption kinetics and contact angles of pharmaceutical powders. J. Pharm. Sci. 94, 861–872. https://doi.org/10.1002/jps.20296.

Pawar, J., Tayade, A., Gangurde, A., Moravkar, K., Amin, P., 2016. Solubility and dissolution enhancement of efavirenz hot melt extruded amorphous solid dispersions using combination of polymeric blends: A QbD approach. Eur. J. Pharm. Sci. 88, 37–49. https://doi.org/10.1016/j.ejps.2016.04.001.

Piñero, J., Furlong, L.I., Sanz, F., 2018. In silico models in drug development: where we are. Curr. Opin. Pharmacol. 42, 111–121. https://doi.org/10.1016/j.coph.2018.08.007.

Pinto, E.C., Cabral, L.M., de Sousa, V.P., 2014. Development of a discriminative intrinsic dissolution method for efavirenz. Dissolution Technol. 21, 31–40. https://doi.org/10.14227/DT210214P31.

Pouton, C.W., 2006. Formulation of poorly water-soluble drugs for oral administration: Physicochemical and physiological issues and the lipid formulation classification system. Eur. J. Pharm. Sci. 29, 278–287. https://doi.org/10.1016/j.ejps.2006.04.016.

Prasad, K., Siddhanta, A.K., Rakshit, A.K., Bhattacharya, A., Ghosh, P.K., 2005. On the properties of agar gel containing ionic and non-ionic surfactants. Int. J. Biol. Macromol. 35, 135–144. https://doi.org/10.1016/j.ijbiomac.2005.01.004.

Rakhmanina, N.Y., van den Anker, J.N., 2010. Efavirenz in the therapy of HIV infection. Expert Opin. Drug Metab. Toxicol. 6, 95–103. https://doi.org/10.1517/17425250903483207.

Reddy, M.S., Reddy, N.S., Reddy, S.M., 2014. Solubility enhancement of poorly water soluble drug efavirenz by solid self emulsifying drug delivery systems. Int. J. Pharma Res. Rev. 3, 20–28.

Ronkart, S.N., Deroanne, C., Paquot, M., Fougnies, C., Lambrechts, J.C., Blecker, C.S., 2007. Characterization of the physical state of spray-dried inulin. Food Biophys. 2, 83–92. https://doi.org/10.1007/s11483-007-9034-7.

Rosen, M.J., Kunjappu, J.T., 2012. Surfactants and Interfacial Phenomena. John Wiley &

Sons, pp. 1–20.

Sathigari, S., Chadha, G., Lee, Y.H.P., Wright, N., Parsons, D.L., Rangari, V.K., Fasina, O., Babu, R.J., 2009. Physicochemical characterization of efavirenz-cyclodextrin inclusion complexes. AAPS PharmSciTech 10, 81–87. https://doi.org/10.1208/s12249-008-9180-3.

Singh, A., Majumdar, S., Deng, W., Mohammed, N.., Chittiboyina, A.., Raman, V., Shah, S., Repka, M.., 2013. Development and characterization of taste masked Efavirenz pellets utilizing hot melt extrusion. J. Drug Deliv. Sci. Technol. 23, 157–163. https://doi.org/10.1016/S1773-2247(13)50024-4.

Tamnak, S., Mirhosseini, H., Tan, C.P., Ghazali, H.M., Muhammad, K., 2016. Physicochemical properties, rheological behavior and morphology of pectin-pea protein isolate mixtures and conjugates in aqueous system and oil in water emulsion. Food Hydrocoll. 56, 405–416. https://doi.org/10.1016/j.foodhyd.2015.12.033.

Taneja, S., Shilpi, S., Khatri, K., 2016. Formulation and optimization of efavirenz nanosuspensions using the precipitation-ultrasonication technique for solubility enhancement. Artif. Cells, Nanomedicine Biotechnol. 44, 978–984. https://doi.org/10.3109/21691401.2015.1008505.

Vitez, I.M., Newman, A.W., Davidovich, M., Kiesnowski, C., 1998. The evolution of hot-stage microscopy to aid solid-state characterizations of pharmaceutical solids. Thermochim. Acta 324, 187–196. https://doi.org/10.1016/s0040-6031(98)00535-8.

Vogt, M., Kunath, K., Dressman, J.B., 2008. Dissolution enhancement of fenofibrate by micronization, cogrinding and spray-drying: Comparison with commercial preparations. Eur. J. Pharm. Biopharm. 68, 283–288. https://doi.org/10.1016/j.ejpb.2007.05.010.

Wan, S., Sun, Y., Qi, X., Tan, F., 2012. Improved bioavailability of poorly water-soluble drug curcumin in cellulose acetate solid dispersion. AAPS PharmSciTech 13, 159–166. https://doi.org/10.1208/s12249-011-9732-9.

Wardhana, Y.W., Hardian, A., Chaerunisa, A.Y., Suendo, V., Soewandhi, S.N., 2020. Kinetic estimation of solid state transition during isothermal and grinding processes among efavirenz polymorphs. Heliyon 6, e03876. https://doi.org/10.1016/j.heliyon.2020.e03876

World Health Organization, 2019. Dissolution test for solid oral dosage forms, in: The International Pharmacopoeia. pp. 1–8.

Zarmpi, P., Flanagan, T., Meehan, E., Mann, J., Fotaki, N., 2020. Biopharmaceutical Understanding of Excipient Variability on Drug Apparent Solubility Based on Drug Physicochemical Properties. Case Study: Superdisintegrants. AAPS J. 22, 1–17. https://doi.org/10.1208/s12248-019-0406-y.